Transcutaneous delivery of anti-breast cancer agents

Zoe Davison

ProQuest LLC
789 East Eisenhower Parkway
P.O. Box 1346
Ann Arbor, MI 48106-1346

For my Mum and my Susan

I would like to acknowledge the following people for their support in the completion of this thesis:

My two supervisors; Dr C.M. Heard and Prof R.I. Nicholson, thank you for your help and guidance throughout my PhD.

My Dad; Mr Ronnie Davison. I would like to thank him for his support, both emotional and financial, throughout my PhD. I would like to thank Mr Ryan Baugh for his continued support, not only in the writing of this thesis, but for everything he has done for me. You are my rock. Elizabeth, Jamie, Megan and William Clayton for their love and support. You brightened up even the darkest days of writing up! Eddie and Lynda, thank you for your hospitality, kindness and support and for all that you do for me and Ryan. I would also like to thank Mrs Kath Addy for all she has done and still does for me.

I would also like to thank members of the Skin and Natural Product Research Group, especially Mr Christopher Thomas for his friendship and help throughout my first few months and Miss Wing Man Lau for her friendship and accompanying me to the lab for late night sample points and members of the Tenovus Research Centre, especially Dr Julia Gee, Mrs Pauline Finnlay, Miss Susan Khyme, Mrs Carol Dutkowski, Mr Hugh Mottram, Dr Steven Hiscox and Mrs Lindy Goddard. I would also like to thank the coffee crew for their friendships, they mean a lot to me and made my time in Cardiff unforgettable.

I am grateful to all the Davison and Watkinson family. Thank you for your love, support and enthusiasm in all that I do. I am honoured to have a family as wonderful as you.

Breast cancer is the most common female malignancy in the western world. Currently, tamoxifen remains the gold standard anti-hormone for ER+ breast cancer. However *de novo* resistance to tamoxifen is a huge clinical problem. What is more, as many as 50% of initial responders develop acquired resistance to tamoxifen and relapse.
Aberrant growth factor signalling has been linked to the resistant phenotype, in particular EGFR and IGF-IR signalling and often gives a more aggressive disease type and poorer patient outlook.
There is a substantial clinical need for new anti-breast cancer therapeutics that target the resistant phenotype or prevent this from occurring. One hypothesis is to combine both anti-hormonal therapies with anti-EGFR therapies, in hope of preventing resistant growth.
Many downstream pathways of EGFR have been targeted to develop novel therapeutics against; however, these compounds are almost certain to give severe adverse reactions, furthermore a complex tablet regime or IV injections have a negative effect on patient compliance. A novel transcutaneous delivery system would give a more patient friendly alternative, with patients re-applying a patch or cream once a day, with rapid termination of dosing in the event of adverse event. This would also go some way to prevent endometrial complications associated with tamoxifen use.

The *in vitro* simultaneous delivery of 4-hydroxytamoxifen and signal transduction inhibitors LY294002 and PD98059 along with EPA determined that all compounds were capable of permeating porcine skin and nipple. Masses able to permeate were; 5.14 ± 0.93, 6.97 ± 0.99, 5.06 ± 0.93 and 1121.6 ± 143 μgcm^{-2} across skin respectively and 21.14 ± 2.75, 18.2 ± 2.55, 25.1 ± 6.89 and 3081.2 ± 252.7 μgcm^{-2} across porcine nipple. These compounds were formulated with 2.5% v/v DMSO and ethanol and 4% w/v Cab-o-sil.
Fish oil was shown to be a skin friendly vehicle. Ki-67 assays confirmed that incubation with fish oil maintained skin viability and H & E staining confirmed no obvious histological effects.
Growth Studies were performed on MCF-7 and TamR cells and showed that the combination of these compounds was able to reduce cell growth to 4.04 ± 0.15 and 2.47 ± 1.4 % of control growth when incubated at 25μM PD98059, 5 μM LY294002, 1×10^{-7}M 4-hydroytamoxifen and 1 μLmL^{-1} fish oil.
This combination of compounds, without 4-hydroxytamoxifen, was able to reduce the migratory capacity of TamR cells ($P = < 0.005$).

Results confirmed that the simultaneous transcutaneous delivery of multiple anti-breast cancer agents is possible and that these show promising anti-tumorogenic actions post skin.

Abbreviations

Abbreviation	Full Name
4OHTam	4-hydroxytamoxifen
AA	Arachadonic Acid
AB	Antibacterial
AF	Antifungal
AF-1	Activating function 1
AF-2	Activating function 2
AP-1	Activating protein 1
BHA	Butylated hydroxyanisole
BSA	Bovine serum albumin
CAM	Cell adhesion molecule
CaMKI	Calcium/calmodium dependant protein kinase 1
CoA	Co-activator
CoR	Co-repressor
COX	Cyclooxygenase
CPE	Chemical penetration enhancer
CTEM	Cyclopore track etched membrane
DCIS	Ductal carcinoma *in situ*
DGLA	Dihomo-γ-linolenic acid
DHA	Docosahexaenoic acid
DMSO	Dimethyl sulfoxide
DNA	Deoxyribonucleic acid

DPX	Di-butylpthalatexylene
E_2	Estradiol
ECL	Enhanced chemiluminescence
ECM	Extracellular matrix
EGF	Epidermal growth factor
EGFR	Epidermal growth factor receptor
EMMPIN	Extracellular matrix metalloproteinase inducer
EnR	Enhancement ration
EPA	Eicosapentaenoic acid
ER	Estrogen receptor
ERE	Estrogen response element
ERK	Extracellular regulated kinase
etOH	Ethanol
FCS	Foetal calf serum
FDA	Food and Drug Administration
FDC	Franz diffusion cell
FGF	Foetal growth factor
FGFR	Foetal growth factor receptor
H & E	Haematoxylin and eosin
HEPES	4-(2-hydroxyethyl)-1-piperazineethanesulfonic acid
HHBBSS	Hanks balanced buffered salt solution
HPLC	High performance liquid chromatography

HRP	Horseradish peroxidase
IC_{50}	Inhibiting concentration 50%
ICC	Immunocytochemistry
IHC	Immunohistochemistry
IGFR-IR	Type 1 insulin-like growth factor receptor
IL	Interleukin
IPK	Intracellular protein kinase
K_p	Permeability coefficient
LK	Leukotriene
LCIS	Lobular carcinoma *in situ*
LogP	Log partition coefficient
LOX	Lipoxygenase
MAPK	Mitogen activated protein kinase
MAPKK/MEK	Mitogen activated protein kinase kinase
MAPKKK/MEKK	Mitogen activated protein kinase kinase kinase
MMP	Matrix metalloproteinase
MRK	Membrane receptor kinase
NGS	Normal goat serum
NHS	Normal human serum
NRS	Normal rabbit serum
NSAID	Non-steroidal anti-inflammatory
PAGE	Polyacrylamide gel electrophoresis
PBS	Phosphate buffered saline

PG	Prostaglandin
PGG_2	Hydroperoxy endoperoxide prostaglandin G_2
PI3K	Phosphotidylinositol-3 kinase
PKA	Protein kinase A
PKC	Protein kinase C
PM	Plasma membrane
PMSF	Phenylmethyl sulphonyl fluoride
POD	Horseradish peroxidase
PTEN	Phosphatase and tensin homolog
PTGS	Prostaglandin-endoperoxide synthase
mRNA	Messanger ribonucleic acid
Rpm	Rotations per minute
SA	Sodium azide
SD	Standard deviation
SDA	Sabouraud dextrose agar
SDS	Sodium dodecyl sulphate
SEM	Standard error of the mean
SERM	Selective estrogen receptor modulator
SFCS	Stripped foetal calf serum
SSM	Sucrose storage media
TamR	Tamoxifen resistant MCF-7 cells
TBS	Tris-buffered saline
TEMED	N,N,N',N'-tetramethylene-diamine

TIMP	Endogenous tissue inhibitor
TK	Tyrosine kinase
TSA	Tryptone soya agar
Tx	Thromboxane
VEGF	Vascular endothelial growth factor
v/v	Volume in volume
w/v	Weight in volume
WB	Western blot

4.3	Permeation profiles for simultaneously applied PD98059, LY294002 and 4-hydroxytamoxifen across excised porcine skin in fish oil (n=6 ± SD)
4.4	Permeation profile for EPA from the fish oil vehicle, through excised porcine skin (n=6 ± SD)
4.5	Permeation profile for PD98059 from the fish oil vehicle, combined with various enhancers and enhancer combinations (n=6 ± SD)
4.6	Permeation profile for LY294002 from the fish oil vehicle, combined with various enhancers and enhancer combinations (n=6 ± SD)
4.7	Permeation profile for 4-hydroxytamoxifen from the fish oil vehicle, combined with various enhancers and enhancer combinations (n=6 ± SD)
4.8	Permeation profile for EPA from the fish oil vehicle, combined with various enhancers and enhancer combinations (n=6 ± SD)
4.9	Photo of a fish oil oleo gel containing 2.5% v/v DMSO and ethanol, 0.05% v/v BHA, $2.54x10^{-4}$ mol PD98059, LY294002 and 4-hydroxytamoxifen. This gel contained 4% Cab-o-sil®.
4.10	Permeation profile for PD98059, LY294002 and 4-hydroxytamoxifen in a fish oil vehicle, when formulated with 2.5% v/v DMSO/etOH, 0.05% v/v BHA and 4.0 % w/v cab-o-sil (n=6 ± SD).
4.11	Permeation profile for EPA when formulated with 2.5% v/v DMSO/etOH, 0.05% v/v BHA and 4.0 % w/v cab-o-sil(n=6 ± SD).
4.12	H & E assay on paraffin embedded excised porcine skin when treated with fish oil plus 2.5% v/v DMSO/etOH, 0.05% v/v BHA and 4.0 % w/v cab-o-sil
4.13	Ki 67 assay on paraffin embedded excised porcine skin when treated with fish oil plus 2.5% v/v DMSO/etOH, 0.05% v/v BHA and 4.0 % w/v cab-o-sil
4.14	ICC assay to detect pERK1/2 in excised porcine skin immediately post dissection
4.15	ICC assay to detect pERK1/2 in excised porcine skin after 3, 6 and 12 hours incubation with water, fish oil (0.05% v/v BHA) or fish oil plus 2.54 x 10^{-4}M PD98059, LY294002, 4-hydroxytamoxifen (plus 0.05 v/v BHA 2.5% v/v DMSO/etOH and 4% w/v cab-o-sil).
4.16	ICC assay to detect pAkt in excised porcine skin immediately post dissection
4.17	ICC assay to detect pAkt in excised porcine skin after 3, 6 and 12 hours incubation with water, fish oil (0.05% v/v BHA) or fish oil plus 2.54 x 10^{-}

	^{4}M PD98059, LY294002, 4-hydroxytamoxifen (plus 0.05 v/v BHA 2.5% v/v DMSO/etOH and 4% w/v cab-o-sil).
4.18	ICC assay to detect pEGFR1068 in excised porcine skin immediately post dissection
4.19	ICC assay to detect pEGFR1068 in excised porcine skin after 3, 6 and 12 hours incubation with water, fish oil (0.05% v/v BHA) or fish oil plus 2.54 x 10^{-4}M PD98059, LY294002, 4-hydroxytamoxifen (plus 0.05 v/v BHA 2.5% v/v DMSO/etOH and 4% w/v cab-o-sil).
4.20	ICC assay to detect total COX-2 in excised porcine skin immediately post dissection
4.21	ICC assay to detect total COX-2 in excised porcine skin after 3, 6 and 12 hours incubation with water, fish oil (0.05% v/v BHA) or fish oil plus 2.54 x 10^{-4}M PD98059, LY294002, 4-hydroxytamoxifen (plus 0.05 v/v BHA 2.5% v/v DMSO/etOH and 4% w/v cab-o-sil).
4.22	Bonding complexes formed between PD98059 and EPA and LY294002
5.1	Growth assays to detect the effects of 1 x 10^{-7}M Faslodex, 1 x 10^{-9}M E_2 and 1 x 10^{-7}M 4-hydroxytamoxifen on MCF-7 cell growth (n=3 ± SD)
5.2	Growth assays to detect the effects of 1 x 10^{-7}M Faslodex and 1 x 10^{-7}M E_2 on TamR cell growth (n=3 ± SD).
5.3	Dose responses of MCF-7 and TamR cells to increasing volumes of fish oil (n=3 ± SD).
5.4	Growth assays to detect the effects of 25μM PD98059, 5μM LY294002, 1 x 10^{-7}M 4-hydroxytamoxifen and 1μlml^{-1} fish oil on MCF-7 cell growth (n=3 ± SD).
5.5	Growth assays to detect the effects of 25μM PD98059, 5μM LY294002 and 1μlml^{-1} fish oil on TamR cell growth (n=3 ± SD)
5.6	Growth assays to detect the effects of permeated concentrations of PD98059, LY294002, 4-hydroxytamoxifen and 1μlml^{-1} fish oil on MCF-7 cell growth (n=3 ± SD)
5.7	Growth assays to detect the effects of permeated concentrations of PD98059, LY294002 and 1μlml^{-1} fish oil on TamR cell growth (n=3 ± SD)
5.8	MCF-7 and TamR cells ICC for total ER (x20).
5.9	MCF-7 and TamR cells ICC for pER118 (x20).
5.10	MCF-7 and TamR cells ICC for pER167 (x20).
5.11	MCF-7 and TamR cells ICC for pERK1/2 (x20).
5.12	MCF-7 and TamR cells ICC for pAkt (x20).

5.13	MCF-7 and TamR cells ICC for total EGFR (x20).
5.14	MCF-7 and TamR cells ICC for pEGFR1068 (x20).
5.15	Western Blot for the levels of total ERα, pERα118 and pERα167 protein in MCF-7 and TamR cells (n=3 ± SD)
5.16	Western Blot for the levels of total ERK1/2 and pERK1/2 protein in MCF-7 and TamR cells (n=3 ± SD)
5.17	Western Blot for the levels of total Akt and phospho-Akt protein in MCF-7 and TamR cells (n=3 ± SD)
5.18	Western Blot for the levels of total EGFR and phospho-EGFR1068 protein in MCF-7 and TamR cells (n=3 ± SD)
6.1	Growth assay to show the growth rates of MCF-7, TamR and FasR cells
6.2	Growth assay to show the growth rates of MCF-7 cells when treated with 4-hydroxytamoxifen, PD98059, LY294002 and fish oil (both singly and in combination)
6.3	Growth assay to show the growth rates of TamR cells when treated with PD98059, LY294002 and fish oil (both singly and in combination)
6.4	Migration assay to show the number of MCF-7, TamR and FasR cells migrating after 48 hours
6.5	Migration assay to show the number of TamR cells migrating after 48 hours, when incubated with control, $1\mu lml^{-1}$ fish oil or $1mgml^{-1}$ fish oil plus 25μM PD98059 and 5μM LY294002 treatments
6.6	**A** Western Blot for the levels of total COX-2 protein **B** Densitometry analysis of total COX-2 protein.
6.7	**A** Western Blot for the levels of total Src and phosphorylated Src (at tyr 416 protein **B** Densitometry analysis of total Src, and phosphorylated Src (at tyr 416) protein
6.8	Western blot to show the levels of β-actin
6.9	Immunocytochemical detection of total COX-2 in MCF-7 and TamR cells
6.10	Immunocytochemical detection of p-Src in MCF-7 and TamR cells
6.11	Flow diagram to show the crosstalk between COX-2/PGE_2, EGFR, Src, PI3K and ERK1/2 in metastasis.
7.1	Gram's stain of bacterial colonies swabbed from porcine ear skin
8.1	Diagram to show the set up of the proposed 'composite model
8.2	Histogram to show the Franz diffusion cell MCF-7 cell counts

	permeated excised porcine skin after 48 hours when formulated with 2.5% DMSO/etOH and various %'s of cab-o-sil
5.1	Dosing concentrations of compounds for phenotypic analysis of MCF-7 and TamR cells.
5.2	Dosing concentrations of 4-hydroxytamoxifen, PD98059, LY294002 and EPA for growth assays.
5.3	Treatments for ICC analysis of cells
5.4	Percentage cell growth compared to control when MCF-7 and TamR cells were incubated with 25μM PD98059, 5μM LY294002, 1 x 10^{-7}M 4-hydroxytamoxifen and 1μlml^{-1} fish oil (and combinations of these).
5.5	H-score analysis of MCF-7 and TamR cells when assayed for the immunocytochemical detection of ER, pER118, pER167, pERK1/2, pAkt, total EGFR and pEGFR1068
6.1	Treatments used in growth assays to detect the effects of formulation constituents on the growth rate of both MCF-7 cells and TamR cells
6.2	Treatments for MCF-7 and TamR cells prior to Western blot and ICC analysis
7.1	Table to show the show the diffusion cell set up when assessing the CTEM at preventing the ingress of microorganisms
7.2	Description of bacterial colonies grown from porcine ear swabs
7.3	Table to show the ability of the CTEM and/or antibiotic and antifungal at preventing bacterial contamination of the receptor phase of Franz diffusion cells
7.4	Table to show the ability of the CTEM and/or antibiotic and antifungal at preventing fungal contamination of the receptor phase of Franz diffusion cells
9.1	Comparison of the mass of PD98059, LY294002, 4-hydroxytamoxifen and EPA reaching the receptor phase after 24 hours when applied to full thickness porcine skin or porcine mammary papilla
9.2	Comparison of the mass of PD98059, LY294002, 4-hydroxytamoxifen and EPA reaching the receptor phase after 24 hours when applied to porcine mammary papilla when formulated with 4 or 10% Cab-o-sil

Chapter 1

General Introduction

1.1 Breast cancer overview

Cancer is commonly (and erroneously) thought of as one single disease, whereas it is in fact a group of diseases. At least 100 different types of cancer have currently been identified, generally sub-grouped due to the tissue in which they originate and also the cell type in which they originate. Cancer is characterized by several criteria, including unregulated cell growth and invasion of cells into other sites of the body from the site of origin (Pecorino, L. 2005). Cell proliferation and cell cycle are tightly controlled in healthy cells, although DNA damage, which escapes cellular repair, leads to uncontrolled cell growth and proliferation, thus leading to tumorogenesis. Breast cancer is a cancer that starts in the cells of the breast in men and women.

As will become clear in the following pages, there is a substantial clinical requirement for new anti-breast cancer systems. This thesis was concerned with the development of a strategy involving the simultaneous transcutaneous delivery of a cocktail of a mitogen-activated protein kinase inhibitor, a phosphotidylinositol 3 kinase inhibitor, tamoxifen and eicosapentaenoic acid. This system was designed as an adjuvant to surgery and/or a prophylactic for individuals with increased risk (family history, genetic predisposition). This novel multi-pronged to combating breast cancer would be expected to confer significant advantages over single treatments, and delay or prevent chemotherapy resistance.

1.1.1 Statistics and incidence rates

Breast cancer is now the most common cancer in the UK, with around 44, 000 new cases diagnosed each year, 1% of which are in males. One in four of all cancers in females are accounted for by breast cancer, with an estimated 1 in 9 women, in the western world, developing breast cancer at some stage in their life (Ali, S. & Coombes, R.C. 2002). Although breast cancer has around the same incidence rates as large bowel cancer and lung cancer, the mortality rate is 50% of these cancers. It is estimated that 77% of woman who are diagnosed with breast cancer live for above 5 years. This lower mortality rate is partly due to the widespread screening, which leads to early detection and so better patient prognosis, along with better treatments, both pre and post operation.

Age is the biggest, but by no means sole, risk factor associated with breast cancer; the risk factor sharply increases after 50 years. The UK has the largest incidence of breast cancer in the world, and so much work is being and still needs to be done to discover any reasons for this trend.

1.1.2 Stages of disease

The breast is composed of glandular, fatty and fibrous tissues, which are positioned over the pectoral muscles and adjoined to the chest wall via Coopers' ligaments (fibrous strands). Each breast is a tear shaped gland composed of between 15-20 lobes, which are arranged in a circular fashion and covered by, and so held in place by a layer of subcutaneous adipose tissue or fat, which extends through the breast (figure 1.1).

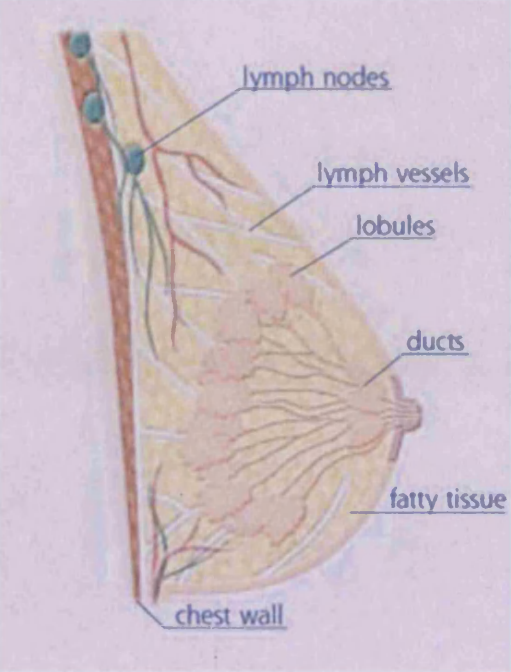

Figure 1.1 Anatomy of the human breast (from www.ribbonofpink.com)

Many bulb-like lobules make up each lobe and ducts connect the lobes and lobule. These ducts are narrow at the lobules, however, diverge and widen at the nipple.

There are many types of breast cancer, which are termed by the location (in the breast) in which the cancer cells begin to grow. For example, ductal carcinoma (the most common form of breast cancer) is called so because it begins within the cells of the ducts. Breast cancers, which remain in the lobule or duct are termed carcinoma *in situ*, however tumors that spread outside these are termed invasive or infiltrating carcinoma.

Breast cancer is also diagnosed according to which 'stage' it is at. The stages (0 to IV) reflect the tumor size, nodal status and metastasis. Stage 0 signifies very early breast cancer, where the tumor is very small and has not spread outside the duct or lobule. Stage I classifies tumors that are no bigger than 2cm and have not spread outside the breast but cancer cells have spread to other parts of the breast. Stage II is used to describe either tumors that are between 2 and 5 cm with no lymph node involvement or tumors that have spread to auxiliary lymph nodes (on the same side of the body). However, these lymph nodes have not stuck down to surrounding tissue or to each other. Stage III includes two sub-stages: stage IIIa and IIIb. Cancers in stage IIIa either have strong lymph node involvement, where lymph nodes have now adhered to surrounding tissue or to other lymph nodes or measure larger than 5 cm. Cancers classed as stage IIIb are invasive cancers, which have spread to internal mammary lymph nodes, the breast skin or the chest wall. Stage IV, the most advanced breast cancer, describes tumors that have spread to other organs within the body. These commonly include bones, the lungs, the liver or the brain.

1.1.3 Risk factors

Despite many advances in breast cancer research over the last few decades the incidence rate and mortality, among females have remained largely unchanged for some time now (Russo, J. *et al* 2000). There have been many risk factors identified, which include genetic, hormonal and environmental.

Age remains of the most significant risk factors related to breast cancer. There has also been a strong relationship recognized between breast cancer risk and weight, however, this is again dependent on age. There has been no evidence that excessive weight alters risk under the age of 50, however at 60+ with each 10kg increase in weight there has been shown to be an 80% in breast cancer risk (Harris, J.R. *et al* 1995). Other risk factors include diet, cigarette intake and alcohol intake.

1.2 Estrogen signalling

Estrogens (Oestrogens) are hormones involved in the female menstrual cycle, of which three exist; estradiol E_2, oesterone and oestriol. They are synthesised from cholesterol in a complex biosynthetic pathway. Aromatase, a cytochrome P450 enzyme, catalyses the final reactions that see testosterone converted to estradiol and androstendione to oesterone. Estrogen is released from the Graafian follicle and controls the proliferative stage of the endometrium. Estrogen not only acts on estrogen receptors in the uterus but also in the vagina, anterior pituitary and mammary gland during the menstrual cycle (Rang, H.P. *et al* 2001).

1.2.1 Estrogen and breast cancer

It has long been known that steroid hormones such as estrogen and progestins are involved in breast cell proliferation, however it wasn't until the late 1800s until these steroid hormones were linked to the development of estrogen positive breast tumors (Jordan V.C. *et al* 2001). Sir George Thomas Beatson

first suggested a link, between the breast and ovaries in the 1890s. He noticed that the removal of the ovaries had effects on lactation of sows. Fundamental research by Beatson and colleagues then revealed that by removing the ovaries, metastatic breast cancer was forced into remission. This groundbreaking work uncovered a link between breast cancer progression and tumour growth with estrogens in endocrine responsive tumours (Beatson, G.T. 1898). In fact, it is now established that estrogens drive the growth of these tumours (Levine, M. *et al* 2001). However, it was this breakthrough, linking cancer progression with estrogens that uncovered many problems with resistance that are still perplexing to date. Beatson showed that only 25% of patients were sensitive to oopherectomy and that many of these responders eventually relapsed and the tumors again progressed. Many more patients did not respond to oopherectomy and were insensitive. This phenomenon is seen today in the clinic with both acquired and *de novo* (from the beginning) resistance to endocrine therapy (Robertson, J.F.R, *et al.* 2002). With this link between ovaries and breast cancer established, anti-estrogen therapies were developed to either deplete the production of estrogen, for example aromatase inhibitors, or to block the estrogen receptor and so oppose the effect of estrogens, such as tamoxifen.

1.2.2 Estrogen receptor

The estrogen receptor (ER) is an important mediator of breast cancer growth and progression and is also an important prognostic and chemotherapeutic target in breast cancer care. Although it is only expressed in 6-10% of normal

breast epithelial cells, over 60% of primary breast cancers express it (Hanstein, B. *et al* 2004).

There are two identified ERs; Erα and Erβ. These receptors belong to a super-family known as the nuclear hormone receptors. They are hormone activated transcription factors and so are responsible for the transcription of genes containing a hormone response element (ERE) (Macgregor, J.I. & Jordan, V.C. 1998). The ER has 6 main functional domains. The E region confers to the steroid-binding domain. This domain undergoes a conformation change upon E_2 binding, which locks this hormone in place in the hydrophobic pocket. The conformational change allows binding of co-activator proteins to the activating function regions 1 and 2 (AF 1 and 2). It also facilitates the interaction of ER with DNA through the DNA binding region (Jordan, V.C. & Morrow, M. 1999). The DNA binding region contains two zinc fingers that facilitate the receptor binding to hormone response elements in the promoter region of hormone responsive genes. ER can alter gene expression in a hormone dependent way (Harris Wooge, C. *et al* 1992). ERs possess both estrogen independent (AF-1) and estrogen dependant (AF-2) domains. They use these domains to recruit co-activator proteins and to interfere with the transcription process (Campbell, R.A *et al* 2001).

1.2.3 Estrogen receptor signalling

There are now several mechanisms understood by which estrogen and ER influence tumorogenesis. The classical mechanism involves estrogen binding

to nuclear ERα at the ligand-binding domain; it is then sealed in this position by helix 12 of the ER. This binding induces receptor homodimerization that leads to a conformational change in the ligand-binding domain of the receptor. This allows the recruitment of co-activator proteins to the AF-2 region. A transcription complex is then formed at an ERE, located in the promoter region of estrogen responsive genes and gene transcription can occur, figure 1.2 shows the suggested mechanism (Jordan, V.C 2001).

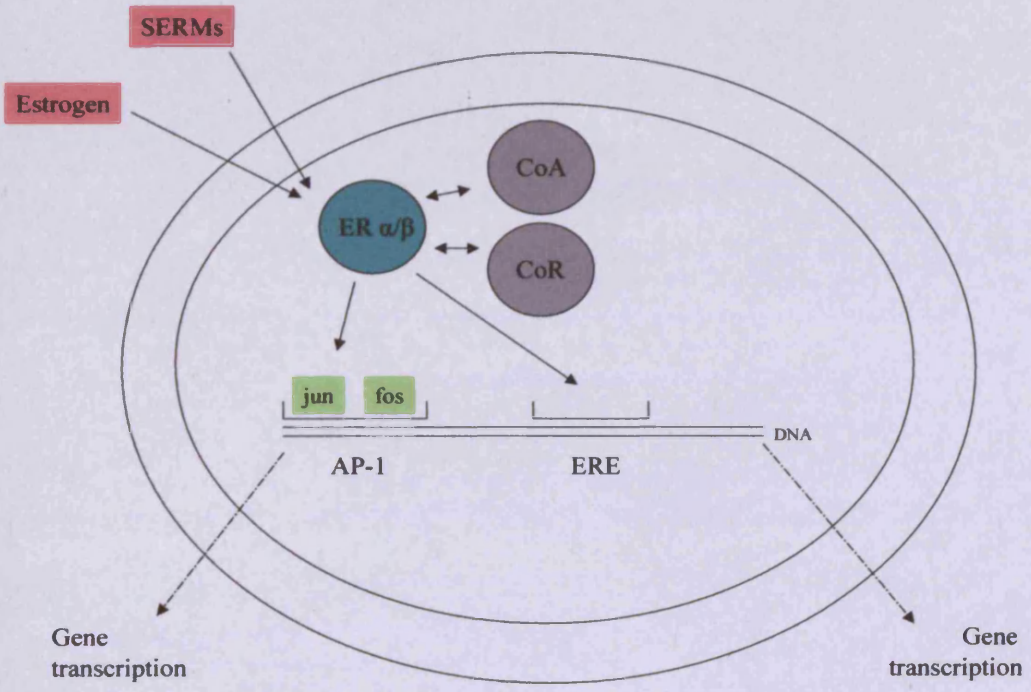

Figure 1.2 Nuclear ER signalling. ERE – estrogen response element. CoA- co-activator. CoR – co-repressor. AP-1 – activating protein 1. SERM – selective estrogen receptor modulator.

Genetic studies revealed that over a third of genes that are regulated by ERs but do not contain EREs (O'Lone, R. *et al* 2004). This new evidence has suggested that this mechanism is not the sole way that ER can regulate gene expression.

ER can regulate gene transcription without binding directly to DNA. Through protein-protein interactions within the nucleus ER can modulate the function of other transcription factors (Gottlicher, M. *et al* 1996). The interaction of ER and the Jun or Fos proteins at AP-1 binding sites leads to the transcription of genes that produce proteins such as ovalbumin and collagenase (Björnström, L. & Sjöberg, M. 2006).

Some actions mediated by ER occur extremely rapidly, therefore eliminating effects on RNA as a plausible mechanism. These actions occur through activation of cell membrane ER and are non-genomic actions of estrogens. Cell membrane ERs remain quiescent in mammary tissue until stimulation by steroid hormones. This stimulation induces the production of growth factors in ER+ cells, which act on neighbouring ER- cells in a paracrine fashion to stimulate growth (Song, X-D. & Santen, R.J. 2006). However, in neoplasia the growth factors predominantly stimulate the growth of the ER+ cells in an autocrine fashion (Streuli, C.H. & Haslam, S.Z. 1998). The membrane receptor has not been fully characterised and its exact role in breast cancer tumorogenesis has not been defined. It is known that the receptor is a G-protein coupled receptor capable of induction of signalling pathways upon

activation by E_2 (Razandi, M. *et al* 1999). Protein kinase signalling pathways are activated in this way, which leads to altered cytoplasmic proteins such as upregulation of eNOS (Björnström, L. & Sjöberg, M. 2006). The membrane ER can also directly interact with and/or activate IGF-IR, PI3K, Src and EGFR (Osbourne, C.K. *et al* 2005).

Activation of the membrane ER can, in turn, also affect gene transcription. Many transcription factors are regulated by protein kinases, which phosphorylate and thus activate them. These actions are termed nongenomic-to-genomic signalling (Björnström, L. & Sjöberg, M. 2006).

1.3 Endocrine therapy

1.3.1 Tamoxifen

For some time now tamoxifen has remained the gold standard treatment for hormone sensitive or ER+ breast cancer.

Tamoxifen is an anti-estrogen and exerts its anti-estrogenic effect by competitively blocking the ER within mammary tissue. Tamoxifen also blocks the transcription of ERE containing genes, thus it has been termed a selective estrogen receptor modulator or SERM (Levine, M *et al* 2001). SERMs show both estrogenic and anti-estrogenic activities at various sites of the body.

SERMs bind to nuclear ERs and alter the conformational shape of these receptors. Tamoxifen binds to ERα at the ligand-binding site. It suppresses AF-2 fully, therefore stopping co-activator molecules from binding and thus giving anti-estrogenic activity (Jordan, V.C 2001). However tamoxifen binding does not silence the charge on a specific amino acid that is important in co-activator binding. This means that binding of few co-activators is still possible in certain cell types, thus suggesting why tamoxifen is estrogenic in certain cell types (Barkhem, T. *et al* 1998).

It has been shown, in clinical trials, that tamoxifen significantly increases survival rate and inhibits the development of metastatic spread compared to placebo. In 1989 the B-14 clinical trial was launched, which was a part of the National Surgical Adjuvant Breast and Bowel Project. This trial studied the benefit of tamoxifen treatment on survival rates, tumor recurrence and second primary tumor development. The B-14 trial randomly assigned post operated patients whom had just had ER+ breast cancer tumors with no auxiliary lymph node involvement removed to either tamoxifen treated (20 mg day^{-1}) or placebo group for 5 years. After 5 years disease free patients from the tamoxifen treated group were then reassigned to new groups and either received tamoxifen for a further 5 years or placebo for the remaining five years. It was demonstrated, through the B-14 clinical trial, that survival rate increased with the length of tamoxifen treatment up to 5 years, however the trial also showed there were no survival benefits of tamoxifen treatment for more than 5 years compared to 5 years only (Fisher, B. *et al* 1996).

Although tamoxifen has been very successful in treating metastatic, ER+ breast cancer, it can give rise to severe, although rare, adverse effects such as endometrial cancer and thromboembolic events and, more commonly, nausea and vomiting. There has been much speculation as to whether tamoxifen administration leads to an increased risk in developing second primary tumors excluding those of the breast, in particular the development of endometrial cancer. The aforementioned B-14 trial monitored closely the incidence of endometrial cancer development after tamoxifen treatment. This trial showed that tamoxifen treatment significantly increased the risk of developing endometrial cancer when compared to placebo (Fisher, B. *et al* 1994). However, there are conflicting and controversial results regarding this issue in the scientific literature. One trial, which took place in Manchester, showed no difference in the risk of developing endometrial cancer between tamoxifen treated and placebo groups. Cases of endometrial cancer were detected in the placebo group, however these were only discovered when the patient had commenced tamoxifen treatment for second primary tumors (Ribeiro, G. & Swindell, R. 1992). So it is questionable whether the data from this trial was accurate. Another trial, which took place in Scotland, also showed that there was no statistically significant link between tamoxifen treatment and endometrial cancer development, when compared to control (Stewart, H.J 1992). These conflicting results highlight the need for a more planned and prepared trial. The trials mentioned above did not follow a standard protocol; in fact they all had differences in treatment time, follow-up time, patient population, group size and doses. So it is not entirely surprising that no

reproducible results have been detected from them. Although there is a need to undertake more trials to ascertain whether or not there is a link between tamoxifen and endometrial cancer, it has to be taken into account whether such a trial is still ethical. We now know the value of tamoxifen in treating all stages of breast cancer. The question is would it be ethical to withhold a beneficial treatment from a patient?

Tamoxifen treatment does not give rise only to unwanted effects, it is suggested that it is cardio-protective. A study by Love, R.R and colleagues in 1994 showed that after 2 or more years of tamoxifen treatment, the risk of cardiovascular disease decreased significantly in post-menopausal women. Tamoxifen was shown to lower total cholesterol (lipoprotein a) and fibrogen and it is this that is thought to contribute to a decreased risk of cardiovascular disease. However, more work is needed to look into the effect on both HDL levels and blood pressure.

Experimental models of breast cancer have shown that the ER can be activated in a ligand-independent manner. It has been suggested that it is this switch to ligand-independent activation of the ER that is a key mechanism that underlies altered ER activity and anti-estrogen resistance (Adeyinka, A. et al 2002). However, it is not yet fully understood what causes this switch to occur.

The development of tamoxifen resistance has also brought limitations to the use of long-term tamoxifen treatment. This is thought to affect around 50% of

patients and leads to a more aggressive phenotype and poorer patient outlook (deGraffenried, L.A 2003). The problems associated with tamoxifen mentioned above have highlighted the need for new treatments to be found.

1.3.2 Aromatase inhibitors

Aromatase inhibitors (AIs) inhibit the conversion of testosterone and androstenedione to estradiol and estrone respectively in peripheral and breast tumor tissues. They exert this effect by inhibiting the cytochrome P450 aromatase enzyme (Nicholson, R.I. *et al* 2004). There are two types of AI: irreversible AIs such as exemestane, which bond and degrade the aromatase enzyme rendering it non-usable. There are also reversible AIs such as anastrozole, which inhibit the aromatase enzyme in a competitive manner allowing re-use of the enzyme.

1.3.3 Fulvestrant

Fulvestrant or faslodex is a non-steroidal, pure anti-estrogen developed to overcome the estrogenic actions seen in tamoxifen treatment. It has a binding efficiency of ~100 times that of tamoxifen (Robertson, J.F. *et al* 2001). It is thought to exert anti-estrogenic actions by downregulating ER and by inhibiting the nuclear/cytoplasm shuttling of the ER and by inhibiting receptor dimerization and DNA binding (McClelland, R.A. *et al* 2001). It is also suggested the faslodex may modulate the recruitment and interaction of co-regulators.

1.4 Anti-hormone resistance and EGFR signalling

The mechanisms by which both primary and acquired resistance occur are only vaguely understood and, so more work needs to be done in this area if new therapies to overcome this obstacle are to be developed. It is now accepted, however, that growth factor signalling is a key, but not sole, factor involved in anti-estrogen resistance. This has led to down stream mediators of these pathways becoming new targets for breast cancer therapy. Increased epidermal growth factor receptor (EGFR) signalling is commonly seen both clinically and in breast cancer cell lines that have developed endocrine resistance (Nicholson, R.I *et al* 2004).

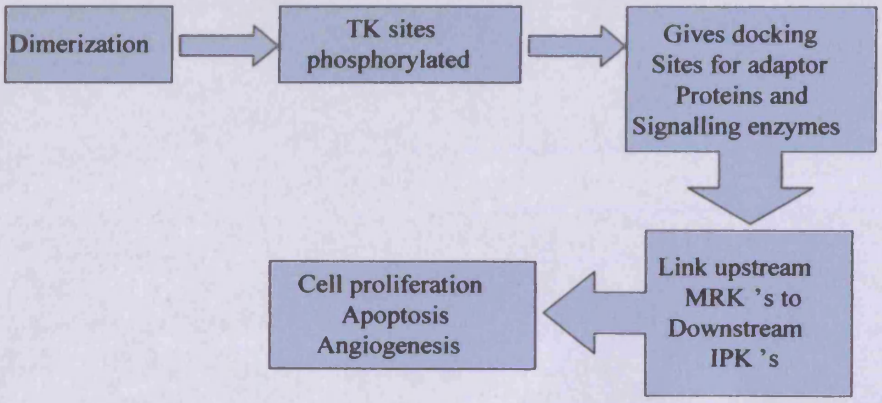

Figure 1.3 A flow chart to show EGFR signalling. TK - tyrosine kinase, MRK - membrane receptor kinase, IPK – intracellular protein kinase.

Epidermal growth factor receptors are a family of 4 protein tyrosine kinase receptors, named EGFR or HER-1, HER-2, HER-3 and HER-4 (Atalay, G. *et al* 2003). They possess both a ligand binding domain (except HER-3) and a

tyrosine kinase domain (except HER-2). Figure 1.3 shows a much simplified flow chart-type representation of EGFR signalling.

Taking into consideration that there are 10 known ligands, several dimer variations and many downstream effectors, the EGFR signalling network is complex and diverse and not fully understood (Atalay, G. *et al* 2003).

Activation of downstream EGFR mediators such as phosphatidylinositol-3-kinase (PI3K) and mitogen activated protein kinase (MAPK) can lead to ligand-independent activation of the estrogen receptor. PI3K and MAPK can phosphorylate key serine residues, serine 118 and 167 respectively on the estrogen receptor within the AF-1 domain. This phosphorylation activates the estrogen receptor in the absence of estrogen. In this instance, if tamoxifen is present the tamoxifen/ER complex is enhanced and results in tamoxifen displaying an estrogenic effect on breast cancer cells, (Nicholson, R.I. *et al* 2004). This highlights the attractiveness and benefit of targeting such kinase pathways in the fight against tamoxifen resistant breast cancer.

1.4.1 Phosphatidylinositol 3 kinase

Phosphatidylinositol 3-kinases are a sub-class of the lipid kinase superfamily that catalyse the addition of phosphates to position 3 of the inositol ring of phosphoinositides. However, 3' phosphorylated phosphoinositides only account for 0.025% of all inositol-containing lipids, suggesting that they are not ubiquitous or homeostatic lipids, but play an important role in cell regulation (Ramelh, L.E. & Cantley, L.C. 1999).

PI3K is heterodimer of two subunits; p85, which is a regulatory subunit and p110, a catalytic subunit. An inter SH (iSH) sequence separates the two SH2 domains of the p85 subunit and links this subunit to the catalytic subunit. The two SH2 domains provide binding sites for tyrosine kinases (TKs). The p110 subunit is also a dual specificity kinase that can phosphorylate serine and threonine residues in addition to phosphoinositides lipids. The regulatory subunit can interact with both the p110 subunit and TKs. This is proposed as the reason behind the membrane targeting of p110 and its subsequent complexation with lipid substrates (Krasilnikov, M.A. 2000). The PI3K enzymes can be activated in a number of ways, by G-protein coupled receptors, proteins with tyrosine kinase activity or by tyrosine-phosphorylated proteins. PI3 kinase signalling revolves around the presence of lipid recognition modules found in target proteins. Two key recognition domains have been described to date; these are the pleckstrin homology (PH) domain and the FYVE domain (Vanhaesebroeck, B.*et al* 1999). 3-phosphorylated inositol lipids are produced in the target membrane upon activation of an appropriate PI3 kinase. This results in the recruitment of proteins containing high affinity binding sites for these lipids, such as Akt (Fry, M.J. 2001). Upon activation, these kinases phosphorylate inositol lipids at the '3 position. The PI3 kinase generated phosphoinositides recruit Akt to the plasma membrane through their affinity for the PH domain of Akt (Scheid, M. *et al* 2002) where it undergoes independent phosphorylation at two residues, a threonine present in the activation loop and a serine at the carboxyl terminus. Once activated, Akt is

capable of phosphorylating a number of proteins involved in metabolism, translational control, control of cell cycle by affecting cyclin D_1 and cell survival by affecting forkhead family transcription factors, BAD and caspase-9. (Campbell, R.A *et al* 2001) The PI3K pathway is one of the pathways over-activated in tamoxifen resistance. Figure 1.4 is a cartoon representation of the PI3 kinase pathway.

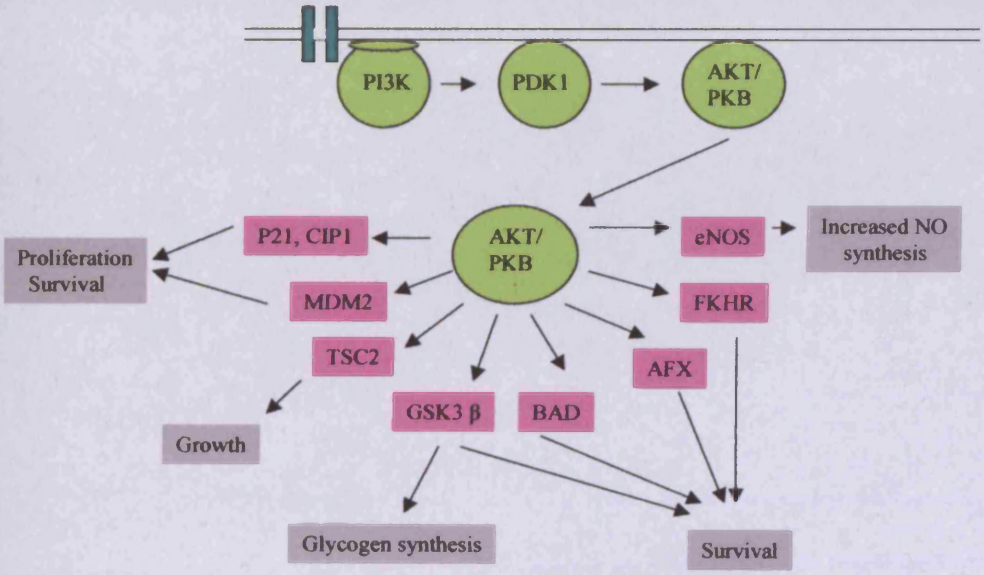

Figure 1.4 The PI3K pathway.

It can be seen from figure 1.4 that activation of PI3 kinase leads to the transcription of many tumor promoting proteins such as BAD, CIP1 and FKHR, which leads to increased cell proliferation, growth and survival and increased glycogen synthesis.

1.4.2 Mitogen-activated protein kinase

Mitogen-activated protein kinases (MAPK), are proline-directed serine/threonine kinases that are widely expressed intracellular signalling molecules involved in mitosis and meiosis and many other facets of cellular regulation (Chang, L. *et al* 2001). Figure 1.5 shows the mitogen-activated protein (MAP) kinase pathway.

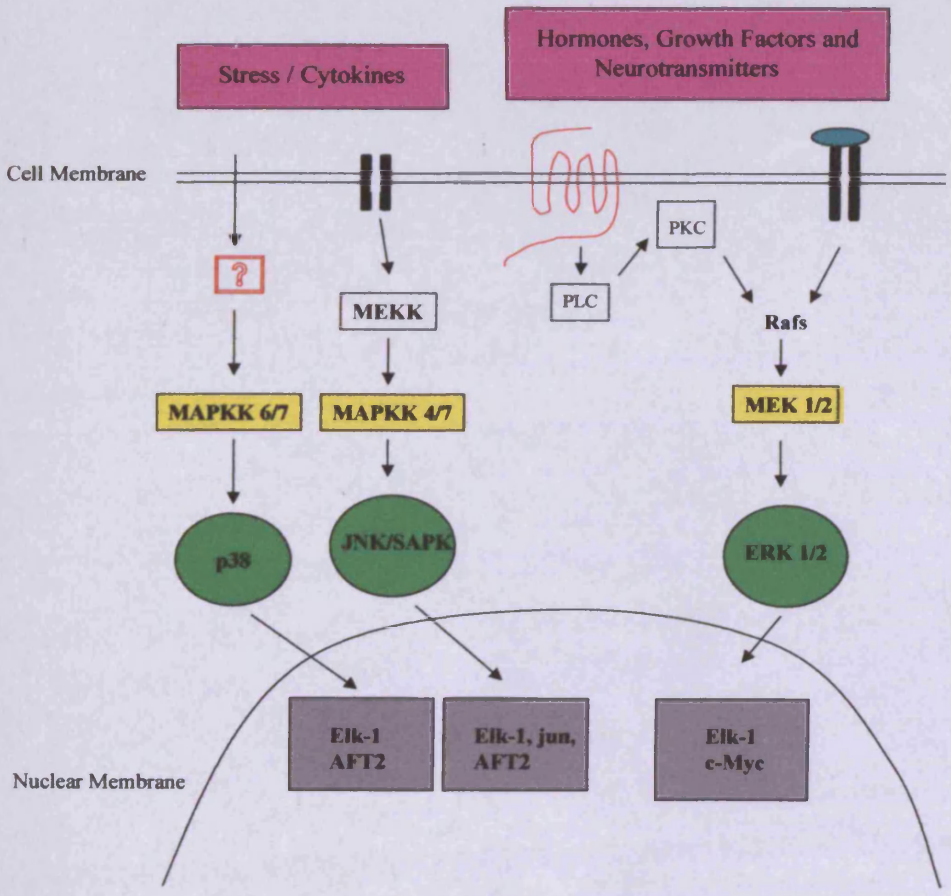

Figure 1.5 MAPK pathway.

They are activated as a result of numerous stimuli and mediate signal transduction from the cell surface to the nucleus (Choi, K-C. *et al* 2003). When activated they catalyse the transfer of the terminal phosphate of ATP onto their target proteins (Choi, K-C. *et al.* 2003). There are three subsets of this family, ERK 1/2, p38MAPK and the c-Jun N terminal kinase/stress activated kinase (JNK/SAPK).

They are organised into three kinase modules consisting of a MAP kinase, an activator of this (MEK or MAP kinase kinase) and a MAP kinase kinase kinase (MEKK or MEK kinase). Figure 1.5 shows that activation of these pathways leads to the transcription of many tumour-promoting proteins.

In the anti-estrogen resistant phenotype, the activation of the MAPK pathway is enhanced, and so inhibition of this pathway could be beneficial in treating tamoxifen resistant breast cancer.

1.5 Inflammation and breast cancer

1.5.1 Inflammation

Inflammation is a tightly controlled process, which occurs in response to tissue damage. The main purpose of this process is to contain and/or destroy the pathogen, repair damaged tissue and remove tissue debris. The following sections will describe how this process may be implicated in malignancies.

1.5.2 Cyclooxygenase

The prostaglandin-endoperoxide synthase (PTGS), cyclooxygenase (COX), is an enzyme that can oxygenate, with varying efficacy, 18-22 carbon polyunsaturated fatty acids (PUFAs), such as arachadonic acid (AA), eicosapentaenoic acid (EPA) and dihomo-γ-linolenic acid (DGLA) (Malkowski, M.G., *et al.* 2001). Physiologically, the pivotal role of these enzymes is to catalyse the conversion of, primarily, AA into a range of biological mediators termed prostanoids. These prostanoids include prostaglandins, prostacyclin and thromboxane (Lee, J.L., *et al* 2003).

The COX enzymes are dimeric, with each monomer containing three folding units. The first folding unit displays heavy sequence homology to that of the EGFR and is thought to be responsible for protein-protein interactions. The second folding unit is responsible for insertion and anchoring into the lipid bilayers. It contains four right-handed helices, which form a motif that allows this insertion to occur. The third folding unit is the catalytic domain and is the largest of the three units. It contains two active sites and so displays two distinct enzymatic activities. The cyclooxygenase enzymes possess both a cyclooxygenase and peroxidase activity. In step 1, shown in figure 1.6, the cyclooxygenase site facilitates the conversion of AA to an intermediate prostaglandin (PG) termed hydroperoxy endoperoxide prostaglandin G_2 (PGG_2).

In this step the peroxidase active site generates a tyrosine radical, which abstracts hydrogen atoms from AA. The tyrosine radical then interacts with two oxygen molecules to form PGG_2. The second step allows the reduction of PGG_2 to PGH_2 via peroxidase activity (Silva, P.J., *et al* 2003). The specific prostaglandins, prostacyclins and thromboxanes are then synthesised via specific enzymes, shown in step 3.

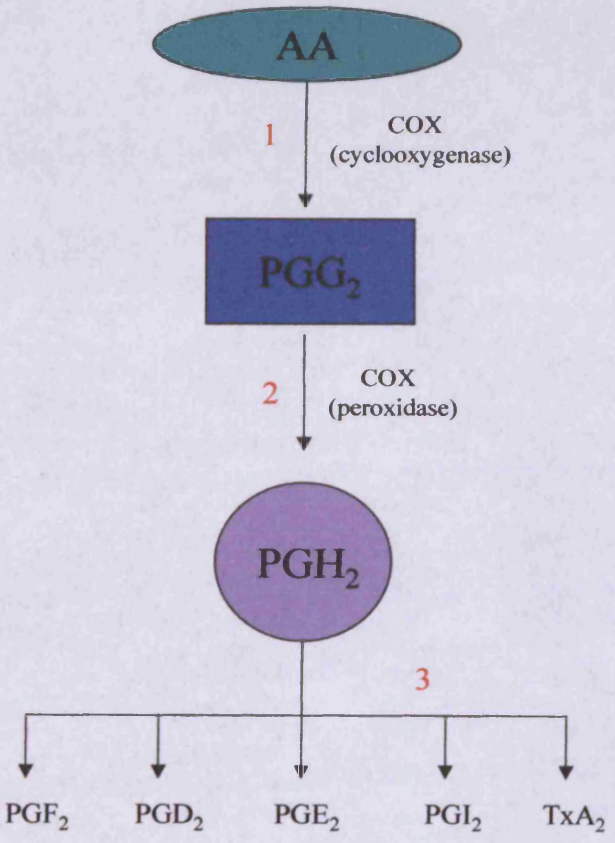

Figure 1.6 Flow chart diagram to show prostanoid biosynthesis (Dubois, R.N., *et al.* 1998).

There are currently 3 identified isoforms of the COX enzymes, namely COX-1, COX-2 and COX-3. COX-1 was first cloned in 1988 and is now known to be a 'housekeeping' enzyme. It is constitutively expressed in most tissues and cell types and is responsible for the management of homeostatic physiological processes including ovulation, bone metabolism and platelet aggregation (Dubois, R.N. *et al* 1998). COX-1 mediated production of PGs occurs via hormone stimulation (Malkowski, M.G., *et al.* 2001).

COX-2, on the other hand, is normally undetectable in most tissues but is induced by a variety of stimuli such as growth factors, tumor promoters and pro-inflammatory cytokines (Méric, J-B. *et al.* 2006). COX-3, the most recently identified form, is now thought to be a splice variant of COX-1 and so is sometimes referred to as COX-1b. It is formed by intron retention, a complex form of alternative splicing (Xie, W. *et al.* 1991).

1.5.3 Prostanoids

Prostanoids are potent and bioactive lipid messengers (Simmons, D.L. *et al.* 2004). There are currently 3 classes of prostanoid identified; prostaglandins (PGs), thromboxanes (Txs) and prostacyclins (PGIs). Each of these classes consists of several different series of prostanoid, depending on the precursor fatty acid.

Precursor Fatty Acid	Series of PG, PGI and TX	Series of LK	Inflammatory potency
AA	2	4	Potent pro-inflammatory
EPA	3	5	Weak pro or sometimes anti-inflammatory
DGLA	1	3	Weak pro or sometimes anti-inflammatory

Table 1.1 Table to show the series of prostanoid and leukotriene (LK) generated from the 3 PUFA pre-cursors and the potency of the inflammatory response produced by the creation of each.

Within each series of prostanoids many of the same class of prostanoid exist, which are distinguished with ABC after their class (e.g. PGE_2, TXA_3). Table 1.1 shows the classes and series of prostanoid and the fatty acid they were derived from.

1.5.4 COX, PGE_2 and breast cancer

It has become evident that the cyclooxygenase enzyme group is involved in many tumors such as prostate, colorectal and breast. A strong correlation between regular non-steroidal anti-inflammatory drug (NSAID) use, which inhibit the cyclooxygenase enzymes, and a reduced risk of colorectal, breast and lung cancer development has also been noted (Liu, C.H., *et al.* 2001).

Both COX-1 and COX-2 isoforms of the enzyme have been found to be expressed in solid tumors, however, addition of selective inhibitors of the two isoforms suggested that only COX-2 contributes to malignant behaviour, as selective COX-1 inhibitors gave no effect on tumor size and grade (Kundu, N. & Fulton, A.M. 2002). It has been widely reported that COX-2 is over-expressed in tumors of the breast, prostate and GIT; this over expression is associated with high tumor grade (Larkins, T.L., *et al.* 2006). The over expression of COX-2 and thus accumulating concentrations of prostaglandins have been suggested to mediate many tumorogenic mechanisms, such as proliferation, angiogenesis and avoidance of apoptosis (Costa, C. *et al.* 2002). In fact, it is now understood that COX-2 overexpression in tumors plays an important role in metastasis and the development of resistance (Dandekar, D.S. & Lokeshwar, B.L. 2004). Various studies have shown this link between up-regulated COX-2 and tumorigenesis. Soslow *et al.* (2000) investigated the expression of COX-2 in ductal carcinomas in situ (DICS), a precursor to invasive breast cancer and compared this to adjacent non-neoplastic breast tissue. They showed that no COX-2 expression was detected in non-neoplastic lesions; although there was a 56% increase in expression found in the DCIS lesion.

There is also evidence suggesting that COX-2 upregulation is not only involved in metastasis and resistance but is enough solely to induce tumorigenesis. Studies using transgenic mice that over-expressed COX-2 by using the mouse mammary tumor virus (MMTV) long terminal repeat

promoter showed that COX-2 was sufficient to induce breast tumorogenesis. This process led to the over-expression of COX-2 in mammary tissue alone and to 85% of mice developing tumors (Liu, C.H. *et al* 2001).

1.6 Metastasis

1.6.1 Extracellular matrix and cellular adhesion

The cells of most tissues remain resident within their tissue and do not possess the ability to spread to other tissues and locations within the body. Metastasis is a multi-step process by which cancer cells spread throughout the body. The process involves a large number of molecules such as growth factors, their receptors and angiogenic factors (Davidson, B. *et al* 2004). This ability of cells to migrate is the fundamental difference between benign and malignant tumors, with only the malignant variant possessing this capacity. Metastasis is the most deadly aspect of cancer and, regrettably, over 50% of malignant tumors have already metastasised at the time of diagnosis (Pecorino, L. 2005).

Malignant tumors contain both neoplastic (cancer) cells and non-neoplastic cellular components, which include macrophages, lymphocytes, fibroblasts and endothelial cells (Hagemann, T. *et al* 2004). The cellular elements of the tumor are surrounded by an extracellular matrix (ECM), and it is the interactions between the cellular and extracellular components that are fundamental in tumorogenesis (Hiscox, S. *et al* 2006).

In order to understand the mechanisms and steps of metastasis, it is first important to understand the typical cellular adhesion mechanisms, which cancer cells must overcome in order to migrate and spread to distant sites.

1.6.1.1 Cell Adhesion molecules and cadherins

Cellular interactions with the cytoskeleton are imperative for normal cell adhesion. Two main families of proteins are responsible for both same cell type (homotypic) and different cell type (heterotypic) recognition; these are the cell adhesion molecules (CAMs) and cadherins.

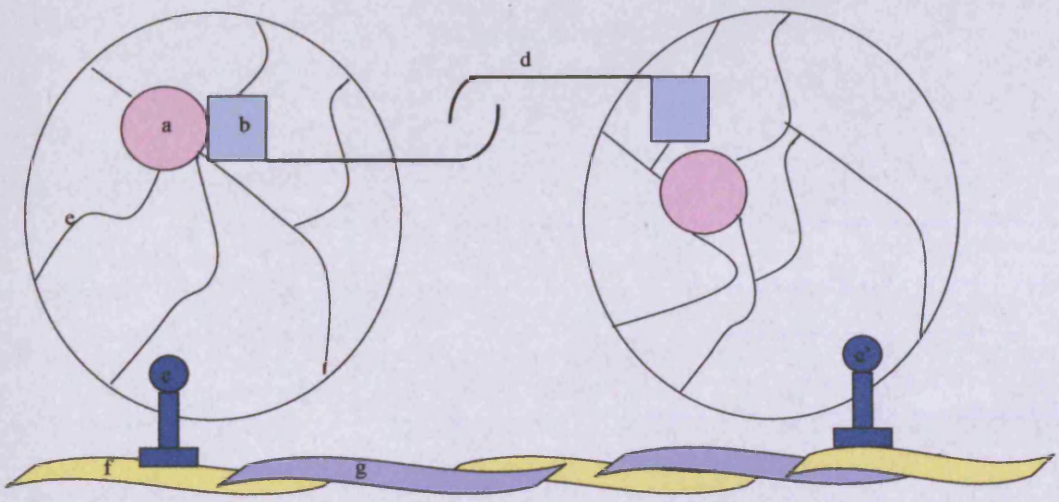

Figure 1.7 Illustration of cell anchorage to the cytoskeleton. a nucleus, b catenins, c and c' different subunits of integrin receptors, d, cadherins, e cytoskeleton, f collagen, g fibronectin.

Figure 1.7 shows the typical method and molecules involved in cell adhesion and anchoring to the cytoskeleton. Cadherins are calcium dependant glycoproteins that traverse the cell membrane. They form 'hooks' by which

cells link together. These proteins interact with catenins, also shown in figure 1.7, which, in turn interact with the cytoskeleton (Pecorino, L 2005).

1.6.1.2 Laminin

Laminin is a component of the ECM and the major non-collagen element of the basal lamina. Laminin molecules have high affinity for other laminin molecules, forming the sheet structure of the basement membrane on which epithelial cells sit (Haralson, M.A. & Hassell, J.R. 1995). Cellular attachment to laminin is a crucial step involved in local and vascular invasion (Davidson, B. *et al* 2004). Laminin receptors can be divided into two distinct categories: integrin and non-integrin receptors.

Integrin receptors, shown in figure 1.7, are responsible for interactions between the cell and the ECM. They also mediate intracellular signal transduction. They are a family of heterodimers made up of a variety of α and β subunits, the assembly of which allows for the recognition of different components of the ECM including fibronectin, collagen and laminin. Upon ligand binding, these integrin receptors cluster and allow actin binding proteins and kinases such as focal adhesion kinase to interact with the cytoskeleton. Several studies have shown that focal adhesion kinase may affect motility of cells by recruiting Src and activating the RAS signalling pathway. Altered integrin receptor expression may promote metastasis by allowing adherence to different ECMs or by modifying the distribution of the receptors. However, in most cancers,

the precise role of integrins in metastasis is still unclear, with the receptors being up regulated in some cases and down regulated in others.

Non-integrin receptors mature from the homodimerisation of two molecules and or the heterodimerisation with an unknown protein to yield a 67KDa receptor (Menard, S. *et al* 1997). The non-integrin lamanin receptor is upregulated by cytokines, and ECM proteins such as fibronectin and laminin and is expressed in a wide array of malignancies (Menard, S. *et al* 1998).

1.6.2 Matrix Metalloproteinases

Matrix metalloproteinases (MMPs) are a family of zinc dependent metalloendopeptidases that are secreted or membrane bound proteins that are involved in the majority of ECM turn over (Birkedal-Hansen, H. *et al* 1993). They are responsible for cleaving many ECM components such as gelatin, fibronectin, elastin, collagen and laminin (Low, J.A. *et al* 1996). MMPs are normally regulated tightly due to being synthesised as latent enzymes and needing proteolytic cleavage to become activated. Endogenous tissue inhibitors (TIMPs) also regulate the function of these proteases (Pecorino, L. 2005). EMMPIN (extracellular matrix metalloproteinase inducer) also regulate MMP expression. Stimulation by EMMPIN is known to upregulate MMP-1, MMP-2 and MMP-3 (Kataoka, K. *et al* 1993). EMMPIN is also capable of binding MMP-1 to the tumor cell surface and is known to co-localise with integrin receptors at the cell membrane (Guo, H. *et al* 2000, Berditchevski, F. *et al* 1997). MMPs are often over activated in tumor cells or in surrounding

stromal cells, enabling breakdown of ECM components and of the basement membrane (Hagemann, T. *et al* 2004). It is understood that MMP-2 and MMP-9 are the key proteases involved in this process (Reich, R. *et al* 1995).

1.6.3 Steps in metastasis

1.6.3.1 Intravasation

As suggested before, the process of metastasis is a multi-step one, illustrated in figure 1.8. Intravasation is the process by which tumor cells attach to the stromal side of the blood or lymphatic vessel, degrade the basement membrane (only present in blood vessels) migrate transendothelially into the blood stream or lymph.

1.6.3.2 Cell transport

The tumor cells are then transported to distant body sites via these two systems. In the blood, they can travel as lone cells or as emboli (groups of cells) in one direction only i.e. the direction of the blood. The specificity of metastatic site is not only due to cell surface receptors, which are specific to some organs and are responsible for the seed and soil theory. A phenomenon called first pass organ also influences the site of metastatic spread. In breast cancer blood flows through the superior vena cava to the lung, therefore the lung is often a site for metastasis in breast cancer. The lung also receives lymphatic drainage from the breast, which also enhances the potential of metastasis to this site (Pecorino, L. 2005).

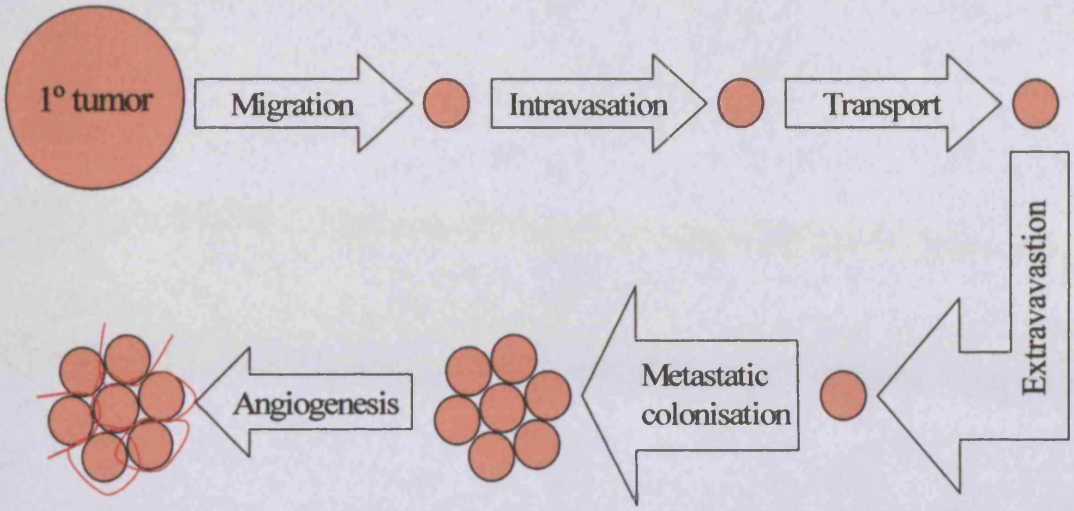

Figure 1.8 A flow chart-type diagram to show the stages of metastatic spread of cancer cells. Adapted from Pecorino, L. 2005.

1.6.3.3 Extravasation

Extravasation is, in effect, intravasation in reverse. It involves the tumor cells attaching to the endothelial side of the vessel, insert through the basement membrane and migrate into the surrounding stromal environment. Calcium dependant specialised adhesion molecules are present on the endothelial cells, which aid the process of extravasation by cancer cells. These molecules are called Selectins and are thought to be, in part, responsible for the seed and soil theory mentioned previously.

1.6.3.4 Metastatic colonisation

Metastatic colonisation goes hand in hand with angiogenesis, without continuous expansion of a capillary network to supply oxygen and nutrients to

the cancer cells; the secondary tumor would not grow. In this instance proliferation and apoptosis would balance out and the secondary tumor or micrometastasis may lay dormant for many years.

A new class of genes have been discovered that encode metastasis suppressors. These suppressors are expressed at an alarmingly low level in metastatic tumor cells when compared with non-metastatic tumor cells and so their loss of function may be key in the induction of metastasis (Pecorino, L. 2005).

1.6.3.5 Angiogenesis

A crucial step in metastasis is the formation of new blood capillary networks to provide tumor cells with oxygen and nutrients, a process called angiogenesis. If the rate of blood vessel formation is not sufficient, distant metastasis cannot grow and so remain a micrometastasis. Angiogenesis hinges on a balance between pro- and anti-angiogenic factors such as proteolytic factors, growth factors, cytokines and chemokines. An increase in inducers or decrease in inhibitors could tip the balance and turn on angiogenesis.

1.6.3.6 c-Src

This protein belongs to the Src family of non-receptor protein tyrosine kinases, which play a variety of critical roles in cell physiology including proliferation, adhesion, angiogenesis and survival (González, L. *et al* 2006). There are eleven members of the Src kinase family; Fyn, Yes, Lck, Hck, Blk, Lyn, Src, Fgr, Brk, Frk and Yrk (Roskoski, R. 2004). Their structures are highly

conserved, with family members containing SH4, SH3, SH2 and SH1 regions along with a short C-terminal tail, which is important for activation (Baggon, T.J. & Eck, M.J. 2004).

All Src family members have a unique SH4 domain and N-terminus that is myristoylated. The SH3 domain is the ligand-binding domain, while the SH2 domain contains protein recognition sites. The arginine at 175 is highly conserved among Src family members and confers to a phosphotyrosyl recognition pocket. The SH2 and SH3 domains are responsible for protein/protein interactions. The SH1 domain is the tyrosine kinase domain and contains the ATP binding site at Lysine 295. The tyrosine residue at 416 is an autophosphorylation site (González, L. et al 2006). The C-terminus contains a tyrosine at residue 527, which regulates Src kinase activity. Phosphorylation of the residue gives an intramolecular interaction with the SH2 domain of Src leading to its inactivation via a conformational change (Thomas, S.M. & Brugge, J.S. 1997). Activation of Src family members can occur by receptor tyrosine kinases such as the EGFR. Activation and thus autophosphorylation of the EGFR allows the receptor to interact with the SH2 domain of the Src family member and disrupts the inactive conformation, allowing activation of Src. Activated Src can then phosphorylate a number of target proteins, such as transcription factors, adaptor proteins and focal adhesion proteins such as focal adhesion kinase (Pecorino, L. 2005).

Cell culture and in vivo data has shown that it is not only the enzymatic activity of the Src kinases that exerts their cellular functions. It has been demonstrated that, through the SH2 and SH3 domains, these kinases can generate complexes of signalling molecules that are involved in a diverse array of signal transduction pathways (Brunton, V.G. 2005).

1.7 Targeting tamoxifen resistant growth

Targeting downstream EGFR mediators supposes beneficial clinical results for *de novo* resistance to endocrine therapy. It may also prevent or somewhat delay the onset of acquired resistance as both of these phenotypes display elevated EGFR, HER2, IGF-IR and downstream signalling.

Quercetin and LY294002, shown in figure 1.9, are selective PI3k pathway inhibitors. Quercetin is a naturally occurring bioflavonoid found in red wine, fruit and vegetables and is especially abundant in onions (Formica, J.V. & Regelson, W. 1995). Flavonoids share a common structure of two phenol rings, which are linked by three carbons (Nanua, S. *et al* 2006). The anti-oxidant properties of bioflavanoids, such as quercetin have long been known and these properties offer cardiovascular protection by preventing low-density lipoprotein oxidation (Moon, J-H. *et al* 2000). Quercetin is known to inhibit several serine/threonine, lipid and protein tyrosine kinases including PI3 kinase (Nanua, S. *et al* 2006).

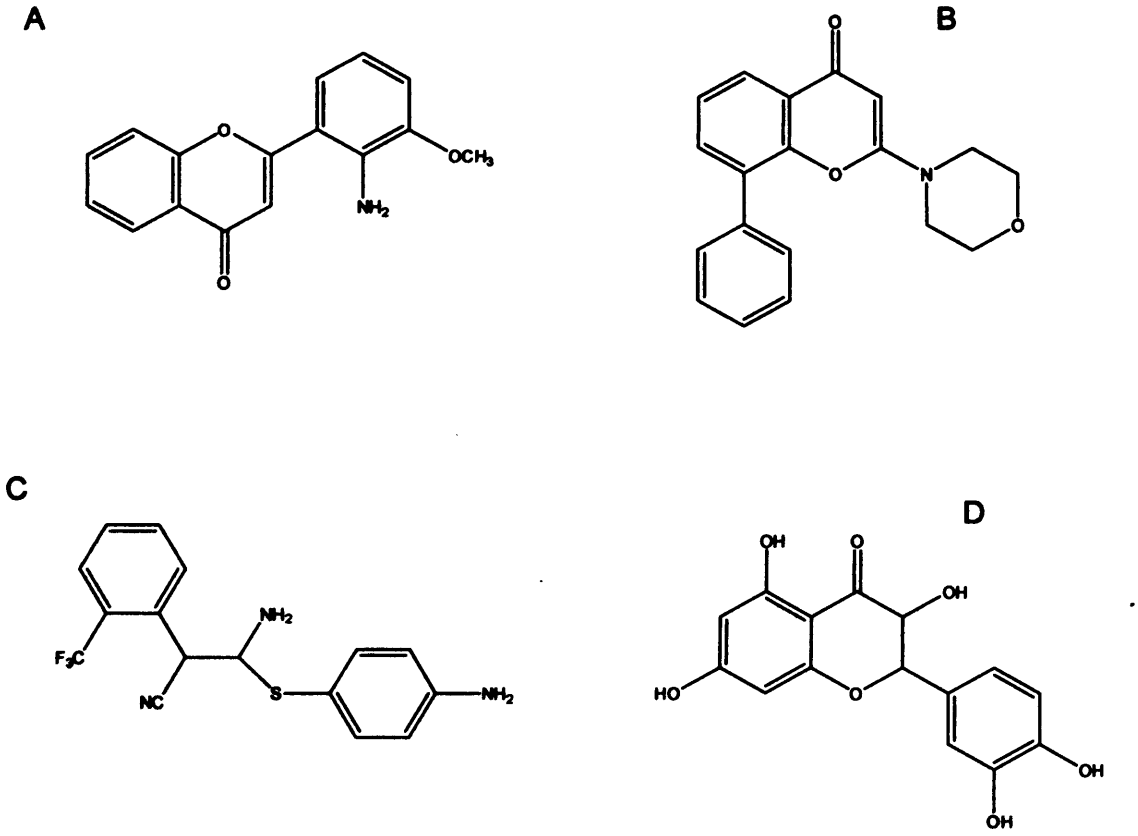

Figure 1.9 Chemical structures of PD98059 (A), LY294002 (B), SL327 (C) and quercetin (D).

LY294002 was developed from the naturally occurring bioflavanoid quercetin, which is known to inhibit PI3 kinase. LY294002 acts by competitively inhibiting the ATP binding site of PI3K, therefore preventing the transfer of the terminal phosphate of ATP to phosphoinositol and so inhibiting the formation of PIP's (Vlahos, C.J. *et al.* 1994).

PD98059 and SL327, shown in figure 1.9 are flavonoid-based compounds that possess the ability to inhibit the MAPK pathway. PD98059 exerts its MAPK

inhibitory effects without directly acting on MAPK. It gives these effects by binding to and preventing phosphorylation of MEK by cRAF or MEK kinase (Dudley, D.T. *et al* 1995). MEK is directly upstream of MAPK, thus this impedes the phosphorylation and activation of this mediator (Alessi, D.R. *et al* 1995).

SL327 also binds to and prevents the activation of MEK, thus inhibiting MAPK, however it has the ability to penetrate the blood brain barrier and reduce cortical phospho-MAPK levels (Dash, P.K. *et al* 2002). It shows selectivity for MEK, without any effects on CaMKI, PKC or PKA (Atkins, C.M. *et al* 1998). Davis, S. and colleges (2000) also reported that SL327 prevented Elk-1 phosphorylation.

Figure 1.10 summarizes the pathways targeted by the multi-pronged transcutaneous device and shows how the pathways crosstalk and overlap in tamoxifen resistance. This cross talk will be discussed later in relevant chapters.

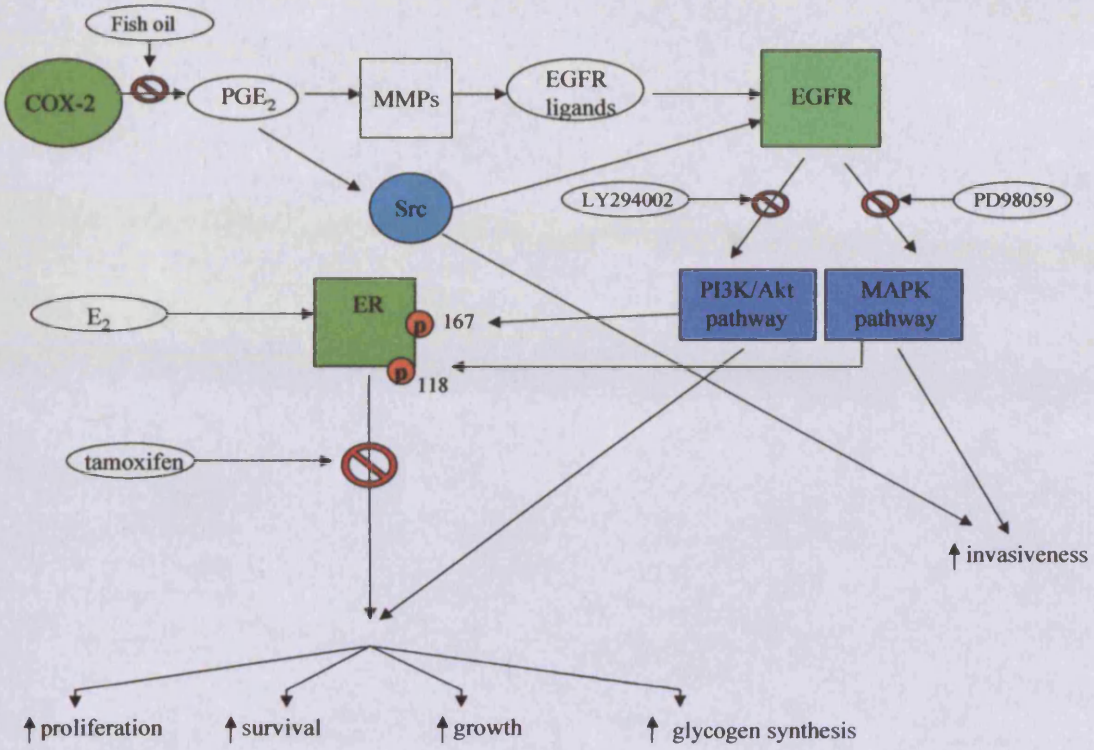

Figure 1.10 Pathways and mediators targeted in the transcutaneous device.

Oral ingestion or IV administration of such compounds is assumed to be problematic due to their non-specific nature for cancer cells and other bodily cells. This, coupled with known adverse events associated oral tamoxifen has lead to the idea of alternative delivery of cocktails of these compounds.

Transcutaneous (permeation across full thickness skin and diffusion to underlying tissue) offers such an alternative delivery route. The benefits of which shall be discussed in detail in the following sections.

1.8 The physiology of skin

The skin is the largest organ of the body, making up 12-16 % of total body mass. It presents as a complex organ and has a range of biological functions including a barrier to control or prevent the entry of chemical or microorganisms into, and water and heat loss from the body (Williams, A.C. 2003). The skin is under constant regeneration and is metabolically active. It comprises of three discrete layers, as displayed in figure 1.11. These will be discussed in the following sections from the outer most to the innermost layer.

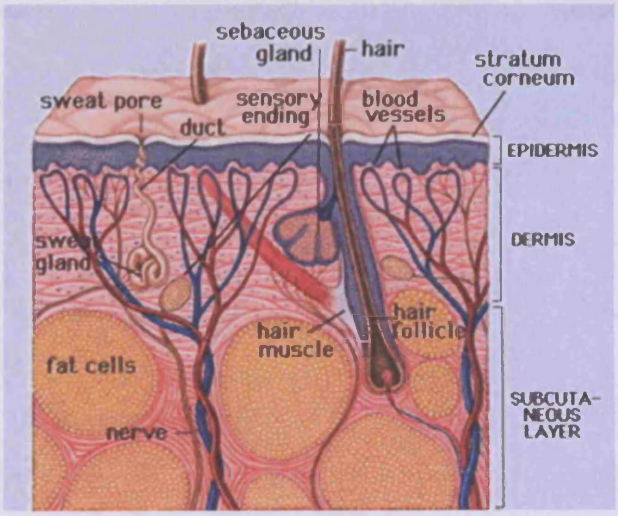

Figure 1.11 Cartoon diagram of the structure of skin (www.natural-skin-health.com).

1.8.1 Stratum corneum

The stratum corneum (SC), (figure 1.12 A), is the outermost structure of the skin and is the end result of epidermal differentiation. This layer comprises of 10-30 cell layers and is only 30-40μm thick when dry, although it can swell,

sometimes to 3 times this thickness when hydrated (Goldsmith, L.A. 1991). It is comprised of corneocytes, which are dead cornified keratinocytes and devoid of all organelles. These largely impenetrable cells have been flattened and keratinised and are tightly and embedded in an interlocking lipid matrix comprised of cholesterol, sphingolipids, fatty acids and ceramides (Charalambopoulou, G.C. *et al* 2004) however, phospholipids are mostly absent. The arrangement of the corneocytes within the lipid matrix is referred to as a wall of bricks, where the corneocytes represent the bricks and the lipid matrix represents the cement (Elias, P.M. 1983). The lipids of the SC are the exocytotic products of lamellar bodies and are suggested to give rise to the SCs remarkable barrier characteristics (Elias, P. 1988, Grubauer, G. *et al* 1989).

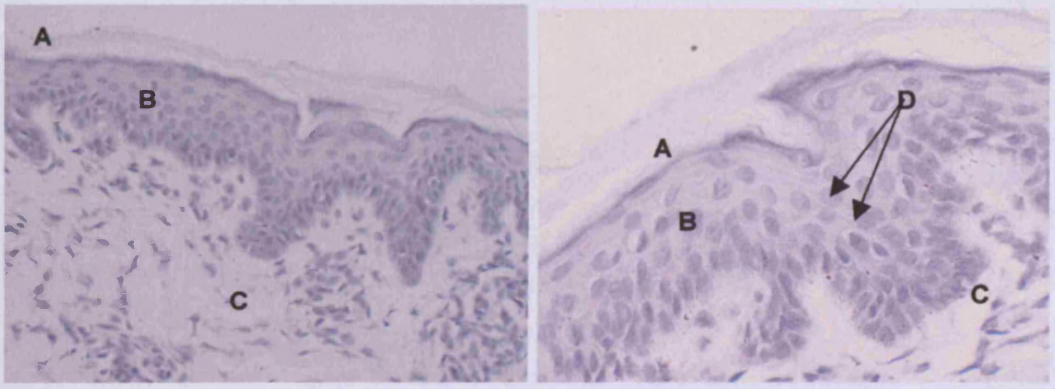

Figure 1.12 Haematoxylin staining of a cross section of freshly excised porcine ear skin using immunocytochemistry. Left is at x20 resolution and right is at x40 resolution using a Olympus BH-2 phase microscope and photographed using an integrated Olympus DP-12 digital camera system (Olympus, Oxford, UK). A. Stratum corneum (SC). B. Epidermis. C. Dermis. D. Keratinocytes.

1.8.2 The viable epidermis

The epidermis (figure 1.12 B) consists of four distinct layers: the stratum germinativum, stratum spinosum, stratum granulosum and the aforementioned stratum corneum, however the stratum corneum is often thought of as a discrete layer. The remaining 3 sub-layers make up the viable epidermis and contain the live epithelial tissue.

The viable epidermis varies in thickness at different parts of the body, with around a 10- fold variation between the thickest and thinnest. It is at its thinnest at the eyelids, where it measures around 0.06mm and it is thickest at the palms and soles, where it is 0.8mm thick. The main cell type within the viable epidermis is keratinocytes, which are produced at the stratum basale and differentiate as they migrate towards the SC, where they are continually sloughed and replaced.

This layer is enzymatically active, containing phosphatases, proteases, lipases and hydrolases (Patil, S. *et al* 1996). However this is only at around 10% of the enzymatic activity seen in the liver (Hotchkiss, S.A.M. 1998). This may seem minimal and somewhat irrelevant, although several studies have shown significant bioconversion of drugs within the skin. A study by Thomas, C.P *et al.* (2007) revealed that eicosapentaenoic acid (EPA) and docosahexaenoic acid (DHA) were significantly metabolised within the epidermis. The bioavailability of nitroglycerin post topical application was shown to be just 56.6 ± 5.8 when compared to IV administration (this event should be borne in

mind when considering transdermal or transcutaneous delivery). The dermis is devoid of blood supply therefore nutrients and waste must pass either to the cells or from them from the dermal vasculature by passive diffusion through the dermo-epidermal layer. The same phenomenon is observed with permeating compounds.

1.8.2.1 Stratum lucidum

The cells within this layer continue to flatten and start to keratinise. The nuclei of the cells also start to degrade in this layer. It is not known for certain to date whether this is in fact a separate membrane, or whether it is just the lower part of the stratum corneum.

1.8.2.2 Stratum granulosum

This layer is termed the granular layer as the cells change and take on granular features. The cells within this layer also continue to differentiate and become flattened; they also start the process of organelle degradation. Membrane coating granules are synthesised in these cells and as the cells migrate towards the surface, these granules begin to extrude and contain the precursor for the stratum corneum lipid lamellae.

1.8.2.3 Stratum spinosum

This layer is also known as the spinous layer. The keratinocytes within this layer change morphologically from those of the stratum germinativum. They become polygonal rather than columnar and begin to differentiate. The cells

within this layer also produce tonofilaments, which condense and make up the desmosomes. It is the role of the desmosome to maintain an equal distance of around 20nm between each keratinocyte.

1.8.2.4 Stratum germinativum/basale

The cells within this layer are metabolically active (germinative) and are histologically similar to cells in other tissues, in that they contain all the normal organelles such as mitochondria and a nucleus. These cells have been shown to produce pro-inflammatory cytokines (Barker, J.N.W.N. *et al* 1991).

The keratinocytes are anchored to the basement membrane or basale lamina by specialised proteinaceous structures termed hemidesmosomes. The cells within the stratum basale are the only cells within the epidermis, which are under constant mitosis, and, in fact, only half of these cells progress onto differentiation, while the other half remain intact to the basement membrane and continue mitosis. Melanocytes are also present within the stratum basale. These are specific cells that synthesise the pigment melanin. Melanin is passed from melanocytes to keratinocytes via dendritic connections. Situated on the dermal side of the basement membrane, there is another specialised cell type, termed the Merkel cell. This cell is fairly specific to the touch-sensitive parts of the body and so is thought to be involved in cutaneous sensation. Langerhans cells, which are the major antigen presenting cells of the skin and also free radical scavengers, are also found in the stratum basale. They are dendritic structures, which are connected to keratinocytes via these processes.

1.8.3 Dermis

The dermis, shown in figure 1.12 C is the major component of the skin in terms of size, measuring between 3 and 5 mm thick. The main structural component of the dermis is a connective tissue network consisting mainly of collagen fibrils and elastic tissue, which provide support and flexibility respectively. These are embedded in a mucopolysaccharide gel, which collectively provides this component of the skin with a hydrophilic nature; this provides an environment more suitable to the permeation of hydrophilic molecules and may hinder the permeation of lipophilic permeants. The dermis is also infiltrated with blood and lymphatic vessels, along with nerve endings. There are also appendageal structures within the dermis, such as hair follicles, sebaceous glands, sweat glands, nerve endings as well as blood and lymphatic vessels, shown in figure 1.11.

1.8.4 Hypodermis

The hypodermis, shown in figure 1.11, is an adipose layer, which acts as a connection between the dermis and underlying body organs and tissues. The main role is to act as a biological shock absorber to protect the organs from physical impact and to insulate the inner constituents of the body from extreme temperature changes. The hypodermis also contains the primary blood vessels and nerves of the skin. The layer of adipose provides the body with energy providing molecules, which are readily available when the body requires them.

1.9 Routes of drug delivery

The most common types of drug administration are oral (p.o) intravenous (i.v). Administration via these two routes means that the drugs either enter directly into the systemic circulation or high quantities of the administered dose diffuse into it via the GI tract.

Topical administration, whereby drugs or other products are applied to the SC surface, can have the benefit of being applied directly to the 'site of action'. An example of this is NSAID formulations for muscle pain, which prove to be a competitive alternative to oral preparations. Also topical drug delivery avoids the 1st pass effect, which can hugely reduce bioavailability of orally administered drugs that undergo extensive and somewhat unwanted metabolism by the liver. Thus lower dosages can be given, which in turn means that any coinciding toxicity could be reduced. Thirdly, topical administration overcomes the problem of pulse dosing, ensuring that the concentration of drug at the site of action lies steadily in the therapeutic window. This again reduces the chances of toxicity associated with overdose and ensures that therapeutically active concentrations remain at the site of action.

When discussing drug administration via the skin, 3 main routes should be considered. Conditions requiring the drug to remain on the skin surface or within the skin itself require minimal permeation through the skin to underlying tissues, whereas condition requiring the drug to diffuse through the

skin and either enter the systemic circulation or pass through to underlying tissues should be formulated in such a way to allow maximum penetration of the skin, including passage through the SC. All three methods of drug administration will be discussed in detail in the following sections; however, all three require successful partition of drug into and passage through the SC. With this in mind, the routes of entry into and channel through the SC shall be discussed first.

1.9.1 Passage through the stratum corneum

There is no evidence of active transport within the skin, therefore entry to compounds must be passive. Permeants may enter via the appendages of the skin; the hair follicle channel or sweat gland. These routes are termed shunt routes. There is still much debate in skin and drug delivery research as to the extent that these two routes contribute to total permeation. This is suggested to be due to the relatively sparse occurrences of these openings in human skin compared many animal counterparts (Roberts, M.S. 2002).

Conflicting reports are found in the literature. One study shows that radiolabelled pesticides were more significantly recovered in the urine of humans when the application site was the head rather than the less hairy forearm (Maibach *et al* 1971). However, another study showed that this route was significant for the permeation of mannitol, a hydrophilic compound but had negligible contributions to the permeation of estradiol, a lipophilic compound (Essa, E.A. *et al* 2002).

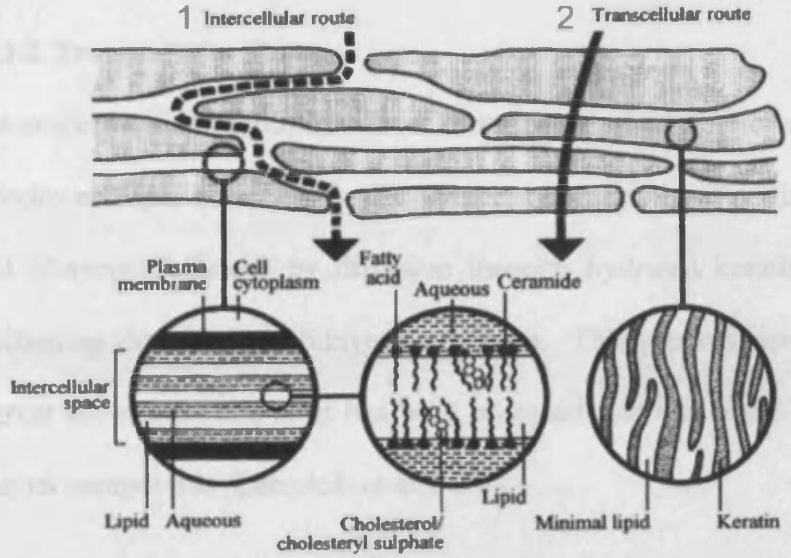

Figure 1.13 Routes of permeation (Moghimi HR Williams AC and Barry BW. Stratum corneum and barrier performance; a model lamellar structural approach. In: Bronaugh RL and Maibach HI. (Eds.) *Percutaneous Absorption.* Marcel Dekker, New York (1999) 515-553)

The final two routes of permeation through the SC are shown in figure 1.13 and described in the next sections.

1.9.1.1 Intercellular Route

The intercellular route is now accepted as the main route of SC penetration for most small non-charged molecules. The lipophilic nature of this region allows moderately lipophilic permeants to penetrate most readily compared to highly lipophilic or hydrophilic molecules. The lipid bilayers within the SC are unique to this site of the body and are present in several states ranging from fluid to solid. It has been suggested that the more fluidic areas allow passage of permeants (Forslind, B. 1994).

1.9.1.2 Transcellular Route

This route provides the most direct route across the SC. However, this route provides multiple obstacles for the permeant in the form of partitioning through lipid bilayers, followed by diffusion through hydrated keratin, followed by partitioning through lipid bilayer once more. This process would be repeated in great succession and so it has been accepted that this route is not followed by most compounds (Lee, A.J. *et al* 1996).

1.9.2 Dermatological formulations

Such formulations are focused on retaining the drug(s) in question within the layers of the skin where they exert a local effect on or in the skin. In many conditions requiring such formulations, such as psoriasis, athletes foot, eczema and burns the SC is compromised and so it becomes difficult to maintain the drug in the desired location, without permeation through and into the systemic circulation. Many mechanisms have been explored to avoid this behaviour; one successful method is the use liposomes. Liposomes are defined in the oxford medical dictionary as 'an artificial vesicle composed of one or more concentric phospholipid bilayers and used especially to deliver microscopic substances to body cells. As the name suggests, the lipophilic liposomes can overcome the SC barrier with relative ease, however cannot partition into the more hydrophilic viable epidermis with such ease. This means that the liposomes accumulate in the SC where they release their encapsulated drug.

Due to the penetration enhancing effects of alcohols and other solvents, dermatological formulations often avoid such ingredients to minimise permeation through the skin.

1.9.3 Transdermal delivery

Transdermal delivery necessitates the permeation of the drug in question through the SC and epidermis into the dermis where it can diffuse into the projecting blood vessels and enter the systemic circulation. From here it can circulate to the site of action. An example of such a preparation is the nicotine patch, where formulated nicotine enters the circulation at the site of application of the patch (usually the arm) and exerts its pleasure-inducing effect in the brain.

1.9.4 Transcutaneous delivery

The aim of transcutaneous delivery is for the drug(s) in question to permeate the lipophilic SC, the more hydrophilic viable epidermis and then partition into the dermis, where it by-passes uptake into blood vessels and so into the systemic circulation and passes into underlying tissues. There are two causes for concern, which may limit transcutaneous delivery; firstly, the drug must be formulated in such a way so that it can permeate both lipophilic and hydrophilic environments, and secondly, the rate of permeation must exceed the rate of clearance by the dermal vasculature to ensure that a certain proportion of the drug reaches underlying tissues.

1.9.5 Permeation enhancement strategies

Often, the desired permeant does not permeate the skin at a sufficiently high rate to be therapeutically useful. Therefore, permeation enhancement strategies are employed to increase the amount of compound able to penetrate the SC. Enhancement may be by either chemical means, by which solvents or other chemicals can be included into the formulation to disrupt the barrier function or by physical means, such as iontophoresis or ultrasound or by bypassing the SC completely via the use of microneedles. Chemical permeation enhancers (CPEs) are added to a drug formulation to increase flux.

1.9.5.1. Sulfoxides

Sulfoxides are a much-studied group of CPEs of which dimethyl sulfoxide (DMSO) is most well known. DMSO is a widely used and studied aprotic industrial solvent. Upon its introduction by Dr Stanley Jacobs in 1963 it was hailed as super solvent, having many pharmacological and therapeutic characteristics (Schaffer, T.E & Pruitt, A.W. 1983). It was envisaged that due to the ability of DMSO to penetrate intact skin, the 'dragging' of a variety of chemicals would replace injections. It was also imagined that its ability to inhibit prostaglandins would lead to an anti-inflammatory treatment. However clinical research was suspended in 1965 due to lens damage seen in animal studies and since this date the use of DMSO has mainly been restricted to use as a scientific tool and industrial solvent. DMSO is now widely established as a CPE and is an effective enhancer for both lipophilic and hydrophilic compounds. It partitions into the stratum corneum and disrupts its barrier

properties, which at low concentrations is said to be a reversible event (Williams, A.C 2003). Fourier transform (FT) Raman spectroscopy has shown that DMSO is capable of transforming stratum corneum keratin to β sheet conformation from an α helical structure. Solutions of 60% and above DMSO enhance permeation by not only protein alterations but by changing SC lipid organization and affecting partitioning of compounds, effects which are not reversible (Anigbogu, A.N.C. *et al* 1995).

1.9.5.2 Terpenes

Terpenes, exemplified by 1,8-cineole have been accepted as permeation enhancers and as fragrances for topical formulations. They enhance permeation by affecting SC lipids. They have been shown to alter transition temperatures of SC lipids, rendering more areas fluidic in state (Narishetty, S.T. & Panchagnula, R. 2005). It is also suggested that hydrocarbon terpenes increase permeation by increasing the diffusivity of the SC lipids, whereas cyclic terpenes act by increasing the partitioning of solute into the skin.

1.9.5.3 Alcohols

Alcohols, such as methanol and ethanol can increase the solubility of solute so increase its partitioning into the skin. They can also affect the skins permeability to the solute irreversibly due to its entry and passage through the skin by extracting lipids from the stratum corneum membrane and so increasing the passage of the permeant through this barrier (Oh, S.Y. *et al* 2003).

1.9.5.4 Fatty acids

Fatty acids can enhance the permeation of both lipophilic and hydrophilic compounds. They are thought to intercalate with the lipid bilayers and exist in separate phases or pools within this. These pools are thought to provide a permeability route for compounds.

1.9.5.5 The Pull or Drag effect

Recent attention has been focused on the pull effect as a viable explanation of the enhancing properties of solvents or fatty acids. It is suggested that the close relationship between the permeation of mefenamic acid and ethanol/1,8-cineole was attributed to the pull effect and not the effect on the SC (Heard, C.M., *et al* 2006). Studies using heat separated membranes devoid of SC saw ethanol giving the same permeation enhancement as seen with full thickness skin, thus suggesting effects on SC lipids was not the reason for permeation enhancement (Heard, C.M., *et al* 2007). Fish oil has also been shown to increase the permeation of ketoprofen in a similar manner (Thomas, C.P. *et al* 2007).

1.10 *In-vitro* models of topical drug delivery

The Franz diffusion cell is the standard method for determining permeation or penetration across a skin membrane, and so all permeation studies throughout this thesis were carried out using all glass Franz diffusion cells.

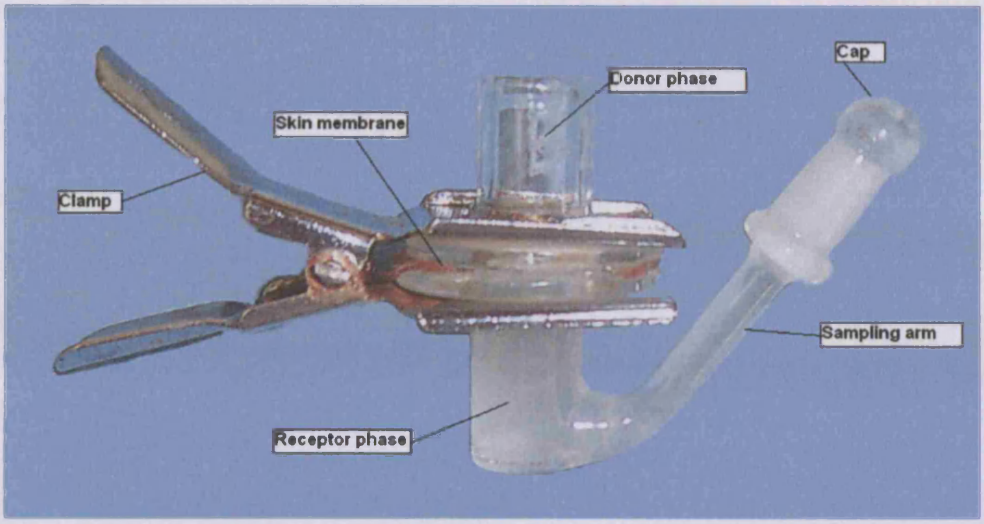

Figure 1.14 An all glass Franz diffusion cell.

These are displayed in figure 1.14 and consist of 2 separate chambers, a receptor (lower) compartment, on which the skin membrane sits stratum corneum up and the donor (upper) compartment. Mating flanges of the two compartments were lined with high vacuum silicon grease (Dow Corning, UK) and the two compartments clamped to minimise leakage.

1.10.1 Choice of skin membrane

Full thickness excised porcine ear skin was used throughout this thesis due to the lack of availability of human skin samples. Porcine skin this provides the most comparable model of human skin (Sekkat, N. *et al* 2002). A noted difference between fresh porcine skin and frozen skin has been established; therefore, fresh skin was used throughout all permeation studies.

1.10.2 Receptor solution

The choice of receptor phase is of utmost importance when designing *in vitro* permeation studies. It must provide a suitable sink in which permeants should be soluble, without modulating the barrier function. To ensure that no retardation of the flux occurs due to an imbalance of the concentration gradient, the permeating species should not exceed 20% of its solubility in the receptor phase. A micro stirrer bar is included to constantly agitate the receptor phase and to mimic the effect of dermal clearance. The receptor phase should exert no effect on the membrane, which would alter the permeation of the permeants in question and should, as much as possible, mimic the *in* vivo situation. Many different solutions have been used as receptor solutions, including ethanol, bovine serum albumin (BSA) and cetrimide. The use of BSA as a receptor phase is currently being scrutinized due to its keratinocyte toxicity (Haberland, A. *et al* 2006).

A recent study has shown that cetrimide does not give rise to any adverse effects on the skin membrane and does not affect the flux of permeants (Morris, A.P. 2003). This receptor phase has also been shown to behave in a similar way to the traditional octanol/water receptor phase (Heard, C.M. *et al* 2002).

1.10.3 Measurements of flux, lag time and k_p

1.10.3.1 Flux

The flux of a permeant is a measure of the mass of a compound permeating per unit area per unit time. It is calculated as the gradient of the linear portion of the permeation profile and is typically measured in $\mu g\ cm^{-2}\ h^{-1}$.

1.10.3.2 Lag time

Lag time is a measure of length of time taken to reach steady state flux. The linear portion of the permeation profile is extrapolated to the x axis in order achieve this value. Lag time is usually measured in hours.

1.10.3.3 Permeability coefficient, k_p

K_p is the permeability coefficient and is derived from using the flux and concentration in the donor phase by using Ficks first law equation 1.1

$$K_p = \frac{\text{flux } (\mu g\ cm^{-2}\ h^{-1})}{\text{Concentration in donor phase } (\mu g)}$$

Equation 1.1

The K_p thus has units of $cm^{-2}\ h^{-1}$ and is a measure of the conductance of skin to a particular permeant (Degim, I.T. 2005).

1.11 Topical delivery of breast cancer therapeutics

Currently, chemotherapy for ER+ breast cancer relies on oral or iv administration of compounds. Complex tablet regimes are often given, which

include; tamoxifen, an aromatase inhibitor and fulfestrant. A transcutaneous device that could deliver combinations of these compounds would provide benefit to the patient, allowing dosing every 1-2 days, with minimal discomfort.

1.12 Aims and objectives

The objectives of this thesis was to test the hypothesis that the combination of tamoxifen and two signal transduction inhibitors downstream of the EGFR could be delivered across skin and be efficacious in the transcutaneous treatment of both tamoxifen sensitive and resistant breast cancer.

Associated aims of this project were:

1. To select signal transduction inhibitors based on their skin permeation and anti-breast cancer activities.
2. To formulate these with tamoxifen or its metabolite to give maximal skin penetration.
3. To investigate the simultaneous effects and biological efficacy of these compounds on breast cancer cell lines
4. To examine the possibility of trans-mammary papilla delivery

Chapter 2

Materials & Methods

The following sections describe all the general materials and methods; however, the details involved in each method are expanded upon in each chapter where necessary.

2.1 Materials

PD98059 and LY294002 (99.8% HPLC) were purchased from Promega UK, Southampton, UK. Super-strength fish oil capsules were purchased from a local Boots store.

Hanks balanced buffered salt solution (HBBSS), HEPEs, gentamycin sulphate, sodium bicarbonate PBS, PBS + 0.02% TWEEN, sodium citrate, citric acid, methyl green, copper sulphate, paraffin wax pellets, 30% hydrogen peroxide solution, sodium hydroxide, hydrogen chloride, acrylamide/bis-acrylamide 29:1 (30% v/v solution), activated charcoal, ammonium persulphate (APS), ampicillin, aprotinin, bovine serum albumen (BSA), crystal violet, di-thiothreitol (DTT), ethylene diamine tetraacetic acid (EDTA), ethylene glycol-bis(2-amino-ethylether)-N,N,N',-tetraacetic acid (EGTA), fibronectin, glycine, leupeptin, N,N,N',N'-tetramethylene-diamine (TEMED),phenylarsine oxide, phenylmethyl sulphonyl fluoride (PMSF), polyoxyethylene-sorbitan monolaurate (Tween 20), ponceau S solution (0.1% w/v in 5% acetic acid, sodium azide, sodium chloride (NaCl), sodium dodecyl sulphate (SDS), sodium fluoride, sodium molybdate, Tris HCl, triton X-100, 17β estradiol (98% HPLC), tamoxifen (99% HPLC), 4-hydroxytamoxifen (98% HPLC), SL327 (98% HPLC), quercetin (98% HPLC), fulvestrant/faslodex (98%

HPLC), 1,8-cineole and cetrimide were from Sigma-Aldrich Company Ltd, Poole, England.

Total and phospho-ERK 1/2 primary antibody, total and phospho-Akt primary antibodies, rabbit total COX-2 primary antibody, mouse phospho-ER 118 monoclonal antibody total and phospho Src antibodies and activated ERα 167 antibody were from Cell Signalling Technology, New England Biolabs, Hitchin, UK.

NeoMarkers total EGFR primary antibody was from LabVision products, Chesire, UK.

HRP labelled anti-rabbit and anti-mouse EnVision™+ system, peroxidase (DAB kits, normal goat serum, liquid DAB$^+$ substrate chromagen system, Ki-67 primary antibody, normal goat serum, normal rabbit serum, total ER clone ID5 mouse antibody and delimiting pen were from Dako UK, Ely, England.

Ethanol, xylene, Whatman filter papers (45μ), Whatman parafilm, high vacuum silicon grease, Corning Standard Transwell inserts 6.5 diameter and 8μm pore size, disposable plastic cuvettes, glycerol, sucrose and chloroform were from Fisher Scientific UK, Loughborough, England.

BioSource phospho-EGFR 1068 primary antibody, amphoteracin B (fungizone), antibiotics (streptomycin and penicillin), RPMI 1640, phenol free

RPMI, L-glutamine, trypsin/EDTA x10 solution and FCS were from Invitrogen Life Technologies, Paisley, UK. Tissue culture plasticware was from Nalge Nunc International, Roskilde, Denmark. Bio-Rad protein assay reagents, lower buffer for SDS-PAGE (tris 1.5M pH 8.8) and upper buffer for SDS-page (tris 0.5M pH 6.8) were from Bio-Rad Laboratories LTD, Hemel Hempstead, UK.

Bromophenol blue and glass coverslips (thickness no2 22mm^2) were from BDH Chemicals LTD, Poole, UK. Cell scrappers and universal containers were from Greiner Bio-One LTD, Gloucestershire, UK.

Chemiluminescent Supersignal® West HRP substrate (pico, dura and femto) were from Pierce and Warriner LTD, Cheshire, UK.

Coulter counter counting cups and lids and sterile, disposable serological pipettes (5, 10 and 25 mL) were from Sarstedt AG and Co, Nümbrecht, Germany. Nitrocellulose transfer membrane (Protran® BA85; 0.45µm pore size was from Schleicher and Schuell, Dassel, Germany. Syringe needles were from Sherwood-Davies and Geck, Gosport, Hampshire, UK.

Syringes were from Becton Dickinson (BD) UK LTD, Oxford, UK. X-ray film developer and film fixative solutions were from X-O-graph Imaging System, Tetbury, UK. Kodak MXB autoradiography film (blue sensitive) was from Genetic Research Instrumentation (GRI), Rayne, UK. Di-butylpthalatexylene (DPX) was from Raymond A Lamb LTD, Eastbourne, UK.

Parental MCF-7 cells were a gift from AstraZeneca, Macclesfield, UK. Porcine skin was obtained from a local abattoir.

2.2 Methods

2.2.1 *In-Vitro* permeation studies

2.2.1.1 Preparation of *ex-vivo* porcine skin membrane

Porcine ears were excised from freshly slaughtered animals and, as soon as practicable, immersed in iced HEPES modified Hanks balanced buffered salt solution (HHBBSS) during transportation to the laboratory to maintain viability (Morris, A.P. 2003, Thomas, C.P. *et al* 2007). On arrival to the laboratory (usually < 1 h post excision) the ears were washed under running water to remove dirt. The epidermal membranes were then liberated from subcutaneous material and cartilage by blunt dissection whilst being continually bathed in HHBBSS. Skin was patted dry and hairs were removed using electric clippers. The skin was cut into 2 cm^2 samples and used immediately.

2.2.1.2 Preparation of receptor phase for *in vitro* permeation studies

To provide an adequate sink for the lipophilic permeants in this work a receptor phase of 30mgml^{-1} cetrimide solution was used. This was made up in de-ionised water was used for all *in vitro* permeation studies throughout the work in this thesis.

2.2.1.3 *In-vitro* transcutaneous delivery

The volume of the receptor phase and the diffusional area were pre-determined in order to calculate accurate permeation measurements. The chosen receptor phase was degassed prior to use to minimize air bubbles, which would have a detrimental effect on the flux of the permeants due to changes between liquid air phases. This was subsequently injected into the receptor compartment via the sampling arm. The complete Franz cell was placed onto a Variomag submersible stirrer plate (Thermo Fisher Scientific, MA, USA) and set in a Clifton unstirred water bath (Nickel Electronics LTD, Weston-super-Mare, UK). This was set to 37 °C to give a skin surface temperature of 32 °C (Bronaugh, R.L *et al* 1982) and the Franz cells were left for 30 minutes prior to dosing to equilibrate at the aforementioned set temperature. A constant concentration gradient was maintained and stagnant diffusion layers were overcome with the addition of a micro stirrer bar.

The Franz cells were dosed after equilibration with the test or control permeant and this time was so called time 0. The donor phase was occluded with Whatman Parafilm to mimic a transdermal patch system. At times 3, 6, 12, 24

and 48 h whole receptor compartment samples were taken and analyzed for permeants via reverse phase HPLC. The receptor compartment was then re-filled with fresh pre-warmed cetrimide solution (30 mg mL^{-1}) until the next sample time.

2.2.1.4 HPLC - Mobile Phase Development

Standards of known concentrations of tamoxifen, PD98059, LY294002, quercetin and SL327 were dissolved in DMSO and analysed using reverse phase HPLC. All analysis was carried out using an Agilent 1100 series automated system with Chemstation software. Samples were separated using a Luna C18 ODS 150 x 4.6 mm, 5 μm column (Phenomenex, Hurdsfield, UK).

A gradient mobile phase of 80:20 methanol:water to 70:30 methanol:water over a time of 20 minutes and detection at 254nm proved successful for the analysis of these two structurally similar compound as it gave good separation of PD98059 and LY294002. Under these conditions the retention times of PD98059 and LY294002 were 14.5 and 16.5 minutes respectively. The mobile phase described for the analysis of PD98059 and LY294002 was used for the analysis of quercetin, which, under these conditions had a retention time of 6.7 minutes. This method did not give adequate separation of SL327. The analysis of SL327 used a mobile phase of 90:10 methanol:water with 0.1% acetic acid, where SL327 had a retention time of 7 minutes. A mobile phase of 80:20 methanol:water with 0.02% v/v TFA was used for the analysis of tamoxifen and 4-hydroxytamoxifen. Run time was 10 min and detection was

at 240 nm. Under these conditions tamoxifen and 4-hydroxytamoxifen had retention times of 6.9 and 4.7 min respectively. Standard solutions (prepared in receptor phase) provided linear responses with $r^2 = 1.000$.

2.2.2 Cell culture

2.2.2.1 Routine cell culture/maintenance

All cell culture procedures were performed in a MDH class II laminar-flow safety cabinet (BIOQUELL UK LTD, Andover, UK). MCF-7 cells are adherent epithelial breast cancer cell line, which have been derived from a pleural effusion adenocarcinoma (Knowlden, J.M. *et al* 2004). Cells were routinely cultured in RPMI-1640, which was supplemented with 5% FCS (v/v), 10U/ml and 10 μg mL^{-1} penicillin/streptomycin and 2.5 μg mL^{-1} fungizone. Cells were grown as a monolayer in T-75 cm^2 sterile plastic flasks and medium was changed every 3-4 days. Cells were maintained in a Sanyo MCO-17AIC incubator (Sanyo, E&E Europe BV, Loughborough, UK) at 37 °C in a humidified atmosphere of 5% CO_2 in air. At 80-90% confluency, culture media was removed by aspiration and 10ml trypsin/EDTA was added to detach and disperse cells. The flask was returned to 37 °C for 3-5 minutes. The detached cells were then transferred to a 25 mL Universal tube and any remaining cells within the flask were recovered with a 10mL wash with routine culture media. This was, again, transferred to the Universal tube and was centrifuged at 1000rpm for 5 minutes using a Jouan C312 centrifuge (Thermo Fisher Scientific, MA, USA). The supernatant was discarded and residual

pellet was re-suspended in fresh routine culture media and added to a sterile T-75 cm^2 flask at a ratio of 1:10 with culture media.

TamR cells were developed in-house at the Tenovus Research Center. MCF-7 cells were routinely cultured in phenol-free RPMI-1640 (wRPMI), to remove the estrogen-like effect of phenol. The wRPMI-1640 was again supplemented with 10 U mL^{-1} and 10 μg mL^{-1} penicillin/streptomycin and 2.5 μg mL^{-1} fungizone. Serum was also included at 5%; however, this was charcoal stripped, SFCS (see appendix 3 for stripping protocol) prior to use to remove any steroid hormones from the serum. The cells were also cultured in the presence of 1 x 10^{-7} M 4-hydroxytamoxifen, the more potent metabolite of the parent compound tamoxifen. The normal metabolism takes place within the liver by the cytochrome P450 enzymes (Dehal, S.S. & Kupfer, D. 1997) whereby this active metabolite is derived. This process would not occur in the *in vitro* cell culture model, for this reason it was deemed necessary to challenge the cells with the metabolite rather than the parent compound. All cell culture experiments throughout this thesis use the potent metabolite (4-hydroxytamoxifen) rather than the parent compound (tamoxifen). After 6 months of culture in the presence of 4-hydroxytamoxifen the MCF-7 cells took on a new phenotype and became resistant to and began to grow in the presence of 4-hydroxytamoxifen. It has been demonstrated that this resistant growth is driven by extreme growth factor signaling, particularly through the EGFR. The cells also take on a new morphology, displaying a spikier structure than their parental MCF-7's and become more aggressive in growth rates and

metastatic potential (Hiscox, S. *et al* 2004). Routine media change and passaging, were as stated for MCF-7 cells.

2.2.2.2 Dose response curves

MCF-7 were grown to ~70% confluency in a T-75 cm^2 sterile plastic flask and then trypsinised as described previously and set up in wRPMI plus 5% SFCS, 10U/ml and 10 $\mu g\ mL^{-1}$ penicillin/streptomycin and 2.5 $\mu g\ mL^{-1}$ fungizone at 1.5 million cells per plate in a 24 well plate. The cells were left overnight to attach to the wells. After this 24 h equilibration, 3 wells were counted to act as base counts and this time point was day 1. In order to count, cells were trypsinised to detach them from the well bottom. The 1mL of cells in trypsin were then separated into a single cell suspension using a 5mL syringe and a 25mm 23 gauge sterile needle. Stabilization of the tryspinisation was ensured with three successive 1ml additions of isoton X-100 solution (see appendix 3) into the well, which was subsequently drawn into the syringe. The 4ml of cells were then syringed into a further 6mL of isoton X-100 contained in a coulter counter counting cup. The lid of which was firmly closed and the contents of the cup were agitated gently to disperse the cells throughout the solution. The cells were counted using the Coulter Multisizer II counter, Beckman Coulter UK Ltd, High Wycombe, UK. Counts were made for 100µL of the cell suspension and were subsequently modified for 1ml. After base counts were completed cells were then treated with each compound or control (vehicle in which compounds were diluted alone). Treatments were repeated in triplicate.

Cells were re-treated on day 4 and counted on day 7 using the same method as for base counts.

This was repeated using TamR cells, however, these cells were also in the continuous presence of $1x10^{-7}$ M 4-hydroxytamoxifen. TamR cells were counted following the same time schedule and also re-treated on day 4.

2.2.2.3 Growth inhibition studies

MCF-7 cells, in log phase growth, were passaged and seeded into 24 well plates, at a density of 1.5 million per plate, on day 0. The cells were left to settle and attach to the wells overnight. On day 1 base counts were taken. Cells were counted as described in section 2.2.2.2. Cells were then treated (9x wells per treatment) with IC_{50} concentrations of test compounds or with control (0.025 % v/v vehicle in media) also on day 1. Cells were subsequently counted on days 3, 5 and 8 and re-treated on day 4. Media was removed on re-treatment, which mimicked dermal clearance.

This was repeated using TamR cells; however, these cells were also in the presence of $1x10^{-7}$ M 4-hydroxytamoxifen. TamR cells were counted following the same time schedule and also re-treated on day 4.

2.2.2.4 Cell migration assays

For migration assays, a modified 24-well plate was used to assess the migratory potential of cells. The wells of aforementioned plates were similar to those of the normal plates; however, these wells had removable Corning Standard Transwell® inserts with an 8μm pore size. On the start of each migration assay, the bottom-facing surface of the insert was coated with fibronectin (from human plasma: 1mg mL^{-1} in 0.05 M TBS pH 7.5) in PBS (1:1000). This was incubated at 37 °C for 2 h. After 2 hours incubation the inserts were allowed to air dry. This was added to mimic the normal composition of the extracellular matrix (Hiscox, S. *et al* 2005).

MCF-7, TamR and FasR cells (80-90% confluency) were passaged using the protocol outlined previously. Fresh culture media (600 μL) was applied to the underside of the coated inserts. Passaged cells were seeded into the insert onto the upper surface of the membrane at a density of 80,000 cells per well. These were then incubated at 37 °C in a humidified atmosphere of 5 % CO_2 in air for 2 days. After 2 day, media was removed from the insert and cells migrated through the membrane to the bottom surface were fixed in 3.7 % formaldehyde (in PBS) for 15 min. Cells were then washed in PBS for 5 min. The inserts were then placed into a 0.5% w/v solution of crystal violet for 15-30 min to stain migrated cells. Inserts were then washed in PBS to remove excess stain, non migrated cells were removed fro the upper surface of the membrane using a fresh cotton bud and the inserts were then left in a dust free environment to dry. Migrating cells were then counted in 7 random fields of view using and

Olympus BH-2 phase microscope integrated with an Olympus DP-12 digital camera system (Olympus, Oxford, UK).

This procedure was then repeated using TamR cells in the presence of 1 μL mL^{-1} fish oil, 25 μM PD98059, and 5 μM LY294002.

2.2.3 Immunocytochemistry (ICC)

2.2.3.1 Paraffin embedded porcine skin sections

2.2.3.1.1 Preparation of HEPES modified Hanks balanced buffered salt solution (HHBBSS)

In order to maintain tissue viability, a suitable physiological media had to be found to bathe the tissue in. It has been shown previously that HHBBSS maintained tissue viability for up to 24 h (Thomas, C.P. *et al* 2007). Hanks balanced buffered salt solution was made up in 1L of de-ionised water. It was then filtered using a vacuum filter and 45μm Whatman filter papers. Furthermore it was modified with the addition of 25 μM HEPES and adjusted to pH 7 with 1M HCL or NaOH. Sodium bicarbonate (0.35 gL^{-1}) and gentamicin sulphate (50 μg mL^{-1}) were also included. The HHBBSS was made up fresh for each experiment and was stored at 2-8 °C until required.

2.2.3.1.2 Preparation of porcine skin membrane

Full thickness excised porcine ear skin was used throughout this thesis for immunocytochemical analysis, as this provides the most comparable model of enzymatic activity of human skin (Middelkoop, E. *et al* 2004). Tissue viability is of utmost importance when studying immunocytochemistry within the tissue, and so tissue preparation was as in 2.2.1.2.

2.2.3.1.3 Diffusion cell set-up and dosing of skin

Franz diffusion cells were set up as stated in section 2.2.1.3. An equimolar (2.54×10^{-4} M) solution of test compounds in vehicle or vehicle alone was dosed onto the surface of the stratum corneum. At 3, 6, 10 and 24 h formulations were removed using a glass pipette and the skin was cleaned to remove residual formulation with a clean cotton bud. Skin was then removed from the diffusion cell apparatus and the area in which the formulation was applied was cut into 2 x 1 mm pieces and placed into labeled white fixation cassettes.

2.2.3.1.4 Fixing and embedding the skin

The white cassettes containing dosed skin were placed in 4% formaldehyde and left to fix for 24 h. Table 2.1 shows the timetable for dehydration of the skin. The skin was put through a series of 70 % to 90 % to 100 % ethanol baths to displace all the water in the skin. The skin was then put through a series of 4 xylene baths to displace all alcohol.

Solvent	Length of Time Skin left in
Formaldehyde	24 h
1st 70% ethanol	Overnight
2nd 70 % ethanol	30 min
90% ethanol	2 x 30 min
100% ethanol	2 x 30 min
1st xylene	60 min
Xylene	3x 30 min

Table 2.1 Timetable for the dehydration and alcohol displacing processes.

Post-dehydration and the ethanol displacement the pre-treated skin was subjected to a series of 3 molten wax baths. The first wax step involved the skin sitting in molten wax for 15 min; a vacuum was then applied for 10 min to remove the xylene from the skin. The skin then was left for a further 5 min without the vacuum on. The skin was then transferred to the second wax bath, where the skin was left in the wax for 10 min, the vacuum was turned on for fifteen minutes and then turned off for a further 5 min. The skin was then transferred into the third bath, where it was left in the wax for 10 min, the vacuum was then turned on for 15 min, finally the vacuum was turned off and the skin was left in the molten wax for 25 min. The lid of the white cassette case was then removed and the skin was embedded in a paraffin wax block.

2.2.3.1.5 Sectioning

The embedded skin was cut using a Shandon Finesse microtome and sections were transferred onto 1" x 3" x 1mm Surgipath pre-cleaned microslides. Sectioned skin was dried overnight at 40 °C.

2.2.3.1.6 Hematoxylin and Eosin staining of excised porcine ear skin

Pre-dried sections were de-waxed and re-hydrated through a series of xylene, ethanol and water baths, as shown in table 2.2.

Solvent	Length of Time Skin left in
Xylene	2 x 7 min
100 % ethanol	2 x 3 min
90% ethanol	2 x 3 min
70% ethanol	2 x 3 min
Water	1 x 5 min
PBS	1 x 5 min

Table 2.2 Timetable for the re-hydration process.

The sections were then incubated with a 10 % (w/v) haematoxylin solution, made up in de-ionised water for 10 min. Sections were the placed under running tap water for 5 minutes and subsequently incubated with a 1% (w/v) eosin solution, made up in de-ionised water for 10 min. The sections were

rinsed in de-ionised water to remove excess dye, air dried and sealed with a coverslip.

2.2.3.1.7 Detection of pMAPK, pAkt, pER, total ER, pEGFR, total EGFR, total COX-2 and ki-67 in excised porcine ear skin

Pre-dried sectioned skin was de-waxed and hydrated as shown in table 2.2. Endogenous peroxidases were subsequently blocked using a 3% hydrogen peroxide solution for 5 min. Excess solution was removed by 2 x 3 min washes in PBS. A heat source was then applied to unmask the antigens present within the skin. This process was specific to the detection of each protein, as shown in table 2.3.

Protein Detecting	Unmasking Process	Non-specific Protein Block	1° Antibody
p-ERK1/2	Microwaved in 1L 0.01M citrate buffer pH 6* for 30 minutes at 560 Watts. Cooled for ten minutes under running tap water	20% Normal Human Serum in PBS solution for fifteen minutes	CST rabbit polyclonal phospho-ERK1/2 kinase antibody at 1/20 in 20% Normal Human Serum in PBS overnight
p-Akt	Microwaved in 1L 0.01M sodium citrate buffer pH 6* for 1 minute at power level 10 and 9 minutes at power level 6. Cooled for ten minutes under running tap water	5% Normal Goat Serum in PBS for 5 minutes	CST rabbit anti-Akt (activated) polyclonal abtibody at 1/30 in PBS overnight
Total-ER	Pressure cooked in 2L of 0.01M sodium citrate buffer pH 6* for 2 minutes at full pressure. Cooled for 10 minutes under running tap water	20% Normal Human Serum in PBS for 10 minutes	DAKO total ER clone ID5 mouse antibody at 1/100 in PBS for 60 minutes
p-EGFR 1068	Microwaved in 1L EDTA 10mM pH8 for 1 minute power 9 and 9 minutes power level 1. Slides were left to cool for 20 minutes	PBS-Tween for 5 minutes	Biosource pEGFR 1068 rabbit primary antibody at 1/25 overnight

Total-EGFR	Enzymatic retrieval: slides warmed in 37°C in PBS for 10 minutes. Transfer into Sigma Protease P6911 (0.02% in PBS) at 37°C for 20 minutes. Reaction was stopped by running under tap water for 10 minutes. Slides were then transferred into PBS.	5% BSA in PBS for ten minutes	NeoMarkers EGFR mouse monoclonal antibody at 1/20 in PBS overnight
Total COX-2	Microwaved in sodium citrate buffer pH 6* for 30 minutes at 590W. Slides cooled in running tap water for 10 minutes	PBS-Tween for 10 minutes	NEB total COX-2 rabbit primary antibody at 1/25 in PBS overnight
Ki-67 (MIB)	Microwaved in 1L 0.01M citrate buffer pH 6* for 30 minutes at 560 Watts. Cooled for ten minutes under running tap water	10% Normal Rabbit Serum in 0.1% BSA/PBS for 20 minutes	DAKO Ki-67 (MIB) mouse Primary antibody at 1/50 in 0.1% BSA/PBS for 2 hours

Table 2.3 Table to show the unmasking process and 1° antibody type and concentration used in the detection of each protein in excised porcine skin. *For buffer recipes see appendix 1.

The sections were then washed in PBS twice for 3 min. Slides were then wiped dry, retaining moisture on the skin sections, and sections were encircled with delimiting pen to retain solution around the section. Once the waxy seal had been applied non-specific proteins were blocked as stated in table 2.3. Excess block was removed before application of the primary antibody, which was applied as stated in table2.3. The length of application of primary antibody was dependant on the protein being detected, however, incubation with 1° antibody was always at 25 °C.

The sections were then washed once in PBS for three minutes and twice in PBS-Tween for 5 min. Horseradish peroxidase (HRP) labeled secondary antibody was then applied for 2 h and was incubated at 25 °C, after which, DAB chromagen was applied for 10 min and subsequently washed off in de-ionised water. The sections were then counter-stained with a 0.5% w/v methyl green solution in de-ionised water for 5 min and washed with de-ionised water. The sections were then dried at 37 °C for 24 h and coverslips mounted using di-butylpthalatexylene (DPX), a xylene based mountant.

After sufficient time for the DPX to dry, sections were inspected on an Olympus BH-2 phase microscope and photographed using an integrated Olympus DP-12 digital camera system (Olympus, Oxford, UK).

2.2.3.2 ICC of breast cancer cells

2.2.3.2.1 Cell culture

Prior to culture, sterile TESPA coated glass coverslips were placed into 60 mm sterile plastic dishes. MCF-7 and Tam-R cells, at log phase growth, were passaged and seeded onto the coverslips at a density of 5 x 10^5 cells per dish. Cells were grown as a monolayer and upon reaching 60-70 % confluency cells were treated with control or test compounds for 3 h. The cells were then fixed according to the protein to be detected (as developed in house by the Tenovus Research Group). Table 2.4 shows the particular fixation protocol for each protein.

Protein Detecting	Fixation Method	1° Antibody	2° Antibody
p-ERK1/2	Formal Saline	CST phospho-ERK1/2 polyclonal at 1/20 in PBS for 60 minutes	DAKO rabbit EnVision HRP labeled polymer antibody for 60 minutes
p-Akt	ER-ICA	CST phospho-Akt polyclonal at 1/100 in PBS for 2 hours	DAKO rabbit EnVision HRP labeled polymer antibody for 2.5 hours
p-ER 118	2% paraformaldehyde	NEB phospho-ER 118 monoclonal antibody at 1/500 in PBS overnight	DAKO mouse EnVision HRP labeled polymer antibody for 60 minutes
p-ER 167	ER-ICA	CST phospho-ER 167 antibody at 1/25 in PBS overnight	DAKO rabbit EnVision HRP labeled polymer antibody for 2 hours
Total-ER	ER-ICA	DAKO total ER clone ID5 mouse antibody at 1/100 in PBS for 90 minutes	DAKO mouse EnVision HRP labeled polymer antibody for 75 minutes
p-EGFR 1068	2.5% Phenol-Formal Saline	Biosource pEGFR 1068 rabbit primary antibody at 1/75 overnight at 37°C	DAKO Rabbit EnVision HRP labeled polymer antibody for 1 hour

Total-EGFR	2.5% Phenol-Formal Saline	NeoMarkers EGFR mouse monoclonal antibody at 1/20 in PBS overnight	DAKO mouse EnVision HRP labeled polymer antibody for 2.5 hours
Total COX-2	Formal Saline	NEB total COX2 rabbit primary antibody 1/40 1.5 hours	DAKO Rabbit EnVision peroxidase labeled polymer antibody for 1.5 hours
Total-Src	Formal Saline	CST total Src mouse polyclonal primary antibody at 1/1000 in 1% w/v dried milk in TBS-Tween with 0.05% sodium azide	EnVision mouse HRP labelled polymer at 1/100000 in 1% w/v dried milk in TBS-Tween
Phospho-Src	Formal Saline	CST p-Src Tyr 414 rabbit polyclonal primary antibody at 1/1000 in 1% w/v dried milk in TBS-Tween with 0.05% sodium azide	EnVision rabbit HRP labelled polymer at 1/100000 in 1% w/v dried milk in TBS-Tween

Table 2.4 Table to show the fixation method, 1° antibody concentration and incubation times, 2° antibody incubation times.

Once fixed, the cells were stored in sucrose storage media (SSM, see appendix for recipe) and were kept at -20 °C until required.

2.2.3.2.2 Detection of pMAPK, pAkt, pER, total ER, phospho-EGFR, total EGFR, total COX-2 and pSrc in fixed MCF-7 and Tam-R cells grown on coverslips

The coverslips bearing the fixed cells were removed from storage at -20 °C and washed in PBS until residual SSM was washed away. The coverslips were subsequently washed twice in PBS-TWEEN for 5 min. After adequate washing, primary antibody was applied as stated in table 2.4. Coverslips were incubated for the stated time in a humidity chamber at 25 °C. After sufficient incubation with the primary antibody, this was washed off with one 3-minute wash in PBS and two 5 min washes in PBS-TWEEN. These washes were followed by application of HRP labeled secondary antibody. The coverslips were incubated in the presence of the secondary antibody for the stated times at 25 °C in a humidity chamber.

Subsequent to ample incubation with secondary antibody, the coverslips were washed once in PBS for 3 min and twice in PBS-TWEEN for 5 min. After these washes the coverslips were incubated with DAB chromagen for ten minutes, washed with de-ionised water and then counterstained with a 10% methyl green solution. Excess methyl green solution was removed with de-ionised water washes and then coverslips were dried at 40 °C for 24 h. The coverslips were then mounted onto Surgipath pre-cleaned microscope slides with DPX mountant. Once DPX had dried, the coverslips were observed and photographed as in 2.2.3.1.7.

2.2.4 Western blot protein analysis

2.2.4.1 Cell culture and preparation of whole cell lysates

MCF-7 and Tam-R cells in log phase growth were passaged and seeded into 90mm dishes at a density of 1.5 x 10^6 cells per dish. Cells were grown in a monolayer to between 60 and 70% confluency with media replenishment every 3 day, at which point they were treated with control or test compounds for 3 h. The cells were then washed 3 times with pre-warmed PBS. Cells were then subjected to 200 μL ice-cold lysis buffer (see appendix for recipe) and kept on ice for 5 min then scraped from the bottom of the dish using a cell scraper and transferred into 1.5 mL Eppendorf tubes and kept on ice for 15 min. After this incubation, cell dispersions were subjected to centrifugation at 13000 rpm and 4 °C. Supernatants were then transferred, in aliquots of 50 μL, to fresh Eppendorf tubes and stored at -20 °C until required.

2.2.4.2 Protein quantification and standard curve

A Bio-rad protein assay was used to construct a standard curve of known concentrations of bovine serum albumin (BSA) made up in de-ionised water, from a starting concentration of 1mgmL^{-1}. All concentrations were made in duplicate to minimise error.

Protein concentration ($mgmL^{-1}$)	Volume of water (μL)	Volume of BSA (μL)
0	1000	0
5	995	5
10	990	10
15	985	15
20	980	20
25	975	25

Table 2.5 Table to show the preparation of protein standard concentrations for the BioRad protein assay.

Protein concentrations were made as outlined in table 2.5. These were made up in 1.5 mL Eppendorf tubes and vortex-mixed 5 s to ensure even dispersion of protein. An 800 μL aliquot was removed from the eppendorf and transferred to a 2 mL plastic spectrophotometer cuvette. To this, 200 μL of Bio-Rad reagent was added and the solution was agitated gently. The solution was allowed to develop for 15 min and was subsequently analysed for optical density using a Cecil CE2041 2000 series spectrophotometer, set at 595 nm.

Once a standard curve of known protein concentrations had been constructed, this was used to determine the amount of protein in whole lysate samples. Protein samples were allowed to thaw gently, then vortexed for 5 s to ensure even dispersion of the protein. To a 5 μL aliquot of protein sample 995 μL of

de-ionised was added and this solution was again vortex-mixed to ensure thorough distribution of the protein into the water. An 800 µL aliquot of this solution was then transferred into 2 ml plastic spectrophotometer cuvette. To this, 200 µL of Bio-Rad reagent was added and the solution was agitated gently. The solution was allowed to develop for 15 min and the amount of protein was determined using a Cecil CE2041 2000 series spectrophotometer (Cecil Instruments, Cambridge, UK), set at 595 nm. The amount of protein in each sample was then calculated to ensure that 50 µg mL^{-1} of protein was loaded in each lane of the SDS-PAGE.

2.2.4.3 Sodium dodecyl sulphate poly acrylamide gel electrophoresis (SDS PAGE)

Gel electrophoresis was completed using a Mini-Protein Slab II Electrophoresis Cell (Bio-Rad Laboratories LTD). Separating and loading gels were prepared as explained in the appendix and set between freshly cleaned glass plates. Once set the electrophoresis apparatus was assembled as described in the manufacturers guidelines and the running buffer (see appendix 1 for recipe) was poured into the electrophoresis cell.

Protein samples were allowed to thaw gently at 4 °C. To each sample 10µl of loading buffer (see appendix 1) was added and samples were subsequently spun down for 10 s in an IEC Micromax RF microcentrifuge (Thermo Electron Corporation, Hampshire, UK) at 1000 rpm. Samples were then heated in a Thermo Scientific (Fisher Scientific UK, Loughborough, England), heating

block set at 100 °C for 10 min to denature the proteins. Next, a rainbow protein marker and the protein samples were loaded into the wells of the loading gel and the electrophoresis cell was subjected to 200V for around 45 min or until the protein samples had reached the bottom of the gel.

2.2.4.4 Transfer of proteins

Following separation of the protein samples the gels were removed from the glass plates in which they were set and assembled in plastic transfer cassettes as shown in figure 2.1, to make a transfer 'sandwich'.

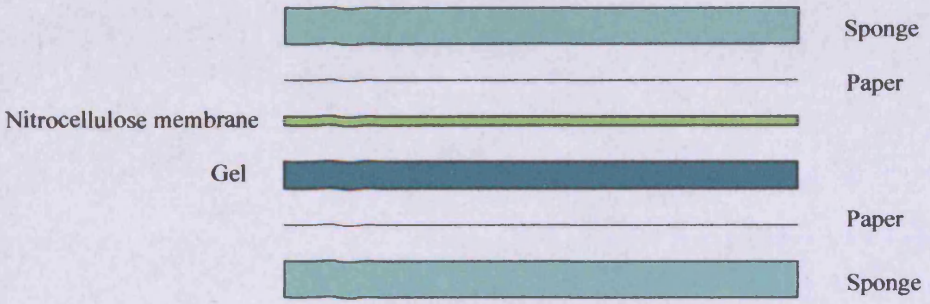

Figure 2.1 Diagram to show the assembly of the blotting sandwich

The sandwich was assembled such that the gel was nearer to the black side of the cassette (cathode) to ensure that the proteins travelled from the gel to the nitrocellulose membrane, which was at the anode side of the cassette. It was then placed in the electrophoresis cell. An ice pack was included to ensure the electrophoresis cell did not overheat. The cell was filled with transfer buffer (see appendix 1) and a magnetic stirrer was added to guarantee adequate circulation of transfer buffer and to maintain a constant temperature. The

electrophoresis cell was then subjected to 100 V for 1 h to transfer the protein from the gel to the nitrocellulose membrane.

The membrane was then incubated with Ponceau S solution to ensure transfer success, which was subsequently washed off with TBS-Tween washes (see appendix 1 for recipes).

2.2.4.5 Application of primary and secondary antibodies

Subject to transfer success, the membrane was then blocked with a 5 % w/v dried milk solution made up in TBS-Tween for 1 h. Whilst blocking, the membrane and block were rocked gently on a Stuart rocker (Bibby Scientific Ltd, Staffordshire, UK). After blocking, the membrane was incubated with primary antibody (see table 2.6) overnight at 4 °C on a Stuart roller (Bibby Scientific Ltd, Staffordshire, UK).

Protein detected	1° antibody concentration	2° antibody concentration
p-MAPK	CST p-MAPk polyclonal at 1/1000 in 1% w/v dried milk in TBS-Tween with 0.05% SA overnight at 4°C	EnVision rabbit HRP labelled polymer at 1/100000 in 1% w/v dried milk in TBS-Tween
p-Akt	CST p-Akt polyclonal at 1/1000 in 1% w/v dried milk in TBS-Tween with 0.05% SA overnight at 4°C	EnVision rabbit HRP labelled polymer at 1/100000 in 1% w/v dried milk in TBS-Tween
p-ER 118	NEB p-ER 118 monoclonal antibody at 1/1000 in 0.05% POD v/v in TBS-Tween overnight at 4°C	EnVision rabbit HRP labelled polymer at 1/100000 in 1% w/v dried milk in TBS-Tween
p-ER 167	CST p-ER 167 antibody at 1/1000 in 1% dried milk w/v in TBS-Tween overnight at 4°C	EnVision rabbit HRP labelled polymer at 1/100000 in 1% w/v dried milk in TBS-Tween
Total-ER	DAKO total ER clone ID5 mouse antibody at 1/1000 in 0.05% v/v POD in TBS-Tween overnight at 4°C	EnVision mouse HRP labelled polymer at 1/100000 in 1% w/v dried milk in TBS-Tween
p-EGFR	Biosource pEGFR 1068 rabbit primary antibody at 1/1000 in 1% w/v dried milk in TBS-Tween with 0.05% SA overnight at 4°C	EnVision rabbit HRP labelled polymer at 1/100000 in 1% w/v dried milk in TBS-Tween

Total-EGFR	NeoMarkers EGFR mouse monoclonal antibody at 1/1000 in 1% w/v dried milk in TBS-Tween with 0.05% SA overnight at 4°C	EnVision mouse HRP labelled polymer at 1/100000 in 1% w/v dried milk in TBS-Tween
Total COX-2	NEB total COX2 rabbit polyclonal primary antibody 1/1000 in 1% w/v dried milk in TBS-Tween with 0.05% sodium azide overnight at 4°C	EnVision rabbit HRP labelled polymer at 1/100000 in 1% w/v dried milk in TBS-Tween
Total Src	CST total Src mouse polyclonal primary antibody at 1/1000 in 1% w/v dried milk in TBS-Tween with 0.05% SA overnight at 4°C.	EnVision mouse HRP labelled polymer at 1/100000 in 1% w/v dried milk in TBS-Tween
p-Src	CST p-Src Tyr 414 rabbit polyclonal primary antibody at 1/1000 in 1% w/v dried milk in TBS-Tween with 0.05% SA overnight at 4°C.	EnVision rabbit HRP labelled polymer at 1/100000 in 1% w/v dried milk in TBS-Tween

Table 2.6 Table to show the concentrations of 1°and 2° antibody for each protein detected.

After sufficient incubation with the primary antibody, the membrane was rocked gently for 3 x 5 min washes in TBS-Tween. The membrane was incubated in the presence of the secondary antibody (as shown in table 2.6) for 75 min.

2.2.4.6 Visualisation of proteins by chemiluminescence

The membranes were washed three times in TBS-Tween for 10 min. The membranes were then placed into a clean plastic folder and were treated with luminol/peroxide based enhanced chemiluminescence (ECL) reagent (Pico, Dura or Femto). The luminol present within this reagent is oxidised by horseradish peroxidase to produce an excited state product, which emits photons of light as it decays to a lower energy state. Kodak autoradiography film was then placed over the membranes and the film was developed using a X-O-graph Compact X2 X-ray developer (X-O-graph Imaging System, Tetbury, UK) in a dark room.

2.2.5 Statistical Analysis

All statistics throughout this thesis were carried out on Minitab for Windows. Confidence intervals were set at 95% and significance was defined as $p=<0.05$.

Chapter 3

Transcutaneous delivery of signal transduction inhibitors and tamoxifen.

3.1 Introduction

Over recent years attention paid to topical drug delivery has increased greatly. The primary benefit of topical delivery is local targeting, which could much reduce quantities of drug administered and thus circulating in the blood stream (and non-target tissues). Other benefits include the elimination of 1st pass hepatic metabolism, controllable 0-order rates of delivery, and rapid termination of dose in event of adverse reaction (Williams, A.C. 2003). Furthermore, skin patches are generally well accepted and tolerated, thus aiding patient compliance.

The FDA approved the first topical preparations in 1981 for the treatment of angina pectoris and motion sickness; however, it took many years to prove the clinical efficacy of these and for researchers to believe that molecules could overcome the physicochemical barrier properties of the skin and reach post skin targets at therapeutic levels.

Early studies had strict exclusion criteria when selecting candidates to deliver across the skin including size and lipophilicity. Compounds above 500 Da and without adequate lipophilicity were not considered for topical delivery. However, the development of chemical and physical enhancers and the manipulation of formulations to increase the thermodynamic activities of compounds have increased the number of products available for topical delivery.

Transcutaneous delivery of compounds involves the permeation of compounds across full thickness skin and diffusion to underlying tissues. The compounds must permeate at a sufficiently high rate to evade clearance by the microvasculature in order to reach their final target destination. Numerous transcutaneous products are now commercially available, such as topical NSAIDs for pain relief.

The breast represents a reasonably accessible target for topical administration, where the drugs can be delivered transcutaneously using a semi-solid formulation or device, which then undergo passive diffusion to the underlying tissues.

Several studies have demonstrated the possibility of percutaneously delivering tamoxifen and 4-hydroxytamoxifen to the breast. Mauvais-Jarvis (1986) and colleagues showed that radio-labelled tamoxifen and 4-hydroxytamoxifen, when formulated in a 60% alcoholic solution, were detected in breast tissue after topical application. Furthermore, these two compounds were retained in the breast tissue significantly when compared to their application to the abdomen. Another study showed that 4-hydroxytamoxifen could permeate the skin sufficiently as to affect tumor proliferation when formulated as a simple gel (Rouanet, P. *et al* 2005). A previous study demonstrated *in vitro* transcutaneous delivery of tamoxifen and γ linolenic acid from a borage oil formulation containing ethanol and 1,8-cineole Ho, S. *et al* 2004).

The aims of this chapter were to incorporate 1 MAPK inhibitor and 1 PI3K inhibitor into a transcutaneous formulation and assess their singular and simultaneous permeation through full thickness porcine skin when combined with tamoxifen.

3.2 Materials and Methods

3.2.1 Materials

The materials for this study were outlined in chapter 2 (section 2.2.1).

3.2.2 Tamoxifen metabolism

It is widely documented that it is the metabolite 4-hydroxytamoxifen that is the potent SERM, rather than the parent compound tamoxifen. In fact, it has been noted that this metabolite is 100 times more efficacious than tamoxifen in inhibiting the ER signalling (Borgna, J-L. & Rochefort, H. 1981). The metabolite exists in two isoforms, with the trans isomer being far more potent than the cis isomer (Robertson, D.W. *et al* 1982). The purchased 4-hydroxytamoxifen exists as trans:cis at 70:30 and remains at this ratio as it enters and penetrates the skin (Malet, C. *et al* 2002). For this reason, only the trans isomer was analysed and quantified by HPLC. 4-hydroxytamoxifen was analysed using the method described in section 3.2.4 for tamoxifen; however, the trans isomer had a retention time of 4.7 minutes.

3.2.2.1 Skin homogenisation

Freshly excised porcine ears were maintained in HHBBSS during transportation from a local abattoir. The ears were then washed in tepid tap water to remove excess surface dirt and the subcutaneous material was removed by blunt dissection. The ears were then cut into small pieces and weighed to provide 2grams of skin per sample. These samples were then transferred to 5mL PBS and homogenised using a Silverson homogeniser (Silverson Machines Ltd, UK) for 3 x 30 seconds.

3.2.2.2 Tamoxifen metabolism study

Tamoxifen was dissolved in 7.5mL PBS to provide a $1mgmL^{-1}$ solution. PBS has been previously shown to maintain viability of skin enzymes for the duration of metabolism studies (Rittirod, T. *et al* 1998). From this solution 1mL was transferred to 14mL of fresh PBS, which was subsequently transferred to the 5mL of PBS containing the homogenised skin, thus giving 20mL of PBS in total (n=5). A further 2 vials contained only tamoxifen (1mL of $1mgmL^{-1}$ tamoxifen in 19mL PBS), while a further 2 vials included only homogenised skin in 20mL PBS. Vials were incubated at 37°C and rotated on a Stuart blood rotator (Barloworld Scientific, Staffordshire, UK) throughout the experiment. Samples were taken at 1,2,5,10 and 24 hours. Vials were mixed thoroughly using a vortex mixer at the stated sample times and 1 mL was removed from the vial and analysed using the HPLC method stated in section 3.2.4. The removed 1mL was not replenished with fresh PBS so as to not unbalance the concentration of tamoxifen and metabolites.

3.2.2.3 Prediction of Log P values

The prediction of LogP was a valuable tool when assessing the potential of compounds to permeate full thickness skin. From this prediction, it was possible to determine whether the compounds were lipophilic or hydrophilic and an estimated Log K_p could be calculated using equation 3.1 and from this an estimated flux could be calculated using equation 3.2.

$$\text{Log } K_p = -6.3 + 0.71 \log \text{octanol/water} - 0.0061 \text{ mol wt}$$

Equation 3.1

$$\text{Log flux} = \log K_p + \text{solubility}$$

Equation 3.2

Using a virtual computational chemistry laboratory website it was possible to estimate the LogP and solubility of the 5 compounds based on their chemical structure. This website was: http://146.107.217.178/lab/ and the program was ALOGPS.

3.2.2.4 Solubility in DMSO and cetrimide solution

It was important to assess the solubility of the 4 signal transduction inhibitors (STIs) and 4, hydroxytamoxifen in both the donor solution and the receptor solution. The compounds should all be soluble in DMSO to provide a high chemical potential between the compounds and vehicle. The receptor solution should provide adequate sink conditions for permeants.

The solubility of PD98059, LY294002, quercetin, SL327 and 4, hydroxytamoxifen was assessed in DMSO and cetrimide solution (30mgmL^{-1}). Compounds were added to 200µl of solution and spun on a Stuart blood rotator (Barloworld Scientific, Staffordshire, UK) at 32°C until excess compound remained. Samples were then centrifuged using a Heraeus (Thermo Scientific, Northumberland, UK) instrument at 1000 rpm for 1 minute to separate the excess drug. Samples of supernatant were then diluted 20-fold and analysed by reverse phase HPLC.

3.2.2.5 Stability in DMSO and cetrimide solution

The stability of the compounds was assessed to ensure that the compounds were stable throughout the time course of the experiment. Poor stability could give misleading results in the permeation experiments.

Compounds were prepared at 1mg mL^{-1} in DMSO or 30mgmL^{-1} cetrimide solution. These were then analysed immediately and then after 1, 5, 12, 24, 48 and 168 hours using reverse phase HPLC.

3.2.2.6 Preparation of porcine skin membranes

The method outlined in chapter 2, section 2.2.1.2 was followed for all skin preparation throughout this chapter.

3.2.2.7 The *in vitro* transcutaneous delivery of PD98059, LY294002, quercetin and SL327

The transcutaneous delivery of 4 compounds was assessed to determine the two compounds with the greatest permeability to take forward and formulate with tamoxifen. Transcutaneous delivery (i.e. across both full thickness porcine skin) was modelled using glass Franz-type diffusion cells in which skin samples were mounted between the greased flanges. A receptor phase of cetrimide 30mg/mL was added, along with a magnetic stirrer bar, to the receptor compartment. The cells were placed in a submersible stirrer plate set up in a water bath and maintained at 37°C. After a 30-minute equilibration period the cells were dosed with 200 µl of PD98059, LY294002, quercetin or SL327 made up in DMSO, previously prepared to provide equimolar aliquots of 2.54×10^{-4} mol. The donor phase compartments were occluded and at 3, 6, 12, 24 and 48 hours the entire contents of the receptor phases were removed for analysis, and replenished with fresh solution.

3.2.2.8 The *in vitro* transcutaneous delivery of PD98059, LY294002, formulated with and without 4-hydroxytamoxifen

The method outlined in section 3.2.7 was repeated, however PD98059 and LY294002 were formulated together and their simultaneous delivery was determined across excised full thickness porcine skin both with and without 4-hydroxytamoxifen present in the formulation. The cells were dosed with 200 µl of PD98059 plus LY294002, with and without tamoxifen made up in DMSO, previously prepared to provide equimolar aliquots of 2.54×10^{-4} mol.

3.2.2.9 Immunocytochemical analysis to determine potential inflammatory activity of DMSO on porcine skin

Immunocytochemistry was performed to detect any potential toxicity of the DMSO vehicle on porcine skin. An assay to detect ki-67, a proliferation marker, was conducted to represent skin viability. Haematoxylin and eosin staining was also carried out to observe the histology of the skin.

Skin was prepared and set up as mentioned in chapter 2, section 2.2.3, but in this case the skin having been dosed with treatments as shown in table 3.1. Treatments were removed and skin samples were processed at the stated times. The skin was processed, embedded and microtomed as in section 2.2.3. Once dried, H&E staining and a ki-67 assay were performed on the sections.

Cell numbers	Treated with	Sample time (hour)
1-3	Water	0
4-6	DMSO	0
7-9	Water	8
10-12	DMSO	8
13-15	Water	24
16-18	DMSO	24
19-21	Water	48
22-24	DMSO	48

Table 3.1. Franz diffusion cells 1-24 treated with either 200µl water or 200µl DMSO. Receptor phase was HHBBSS and skin was maintained at 32°C.

3.2.3 Statistical analysis

Unpaired t-tests were used to compare the permeation of each compound when applied to the skin individually, simultaneously and then together with tamoxifen. T-tests were also used to compare the concentration of tamoxifen present with and without homogenised skin to assess the levels of tamoxifen metabolism. All statistics were performed using Minitab for Windows.

3.3 Results

3.3.1 Tamoxifen metabolism

Tamoxifen is metabolised in the liver by cytochrome P450 enzymes to, among other metabolites, 4-hydroxytamoxifen. Potential metabolism within the skin has not been investigated or reported. Understanding that 4-hydroxytamoxifen is significantly more potent at inhibiting ER signalling, this small study was aimed at determining the extent, if any, of tamoxifen metabolism to its more active metabolite within the skin. Figure 3.1 shows the concentration of tamoxifen throughout the metabolism study.

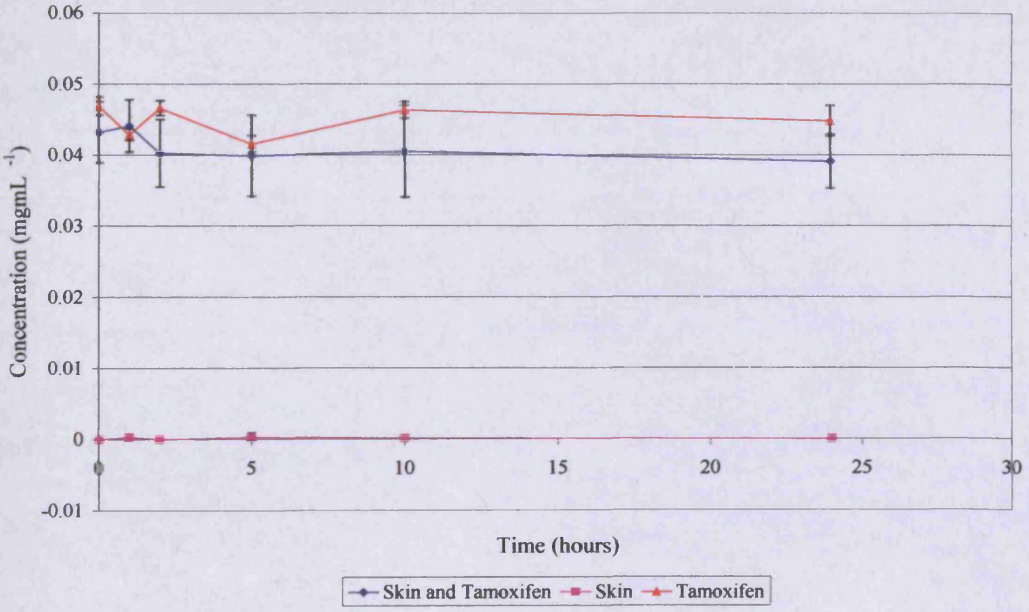

Figure 3.1 Tamoxifen metabolism assay. Concentration of tamoxifen ($mgmL^{-1}$) with increased incubation with 2g homogenised porcine skin in PBS. Starting concentration was $0.05mgmL^{-1}$. Samples were maintained at 37°C and agitated on a blood rotator throughout the experiment (n=15 ± SD).

The metabolism study shows no significant decrease in the concentration of tamoxifen when the homogenised skin was present compared to when the skin was absent (P = 0.184). No HPLC peaks were detected at 4.7 or 6.1, using the previously described method, suggesting the absence of trans- or cis-4-hydroxytamoxifen in each sample. Analysis of samples containing only homogenised skin showed no peaks at 6.9 minutes or at 4.7 or 6.1 minutes. This ensured that that peaks quantified as tamoxifen in the test samples were true peaks and not homogenised skin material. No metabolism of tamoxifen was detected in the presence of the homogenised skin.

3.3.2 Predicted log P

The predicted log P of PD98059, LY294002, quercetin. SL327 and 4-hydroxytamoxifen using the ALOGPs software package were 2.89, 3.46, 0.95, 3.7 and 5.44 respectively. The ALOGSs using the same software were predicted as -3.99, -3.38, -2.42, -4.82, and -5.11 respectively. Therefore predicted solubilities were 0.102, 0.42, 0.38, 0.015 and 0.007mgmL^{-1}. The predicted flux values of the compounds were 129, 899, 95, 36.7 and 172 μgcm^{-2}h^{-1}.

3.3.3 Solubility of PD98059, LY294002, quercetin SL327 and 4, hydroxytamoxifen in DMSO and cetrimide solution at 32°C

The solubility of PD98059, LY294002, quercetin, SL327, 4-hydroxytamoxifen in DMSO was 6.98 ± 0.34, 14.76 ± 1.08, 12.54 ± 1.68, 6.57 ± 0.86 and 21.03 ± 3.22 $mgmL^{-1}$ respectively. Solubility of PD98059, LY294002, quercetin, SL327, 4-hydroxytamoxifen in cetrimide was 4.57 ± 0.76, 9.42 ± 0.9841, 6.43 ± 0.11, 2.87 ± 0.34 and 16.23 ± 1.13 $mgmL^{-1}$ respectively.

3.3.4 Stability of PD98059, LY294002, quercetin SL327 and 4, hydroxytamoxifen in DMSO and cetrimide solution

Table 3.2 and 3.3 show the stability of all 5 compounds in DMSO and cetrimide solution respectively by presenting the percentage of degradation of each compound over 168 hours.

Time (hours)	PD	LY	Q	SL	4OHTam
0	0	0	0	0	0
5	0	0	0	0	0
12	0	0	0	0	0
24	0.21 ± 0.011	0.39 ± 0.04	0.99 ± 0.13	1.01 ± 0.22	1.54 ± 0.067
48	1.96 ± 0.24	2.27 ± 0.23	3.22 ± 0.015	2.74 ± 0.24	2.88 ± 0.19
168	5.27 ± 0.47	6.11 ± 0.82	7.93 ± 0.43	5.48 ± 0.47	4.72 ± 0.66

Table 3.2 Table to show the percentage degradation of PD98059, LY294002, SL327, quercetin and 4-hydroxytamoxifen in DMSO over 1 week. Solutions were made at 1mgmL^{-1} and left on the bench top. Samples were taken at the stated times (n=3 ± SD).

All 5 compounds show good stability in DMSO up to 48 hours, with 4, hydroxytamoxifen showing the worst stability after 48 hours. 4,hydroxytamoxifen degraded by 2.88 ± 0.19%. After 168 hours, however, considerable degradation was seen with all 5 compounds, with quercetin showing the most degradation (7.93 ± 0.43%).

Each compound showed reduced stability in cetrimide when compared to DMSO. Up to 24 hours all compounds showed negligible degradation when dissolved in cetrimide solution, with the highest degradation being seen with

LY294002, which degraded by 2.76 percent. However, at 48 and 168 hours degradation was as high as 10.6 % for PD98059.

Time (hours)	PD	LY	Q	SL	4OHTam
0	0	0	0	0	0
5	0	0	0	0	0
12	0.1 ± 0.005	0.248 ± 0.026	0.13 ± 0.011	0.054 ± 0.0018	0
24	2.44 ± 0.35	2.76 ± 0.048	2.276 ± 0.022	1.242 ± 0.089	0.98 ± 0.025
48	4.872 ± 0.63	5.12 ± 0.78	3.891 ± 0.55	3.987 ± 0.27	2.795 ± 0.77
168	10.576 ± 1.28	9.598 ± 0.92	9.154 ± 1.73	6.905 ± 0.88	7.58 ± 0.32

Table 3.3 Table to show the percentage of degradation of PD98059, LY294002, SL327, quercetin and 4-hydroxytamoxifen in cetrimide over 1 week. Solutions were made at 1mgmL^{-1} and left on the bench top. Samples were taken at the stated times (n=3± SD).

It was important for the compounds to be stable in DMSO for 48 hours because the compounds are applied to the skin and remain dissolved in this solvent throughout the skin permeation experiment, which is over a 48 hour time period. Samples taken from the receptor phase were frozen and analysed over

12 hours, and so it was important that the compounds showed negligible degradation over 12 hours.

3.3.5 Permeation studies for PD98059, LY294002, quercetin and SL327

The permeation of the 4 compounds when dosed at equimolar concentrations (2.54×10^{-4}mol) individually to excised, full thickness porcine skin in DMSO is shown in figure 3.2. This figure shows typical 0-order permeation profiles for all 4 compounds. LY294002 permeated significantly more readily than quercetin ($P = 0.001$) and PD98059 permeated more readily than SL327 ($P = 0.012$). These conditions allowed 3.81 ± 0.62, 5.38 ± 0.78, 1.15 ± 0.37 and 2.3 ± 0.48 μgcm^{-2} of PD98059, LY294002, quercetin and SL327 to permeate after 48 hours respectively. Steady state flux was seen between 6 and 12 hours for PD98059 and SL327 and between 12 and 24 hours for LY294002 and quercetin. These were 0.09 ± 0.08, 0.14 ± 0.015, 0.03 ± 0.009 and 0.066 ± 0.01 $\mu gcm^{-2}h^{-1}$ for PD98059, LY294002, quercetin and SL327 respectively. Lag times varied between the 4 compounds, with PD98059 having the shortest lag time of 2.73 ± 0.66 hours, while quercetin showed the longest lag time of 6.17 ± 0.499 hours.

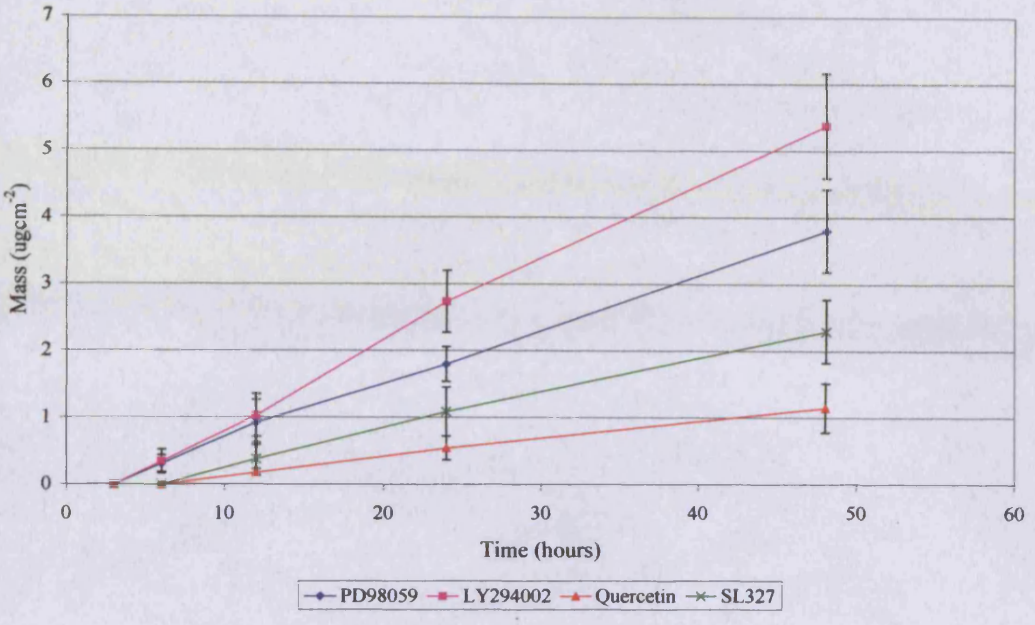

Figure 3.2 Permeation profiles for PD98059, LY294002, quercetin and SL327. Excised porcine skin was maintained at 32°C. Receptor phase was 30mgmL^{-1} cetrimide solution, which was agitated with a micro-stirrer. Donor phase was 2.54 x 10^{-4} mol PD98059, LY294002, quercetin or SL327 in DMSO (n=6 ± SD)

The lag times of LY294002 and SL327 were 4.84 ± 0.84 and 6.01 ± 0.01 hours respectively. The Kp of the four compounds was 1.06 x 10^{-3} ± 1.5 x 10^{-4}, 9.28 x 10^{-4} ± 9.8 x 10^{-5}, 2.68 x 10^{-4} ± 7.9 x 10^{-5} and 4.65 x 10^{-4} ± 7.04 x 10^{-5} cm^{-2}h^{-1} respectively for PD98059, LY294002, quercetin and SL327.

3.3.6 Permeation studies for PD98059 and LY294002 with and without 4-hydroxytamoxifen

The permeation of individually dosed PD98059 and LY294002 was described in section 3.3.3. This study was aimed at concluding whether simultaneous

dosing of PD98059 and LY294002 changed the permeation of the two compounds compared to separate dosing. It also determined if the inclusion of 4-hydroxytamoxifen altered the permeation of the 2 compounds.

The permeation profiles detailed in figure 3.3 show typical 0-order permeation profiles. Surprisingly the permeation of both compounds increased significantly (P = 0.018 and 0.006) when applied to the skin simultaneously. Table 3.5 compares the mass and number of moles permeated after 24 and 48 hours, the steady state flux, lag time and K_p of the two compounds when applied to the skin individually and simultaneously.

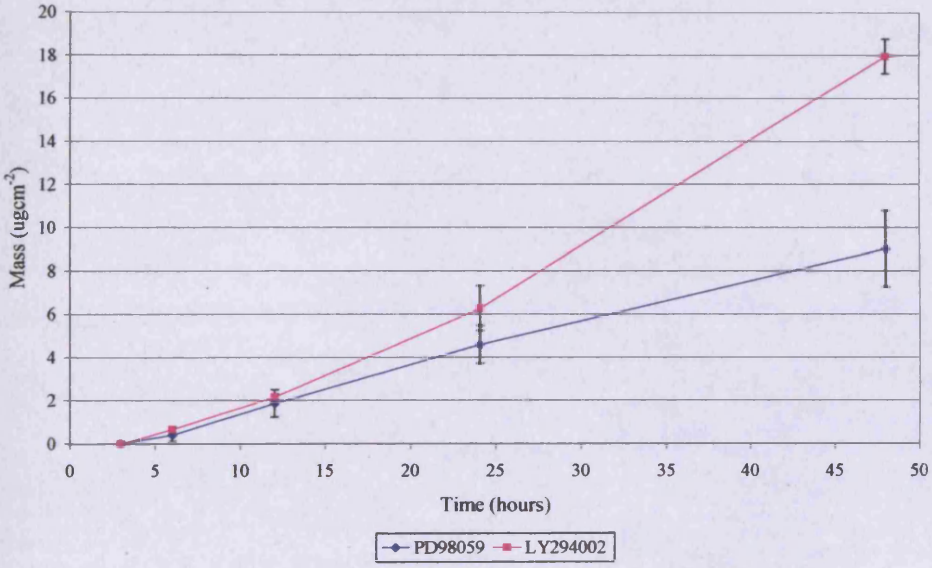

Figure 3.3 Permeation profiles for simultaneously dosed PD98059 and LY294002. Excised porcine skin was maintained at 32°C. Receptor phase was 30mgmL^{-1} cetrimide solution, which was agitated with a micro-stirrer. Donor phase was 2.54 x 10^{-4} mol PD98059 plus LY294002 in DMSO (n=6 ± SD).

	Dosed individually		Dosed simultaneously		Simultaneously with 4-OHT	
	PD98059	LY294002	PD98059	LY294002	PD98059	LY294002
J_{ss} ($\mu g\ cm^{-2}\ h^{-1}$)	0.09 ± 0.008 (@6-12h)	0.14 ± 0.015 (@12-24h)	0.24 ± 0.045 (@6-12h)	0.49 ± 0.051 (@24-48h)	0.38 ± 0.098 (@6-12h)	0.61 ± 0.081 (@12-24h)
Lag time (h)	2.73 ± 0.66	4.84 ± 0.84	4.31 ± 0.62	11.1 ± 1.22	5.24 ± 0.87	7.14 ± 1.42
Q_{24} ($\mu g\ cm^{-2}$)	1.8 ± 0.26	2.74 ± 0.46	4.59 ± 0.88	6.28 ± 1.04	5.64 ± 0.98	10.99 ± 1.39
Q_{48} ($\mu g\ cm^{-2}$)	3.81 ± 0.62	5.38± 0.78	9 ± 1.77	17.95 ± 1.30	10.51 ± 1.81	23.31 ± 2.83
Q_{24} ($\mu mol\ cm^{-2}$)	0.007 ± 0.001	0.009 ± 0.001	0.017 ± 0.004	0.02 ± 0.003	0.021 ± 0.004	0.036 ± 0.005
Q_{48} ($\mu molcm^{-2}$)	0.014 ± 0.002	0.018 ± 0.003	0.034 ± 0.008	0.058 ± 0.09	0.04 ± 0.007	0.076 ± 0.006
K_p ($cm\ h^{-1}$)	1.06×10^{-3} ± 1.5 x10^{-4}	9.28×10^{-4} ± 9.8 x 10^{-5}	1.25×10^{3} ± 1.77 x 10^{-4}	2.99×10^{-3} ± 2.65 x 10^{-4}	3.28×10^{3} ± 8.92 x 10^{-4}	3.995×10^{-3} ± 6.21 x 10^{-4}

Table 3.4 Steady state flux (J_{ss}), cumulative permeation at 24 hours (Q_{24}) and at 48 hours (Q_{48}) and permeability coefficient (K_p) data for the delivery of PD98059 and LY 294002 across excised full thickness porcine skin when applied separately or simultaneously. Simultaneous delivery includes both data with and without the addition of 4-hydroxytamoxifen (n=6, ± SD)

Table 3.4 clearly reveals that the mass and number of moles of both compounds permeating after 48 hours increased significantly when the compounds were dosed together, with enhancement ratios (EnRs) of 2.36 and 3.71 for PD98059 and LY294002 respectively.

Interestingly the steady state flux (P = 0.004, 0.001 PD and LY) and lag times (P = 0.05, 0004 PD and LY) of both compounds were also significantly increased when the two compounds were dosed simultaneously.

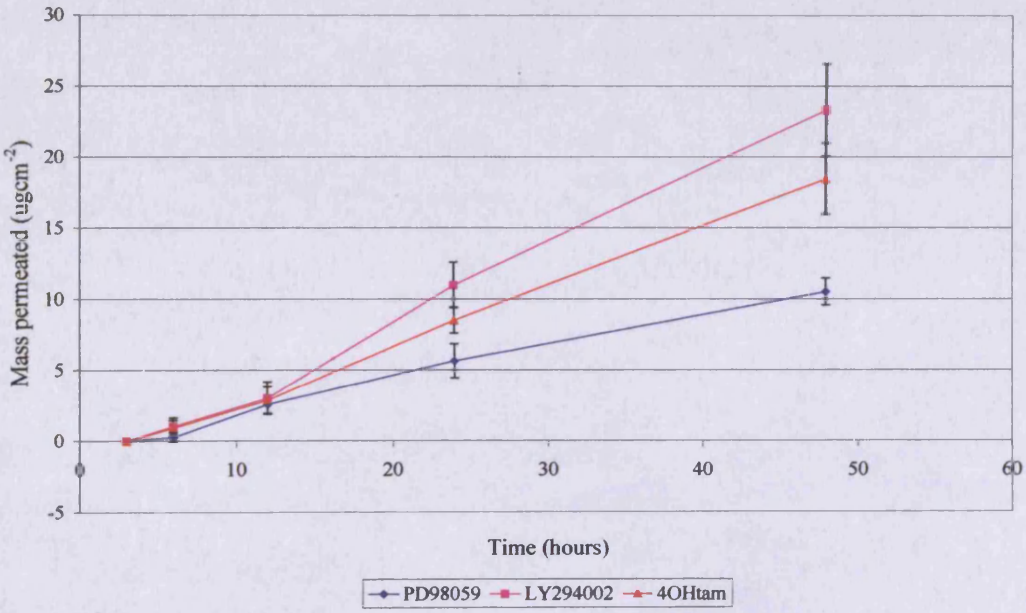

Figure 3.4 Permeation profiles for PD98059, LY294002 and 4-hydroxytamoxifen (4Ohtam) when dosed simultaneously. Excised porcine skin was maintained at 32°C. Receptor phase was 30mgmL^{-1} cetrimide solution, which was agitated with a micro-stirrer. Donor phase was 2.54 x 10^{-4} mol PD98059, LY294002 or 4- hydroxytamoxifen in DMSO (n=6 ± SD).

Figure 3.4 shows the permeation of PD98059, LY294002 and 4-hydroxytamoxifen when formulated and dosed together in DMSO. The data

show typical 0-order permeation profiles for all 3 compounds. The addition of 4-hydroxytamoxifen did not significantly alter the mass permeated, flux or lag time of PD98059 (P = 0.961, 0.116 and 0.301). No significant difference in mass permeated and flux of LY294002 was seen with the inclusion of tamoxifen compared to the when PD98059 and LY294002 were dosed simultaneously without 4-hydroxytamoxifen (P = 0.367 and 0.08 respectively). However the lag time of LY294002 was significantly reduced (P = 0.018) when 4-hydroxytamoxifen was included in the formulation.

Figure 3.4 demonstrates the permeation of 4-hydroxytamoxifen, showing that 18.5 ± 2.52 μgcm^{-2} permeated into the receptor compartment after 48 hours. Steady state flux was detected between 12 and 24 hours and was determined as 0.47 ± 0.045$\mu gcm^{-2}h^{-1}$. The lag time of 4-hydroxytmoxifen, under these conditions, was 5.72 ± 0.86 hours and the k_p was 3.87 x 10^{-3} ± 3.68 x 10^{-4} $cm^{-2}h^{-1}$.

3.3.7 Immunocytochemical analysis of the effect of DMSO on porcine skin

3.3.7.1 H & E staining

The anatomy of the skin was examined using a standard haematoxylin and eosin assay, where cell nuclei stain blue and the cytoplasm stains pink. The effect of DMSO compared to water control on the structure of the skin using this assay, as skin toxicity in response to DMSO administration has previously been reported when DMSO is over 60%.

Figure 3.5 shows the result of the H & E assay, showing clearly the dermis, epidermis and stratum corneum. Figure 3.5 A-B show H & E staining of skin freshly dissected and fixed. The staining shows healthy epidermal keratinocytes and shows the stratum corneum still attached to the epidermis.

Figure 3.5 C-D shows H & E staining on excised porcine skin of which the SC was incubated with water for 3 hours. Viability was maintained by using a receptor phase of HHBBSS.

The H & E assay revealed that incubation with water gave no observable changes in the structure of the skin, suggesting that no skin toxicity was caused.

Figure 3.5 E-F, however did show considerable structural changes. This skin was incubated with DMSO for 3 hours and seemed to cause detachment of the stratum corneum and some evidence of keratinocyte damage, which has been highlighted with an arrow.

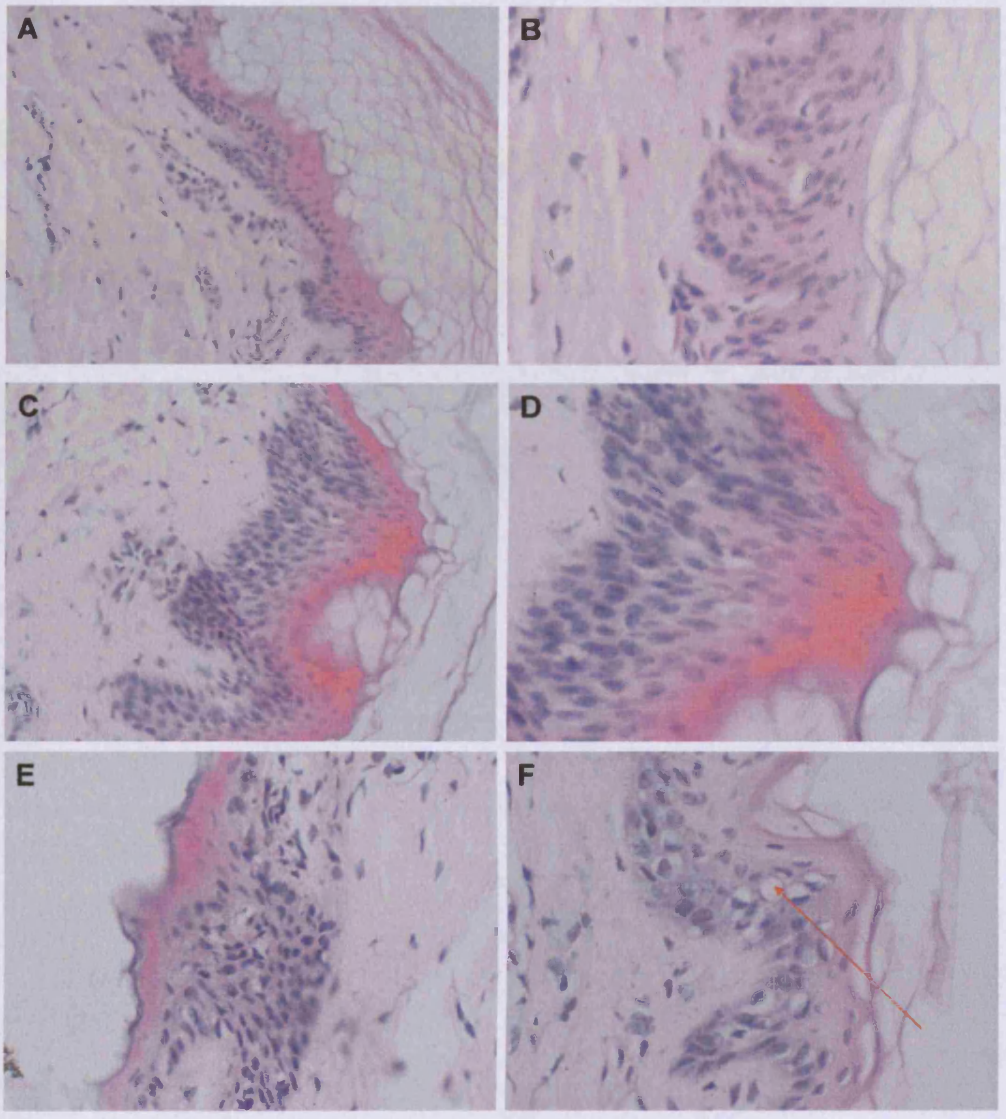

Figure 3.5 A-F H & E staining of freshly excised porcine skin, immediately post dissection (A x10, B x20), incubated with 200µl water for 3 hours (C x20, D x40) and with 200µl DMSO for 3 hours (E x 20, F x 40). Skin was fixed in formaldehyde, dehydrated and embedded in wax. Sections (5µm) were then cut using a Shandon microtome and placed onto Surgipath pre-cleaned microscope slides and dried at 37°C. A standard H & E assay was performed and slides were dried at 37°C and images were viewed and recorded using an Olympus BH-2 phase microscope and photographed using an integrated Olympus DP-12 digital camera system (Olympus, Oxford, UK).

3.3.7.2 Ki 67 assay

The ki-67 assay was performed to examine the effect of DMSO on skin viability. Figure 3.6 shows the ki-67 assay performed on excised porcine skin when treated with either water or DMSO. Figure 3.6 A-B shows skin assayed immediately post dissection. It shows significant ki-67 staining within the lower stratums of the epidermis, which is localised to the nuclei of these cells. Figure 3.6 C-D shows the results of the ki-67 assay completed on skin incubated with water for 3 hours. Again, ki-67 was found predominantly within the lower layers of the epidermis and was confined to the nuclei of these cells. Comparing ki-67 staining in both time 0 and after 3 hours incubation with water, showed no visible differences in extent of ki-67 presence.

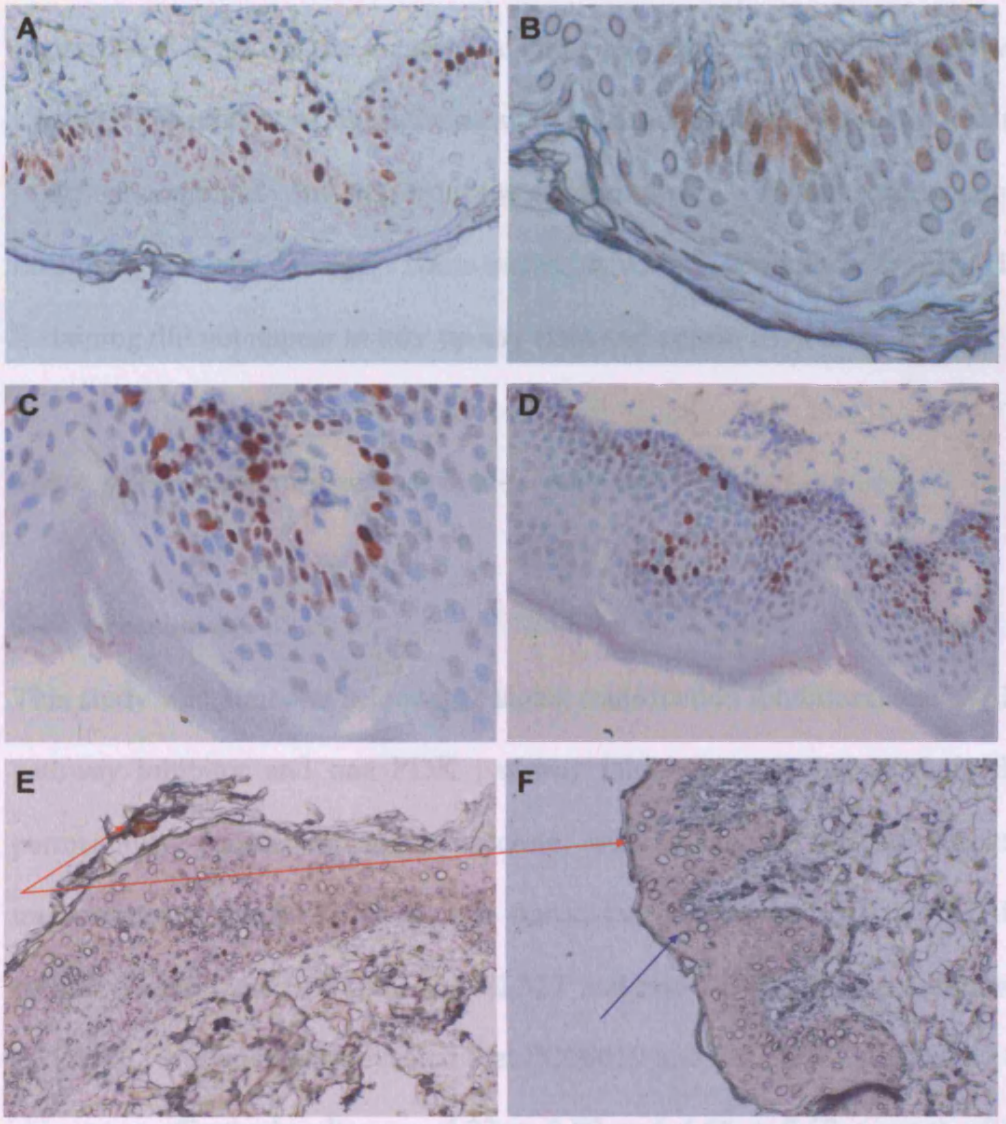

Figure 3.6 A-F Ki-67 assay on freshly excised porcine skin, immediately post dissection (A x20, B x40), incubated with 200µl water for 3 hours (C x40, D x20) and with 200µl DMSO for 3 hours (E x 20, F x 20). Sections (5µm) were then cut using a Shandon microtome and placed onto Surgipath pre-cleaned microscope slides and dried at 37°C. A DAKO corporation ki-67 mouse monoclonal primary antibody was used at 1/50 in 1% BSA in PBS for two hours and a DAKO EnVision detection system was applied for 2 hours. Counter stain was with methyl blue. Slides were dried at 37°C and images were viewed and recorded using an Olympus BH-2 phase microscope and photographed using an integrated Olympus DP-12 digital camera system (Olympus, Oxford, UK).

Figure 3.6 E-F shows the outcome of the ki-67 assay on skin incubated with DMSO. The red arrow highlights stratum corneum damage, where this stratum is almost completely missing from the section of skin. The blue arrow shows keratinocyte nuclei damage. These nuclei, as with those in the respective H & E staining did not appear to take up any stain and appear as holes.

There was also a significant loss in ki-67 staining.

3.4 Discussion

This study was aimed at selecting 2 signal transduction inhibitors, one MAPK pathway inhibitor and one PI3K pathway inhibitor according to their skin permeability properties, to incorporate with tamoxifen into a cocktail transcutaneous patch. The *in-vitro* transcutaneous delivery of two MAPK pathway inhibitors; PD98059 and SL327 and two PI3K pathway inhibitors; LY294002 and quercetin revealed that PD98059 and LY294002 permeated the skin most effectively allowing 4.23 ± 0.69 and 4.68 ± 0.68 percent of the applied dose to permeate after 48 hours.

The predicted flux values of all compounds were significantly greater than the flux values seen in the permeation experiments. This could be due to the donor phase containing sub-saturated concentrations of all compounds due to cost limitations; however, the average permeation of active ingredients of commercially available transdermal and transcutaneous formulations is around

ten percent. Considering that this simple drug in vehicle delivered 5% of applied dose and that manipulation with chemical penetration enhancers could improve these results, the preliminary results appeared promising.

The permeation of PD98059 through skin has had little attention paid to it, however, it has been previously described that a 5-10mM dose of PD98059 permeated the stratum corneum and entered the viable epidermis of mouse ears sufficiently after 30 minutes to affect CCL2, CXCL8, CCL5 and CXCL10 expression (Pastore, S. *et al* 2005). The permeation of LY294002 across or into skin has received more consideration. Bedogni, B *et al.* (2004) described how LY294002 was able to permeate the skin and inhibited the growth of TPras transgenic melanomas, their invasive behaviour and angiogenesis in mice. They also showed that the invasion inhibitory effects seen with topical administration of LY294002 or U0126 (a MAPK inhibitor) correlated with a reduction in MMP expression. It has also been shown that 5 μmol solution of LY294002 was able to permeate the skin and inhibit TPA-induced p-Akt expression (Hwang, D-M. *et al* 2006). However, the two remaining STIs; SL327 and quercetin, did not permeate full thickness porcine skin with such ease. In fact, only 0.87 ± 0.2 percent of the applied dose of quercetin permeated the skin membrane after 48 hours. The skin permeation of quercetin has been investigated intensively due to its poor oral bioavailability. Casagrande, R. *et al.* (2007) reported similar observations as seen in the present transcutaneous permeation study. Quercetin showed very poor permeation through porcine skin, even though release studies showed that

quercetin was released from each formulation sufficiently. However, this investigation revealed that topical quercetin could inhibit oxidative stress and inflammation within the skin caused by UVB damage, suggesting that quercetin was capable of partitioning into the stratum corneum and viable epidermis to inflict these effects and was retained in this location (Casagrande, R. *et al* 2007). It has also been shown that without the presence of either a fatty acid or fatty alcohol enhancer present, quercetin did not permeate into the receptor phase. This study also concluded that without the presence of an anti-oxidant such as BHA, quercetin degraded rapidly in the donor phase (Kim, H.W. *et al* 2004). This oxidation of quercetin would offer an explanation on the poor permeation seen in this chapter; however, the stability of quercetin was measured in both these experiments and those in the study conducted by Casagrande, suggesting this was not the reason for poor permeation in both of these cases. Saija, A. and co-workers (1998) investigated the permeation of three flavanoids; quercetin, hesperetin and naringenin. They discovered that while hesperetin and naringenin permeated the skin sufficiently, quercetin, which is not structurally unlike these two compounds, did not permeate the skin. The skin has both lipophilic and hydrophilic stratums and so compounds that are either highly lipophilic or hydrophilic often have inferior permeation properties (Williams, A.C, 2003). The poor water solubility of quercetin has been suggested as another possible reason for the absence of skin permeability properties (Bonina, F.P. *et al* 1996).

SL327 permeated slightly more readily, with 2.42 ± 0.5 percent of the applied dose permeating after 48 hours. The topical administration of SL327 has not been previously described.

DMSO proved a successful vehicle for the delivery of PD98059, LY294002 and, to some extent, SL327. The permeation enhancing properties of DMSO are widespread throughout the topical drug delivery literature, with increasing bodies of evidence suggesting that at concentrations above 60% particularly DMSO increases the permeation of a wide variety of compounds by altering SC protein conformation and lipid organization (Anigbogu, A.N.C. *et al* 1995). Several studies have demonstrated the value of DMSO in aiding the permeation of a variety of compounds. It was shown that where PEG, a known permeation enhancer, failed to deliver acyclovir through human skin, 5% acyclovir in a 95% DMSO solution improved the permeation of the compound significantly. A subsequent study by the same authors showed that a 95% solution of DMSO had the same penetration enhancing effect on another anti-viral compound; indoxuridine. A study by Bugaj and co-workers in 2006 illustrated that DMSO gave rise to the most significant increase in the permeation of the methyl ester of 5-aminolevulinic acid measured by the formation of porphyrins in mouse skin. In this study the authors suggest that DMSO acts as a stratum corneum emollient. DMSO does not always improve permeation, however. Jantharapprapap, R. & Stagni, G. (2007) showed that neither DMSO nor Tween 20 enhanced the permeation of meloxicam gels through human cadaver skin, although DMSO was only included at 1, 5 and

10% compared to 100% in this chapter. The extent of permeation enhancing effects related to the concentration of DMSO has already been discussed, which may explain the results obtained by Jantharapprapap, R. & Stagni, G. (2007).

The permeation rates of the two STIs increased when applied together compared to when they were applied individually. This is could be a consequence of the increased thermodynamic activity when both compounds were present in the vehicle; alternatively, it could have been due to a complexation effect.

.

This chapter has also illustrated that tamoxifen cannot be metabolised within the skin. Tamoxifen, when administered orally, is readily metabolised in the liver and small intestine by the cytochrome P450 (CYP450) enzymes, particularly the CYP4503A subfamily (Tucker, A.N. *et al* 2005). CYP4502D and CYP4502C have also been linked to the formation of N-desmethyltamoxifen (N-DMT), 4-hydroxytamoxifen (4-OHT), and 4-hydroxy-N-desmethyl-tamoxifen (4OHNDMT) (Gallicchio, L. *et al* 2004). The skin does not contain CYP450 enzymes, and so it was necessary to examine if epidermal enzymes, including esterases, were capable of metabolizing tamoxifen into identified or novel metabolites. The presence of homogenized skin, and so liberated epidermal enzymes did not affect the concentration of tamoxifen, suggesting that tamoxifen metabolism is a CYP450 specific process.

Several studies, including the aforementioned study by Mauvais-Jarvis have demonstrated that 4-hydroxytamoxifen readily permeates breast skin *in* vivo. A further study compared gel formulations with increasing 4-hydroxytamoxifen concentrations to oral tamoxifen on several breast cancer markers. The authors reported that the topical formulations were capable of significantly reducing tumor tissue proliferation indexes, such as ki-67 and PCNA and that this reduction was comparable to that seen with oral tamoxifen administration, however, no benefit was seen with increased 4-hydroxytamoxifen concentrations. The 4-hydroxytamoxifen gels did not effect the expression of the apoptotic marker BCL-2. Although plasma levels of 4-hydroxytamoxifen was consistently higher when tamoxifen was administered orally and although the topical 4-hydroxytamoxifen gels were generally well tolerated, hot flushes were as common in the higher gel doses as with oral tamoxifen (Rouanet, P. *et al* 2005).

Immunocytochemical assessment of DMSO treated skin revealed alarming toxicological effects. H&E analysis showed that DMSO caused the stratum corneum to separate from the underlying epidermis and keratinocyte nuclei loss after just 3 hours incubation with DMSO. Smith, E.R. *et al.* (1966) demonstrated that repeated exposure of up to 80% DMSO gave rise to punctate ulcerative lesions on the skin.

3.5 Conclusions

These studies have demonstrated several things. Firstly, preliminary permeation studies revealed that compounds only differing in structure slightly can have drastically different skin permeating capabilities. LY294002, a compound developed from quercetin showed a significantly superior ability to permeate full thickness porcine skin. These permeation studies highlighted PD98059 and LY294002 as the best candidates to take forward to develop into a transcutaneous formulation based on their permeating capabilities compared to SL327 and quercetin.

It was also noted that epidermal enzymes were not capable of metabolising tamoxifen to its more potent metabolite 4, hydroxytamoxifen.

These studies also showed that when PD98059 and LY294002 were formulated together in DMSO, the permeation of both compounds was significantly enhanced, in-fact, each compound seemed to enhance the permeation of the other synergistically. However, the addition of 4-hydroxytamoxifen did not affect the permeation of the two compounds further. 4-hydroxytamoxifen was capable of permeating full thickness porcine skin when formulated with PD98059 and LY294002.

Upon assessment of DMSO as a clinically suitable vehicle, it soon became clear that the pure DMSO solution gave rise to skin toxicity by damaging the stratum corneum and keratinocytes. This observation on the skin toxicity

eliminated DMSO as a possible vehicle for further development, and so another 'skin friendly' vehicle must be found.

Chapter 4

Transcutaneous delivery of PD98059, LY294002 and 4-hydroxytamoxifen from a fish oil vehicle.

4.1 Introduction

Chapter 3 demonstrates the plausibility of delivering 4-hydroxytamoxifen, PD98059 and LY294002 across excised porcine skin. However, the use of ICC revealed that DMSO inflicted severe skin toxicity. This analysis showed stratum corneum toxicity and keratinocyte nuclei loss, thus keratinocyte toxicity. At high concentrations, above 60%, DMSO can cause delamination of the stratum corneum and protein denaturing. Moreover these effects are not reversible which limits the usefulness of DMSO as a vehicle (Williams, A.C. 2003). The issue regarding skin toxicity eliminated DMSO as a viable vehicle to develop an anti-breast cancer formulation and so an alternative vehicle had to be found.

Fatty acids are widely established as being successful topical penetration enhancers. Green, P.G. and colleagues (1988) suggested that fatty acids achieve this enhancing quality by having a kinked structure due to their double bond. As the kinked fatty acid enters the straight chain structured stratum corneum lipid environment they intercalate and cause perturbation of the ordered lipid array (Walker, R.B. & Smith, E.W. 1995). It has also been proposed that oleic acid may increase the fluidity of the stratum corneum lipids by decreasing the phase transition temperatures of these lipids, therefore, simplifying the permeation of many compounds of differing polarities (Golden, G.M., *et al* 1987). It has also been demonstrated that the combination of fatty acids with polar solvents such as propylene glycol augments permeation of many compounds. It is postulated that this combination may reduce the

resistance of the stratum corneum or the diffusional path length by making the route of administration less tortuous. The authors suggest that the combination achieves this by stimulating severe alterations in the membrane lipid structure, which causes faults between solid and liquid phases (Ongpipattanakul, B. *et al* 1991).

It has been previously reported that fish oil provides a useful vehicle for several non-steroidal anti-inflammatory drugs (NSAIDs) including ketoprofen (Thomas, C.P. & Heard, C.M. 2004). It has also been suggested that thermodynamic activity is not responsible for the penetration of these NSAIDs into the skin, rather, the permeants enter the skin bound to the fish oil vehicle and permeate via a 'pull effect' phenomenon. This phenomenon involves the binding of compound and vehicle in a solvation cage (Heard, C.M. *et al* 2003). Indeed it was later proposed, through the use of NMR studies, that ketoprofen bound to EPA as it permeated the skin and that EPA along with DHA were quantitively detected in the receptor phase of diffusion cell studies (Thomas, C.P. *et al* 2007).

Other oils and fatty acids have also been shown to permeate the skin and act as permeation enhancers. Topically applied safflower oil was shown to be absorbed and provide nutritional benefits (Solanki, K. *et al* 2005). The permeation of tamoxifen has also been shown when formulated in borage oil, this formulation allowed the simultaneous delivery of tamoxifen and gamma linolenic acid. (Karia, C. *et al* 2003). Later, permeation studies and HNMR

spectral data revealed that complexation occurred between polyunsaturated constituents of borage oil (eg γ linolenic acid) and tamoxifen and that these complexes permeated intact (Heard, C.M. *et al* 2005).

The use of fish oil would provide a superior vehicle in which to formulate tamoxifen and the two STIs; however, to develop this into a clinically acceptable formulation it would need to be thickened to produce a more viscous gel, cream or paste. HPC has previously been investigated as a thickening agent for fish oil based formulations. It was shown that while this formulation did not affect the permeation of ketoprofen, the permeation of the constituents of fish oil, such as EPA and DHA were retarded significantly.

Cab-o-sil® is an amorphous, synthetic and untreated fumed silicon dioxide. It is an inert thickening agent, which is used to thicken many liquids including tomato ketchup. Omran, M.O. and colleges (1996) used cab-o-sil to thicken oily suspensions for the oral delivery of sodium salicylate. Here they show that up to 0.3% Cab-o-sil allows adequate release of the active ingredient into the blood, however, at 1% and above strong H-bonds between the cab-o-sil silanol groups and sodium salicylate prevent its release. Previously, Cab-o-sil was also employed to increase the viscosity of topical preparations containing NSAIDs. (Gallagher, S.J. *et al* 2003).

The utilisation of fish oil as a vehicle, and the subsequent permeation of EPA, an n-3 fatty acid, would provide a possible additional therapeutic benefit to the

formulation. Many studies have investigated the role of inflammation, in particular the role of the cyclooxygenase enzymes, in cancer. These studies link it to breast cancer tumor initiation, progression and metastatic spread. With this in mind, the inclusion of an inhibitor of these cyclooxygenase enzymes seems attractive.

As 4-hydroytamoxifen, PD98059 and LY294002 are lipophilic compounds; the aims of this work were to incorporate fish oil as an alternative vehicle to DMSO and to probe the effect of chemical permeation enhancers and Cab-o-sil® on the transcutaneous delivery of 4-hydroxytamoxifen, PD98059 and LY294002.

4.2 Materials and Methods

4.2.1 Materials

The materials used in this chapter have been discussed in chapter 2.

4.2.2 Methods

4.2.2.1 Solubility and stability of 4-hydroxytamoxifen, PD98059 and LY294002 in fish oil

Solubility and stability of 4-hydroxytamoxifen, PD98059 and LY294002 in fish oil was performed as described for their solubility and stability in DMSO in chapter 3.

Samples were diluted 1/20 in methanol before analysis.

4.2.2.2 Preparation of porcine skin membrane

Skin membranes were prepared as previously stated in chapter 2.

4.2.2.3 *In vitro* transcutaneous delivery of 4-hydroxytamoxifen, PD98059 and LY294002 in a fish oil vehicle

Transcutaneous delivery (i.e. across full thickness skin) was modelled using glass Franz-type diffusion cells as described in chapter 2. A receptor phase of cetrimide 30mgmL^{-1} plus 0.05% butylated hydroxyanisole (BHA) to prevent oxidation of any permeating polyunsaturated fatty acid (Howard, F.A. & Henderson, C. 1999) was added along with a magnetic stirrer bar. The cells were dosed with 200µl of 4-hydroytamoxifen, PD98059 or LY294002 made up in fish oil, previously prepared to provide equimolar aliquots of 2.54 x 10^{-4} mol. The donor phase compartments were occluded with Whatman Parafilm and at 3, 6, 12, 24 and 48 hours the entire contents of the receptor phases removed for analysis, and replenished with fresh solution. Removed receptor phase was separated into 3 x 1mL aliquots and stored at -20°C until required.

4.2.2.4 Probing the effect of permeation enhancers on the permeation of 4-hydroxytamoxifen, PD98059 and LY294002

The addition of various chemical penetration enhancers was assessed for their ability to improve the permeation of 4-hydroxytamoxifen, PD98059 and

LY294002. The in vitro transcutaneous delivery protocol as stated in 4.2.2.4 was followed; however, the cells were dosed as shown in table 4.1.

Cell numbers	Vehicle	Enhancer
1-5	Fish oil	5% DMSO
6-10	Fish oil	5% Ethanol
11-15	Fish oil	5% 1,8-cineole
16-20	Fish oil	2.5% DMSO / 2.5% ethanol
21-25	Fish oil	2.5% DMSO / 2.5% 1,8-cineole
26-30	Fish oil	2.5% ethanol / 2.5% 1,8-cineole

Table 4.1 Table to show the vehicle and enhancer combinations used.

Donor phases were dosed with 200µl of each formulation, with each dose containing equimolar concentrations of 4-hydroxytamoxifen, PD98059 and LY294002 at 2.54 x 10^{-4} mol. Enhancers were tested firstly alone and then in combination to establish whether synergy or additive benefit could be achieved.

4.2.2.5 Probing the effect of Cab-o-sil® on the permeation of tamoxifen, PD98059 and LY294002

The effect of the addition of the thickening agent Cab-o-sil on the permeation of all 3 compounds and EPA was assessed to evaluate the possibility of creating a viscous gel formulation. The in vitro transcutaneous delivery

protocol as stated in 4.2.2.4 was followed; however, the cells were dosed as shown in table 4.2.

Cell numbers	% Cabosil
1-5	0
6-10	4
11-15	4.5
16-20	5
21-25	5.5
26-30	6

Table 4.2 Table to show the percentage of Cab-o-sil used in the fish oil and enhancer formulations. This was repeated for formulations containing 2.5% DMSO/ethanol, DMSO/1,8 cineole and 1,8 cineole/ethanol n=5.

The donor phase of each diffusion cell was dosed with 200µl of each formulation containing equimolar concentrations of each compound (2. 5 x 10^{-4} mol). The compounds were formulated in a fish oil vehicle and various concentrations of Cab-o-sil were added.

4.2.2.6. HPLC analysis

Samples were analysed using methods stated in chapter 2. Samples were also analysed for EPA. Again, samples were separated on a Phenomenex Luna C18 column (150 x 4.6 mm, 5µm). However an isocratic mobile phase of 20:80

methanol:water with 2.5% acetic acid was employed and detection was at 210nm. EPA, under these conditions, had a retention time of 6.5 minutes.

4.2.2.7 Immunohistological analysis of porcine skin

4.2.2.7.1 Haematoxylin assay to reveal the histological effects of fish oil on porcine skin

The immunohistological procedure as outlined in chapter 3 was followed. However, in this case, freshly excised and HHBBSS maintained porcine skin was dosed with the following treatments, shown in table 4.3. The fish oil formulation included 0.05% v/v BHA to prevent the oxidation of the fish oil constituents. At the times stated within table 4.3 the skin to which the treatments were applied was cut into 3 x 1 mm pieces and transferred to 3.7% formaldehyde solution.

Processing of the skin tissue, embedding and microtoming was followed as stated in chapter 3.

Cell number	Treatment	Time Processed at (hour)
1-3	Water	0
7-9	Water	5
10-12	Fish oil	5
13-15	Water	12
16-18	Fish oil	12

Table 4.3 Table to show the treatment and processing regime prior to H&E staining and ki67 assay.

4.2.2.8 Immunocytochemical analysis of porcine skin

The immunocytochemical procedure as outlined in chapter 2 was followed, however freshly excised and HHBBSS maintained porcine skin was dosed with the following treatments, shown in table 4.4. The fish oil formulation included 0.05% v/v BHA, 2.5% v/v DMSO/etOH and 4% w/v cab-o-sil. At the times stated within table 4.4 the skin to which the treatments were applied was cut into 3 x 1 mm pieces and transferred to 3.7% formaldehyde solution.

4.2.2.8.1 Ki-67 assay

ICC was performed as outlined in chapter 3, however freshly excised and HHBBSS maintained porcine skin was dosed with the following treatments, shown in table 4.3. . The fish oil formulation included 0.05% v/v BHA0.05% v/v BHA, 2.5% v/v DMSO/etOH and 4% w/v cab-o-sil. At the times stated within table 4.3 the skin to which the treatments were applied was cut into 3 x 1 mm pieces and transferred to 3.7% formaldehyde solution. Processing of skin tissue, embedding, microtoming and Ki-67 assay were performed as stated in chapter 2.

4.2.2.8.2 pERK1/2, pAkt, pEGFR1068 and total COX-2

To examine the effects of the cocktail formulation on pERK1/2, pAkt, pEGFR1068 and COX-2 in the skin ICC analysis of skin treated with either water, fish oil (plus 2.5% v/v DMSO/etOH and 4% w/v cab-o-sil) or fish oil,

and 2.54 x 10^{-4}M PD98059, LY294002, 4-hydroxytamoxifen (plus 2.5% v/v DMSO/etOH and 4% w/v cab-o-sil) was determined. Skin was dosed with formulations as stated in table 4.4 and fixed at the stated times.

Cell number	Treatment	Time Processed at (hour)
1-3	Water	0
4-6	Water	3
7-9	Fish oil	3
10-12	PD LY 4OHTam fish oil	3
13-15	Water	6
16-18	Fish oil	6
19-21	PD LY 4OHTam fish oil	6
22-24	Water	12
25-27	Fish oil	12
28-30	PD LY 4OHTam fish oil	12

Table 4.4 Table to show the treatment and processing regime prior to ICC analysis. PD = 25μM PD98059, LY = 5μM LY294002, 4OHTam = 1 x 10^{-7} M 4-hydroxytamoxifen.

Processing of skin tissue, embedding and microtoming protocol was followed as stated in chapter 2. The skin sections were then assayed for pERK1/2, pAkt, pEGFR1068 and total COX-2 as stated in chapter 2.

4.2.3 Statistical analysis

Comparison between the mass permeated, flux and lag times of compounds were compared between each formulation using un-paired t-tests. All statistical analysis was performed using Minitab for Windows.

4.3 Results

4.3.1 The effect of fish oil on excised porcine skin

4.3.1.1 H & E staining

Haematoxylin and eosin staining revealed a clear histology of the porcine skin and showed that it was very similar in appearance to human skin. Figure 4.1 shows the H & E staining of fish oil treated skin compared to skin treated with water. Figure 4.1A shows haematoxylin and eosin staining on excised porcine skin at 0 hours post-dissection.

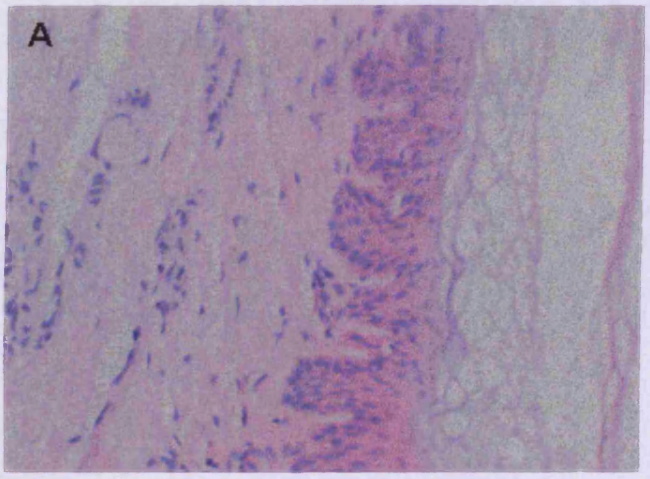

Figure 4.1 A H & E assay on paraffin embedded excised porcine skin after 0 hours. Sections were cut at 5µm on a Shandon Finesse 325 microtome. A- x 20

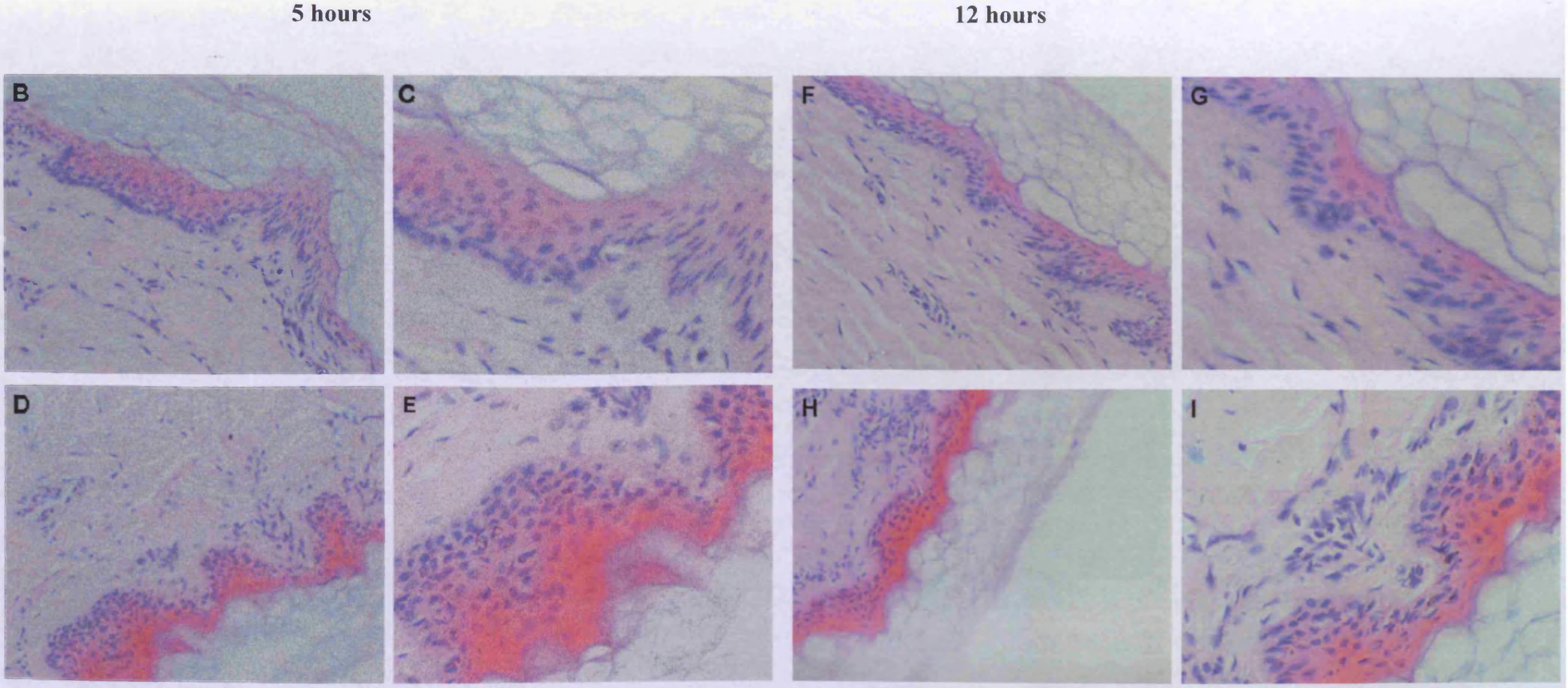

Figure 4.1 C-J. H & E assay on paraffin embedded excised porcine skin after 5 hours (B-E) and 12 hours (F-I) incubation with water control (B-C, F-G) or 200µl fish oil (D-E, H-I). Sections were cut at 5µm on a Shandon Finesse 325 microtome. F, H x 10, B, D- x 20 C, E, F, I- x 40.

4.3.1.2 Ki-67 assay

A ki-67 assay was used to determine the viability of fish oil treated skin compared to water controls. This assay is displayed in figure 4.2. Figure 4.2A shows a negative control, in which PBS was applied to the section instead of primary antibody. This demonstrates that any staining seen in figure 4.2B is specific ki-67. Figure 4.2B shows a section of skin at 0 hours. This displays the time point where the skin is most viable and so was used as a reference for the other time points.

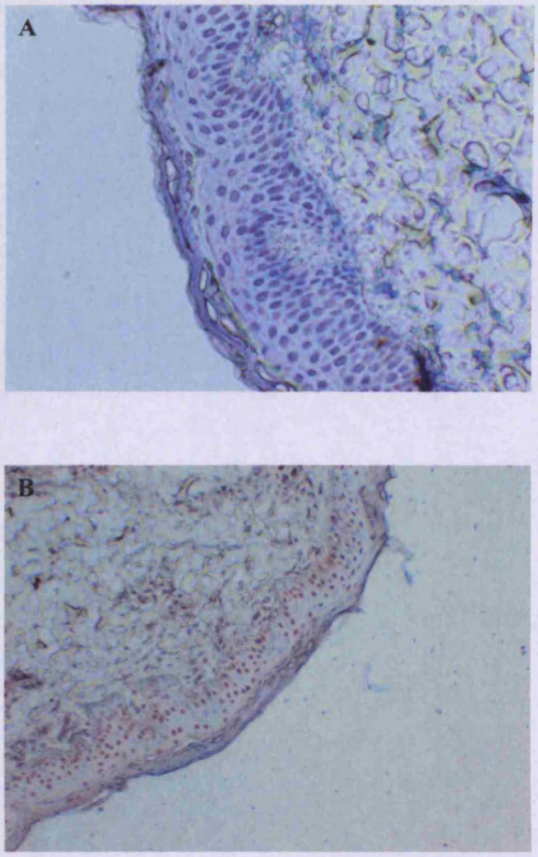

Figure 4.2 A-B. ICC assay to detect ki-67 in excised porcine skin after 0 hours incubation with water control A - ICC negative control. PBS applied instead of primary antibody. B - ICC positive control. Primary antibody was DAKO MIB made up in 0.1% BSA in PBS at 1/50. Sections were cut at 5μm on a Shandon Finesse 325 microtome. A- x 20 B- x 10.

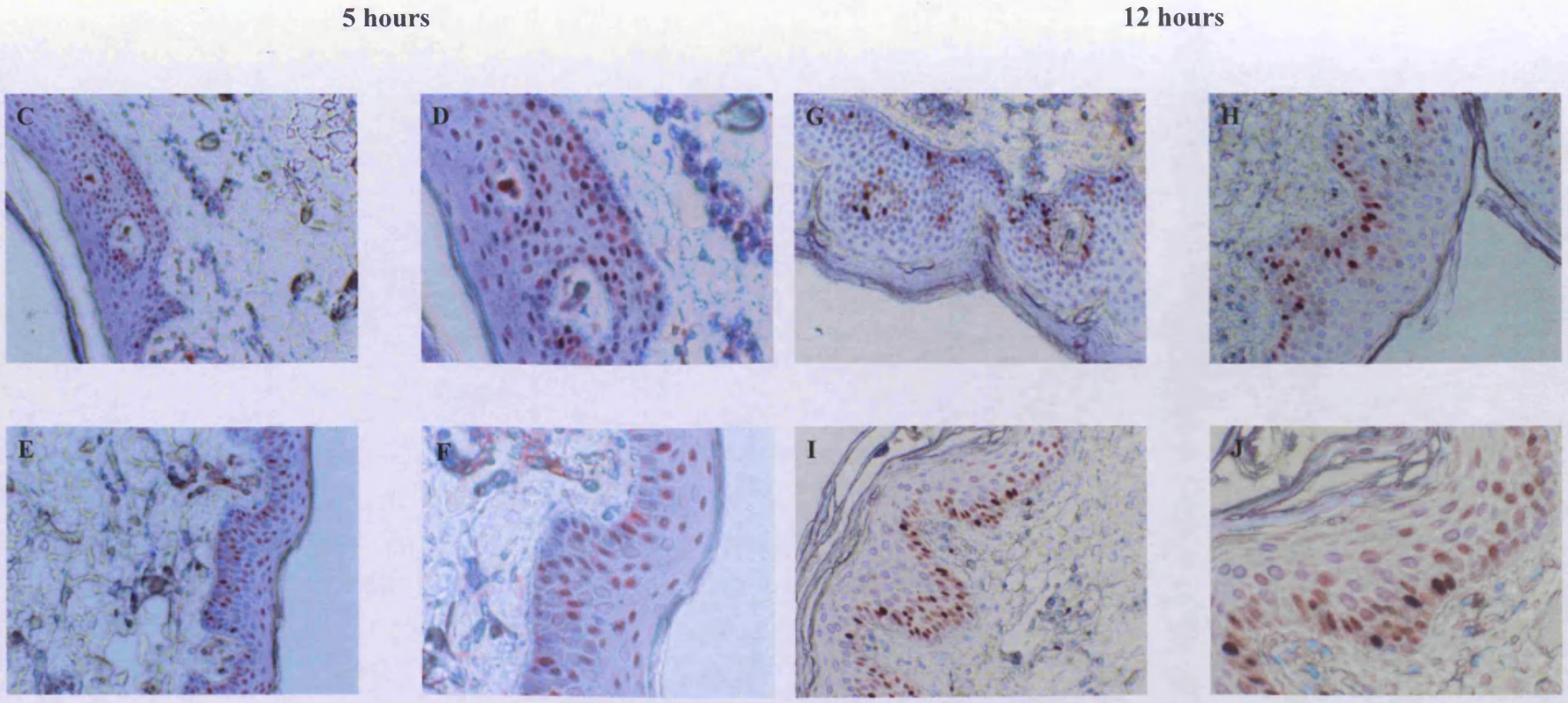

Figure 4.2 C-F. ICC assay to detect ki-67 in excised porcine skin after 5 hours (C-F) and 12 hours (G-J) incubation with water control (C-D, G-H) or fish oil (E-F, I-J). Receptor phase was HHBBSS and skin was maintained at 32°C. Primary antibody was DAKO MIB made up in 0.1% BSA in PBS at 1/50. Sections were cut at 5µm on a Shandon Finesse 325 microtome microtome. C, E, G, I- x 20, D, F- x 40.

Figure 4.2 C-F shows sections of skin left in the presence of either water or fish oil for five hours. C-D shows water treated skin, which shows positive ki-67 staining of the same degree as seen in E-F, which was treated with fish oil. In figure 4.2 C and D it is clear that the stratum corneum has detached from the underlying epidermis, whereas, the fish oil formulation does not cause this detachment to occur.

Figure 4.2 G-J shows sections of porcine skin after incubation for 12 hours. Again, both water and fish oil treated sections are positive for ki-67. In these sections, however, it is predominantly seen within the basal layer of the epidermis compared to staining throughout the epidermis that was seen at 5 hours. Stratum corneum damage is seen with both treatments at this time point, although is much less severe than that seen with DMSO treated skin.

4.3.2 Suitability of fish oil as vehicle for the permeation of 4-hydroxytamoxifen, PD98059 and LY294002

4.3.2.1 Solubility and Stability of 4-hydroxytamoxifen, PD98059 and LY294002 in fish oil

The solubility of PD98059 LY294002 and 4-hydroxytamoxifen in fish oil was $2.47 \pm 0.13 mgmL^{-1}$, $5.16 \pm 0.41 mgmL^{-1}$ and $3.83 \pm 0.17 mgmL^{-1}$ respectively when assessed separately. The solubility of all 3 compounds did not change significantly when determined within the same solution. These were $2.21 \pm 0.1 mgmL^{-1}$, $5.48 \pm 0.62 mgmL^{-1}$ and $4.12 \pm 0.46\ mgmL^{-1}$ respectively.

Table 4.5 displays the stability and degree of degradation of 4,hydroxytamoxifen, PD98059 and LY294002 singly and together.

Time (hours)	% Degradation							
	PD	LY	Tam	PD + LY		All 3		
				PD	LY	PD	LY	Tam
0	0	0	0	0	0	0	0	0
5	0	0	0	0	0	0	0	0
12	0.1	0.248	0.13	0.035	0.165	0.054	0.065	0
24	1.44	0.76	1.276	1.87	1.487	1.242	1.232	0.98
48	1.872	2.12	1.891	2.18	1.845	1.987	2.141	2.795
168	10.576	9.598	9.154	7.15	8.186	6.905	7.86	7.58

Table 4.5 Table to show the degree of degradation of PD98059 and LY294002, both singly and together in a fish oil vehicle.

This degradation data suggests that all 3 compounds can be left at room temperature for 48 hours and overnight analysis can be performed without causing errors in results obtained. It can also be seen that the combination of compounds seems to slightly reduce the amount of degradation of all 3 compounds.

4.3.2.2 *In vitro* transcutaneous delivery of PD98059, LY294002 and 4-hydroxytamoxifen

As stated in chapter 3, the mass of PD98059, LY294002 and 4-hydroxytamoxifen that permeated after 48 hours when applied simultaneously in a DMSO vehicle was 9.1μgcm^{-2} ± 2.19, 20.18μgcm^{-2} ± 2.83 and 15.99μgcm^{-2} ± 0.963 respectively. However, a replacement vehicle had to be found due to the skin toxicity of DMSO. Fish oil was chosen to replace DMSO and assessed as a vehicle for the delivery of both PD9805 and LY294002. Figure 4.3 shows the cumulative mass of PD98059, LY294002 and 4-hydroxytamoxifen that permeated across excised porcine skin after 48 hours when applied simultaneously in a fish oil vehicle.

Figure 4.3 shows that the order of permeation of the two compounds changed from 0-order when combined in a DMSO vehicle to first order when formulated in a fish oil vehicle.

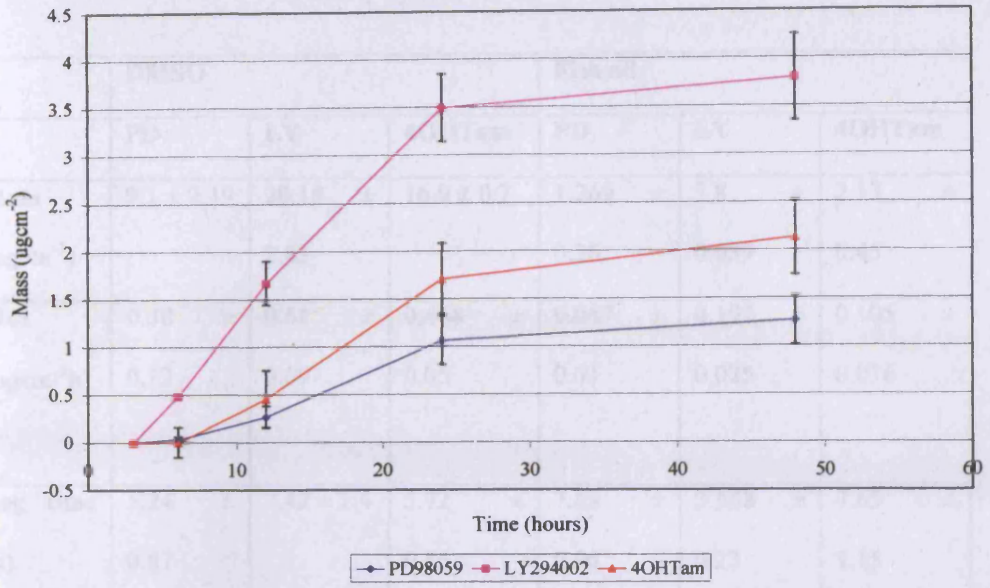

Figure 4.3 Permeation profile to compare the mass (μgcm^{-2}) of simultaneously applied PD98059, LY294002 and 4-hydroxytamoxifen across excised porcine skin. Donor phase was 2.54 x 10^{-4}mol PD98059, LY294002 and 4-hydroxytamoxifen in 200µl fish oil with 0.05% BHA. Receptor phase was 30mgmL^{-1} cetrimide solution, it was stirred continuously and maintained in a water bath set to maintain a skin surface temperature of 32°C (n=6 ± SD).

Permeation data for PD98059, LY294002 and 4-hydroxytamoxifen when applied to the skin simultaneously in fish are displayed in table 4.6. This table also compares permeation this data to that obtained in chapter 3, when compounds were formulated in a DMSO. This comparison highlights many interesting data. The extent of the reduction in permeation when formulated in fish oil compared to DMSO is clear and was significant for all compounds (P = 0.006, 0.001 and 0.0005 for PD98059, LY294002 and 4-hydroxytamoxifen respectively).

	DMSO			Fish oil		
	PD	LY	4OHTam	PD	LY	4OHTam
Mass (μgcm^{-2})	9.1 ± 2.19	20.18 ± 2.83	16.0 ± 0.7	1.269 ± 0.26	3.8 ± 0.039	2.13 ± 0.45
Flux ($\mu gcm^{-2}h^{-1}$)	0.38 ± 0.12	0.61 ± 0.09	0.468 ± 0.05	0.067 ± 0.01	0.197 ± 0.025	0.105 ± 0.016
Lag time (h)	5.24 ± 0.87	7.42 ± 1.4	5.72 ± 0.86	7.83 ± 0.96	3.558 ± 0.23	7.65 ± 1.15
Kp (cm^2h^{-1})	$1.96 \times 10^{-2} \pm 6.2 \times 10^{-3}$	$1.993 \times 10^{-2} \pm 2.9 \times 10^{-3}$	$1.93 \times 10^{-2} \pm 2.1 \times 10^{-3}$	$3.45 \times 10^{-3} \pm 5.2 \times 10^{-4}$	$6.44 \times 10^{-3} \pm 8.2 \times 10^{-4}$	$4.34 \times 10^{-3} \pm 6.6 \times 10^{-4}$

Table 4.6 Table to show the mass of PD98059, LY294002 and 4-hydroxytamoxifen permeated, flux, lag time and Kp when formulated in DMSO and fish oil vehicle.

The table also shows that the flux of all 3 compounds was reduced significantly ($P = 0.014$, 0.003 and 0.001) for PD98059, LY294002 and 4-hydroxytamoxifen respectively.

Lag times did not follow this pattern. The lag time of PD98059 was significantly increased when formulated with fish oil ($P = 0.039$), whereas the lag time of LY294002 was significantly reduced ($P = 0.02$) while there was no significant effect on the lag time of 4-hydroxytamoxifen ($P = 0.263$). Overall,

it is obvious that the use of fish oil as a vehicle limits the permeation of all 3 compounds significantly compared to when applied in DMSO.

However, formulation into a fish oil vehicle gave a fourth prong to this cocktail therapeutic with the delivery of COX inhibitors. One such inhibitor found in fish oil is eicosapentaenoic acid (EPA). The mass of EPA permeating the skin, therefore, was calculated.

Figure 4.4 shows the mass (μgcm^{-2}) of EPA that permeated the skin from the fish oil vehicle when formulated with PD98059, LY294002 and 4-hydroxytamoxifen. In these conditions 266.95 ± 31.18μgcm^{-2} of EPA permeated excised porcine skin after 48 hours. However, when applied to the skin in the absence of the two signal transduction inhibitors and 4OH tamoxifen, no EPA permeation was detected.

Compared to the permeation of PD98059, LY294002 and 4OH tamoxifen, a large amount of EPA seemed to permeate, however, when converted into the percentage of applied dose permeated it was obvious that a huge concentration gradient existed between the dosed mass and that within and permeating the skin.

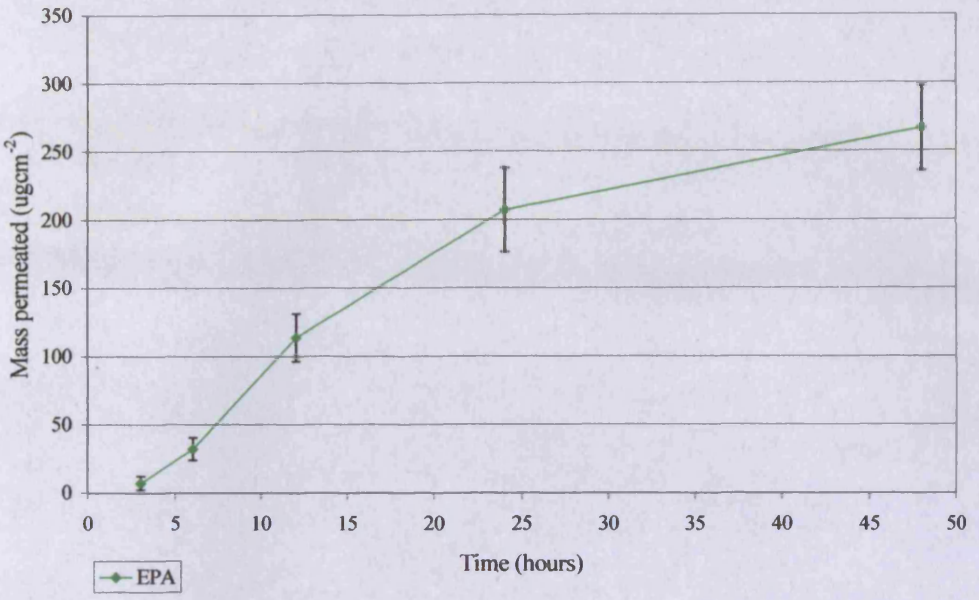

Figure 4.4 Permeation profile showing the mass (μgcm^{-2}) of EPA permeated from the fish oil vehicle, through excised porcine skin. Donor phase was 2.54 x 10^{-4}mol PD98059 and LY294002 in 200µl fish oil with 0.05% BHA. Receptor phase was 30mgmL^{-1} cetrimide solution, it was stirred continuously and maintained in a water bath set to maintain a skin surface temperature of 32°C (n=6 ± SD).

Steady state flux of EPA was reached after 6 hours. The flux of EPA under these conditions was 7.798 ± 1.31$\mu gcm^{-2}h^{-1}$ and the lag time was 3.744 ± 0.31 hours. The permeability coefficient was determined as 1.2 x 10^{-4} ± 1.98 x $10^{-5}cm^2h^{-1}$.

4.3.3 The effect of chemical penetration enhancers and their combinations on the permeation of 4-hydroxytamoxifen, PD98059 and LY294002

Due to the poor permeation of all 3 compounds in fish oil, this section aimed to improve permeation with the addition of three well known CPEs and

combinations of these. DMSO, ethanol and 1,8-cineol were the chosen as CPEs and were used at 5% (v/v) when assessing their effect separately and at 2.5% (v/v) when combining CPEs.

Figure 4.5 shows the permeation of PD98059 when formulated with the three CPEs and combinations of enhancers.

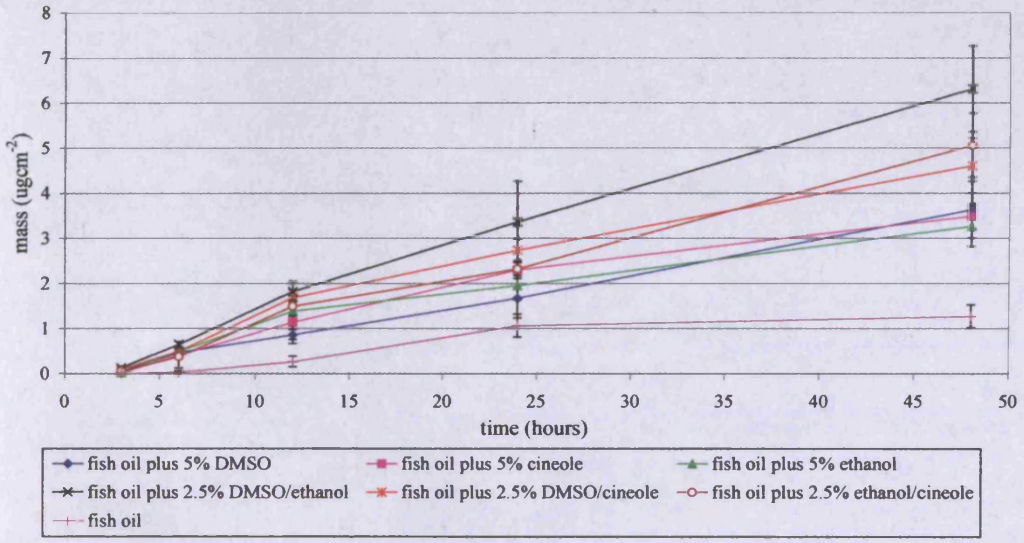

Figure 4.5 Permeation profile showing the mass (μgcm^{-2}) of PD98059 permeating from the fish oil vehicle, combined with various enhancers and enhancer combinations. Donor phase was 2.54 x 10^{-4}mol PD98059 and LY294002 in 200µl fish oil with 0.05% BHA. Receptor phase was $30mgmL^{-1}$ cetrimide solution, it was stirred continuously and maintained in a water bath set to maintain a skin surface temperature of 32°C (n=6 ± SD).

Figure 4.5 shows that the mass of PD98059 permeated could be manipulated with addition of various enhancers. All enhancers and enhancer combinations increased the permeation of PD98059 when compared to the permeation seen with fish oil alone. The highest mass permeated was seen when fish oil was

formulated with a combination of 2.5% DMSO/ethanol. This formulation allowed 6.31 ± 0.95 μgcm^{-2} of PD98059 to permeate after 48 hours, which was significantly greater than from fish oil alone (P = 0.01). This was statistically indistinguishable from the mass permeating from a DMSO vehicle (P = 0.092). PD98059 permeated with a flux of 0.195 ± 0.02 $\mu gcm^{-2}h^{-1}$ and the lag time was 2.39 ± 0.5 hours when formulated with these two CPEs. Steady-state flux was statistically greater with the presence of 2.5% DMSO/ethanol (P = 0.016) and lag time was significantly shorter (P = 0.003). The permeation coefficient of PD98059 in this formulation was $1.02 \times 10^{-2} \pm 3.09 \times 10^{-3}$ cm^2h^{-1}, which was higher than that seen when PD98059 was formulated with fish oil alone.

Table 4.7 shows the enhancement ratio (EnR) of the mass permeated of PD98059 with the various CPEs and combinations. It shows that the combinations of CPEs enhance the permeation of PD98059 greater than when included individually. The EnR data also highlights that the combination of DMSO and ethanol (both at 2.5% v/v) gave the greatest enhancement.

The inclusion of the enhancers also affected the permeation of LY294002 through excised porcine skin. Figure 4.6 shows permeation profiles for LY294002 when formulated with the various enhancers (PD98059 and 4-hydroxytamoxifen also present in formulation).

Again, as with the permeation of PD98059, the combination of DMSO and ethanol gave maximal permeation of LY294002. This formulation allowed 9.4

± 0.95 μgcm^{-2} of LY294002 to permeate after 48 hours. This was significantly greater than the mass that permeated when LY294002 was formulated in fish oil alone (P = 0.003). However, this was still significantly less than that seen with a pure DMSO vehicle (P = 0.0026).

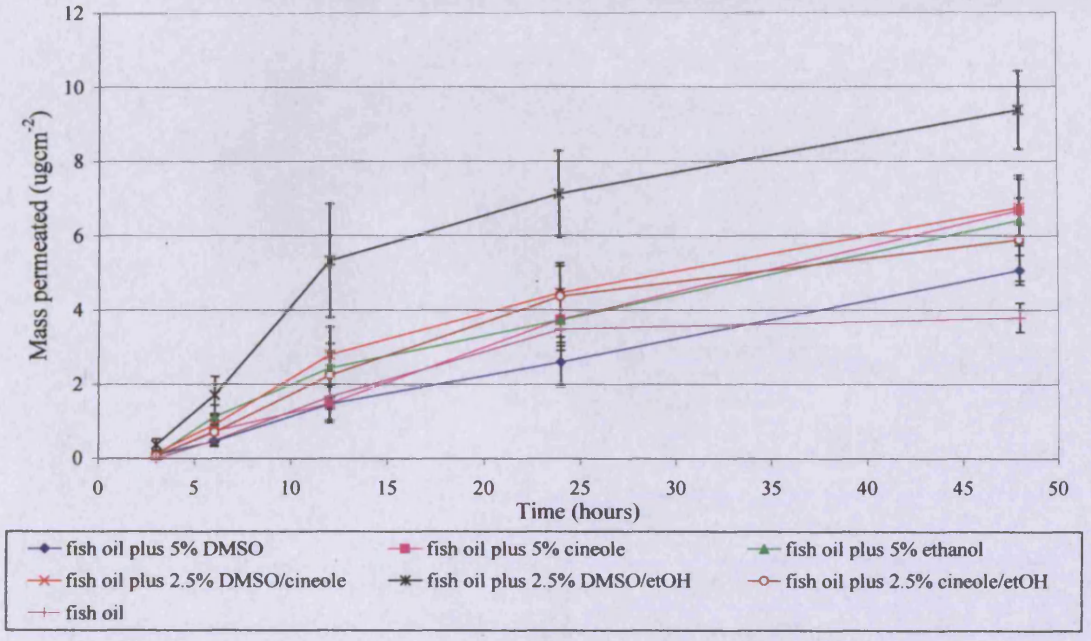

Figure 4.6 Permeation profile showing the mass (μgcm^{-2}) of LY294002 permeating from the fish oil vehicle, combined with various enhancers and enhancer combinations. Donor phase was 2.54 x 10^{-4} mol PD98059 and LY294002 in 200μl fish oil with 0.05% BHA. Receptor phase was 30mgmL^{-1} cetrimide solution, it was stirred continuously and maintained in a water bath set to maintain a skin surface temperature of 32°C (n=6 ± SD).

LY294002 permeated with a flux of 0.6 ± 0.08 μgcm^{-2}h^{-1}, which was significantly greater than from fish oil alone (P = 0.001) and the lag time was 3.03 ± 0.54 hours, which was not significantly changed by the addition of DSMO/ethanol to the formulation (P = 0.145). The permeation coefficient of

LY294002 in this formulation was $2.0 \times 10^{-2} \pm 2.26 \times 10^{-3}$ cm^2h^{-1}, which was greater than that seen when LY294002 was formulated in fish oil alone.

CPE(s)	EnR PD	EnR LY	EnR 4OHTam	EnR EPA
DMSO	2.8	1.3	1.53	4.4
etOH	2.76	1.7	1.22	2.4
1,8-cineole	2.5	1.76	1.28	3.5
DMSO/etOH	5.0	2.5	2.5	5.0
DMSO/1,8-cineole	3.6	1.78	1.96	4.1
1,8-cineole/etOH	3.9	1.55	1.96	3.4

Table 4.7 Table to show the enhancement ratio (EnR) in the mass permeated of PD98059 (PD), LY294002 (LY), 4-hydroxytamoxifen and EPA when formulated in a fish oil vehicle with various enhancers present compared to fish oil alone.

Table 4.7 shows that the addition of ethanol, 1,8-cineole, DMSO/1,8-cineole or 1,8-cineole/ethanol all gave rise to similar EnRs for the mass of LY294002 permeating after 48 hours. The EnR data also confirms that the formulation containing the combination of DMSO and ethanol gave maximal enhancement of LY294002.

The permeation of 4-hydroxytamoxifen was also assessed in the presence of the CPEs.

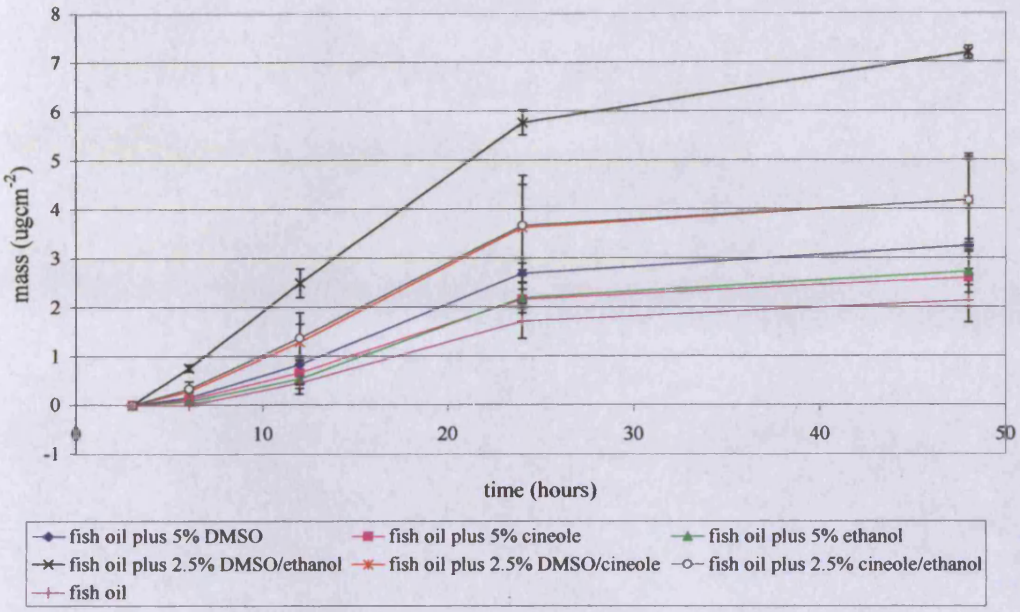

Figure 4.7 Permeation profile showing the mass (μgcm^{-2}) of 4-hydroxytamoxifen permeating from the fish oil vehicle, combined with various enhancers and enhancer combinations. Donor phase was 2.54 x 10^{-4} mol PD98059 and LY294002 in 200µl fish oil with 0.05% BHA. Receptor phase was $30mgmL^{-1}$ cetrimide solution, it was stirred continuously and maintained in a water bath set to maintain a skin surface temperature of 32°C (n=6 ± SD).

Figure 4.7 shows permeation profiles for 4-hydroxytamoxifen when formulated with the various enhancers. Again, the combination of DMSO and ethanol gave maximal permeation of 4-hydroxytamoxifen. This formulation allowed 7.19 ± 0.13 μgcm^{-2} of 4-hydroxytamoxifen to permeate after 48 hours, which was significantly greater that that permeation seen without CPEs present ($P = < 0.001$), however was still significantly less than that permeating when 4-hydroxytamoxifen was formulated in DMSO ($P = 0.001$). This was a significant increase from 2.13 ± 0.45 μgcm^{-2} that permeated when 4-hydroxytamoxifen was formulated without CPEs present.

4-hydroxytamoxifen permeated with a flux of 0.27 ± 0.02 $\mu g cm^{-2} h^{-1}$, which was significantly greater than the flux seen when 4-hydroxytamoxifen was applied in fish oil alone (P = 0.002). Lag time was 3.61 ± 0.66 hours, which was significantly shorter than when CPEs were absent (0.012). The permeation coefficient of 4-hydroxytamoxifen in this formulation was 1.12 x 10^{-2} ± 8.26 x 10^{-3} $cm^2 h^{-1}$, which was greater than that seen when 4-hydroxytamoxifen was formulated in fish oil alone.

Figure 4.8 shows permeation profiles for EPA when formulated with the various enhancers.

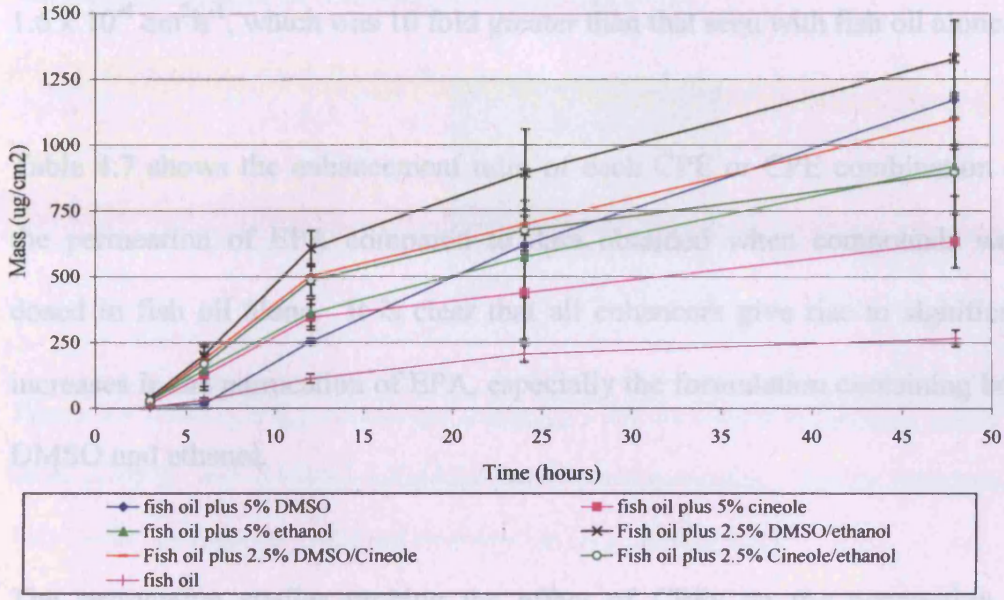

Figure 4.8 Permeation profile showing the mass (μgcm^{-2}) of EPA permeating from the fish oil vehicle, combined with various enhancers and enhancer combinations. Donor phase was 2.54 x 10^{-4} mol PD98059 and LY294002 in 200µl fish oil with 0.05% BHA. Receptor phase was 30mgmL^{-1} cetrimide solution, it was stirred continuously and maintained in a water bath set to maintain a skin surface temperature of 32°C (n=6 ± SD).

All formulations increased the permeation of EPA. However, formulations containing DMSO seemed to offer the most benefit. Again, the combination of DMSO and ethanol gave maximal permeation of EPA. This mass of EPA able to permeate when 2.5%DMSO/ethanol was added was significantly greater than when no CPEs were present (P = 0.006). The mass able to permeate from this formulation was 1329 ± 142 μgcm^{-2} after 48 hours. Steady-state flux was seen between 6 and 12 hours and was 67.67 ± 10.8 $\mu gcm^{-2}h^{-1}$ and the lag time was 3.01 ± 0.44 hours. The flux increased significantly (P = 0.011) but lag time remained statistically unchanged (P = 0.1). The permeation coefficient of

EPA seen in the presence of the DMSO/ethanol combination was $1.03 \times 10^{-3} \pm 1.6 \times 10^{-4}$ cm^2h^{-1}, which was 10 fold greater than that seen with fish oil alone.

Table 4.7 shows the enhancement ratio of each CPE or CPE combination on the permeation of EPA compared to data obtained when compounds were dosed in fish oil alone. It is clear that all enhancers give rise to significant increases in the permeation of EPA, especially the formulation containing both DMSO and ethanol.

The permeation studies probing the effect of CPEs on the permeation of PD98059, LY294002, 4-hydroxytamoxifen and EPA revealed that the formulation containing 2.5% (v/v) DMSO/ethanol gave maximal enhancement of all 4 actives.

4.3.4 Probing the suitability of Cab-o-sil ® as a thickening agent

Cab-o-sil ® was assessed as a thickening agent for the fish oil based formulation containing 2.54×10^{-4} mol PD98059, LY294002 and 4-hydroxytamoxifen, along with 2.5% v/v DMSO and ethanol and 0.05% v/v BHA.

Cab-o-sil, at various percentages, was added to the liquid formulation to produce a series of oleo gels, as described in section 4.2.2.6.

Thermodynamically stable oleo gels were generated from the addition of the various percentages of cab-o-sil, shown in figure 4.9.

Figure 4.9 Photo of a fish oil oleo gel containing 2.5% v/v DMSO and ethanol, 0.05% v/v BHA, 2.54×10^{-4} mol PD98059, LY294002 and 4-hydroxytamoxifen. This gel contained 4% Cab-o-sil®. Gels were prepared and maintained at 32° C until required.

The viscosity of these gels increased as the percentage of Cab-o-sil added increased, however, this percentage range yielded gels that could still be measured and dosed using a Gilson 1mL pipette.

Permeation data revealed all three compounds were released from all percentage Cab-o-sil oleo gels. The addition of Cab-o-sil did not affect the cumulative mass of PD98059, LY294002 or 4-hydroxytamoxifen permeating excised porcine skin after 48 hours when compared to un-thickened formulation ($P = 0.111$, 0.091 and 0.366 respectively).

% Cab-o-sil		0	4	4.5	5	5.5	6
Mass permeated after 48 h (μgcm^{-1})	EPA	1660.9 ± 98.1	1420.12 ± 119	541.89 ± 88.7	417.56 ± 56.34	16.26 ± 3.22	8.99 ± 0.76
	4OHtam	8.09 ± 0.67	8.25 ± 0.36	7.44 ± 0.81	7.28 ± 0.69	7.99 ± 0.84	8.27 ± 0.53
	LY294002	8.21 ± 0.47	9.17 ± 0.77	8.03 ± 0.82	7.86 ± 0.46	7.92 ± 0.53	9.01± 0.64
	PD90859	6.56 ± 0.24	6.92 ± 0.55	5.57 ± 0.68	5.71 ± 0.33	5.97 ± 0.81	6.18 ± 0.7

Table 4.8 Table to show the mass (μgcm^{-1}) of PD98059, LY294002, 4-hydroxytamoxifen and EPA permeated excised porcine skin after 48 hours when formulated with 2.5% DMSO/etOH and various %'s of Cab-o-sil.

The addition of Cab-o-sil did affect the release of EPA. At percentages of 4.5% and above the mass of EPA that permeated after 48 hours was significantly lower than the mass that permeated from the un-thickened formulation ($P = 0.001$ for 0% cab-o-sil vs 4.5% and less than 0.001 for other percentages of Cab-o-sil). At 4% Cab-o-sil, however, there was no statistical difference in the mass of EPA permeating after 48 hours compared to when the formulation was absent of Cab-o-sil ($P = 0.075$).

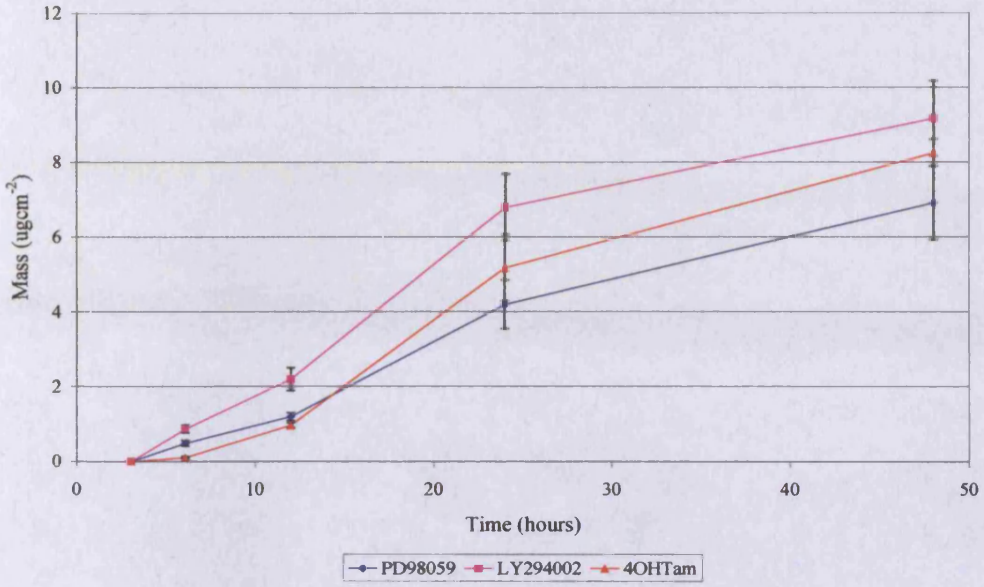

Figure 4.10 Permeation profile showing the mass (μgcm^{-2}) of PD98059, LY294002 and 4-hydroxytamoxifen permeating from the fish oil vehicle, when formulated with 2.5% v/v DMSO/ethanol, 0.05% v/v BHA and 4.0 % w/v Cab-o-sil. Donor phase was 2.54×10^{-4} mol PD98059 and LY294002 in 200µl fish oil with 0.05% BHA. Receptor phase was $30mgmL^{-1}$ cetrimide solution, it was stirred continuously and maintained in a water bath set to maintain a skin surface temperature of 32°C (n=6 ± SD).

Figure 4.10 shows permeation profiles for PD98059, LY294002 and 4-hydroxytamoxifen when 4.0% cab-o-sil was incorporated. Due to the retardation in release of EPA beyond this percentage of cab-o-sil, this formulation was deemed the most effective.

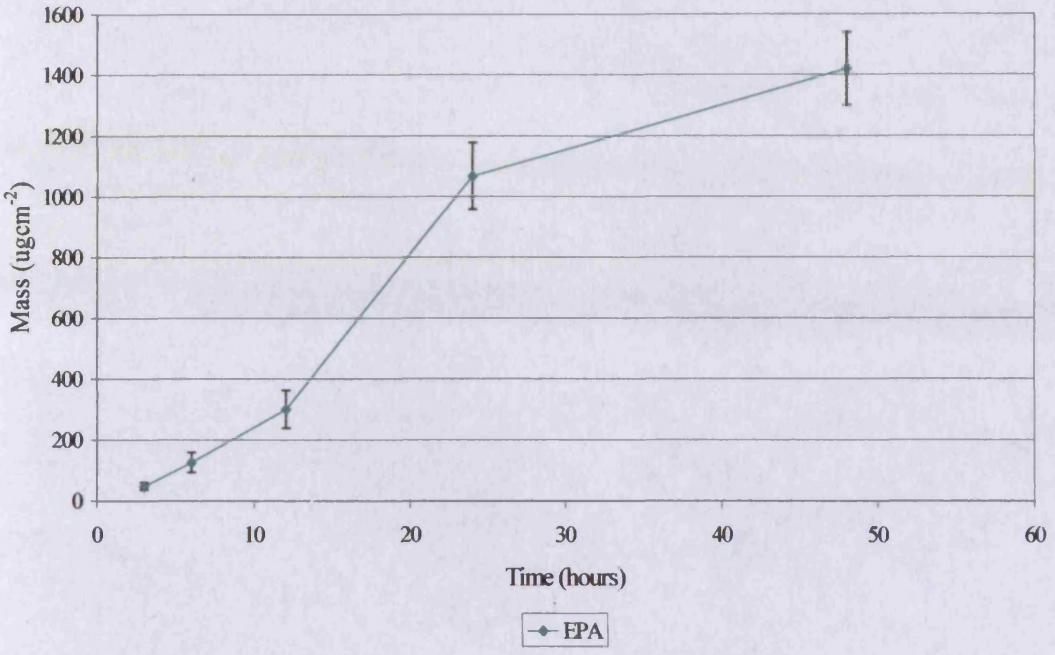

Figure 4.11 Permeation profile showing the mass (μgcm^{-2}) of EPA permeating from the fish oil vehicle, when formulated with 2.5% v/v DMSO/ethanol, 0.05% v/v BHA and 4.0 % w/v Cab-o-sil. Donor phase was 2.54 x 10^{-4} mol PD98059 and LY294002 in 200µl fish oil with 0.05% BHA. Receptor phase was 30mgmL^{-1} cetrimide solution, it was stirred continuously and maintained in a water bath set to maintain a skin surface temperature of 32°C (n=6 ± SD).

The steady state fluxes for the three actives were seen at 12-24 hours, which was later than seen with the absence of 4% Cab-o-sil. The steady-state flux of PD98059, LY294002 and 4-hydroxytamoxifen when 4.0% Cab-o-sil was incorporated was not significantly different from when cab-o-sil was absent from the formulation (P = 0.122, 0.72, 0.993 respectively). These were 0.25 ± 0.034$\mu gcm^{-2}h^{-1}$, 0.529 ± 0.078$\mu gcm^{-2}h^{-1}$and 0.35 ± 0.056$\mu gcm^{-2}h^{-1}$ respectively. The lag times were 7.2 ± 0.98, 8.15 ± 0.76 and 9.2 ± 0.93 hours and were significantly longer than those seen when cab-o-sil was not included

($P = < 0.001$ for each compound). The permeability coefficients for PD98059, LY294002 and 4-hydroxytamoxifen under these conditions were $2.58 \times 10^{-3} \pm 3.51 \times 10^{-4}$ μgcm^{-2}, $2.8 \times 10^{-3} \pm 5.1 \times 10^{-4}$ μgcm^{-2} and $2.9 \times 10^{-3} \pm 4.63 \times 10^{-4}$ μgcm^{-2}.

Figure 4.11 shows the permeation profile for EPA with the inclusion of 4% Cab-o-sil. Steady state flux was again seen later at 12-24 hours. Under these conditions the flux of EPA was statistically unchanged from that seen in the absence of Cab-o-sil ($P = 0.692$) however, was still significantly greater than the flux of EPA seen from fish oil vehicle without enhancers or Cab-o-sil present ($P = 0.01$). The lag time followed the same pattern. Flux of EPA with 4% Cab-o-sil present was 63.967 ± 9.93 $\mu gcm^{-2}h^{-1}$. Lag time was statistically longer than in formulations of fish oil alone and with 2.5%DMSO/ethanol ($P = 0.023$ and 0.017). With the inclusion of 4% Cab-o-sil the lag time of EPA was 7.29 ± 0.89 hours respectively. The permeability coefficient for EPA was $9.7 \times 10^{-4} \pm 1.5 \times 10^{-4}$ μgcm^{-2}.

4.3.5 The effect of Cab-o-sil ® on the viability of porcine skin

4.3.5.1 H & E staining

The H&E assay as used in section 4.3.2.1 was followed, however, skin was dosed with either water, which acted as control, or fish oil with 2.5% (v/v) of both DMSO and ethanol and with 4.0% (w/v) Cab-o-sil. Figure 4.12 shows the sections of skin from each treatment and reveals that the inclusion of the two

enhancers and Cab-o-sil causes no obvious histological changes to the porcine skin when compared to skin incubated with fish oil alone.

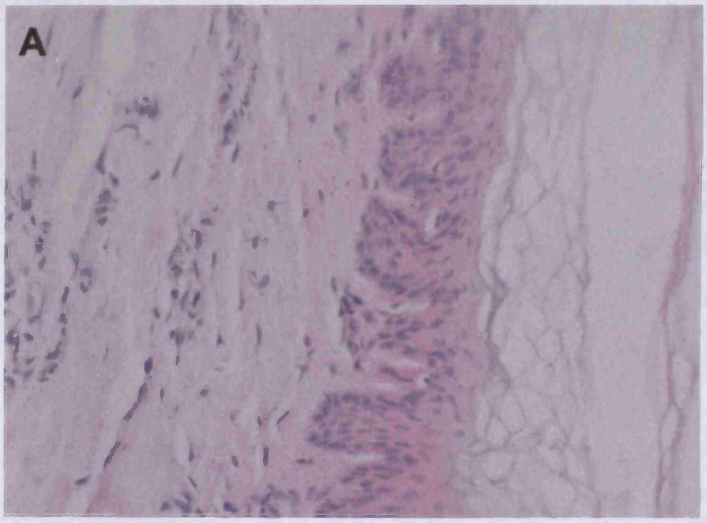

Figure 4.12. A- H & E assay on paraffin embedded excised porcine skin at 0 hours. Sections were cut at 5μm on a Shandon Finesse 325 microtome. A- x 20

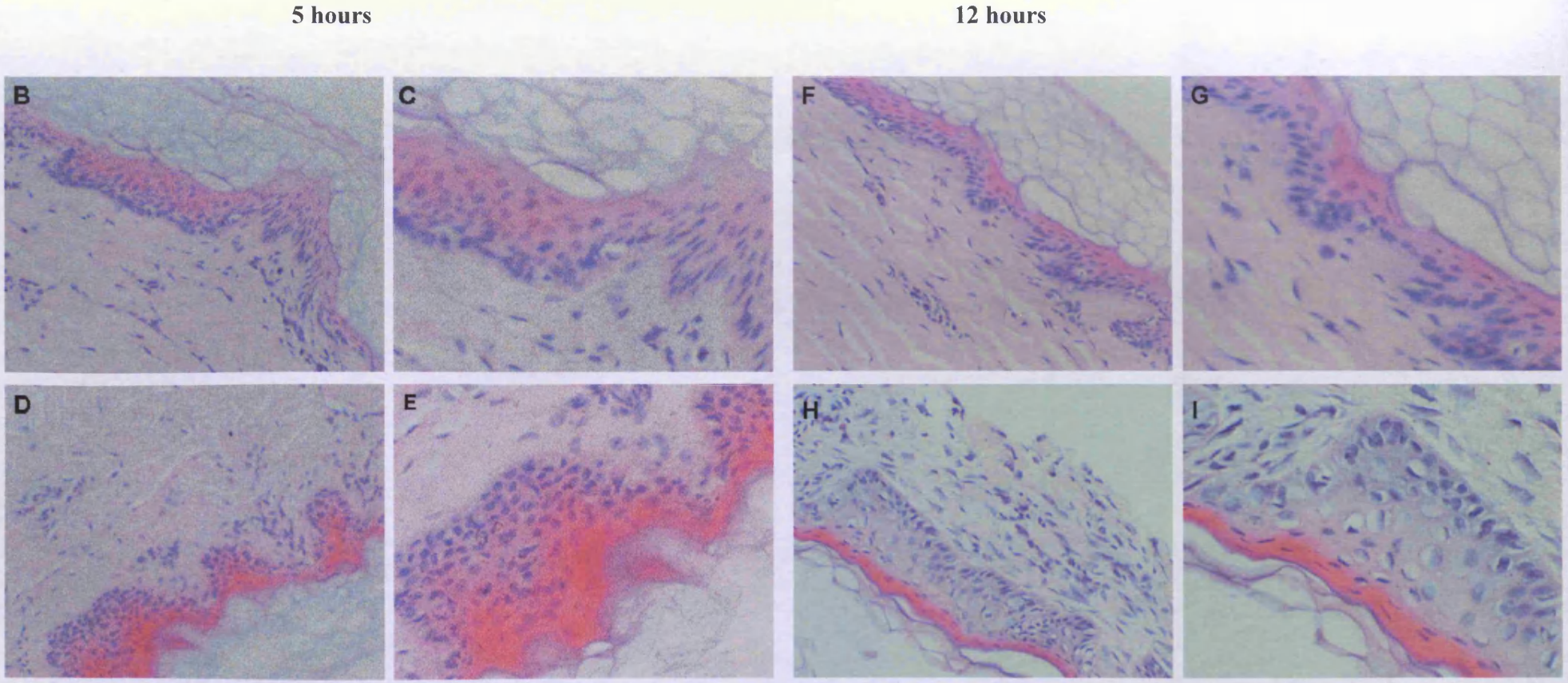

Figure 4.12 B-I. H & E assay on paraffin embedded excised porcine skin after 5 hours (B-E) and 12 hours (F-I) incubation with water control (B-C, F-G) or 200µl fish oil plus 2.5% v/w DMSO/ethanol and 4% w/v Cab-osil (D-E, H-I). Sections were cut at 5µm on a Shandon Finesse 325 microtome. F x 10, B, D, H- x 20 C, E, G, I- x 40.

4.3.5.2 Ki-67 assay

It was of paramount importance to make sure that fish oil plus 2.5% (v/v) of both DMSO and ethanol and also with 4.0% (w/v) Cab-o-sil was able to maintain skin viability

Figure 4.13 shows the ki-67 assay carried out skin incubated with each formulation. The assay shows Ki-67 staining was maintained throughout the duration of the 12 hour experiment when skin was incubated with each formulation, suggesting that fish oil plus 2.5% (v/v) of both DMSO and ethanol and also with 4.0% (w/v) Cab-o-sil did not affect skin viability.

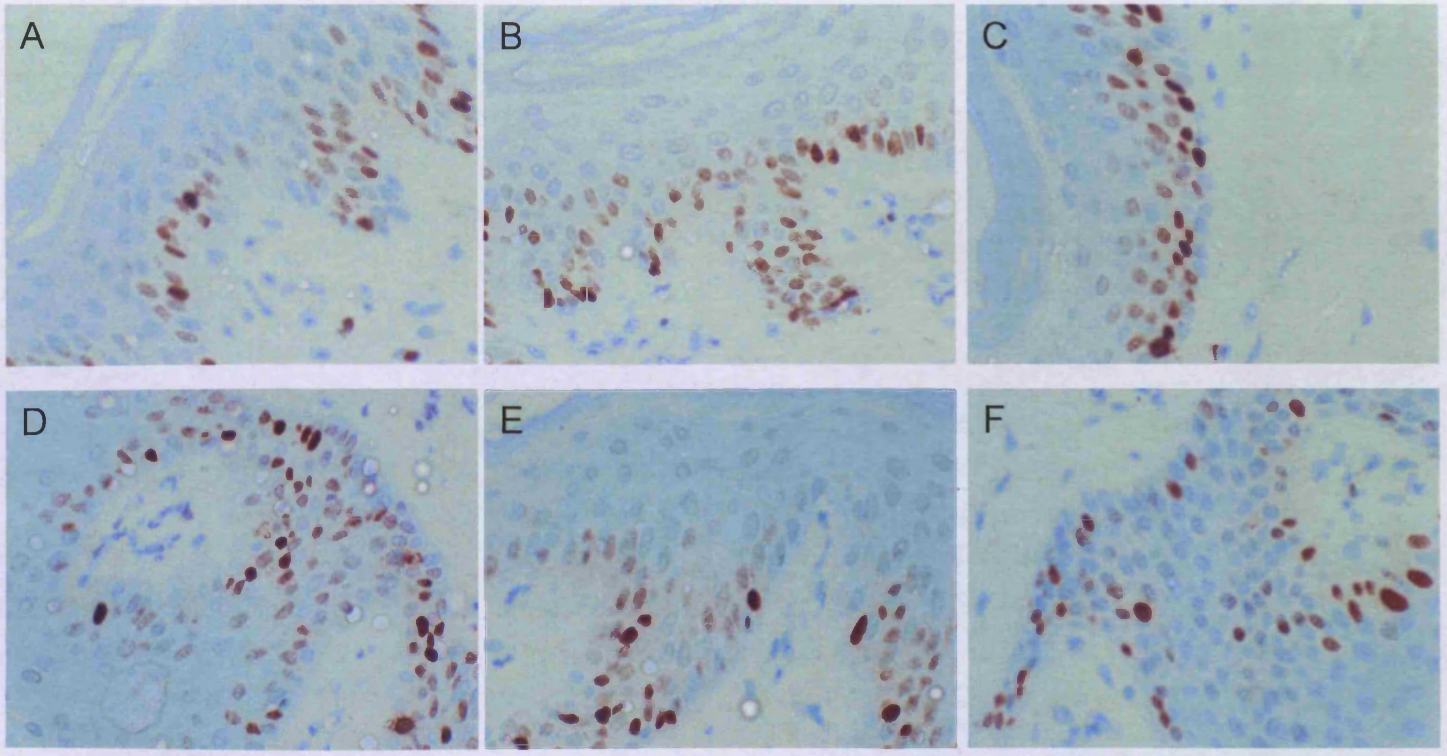

Figure 4.13 ICC assay to detect ki-67 in excised porcine skin (x40) after 0 (A, D), 5(B, E) and 12 (C, F) hours incubation with water (A-C) or fish oil (D-F). Primary antibody was DAKO MIB made up in 0.1% BSA in PBS at 1/50. Sections were cut at 5µm on a Shandon Finesse 325 microtome.

4.3.5.3 pERK1/2

Figure 4.14 displays porcine skin immediately post dissection. Figure 4.15A represents a negative control, where the pERK1/2 primary antibody was replaced with PBS. Figure 4.14 shows porcine skin assayed for the detection of pERK1/2 after 0 hours. The negative control displays no staining; suggesting that staining seen in figure 4.14B and the sections throughout this experiment was specific for pERK1/2.

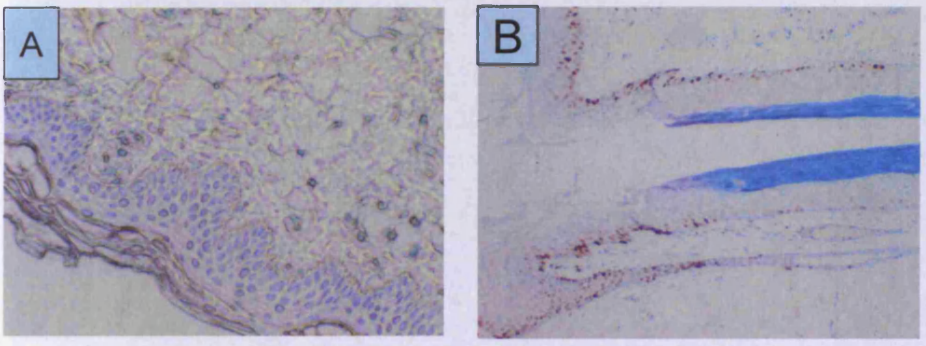

Figure 4.14 ICC assay to detect pERK1/2 in excised porcine skin immediately post dissection (A= negative control x 20, B = 0 hours control x 10) Primary antibody was a CST rabbit polyclonal phospho-ERK1/2 kinase antibody at 1/20 in 20% Normal Human Serum in PBS overnight. Sections were cut at 5μm on a Shandon Finesse microtome.

Figure 4.15 displays sections of porcine skin assayed for the detection of pERK1/2 over 12 hours. The assayed revealed that pERK1/2 was localised to the nucleus of epidermal keratinocytes, although some cytoplasmic staining was seen. Figure 4.15 A-C shows that water has no effect on pERK1/2 levels, with staining remaining at a constant level from the 0 hour control and throughout the 12 hours when the skin was incubated with water.

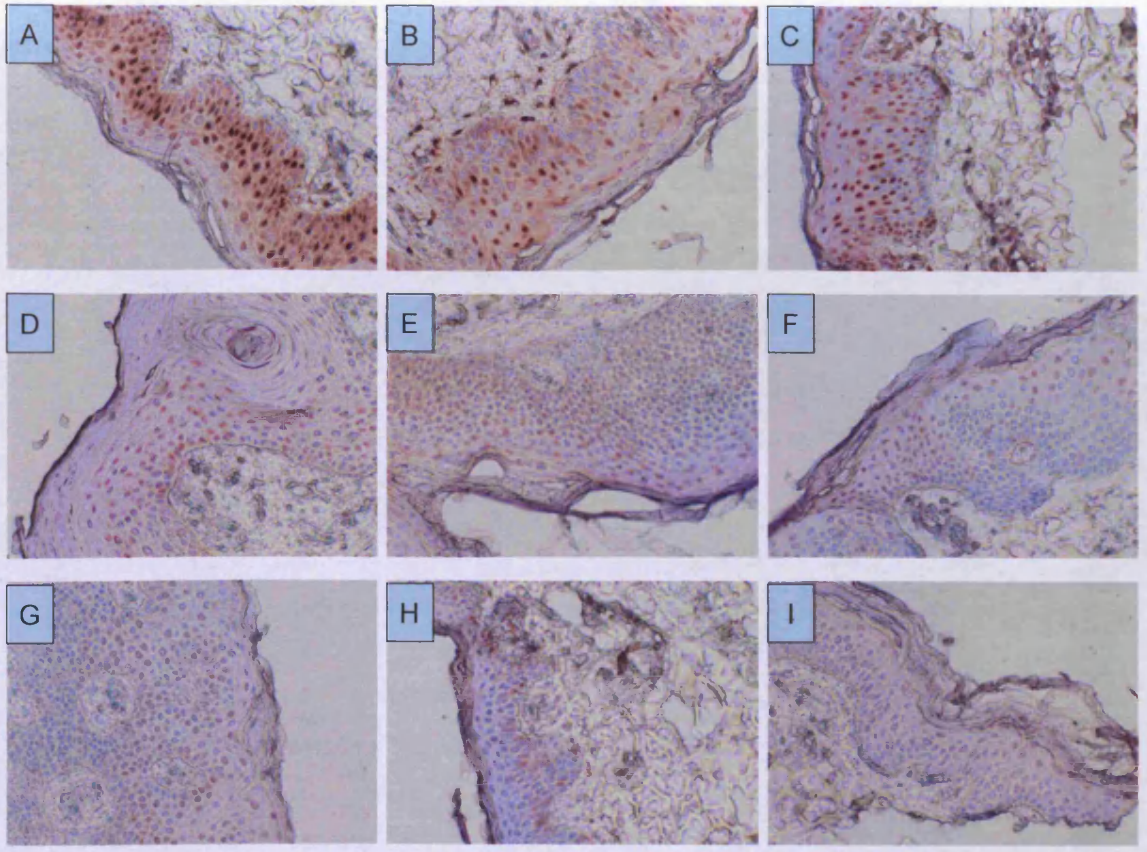

Figure 4.15 ICC assay to detect pERK1/2 in excised porcine skin (x40) after 3 (A, D, G), 6 (B, E, H) and 12 (C, F, I) hours incubation with water (A-C), fish oil (0.05% v/v BHA) (D-E) or fish oil plus 2.54 x 10^{-4}M PD98059, LY294002, 4-hydroxytamoxifen (plus 0.05 v/v BHA 2.5% v/v DMSO/ethanol and 4% w/v Cab-o-sil). Primary antibody was a CST rabbit polyclonal phospho-ERK1/2 kinase antibody at 1/20 in 20% Normal Human Serum in PBS overnight. Sections were cut at 5μm on a Shandon Finesse microtome

4.3.5.4 pAkt

Figure 4.16 displays porcine skin immediately post dissection. It revealed that pAkt was localised to the cytoplasm of the epidermis. Figure 4.16A represents a negative control, where the pAkt primary antibody was replaced with PBS. Figure 4.16B shows porcine skin assayed for the detection of pAkt after 0 hours. The negative control displays no staining; suggesting that staining seen in figure 4.16B and the sections throughout this experiment was specific for pAkt.

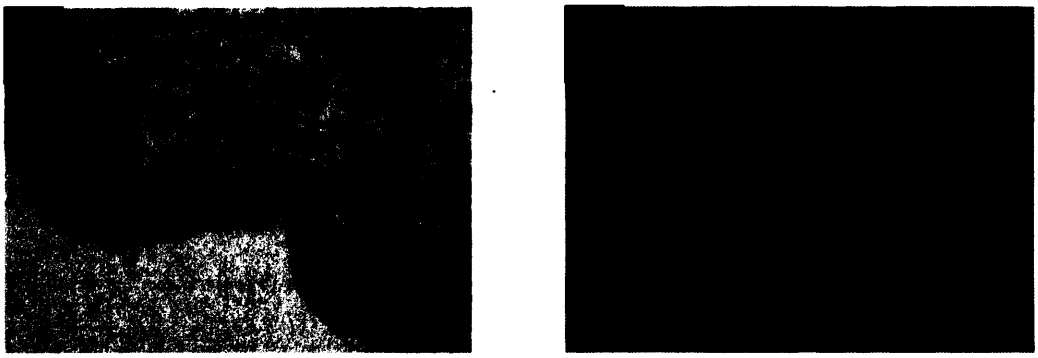

Figure 4.16 ICC assay to detect pAkt in excised porcine skin immediately post dissection (A= negative control x10, B = 0 hours control x40) Primary antibody was CST rabbit anti-Akt (activated) polyclonal antibody at 1/30 in PBS overnight Sections were cut at 5μm on a Shandon Finesse microtome

Figure 4.17 demonstrates excised porcine skin assayed to detect pAkt over 12 hours when treated with water, fish oil or fish oil and 2.54 x 10^{-4}M PD98059, LY294002, 4-hydroxytamoxifen (plus 2.5% v/v DMSO/ethanol and 4% w/v Cab-o-sil).

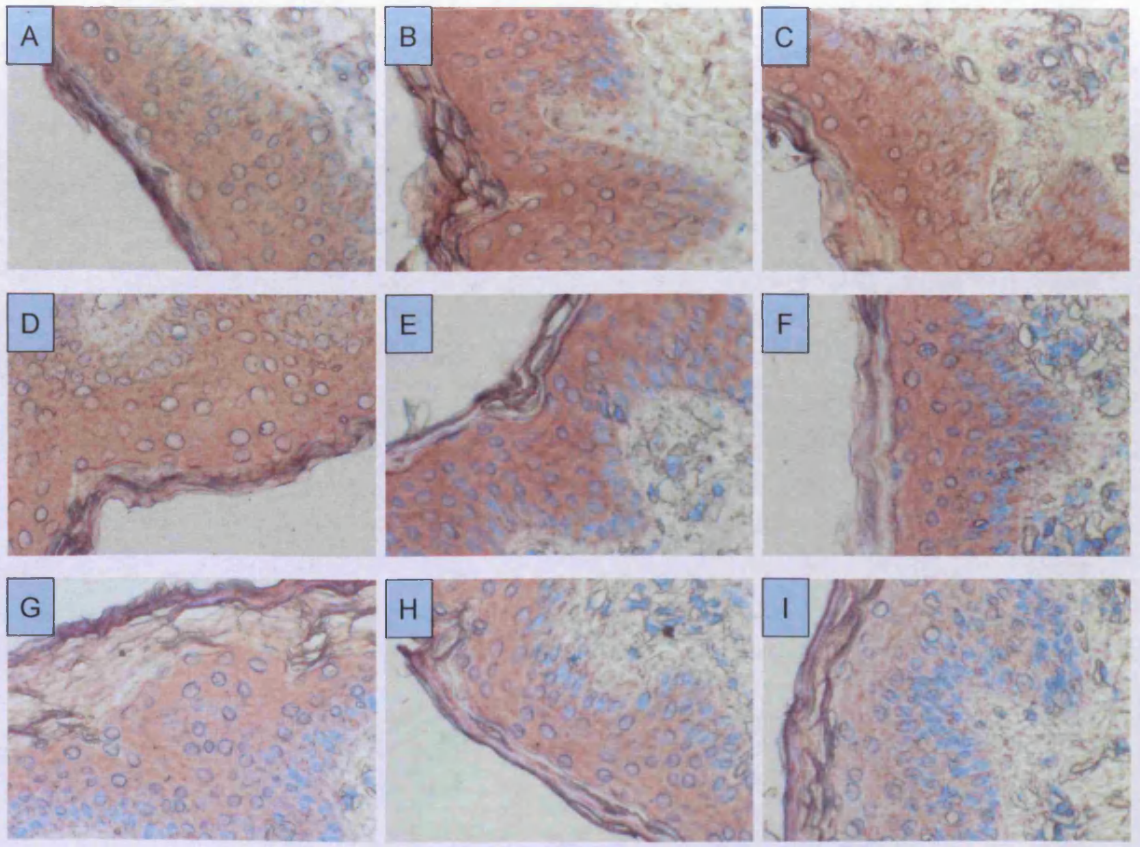

Figure 4.17 ICC assay to detect pAkt in excised porcine skin (x40) after 3 (A, D, G), 6 (B, E, H) and 12 (C, F, I) hours incubation with water (A-C), fish oil (0.05% v/v BHA) (D-E) or fish oil plus 0.05% v/v BHA, 2.54 x 10^{-4}M PD98059, LY294002, 4-hydroxytamoxifen (plus 2.5% v/v DMSO/ethanol and 4% w/v Cab-o-sil). Primary antibody was CST rabbit anti-Akt (activated) polyclonal antibody at 1/30 in PBS overnight. Sections were cut at 5μm on a Shandon Finesse microtome

Figure 4.17 shows that epidermal pAkt expression was not affected when water was applied to the stratum corneum (figure 4.17 A-C). The application of fish oil (plus 2.5% v/v DMSO/ethanol and 4% w/v Cab-o-sil) did not affect the protein expression of pAkt throughout the 12 hour experiment (4.17 D-F). The application of fish oil (plus 2.5% v/v DMSO/ethanol and 4% w/v Cab-o-sil ,2.54 x 10^{-4}M PD98059, LY294002, 4-hydroxytamoxifen) to the surface of the skin was capable of inhibiting pAkt within the epidermis after 3 hours (4.17G), furthermore, this inhibition was maintained for the 12 hour experiment

4.3.5.5phospho EGFR

Figure 4.18 displays porcine skin immediately post dissection. The assay revealed that pEGFR1068 was only found within the epidermis and was localised to the cytoplasm. Figure 4.18A represents a negative control, where the pEGFR1068 primary antibody was replaced with PBS. Figure 4.18B shows porcine skin assayed for the detection of pEGFR1068 after 0 hours. The negative control displays no staining; suggesting that staining seen throughout this assay was pEGFR specific.

Figure 4.19 displays the pEGFR1068 assay performed on porcine skin treated with water, fish oil or fish oil plus 2.54 x 10^{-4}M PD98059, LY294002, 4-hydroxytamoxifen (plus 2.5% v/v DMSO/ethanol and 4% w/v Cab-o-sil). It revealed that pEGFR protein expression remained constant throughout the 12 hour experiment when water was applied to the SC surface (4.19 A-C).

Application of both the fish oil vehicle and the cocktail of compounds reduced pEGFR1068 within porcine skin after 3 hours (4.19 D & G). At 12 hours (4.20 F & I), however, pEGFR specific staining was elevated compared to at 3 hours.

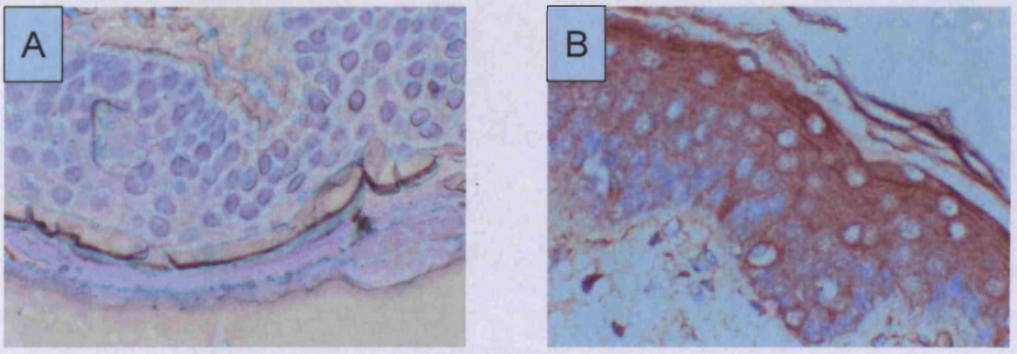

Figure 4.18 ICC assay to detect pEGFR1068 in excised porcine skin immediately post dissection (A= negative control x40, B = 0 hours control x40) Primary antibody was Biosource pEGFR 1068 rabbit primary antibody at 1/25 overnight. Sections were cut at 5µm on a Shandon Finesse microtome.

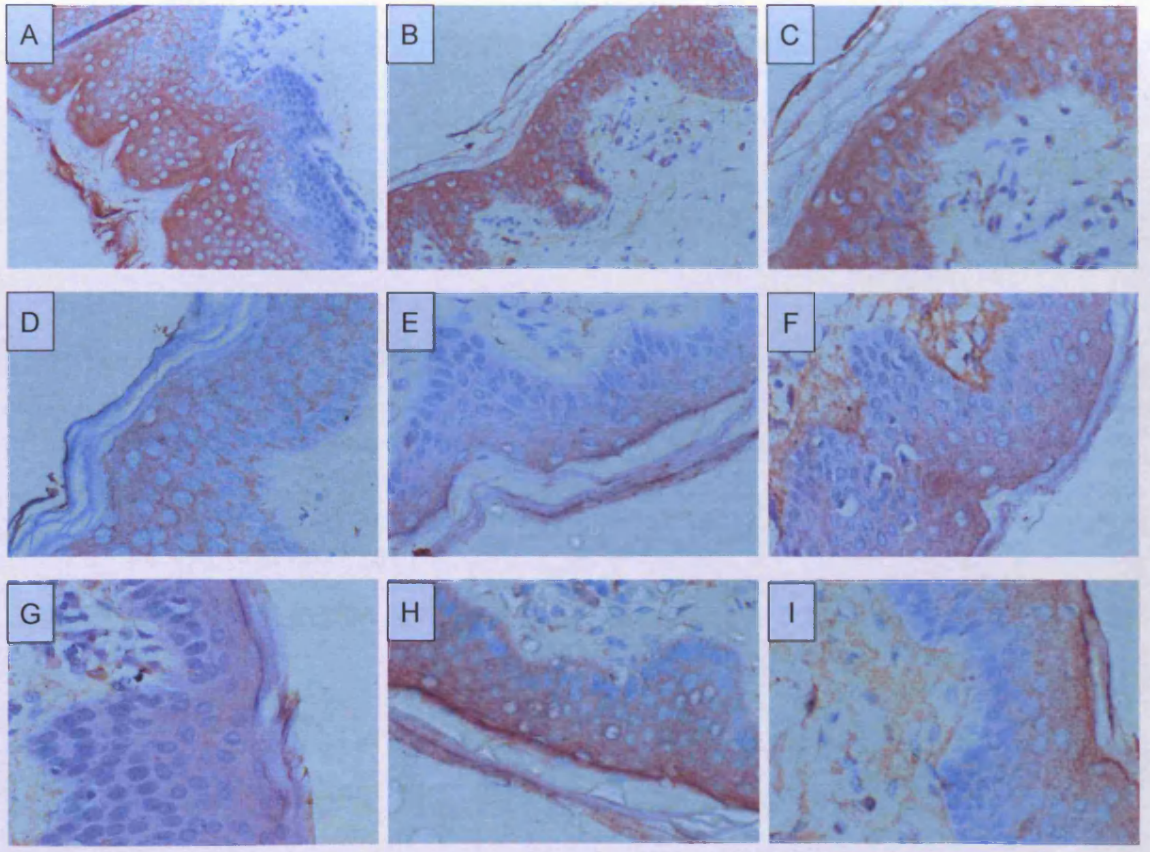

Figure 4.19 ICC assay to detect pEGFR1068 in excised porcine skin (A, B, x20 C-I x40) after 3 (A, D, G), 6 (B, E, H) and 12 (C, F, I) hours incubation with water (A-C), fish oil (0.05% v/v BHA) (D-E) or fish oil plus 0.05% v/v BHA, 2.54 x 10^{-4}M PD98059, LY294002, 4-hydroxytamoxifen (plus 2.5% v/v DMSO/etOH and 4% w/v cab-o-sil). Primary antibody was Biosource pEGFR 1068 rabbit primary antibody at 1/25 overnight. Sections were cut at 5µm on a Shandon Finesse microtome

4.3.5.6 Total COX-2

Figure 4.20 displays porcine skin immediately post dissection. The assay revealed that total COX-2 protein was only found within the epidermis and was cytoplasmic and nuclear. Figure 4.20A represents a negative control, where the total COX-2 primary antibody was replaced with PBS. Figure 4.20B shows porcine skin assayed for the detection of total COX-2 after 0 hours. The negative control displays no staining; suggesting that staining seen throughout this assay was total COX-2 specific.

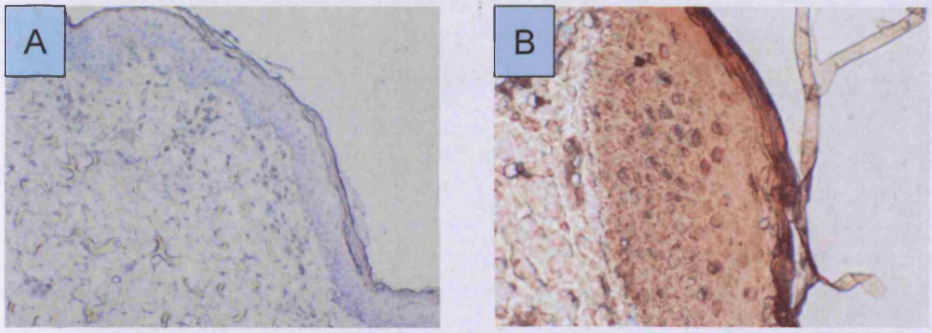

Figure 4.20 ICC assay to detect total COX-2 in excised porcine skin immediately post dissection (A= negative control x10, B = 0 hours control x40) Primary antibody was New England Biolabs total COX-2 primary antibody at 1/25 overnight. Sections were cut at 5µm on a Shandon Finesse microtome.

Figure 4.21 displays the total COX-2 assay performed on porcine skin treated with water, fish oil or fish oil plus 2.54 x 10^{-4}M PD98059, LY294002, 4-hydroxytamoxifen (plus 2.5% v/v DMSO/ethanol and 4% w/v cab-o-sil). It revealed that total COX-2 protein expression remained constant up to 6 hours when water was applied to the SC surface. At 12 hours, however, total COX-2 staining was greater than that at 3 and 6 hours.

Application of fish oil knocked down total COX-2 protein expression within the epidermis after 3 hours (figure 4.21D). Total COX-2 staining increased in intensity at 6 hours (4.21E) and again at 12 hours (4.21F) post fish oil application. Application of fish oil plus PD98059, LY294002 and 4-hydroxytamoxifen gave a continual knockdown in total COX-2 protein throughout the 12 hour experiment (4.21 G-I).

4.4 Discussion

The aims of this study were to investigate the plausibility of fish oil as an efficacious replacement for the DMSO vehicle and to probe whether it offered a skin friendly alternative.

Immunohistological and immunocytochemical data suggested that fish oil met the first criterion of the aims. H&E staining showed no obvious detrimental effects of fish oil, after 12 hours treatment, on the structure of the skin and showed no obvious keratinocyte toxicity, as observed with only 3 hours incubation with DMSO. It is widely documented that the mechanism by which DMSO exerts its permeation enhancement is by modifying the structure of the SC by removing the lipid content of it (Williams, A.C 2003) which is thought to be the reason that skin toxicity was seen.

The ki-67 assay determined that fish oil could be superior to water at maintaining the viability of excised porcine skin, possibly due to incorporation of fatty acids into cell membranes (Walker, R.B. & Smith, E.W. 1995). The

staining was seen throughout the 12-hour timescale of the study, localised mainly to the lower layers of the epidermis.

The epidermis is the main enzymatic site within the skin, with most phase 1 and phase 2 catalytic reactions occurring here, however only at a much reduced level (~10%) compared to that seen in the liver (Williams, A.C. 2003). The main sub-layer of the epidermis actively proliferating is the stratum basale, which explains the localisation of the ki-67 staining to this layer.

After the successful determination of fish oil as a non-toxic vehicle, it was then assessed for its' ability to enhance the permeation of PD98059, LY294002 and 4-hydroxytamoxifen. Permeation data and steady state flux of both PD98059 and LY294002 with and without 4-hydroxytamoxifen present was vastly reduced compared to that seen with DMSO. The mechanism by which the PUFAs within the fish oil enhance permeation is different to that seen with DMSO. PUFAs are known to intercalate into the lipid domain of the stratum corneum, where the kink in their structures disrupts the linear array of lipids. DMSO at percentages over 60% is thought to cause an irreversible effect on the skin, causing loss of SC lipids and, in effect, forming a hole in the barrier. Taking the mechanisms into account, the severity in the permeation enhancing mechanism of DMSO compared to the more subtle mechanism of the PUFAs may be a plausible explanation for the results. Another theory, involving the pull effect, may explain the retardation in the permeation of all 3 compounds when formulated with fish oil. NSAIDs formulated within a fish oil vehicle

have been shown to permeate proportionally to EPA and DHA, two PUFAs present within the fish oil. The permeation of ketoprofen and ibuprofen were assessed when both were formulated in fish oil. Interestingly the flux of EPA and DHA were greater when formulated with the fastest permeating NSAID. The authors suggest that this could be explained by the solute permeating in its solvent cage (Heard, C.M *et al* 2003). Later the permeation of ketoprofen and EPA was probed using NMR studies. Here it was discovered that ketoprofen and EPA permeated the skin whilst bound together (Thomas, C.P. *et al* 2007). With this in mind, possible binding complexes between PD98059, LY294002 and 4-hydroxytamoxifen with EPA were studied.

Complexation between PUFAs and tamoxifen have already been shown, where HNMR showed that tamoxifen and γ linolenic acid permeated full thickness skin bound together.

Figure 4.23 shows the most likely bonding complexes of PD98059/EPA and LY294002/EPA.

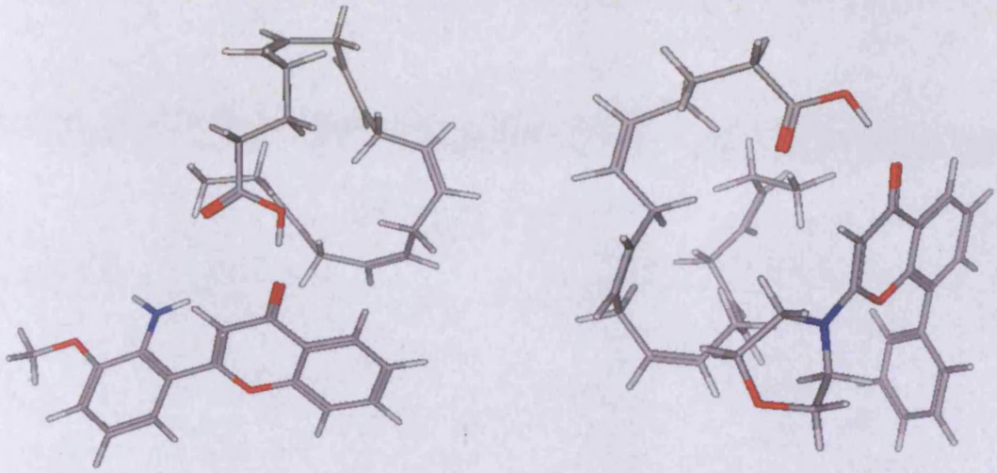

Figure 4.23 Bonding complexes formed between PD98059 and EPA (left) and LY294002 (right).

H-bonding interactions between the acid group of EPA and the ring carbonyl group of each of the compounds are responsible for the complexes and the similar binding energies produced. These were 98.7KJ/mol and 101.0KJ/mol for PD98059 and LY294002 respectively.

This binding could be responsible for the retardation of permeation of all 3 compounds if the mechanism by which PUFAs compromise the barrier properties of skin is examined. If the PUFAs bind the three compounds and then are intercalated within the skin, unless the binding is overcome, the compounds may be retained within the skin. This is also supported by the fact

that EPA did not permeate the skin in the absence of the three compounds, suggesting that all permeating EPA was intercalated into the lipid environment of the SC. Incorporation of the compounds allowed small amounts of EPA to permeate via the pull effect.

The addition of the three permeation enhancers and combinations of these was aimed at improving the permeation of PD98059, LY294002 and 4-hydroxytamoxifen. The inclusion of all enhancers and enhancer combinations increased the permeation and steady state flux of all 4 actives. The method of enhancement caused by DMSO has been mentioned. The addition of ethanol may have enhanced the permeation of all 3 compounds in a wide range of ways. Ethanol can increase the solubility of solute so increase its partitioning into the skin. It can also affect the skins permeability to the solute irreversibly due to its entry and passage through the skin (Oh, S.Y. *et al* 2003). It has also been suggested by Liu, H. and colleagues (2006) that ethanol can extract lipids from the stratum corneum membrane and so increase the passage of the permeant through this barrier. Recent attention has been focused on the pull effect as a viable explanation of the enhancing properties of ethanol. It is suggested that the close relationship between the permeation of mefenamic acid and ethanol or 1,8-cineole was attributed to the pull effect and not the effect on the SC (Heard, C.M., *et al* 2005). Indeed, it was later established that ethanol gave rise to the same permeation enhancement in both full thickness skin and in heat separated dermal membranes. The absence of the SC in these

membranes eliminates effects on the SC lipid content as a mechanism of permeation enhancement (Heard, C.M., *et al* 2007).

Terpenes, such as 1,8-cineole, have been widely used as penetration enhancers and have GRAS (generally regarded as safe) status (Narishetty, S.T.K. & Panchagnula, R. 2004). They are used to increase the permeation of compounds such as estradiol, ketoprofen and haloperidol (Monti, D. *et al* 2002, Rhee, Y.S. *et al* 2001, Vaddi, H.K. *et al* 2002). It has also previously been demonstrated that terpenes can enhance the permeation of tamoxifen (Gao, S. & Singh, J. 1998). The addition of 1,8-cineole may have enhanced the permeation of PD98059, LY294002 and 4-hydroxytamoxifen by disrupting stratum corneum lipid bilayers. Narishetty and co-workers (2004) showed, by differential scanning calorimetry, that terpenes caused a shift in endothermic transition temperature of SC lipids and suggested this was the main mechanism of their penetration enhancing actions. Moghimi, H.R. and colleagues, (1996-1997) throughout many short studies, concluded that hydrocarbon terpenes increase permeation by increasing the diffusivity of the SC lipids, whereas cyclic terpenes act by increasing the partitioning of solute into the skin.

Investigations looking at the effect of combination of two or more CPEs on permeation have received little attention in the literature, mainly due to the enormous quantity of combinations that exist. The combination of DMSO and ethanol gave an additive increase in permeation compared to the enhancement seen with the individual CPEs. Synergy was not seen with any combinations,

which was similar to results seen by Karande, P. and colleagues (2006). This group showed, using a high through-put screening of CPE combinations that combinations of two or more CPEs very rarely displayed synergy and more often show additive benefit. Additive interactions may have caused an increase in permeation due to the different mechanisms of permeation enhancement of each individual CPE. However, as the definitive permeation enhancement mechanism of each CPE has not been elucidated, this can only be speculated.

Cab-o-sil forms gels due to its fumed silica network forming H-bonds with either solvents or with actives within the formulation. The inclusion of each percentage of cab-o-sil did not significantly alter the mass permeated or steady state flux of PD98059, LY294002 or 4-hydroxytamoxifen. This result suggests that each compound was released from the thickener sufficiently to allow maximal flux. However, the lag time of each compound was increased significantly, suggesting that cab-o-sil did slow down the initial release of the compounds. Interestingly, studies by Gallagher, S.J. and colleagues (2003) revealed that even the inclusion of 0.5% cab-o-sil retarded the permeation of ketoprofen and ibuprofen significantly. The inclusion of cab-o-sil above 4.0% (w/v) significantly impeded the permeation of EPA, suggesting that cab-o-sil formed H-bonds preferentially with constituents of the fish oil rather than with the active compounds.

The inclusion of the two enhancers and 4% cab-o-sil showed no obvious detrimental effects on the skin. Cab-o-sil is commonly used commercially as a

non-matrix forming thickening (Gallagher, S.J. *et al* 2003). It is even used to thicken tomato ketchup so it is not surprising that this did not exert any toxicity on the skin. What was surprising, however, was evidence suggesting that the two enhancers (DMSO and etOH) did not display any skin toxicity when both were included at 2.5%. Common sense would dictate that if these two enhancers enhanced the permeation of PD98059, LY294002 and 4-hydroxytamoxifen in the classical method (by removing SC lipids and elevating SC lipid fluidity then some SC damage would be expected. This was not seen, either in H&E staining or with the ki-67 assay. These data may provide support that the enhancement seen is due to the pull effect rather than severe SC structural alterations. One other explanation could be that the percentages of each CPE used were enough to cause permeation enhancement by the classical mechanism but the alterations seen in the SC were too subtle to be seen in the ICC and IHC.

ICC detection of pERK1/2, pAkt, pEGFR and total COX-2 demonstrated, qualitatively, that the active constituents permeated through into the epidermis, where they inhibited the target molecules. After 3 hours the formulation containing fish oil plus PD98059, LY294002 and 4-hydroxytamoxifen was capable of inhibiting these mediators within the epidermis, compared to water control. This inhibition was maintained during the 12 hour experiment. Interestingly, COX-2 expression seemed to increase with time when skin was treated with water and increased after 3 hours incubation with fish oil. This suggests that the inflammatory response invoked by amputation and dissection

of the ear caused a sustained induction of COX-2 protein, which overcame the concentrations of EPA and DHA within the epidermis. The cocktail formulation, however, maintained COX-2 knockdown throughout the 12 hour experiment, suggesting that PD98059, LY294002 or 4-hydroxytamoxifen affected total COX-2. A recent study supports this and linked the regulation of COX-2 expression in HT29 colon cancer cell lines to pERK1/2 activity, showing that PD98059 (20μmol/L) inhibited serum-induced COX-2 expression (Tominga, K. *et al* 2004). The pull effect could be another plausible explanation as to the maintained knockdown of COX-2. The permeation of EPA and DHA are significantly increased when compounds such as ketoprofen and ibuprofen were applied simultaneously (Thomas, C.P. & Heard, C.M. 2004). This result was observed in this chapter, where EPA was only detected in the receptor fluid when PD98059, LY294002 and 4-hydroxytamoxifen were included. This increased permeation suggests that there would be more EPA and DHA within the epidermis to act on COX-2 localised there.

This limited investigation has shown that choice of vehicle and exipients is of paramount importance in the development of topical formulations. Even the replacement of one enhancer for another can, and has had significant effects on the permeation of different compounds. It has been very fortunate that the combination of DMSO and ethanol gave maximal enhancement of all 3 compounds and EPA.

4.5 Conclusions

Fish oil has been demonstrated as a potentially skin friendly vehicle, and with the correct mixture of enhancers and the optimum percentage of thickener can provide a suitable vehicle for the permeation of PD98059, LY294002 and 4-hydroxytamoxifen.

Although the permeation seen with the addition of CPEs was still not to the magnitude observed with the pure DMSO vehicle, a compromise must be made between safety and efficacy. Permeation studies and ICC have shown quantitatively and qualitatively that the constituents of the cocktail formulation permeate full thickness skin at potentially useful rates.

Chapter 5

Probing the effect of PD98059, LY294002, 4-hydroxytamoxifen and fish oil on human breast cancer cells.

5.1 Introduction

The work in the earlier chapters detailed the development of an anti-breast cancer therapeutic system comprised of a MAPK inhibitor, a PI3K inhibitor and 4-hydroxytamoxifen and EPA (fish oil vehicle). This combination was derived primarily based upon their skin permeation characteristics, although assessment of their effects on human breast cancer cells is of key importance.

Two human breast cancer cell lines were used in this chapter to represent two phenotypes of the disease. MCF-7 cells are an adherent epithelial breast cancer cell line, derived from a pleural effusion adenocarcinoma. They are ER positive (ER+) and are steroid hormone sensitive (Hiscox, S. *et al* 2006), representing the ER+ phenotype that responds to tamoxifen (figure 5.1). TamR cells were developed 'in house' at the Tenovus Cancer Research Centre, Cardiff University. The cells were developed from parental MCF-7 cells that were grown in the presence of 4-hydroxytamoxifen until normal growth was restored (Knowlden, J.M. *et al* 2003). These cells were used to represent the patient population that develop acquired resistance to tamoxifen. The cells have lost sensitivity to E_2 and tamoxifen but still have a growth inhibitory response to the pure anti-estrogen Faslodex (figure 5.2).

The use of fish oil not only provided a beneficial effect on the delivery of both PD98059 and LY294002 but research has shown that EPA, contained in fish oil, could provide an additional prong to the transcutaneous anti-breast cancer cocktail.

It has been widely documented that many breast tumors overexpress COX-2, the inducible isoform of the cyclooxygenase enzyme (Davis, G. *et al* 2002). However the exact role for COX-2 in tumorogenesis is still unclear. Wild, P.J. and colleagues (2004) conducted a high throughput tissue microarray trial but used immunocytochemical techniques to assess the correlation of COX-2 expression with molecular, clinical and pathologic markers involved in breast cancer. This study concluded that strong COX-2 staining was significantly correlated with high tumor stage and BRE grade and that there was a strong correlation with metastatic status and in hormone-refractory tumors compared to those confined to one organ suggesting that COX-2 may play a role in breast cancer cell motility and metastasis (Parrett, M.L. *et al* 1997).

5.1.1 Aims

Using a combination therapy comprising of 4-hydroxytamoxifen, LY294002 and PD98059 it is postulated that tamoxifen resistance could be largely delayed or even eradicated. The aims of this chapter therefore, were to assess the effects of the cocktail formulation, developed in chapter 4, on tamoxifen sensitive and resistant cell lines. Growth assays were conducted to examine the effects of the compounds singly and simultaneously, while ICC analysis was employed to visualise the effect of the cocktail of compounds on key mediators of tumorogenesis such as COX-2, EGFR, ER, Akt, and ERK 1/2.

5.2 Materials and Methods

5.2.1 Materials

The materials for this chapter have been outlined in chapter 2 (section 2.1).

5.2.2 Methods

5.2.2.1 Dose response curve for fish oil on growth of MCF-7 and TamR cells

The IC_{50} concentrations of 4-hydroxytamoxifen, PD98059 and LY294002 had already been determined in house on MCF-7 and TamR cells as 1 x 10^{-7} M, 25 x 10^{-6} M and 5 x 10^{-6} M respectively, however the optimum volume of fish oil to deliver the optimum concentration of EPA on these cell lines had not been explored.

MCF-7 and TamR cells were grown to ~70 % confluency, trypsinised and seeded into 24 well plates at a density of 1.5 x 10^6 per plate on day 0. Dose response assays were carried out as stated in chapter 2. Cells were dosed with volumes of filter sterilised fish oil made up in 2:1 with ethanol to give final concentration of 0.1, 0.5, 1, 2 and 5 μl mL^{-1} on days 1 and 4 and counted on day 7.

5.2.2.2 Growth assays

Growth assays were performed as stated in section 2.2.2.3. Firstly the phenotype of both MCF-7 and TamR cells were checked to ensure the cells were behaving characteristically. Cells were seeded on day 0 and on days 1 and 4 treated with compounds as shown in table 5.1.

Cell Line	Treatment
MCF-7	0.1 μL mL^{-1} DMSO (Control)
	1 x 10^{-7} M Faslodex
	1 x 10^{-7} M 4OHTam
	1x 10^{-9} M E_2
TamR	0.1 μL mL^{-1} DMSO (Control)
	1 x 10^{-7} M Faslodex
	1x 10^{-9} M E_2

Table 5.1 Dosing concentrations of compounds for phenotypic analysis of MCF-7 and TamR cells.

Secondly, MCF-7 and TamR cells were seeded on day 0. On day 1 base counts were taken and cells were dosed with IC_{50} and secondly permeated concentrations of 4-hydroxytamoxifen, PD98059, LY294002 and EPA as shown in table 5.2.

Cell Line	IC_{50} Treatment
MCF-7	0.1μL mL^{-1} DMSO (Control)
	1μL mL^{-1} Fish oil
	1 x 10^{-7}M 4OHTam
	25μM PD98059
	5μM LY294002
	1 x 10^{-7}M 4OHTam, 25μM PD98059, 5μM LY294002
	1μL mL^{-1} Fish oil,1 x 10^{-7}M 4OHTam, 25μM PD98059, 5μM LY294002
	1 x 10^{-9} M E_2
TamR	0.1μL mL^{-1} DMSO (Control)
	1μL mL^{-1} Fish oil
	25μM PD98059
	5μM LY294002
	1 x 10^{-7}M Faslodex
	25μM PD98059, 5μM LY294002
	1μL mL^{-1} Fish oil, 25μM PD98059, 5μM LY294002
	1 x 10^{-9} M E_2

Table 5.2 Dosing concentrations of 4-hydroxytamoxifen, PD98059, LY294002 and EPA for growth assays.

Concentrations were taken from the in vitro permeation studies (0.65 μM PD98059, 0.8 μM LY294002 and 0.41 μM 4-hydroxytamoxifen). The studies were conducted as above, except that cells were treated 0.65 μM PD98059, 0.8 μM LY294002 and 0.41 μM 4-hydroxytamoxifen on day 1 and then with the concentration permeated after 24 h, each day thereafter (0.325 x 10^{-6} M PD98059, 0.4 10^{-6} M LY294002 and 0.205 μM 4-hydroxytamoxifen).

The effect of permeated concentration of EPA was also assessed on the growth of MCF-7 cells. Cells were set up as in previous growth studies. Cells were dosed with 4μl of fish oil per 1ml of media to deliver the accurate permeated amount of EPA to the cells on days 1 and 4. Fish oil was dissolved 2:1 with ethanol. Counts were taken on days 1, 3, 5 and 8.

5.2.2.3 ICC of cell lines

Cells were grown to ~70% confluency on TESPA coated glass coverslips placed at the bottom of sterile petri dishes. The cells were then treated as described in table 3 for 3 h. Cells were then fixed post treatment according to the assay to be performed (chapter 2). Coverslips were then frozen at -20 °C until required.

Cell Line	IC_{50} Treatment
MCF-7	0.1μlml^{-1} DMSO (Control)
	1μlml^{-1} Fish oil
	1 x 10^{-7}M 4OHTam
	25μM PD98059
	5μM LY294002
	1μlml^{-1} Fish oil,1 x 10^{-7}M 4OHTam, 25μM PD98059, 5μM LY294002
TamR	0.1μlml^{-1} DMSO (Control)
	1μlml^{-1} Fish oil
	25μM PD98059
	5μM LY294002
	1μlml^{-1} Fish oil, 25μM PD98059, 5μM LY294002

Table 5.3 Treatments for ICC analysis

ICC assays to detect, total ER, pER 118, pER 167, EGFR, pEGFR 1068, pAkt and pERK1/2 were performed; coverslips were then dried and mounted onto glass microscope slides using DPX.

H-score was used as a semi-quantitative method of measuring specific staining. It was determined by equation 5.1 (McClelland, R. *et al* 2001).

H-score = Σ (% of cells very weakly stained cells x 0.5) + (% weakly stained cells x 1) + (% of moderately stained cells x 2) + (% strongly stained cells x 3)

Equation 5.1

This analysis gives H Scores of between 0-300, where 0 is no staining seen and 300 is the strongest staining possible.

5.2.2.4 Western blot

Western blot analysis was carried out as described in chapter 2. Cells were grown to ~70% confluency, at which point they were dosed with either control (0.1μlml^{-1} DMSO) or test (1 μL mL^{-1} Fish oil,1 x 10^{-7} M 4OHTam, 25 μM PD98059, 5 μM LY294002 for MCF-7 cells and 1 μL mL^{-1} Fish oil, 25 μM PD98059, 5μM LY294002 for TamR cells) treatments. These were incubated for 3 h, after which protein was extracted and frozen at -20 °C until required. Samples were probed for protein concentrations of total ER, pER 118, pER 167, EGFR, pEGFR 1068, pAkt and pERK1/2.

Western blot analysis of β-actin using a CST β-actin was used as an internal control to ensure equal protein loading between lanes was achieved. β-actin is a ubiquitous protein and a major component of the cytoskeleton and has been proved as a positive control for protein loading (Grände, M. *et al* 2002, Suliburk, J. *et al* 2005).

5.3 Results

5.3.1 Phenotypic analysis of cell lines

Before any experimentation in this chapter both cell lines were analysed for typical phenotypic behaviour. MCF-7 cells were chosen to represent hormone responsive breast cancer cells, while TamR cells were chosen to represent the clinical problematic situation of tamoxifen resistance. Therefore, it was of paramount importance that the cells behaved as expected.

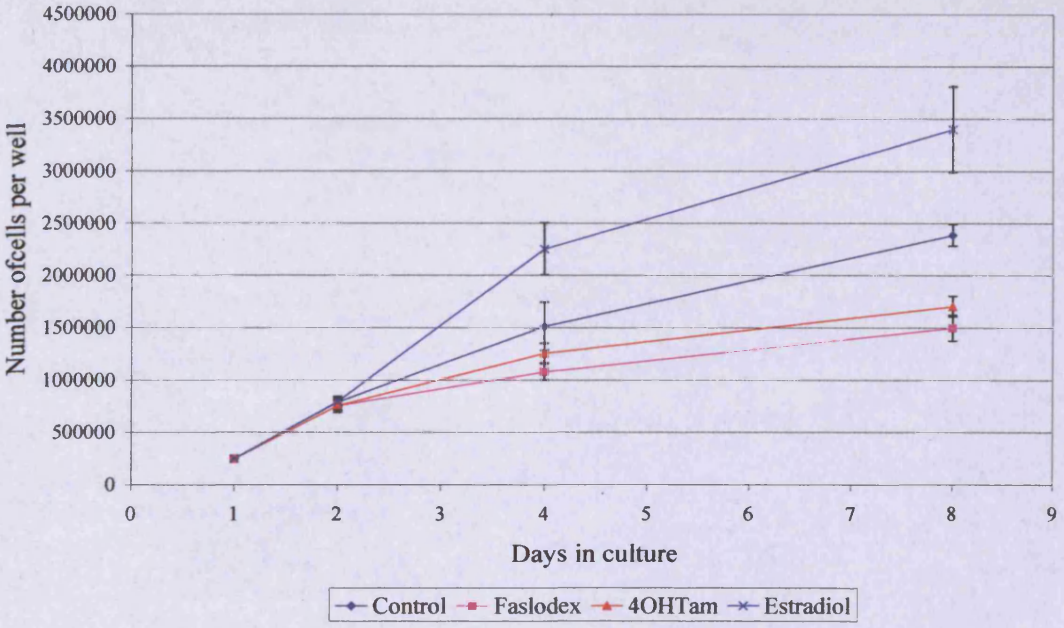

Figure 5.1 Growth assays to detect the effects of 1 x 10^{-7}M Faslodex, 1 x 10^{-9}M E_2 and 1 x 10^{-7} M 4-hydroxytamoxifen on MCF-7 cell growth. Cells were maintained in wRPMI + 5% SFCS for the duration of the experiment and were incubated at 37°C with 5% CO_2. Cells were dosed on days 1 and 4 and media replenished on doing. Passage numbers used were 25, 26 and 28 (n=3 ± SD).

Figure 5.1 shows growth assays for MCF-7 cells treated with 0.1 μL mL^{-1} DMSO (control), 1 x 10^{-7} M Faslodex, 1 x 10^{-9} M E_2 and 1 x 10^{-7} M 4-hydroxytamoxifen. It shows that the MCF-7 cells behaved as expected with Faslodex and 4-hydroxytamoxifen reducing cell growth to 64.3 ± 7.2 and 72.4 ± 10.1 % of control growth after 8 days. Treatment with 1 x 10^{-9} M E_2 elevated growth to 143 ± 12.7 % of control growth after 8 days.

Figure 5.2 shows growth assays for TamR cells when incubated with 0.1 μL mL^{-1} DMSO (control), 1 x 10^{-7} M Faslodex and 1 x 10^{-9} M E_2.

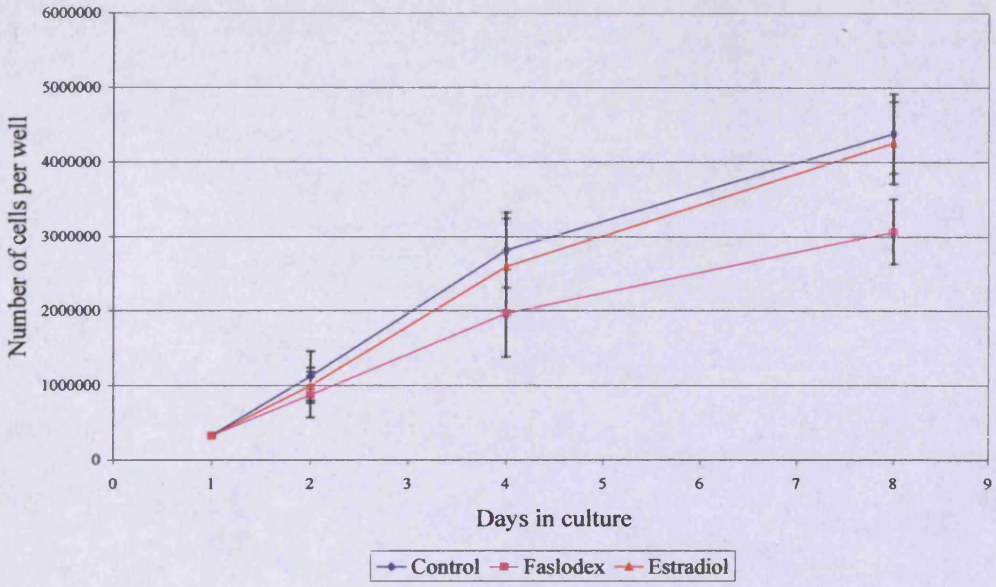

Figure 5.2 Growth assays to detect the effects of 1 x 10^{-7}M Faslodex and 1 x 10^{-7}M E_2 on TamR cell growth. Cells were maintained in wRPMI + 5% SFCS (with 1 x 10^{-9} M 4-hydroxytamoxifen present in the media) for the duration of the experiment and were incubated at 37°C with 5% CO_2. Cells were dosed on days 1 and 4 and media replenished on day 4. Passage numbers used were 13, 15 and 18 (n=3 ± SD).

The cells behaved characteristic of tamoxifen resistant cells, showing insensitivity to E_2 but still displaying a growth inhibition in response to incubation with the true anti-estrogen Faslodex. Growth was 69.9 ± 9.97 and 97.19 ± 12.5 % of control cell growth when TamR cells were incubated with 1 x 10^{-7}M Faslodex and 1 x 10^{-9} M E_2 respectively.

5.3.2 Dose response for fish oil on the growth of MCF-7 and TamR cells

Before growth assays showing the effect of fish oil over 8 days could be achieved, the IC_{50} of fish oil needed to be discovered.

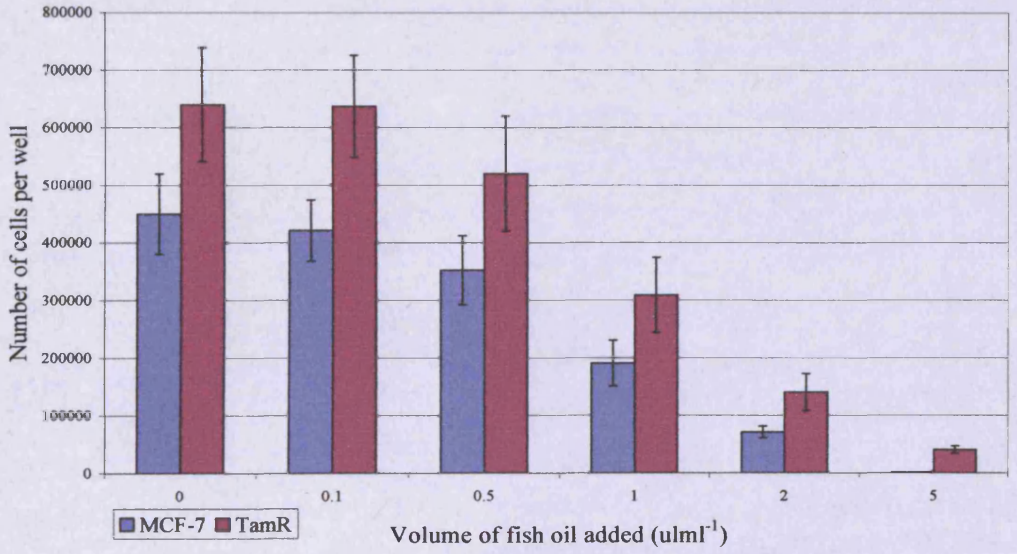

Figure 5.3 Dose responses of MCF-7 and TamR cells to increasing volumes of fish oil. Cells were maintained in wRPMI + 5% SFCS (with 1 x 10^{-9} M 4-hydroxytamoxifen present in the media for TamR cells) for the duration of the experiment and were incubated at 37°C with 5% CO_2. Cells were dosed on days 1 and 4 and media replenished on day 4. Passage numbers used were 18, 19 and 23 for MCF-7 cells and 20, 22 and 23 for TamR cells (n=3 ± SD).

Figure 5.3 demonstrates that there was an inverse relationship between increased fish oil and cell count, suggesting that fish oil inhibited MCF-7 and TamR cell growth in a dose dependant manner. Interestingly, both cell lines gave the same IC_{50} concentration of $1\mu L\ mL^{-1}$.

5.3.3 Growth assays

5.3.3.1 IC_{50} concentrations

The growth of MCF-7 and TamR cells were measured when insulted with PD98059, LY294002, 4-hydroxytamoxifen and fish oil. Figure 5.4 shows growth assays performed on MCF-7 cells.

Again the assay showed that the MCF-7 cells were hormone sensitive as they showed growth acceleration in response to estradiol and growth inhibition in response to 4-hydroxytamoxifen. These treatments altered growth rates to 130.9 ± 11.9 and 65.6 ± 5.8 % of control growth respectively. The incubation of MCF-7 cells with PD98059, LY294002, fish oil and combinations of compounds all reduced cell growth as displayed in table 5.4

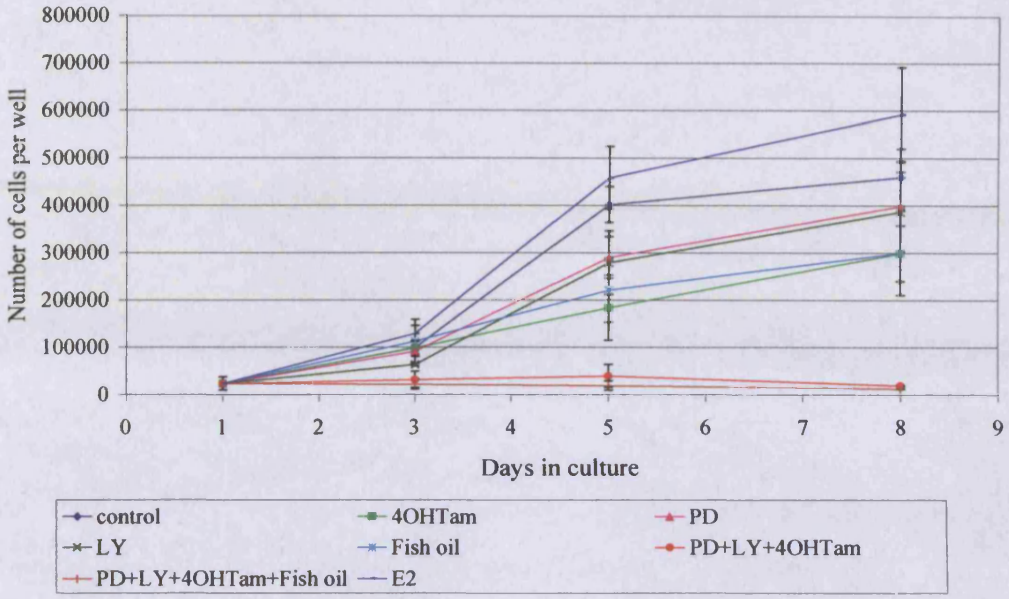

Figure 5.4 Growth assays to detect the effects of 25μM PD98059, 5μM LY294002, 1 x 10^{-7} M 4-hydroxytamoxifen and 1 μl ml^{-1} fish oil on MCF-7 cell growth. Cells were maintained in wRPMI + 5% SFCS for the duration of the experiment and were incubated at 37°C with 5% CO_2. Cells were dosed on days 1 and 4 and media replenished on day 4. Cell passage numbers were 14, 16 and 17 n=3 ± SD).

Figure 5.4 shows the effects of insult with 25 μM PD98059, 5 μM LY294002 and 1 μL mL^{-1} fish oil (individually and simultaneously) on TamR cell growth.

The growth assays for TamR cells, again, show that this cell line has lost sensitivity to E_2, however, PD98059, LY294002, Faslodex and fish oil gave growth inhibitory results.

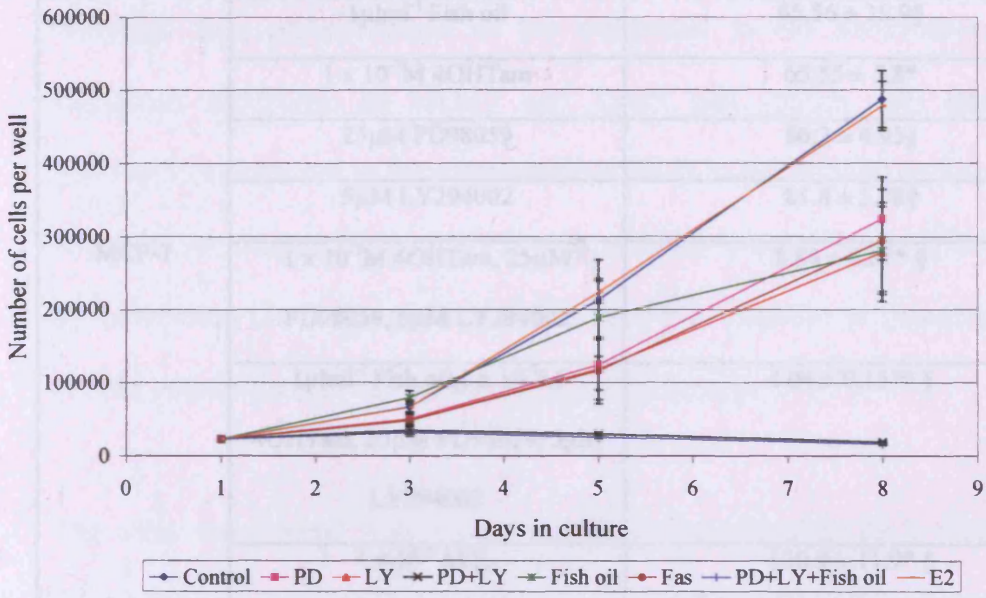

Figure 5.5 Growth assays to detect the effects of 25μM PD98059, 5μM LY294002 and 1μlml^{-1} fish oil on TamR cell growth. Cells were maintained in wRPMI + 5% SFCS for the duration of the experiment and were incubated at 37°C with 5% CO_2. Cells were dosed on days 1 and 4 and media replenished on day 4. Cell passage numbers were 12, 14 and 17 (n=3 ± SD).

As with MCF-7 cells, the simultaneous incubation of PD98059 plus LY294002, with and without fish oil present, gave significantly greater cell growth inhibition than incubation of these compounds individually. Percentage growth compared to control when incubated with these compounds can be seen in table 5.4

Cell Line	Treatment	% growth compared to control
MCF-7	1μlml^{-1} Fish oil	65.56 ± 15.9§
	1 x 10^{-7}M 4OHTam	65.55 ± 5.8*
	25μM PD98059	86.2 ± 4.95§
	5μM LY294002	81.8 ± 5.78§
	1 x 10^{-7}M 4OHTam, 25μM PD98059, 5μM LY294002	8.84 ± 0.2** §
	1μlml^{-1} Fish oil,1 x 10^{-7}M 4OHTam, 25μM PD98059, 5μM LY294002	4.04 ± 0.15** §
	1 x 10^{-9} M E_2	130.9 ± 11.9* §
TamR	1μlml^{-1} Fish oil	65.1 ± 16.8*
	25μM PD98059	66.4 ± 15.3*
	5μM LY294002	55.7 ± 14.5*
	1 x 10^{-7}M Faslodex	59.7 ± 16.3*
	25μM PD98059, 5μM LY294002	3.7 ± 0.9**
	1μlml^{-1} Fish oil, 25μM PD98059, 5μM LY294002	2.47 ± 1.4**
	1 x 10^{-9} M E_2	98.7 ± 14.5

Table 5.4 Percentage cell growth compared to control when MCF-7 and TamR cells were incubated with 25μM PD98059, 5μM LY294002, 1 x 10^{-7}M 4-hydroxytamoxifen and 1μlml^{-1} fish oil (and combinations of these). * $p = <0.05$ compared to control growth, ** $p = < 0.004$ compared to control growth, § $p = < 0.05$ compared to same treatment between cell lines.

5.3.3.2 Effect of levels of drug found to permeate full thickness skin

Although IC_{50} concentrations of the compound in the formulation gave significant reductions of MCF-7 and TamR cell growth, this does not necessarily extrapolate to the concentrations likely to reach breast cancer tissue when delivered transcutaneously. A more realistic assessment could be made by calculating the concentrations found in earlier chapters to permeate skin (4.3.4), correct for a 25 cm^2 patch and apply to the cells.

The cells were dosed with concentrations permeated after 48 h (from the formulation consisting of 4 % cab-o-sil and 2.5 % DMSO ethanol) on day 1 (0.65 μM PD98059, 0.8 μM LY294002 and 0.41 μM 4-hydroxytamoxifen) and then with concentrations permeated after 24 h each day thereafter (half of those stated above).

Figure 5.6 shows the effects of the permeated doses of compounds on MCF-7 cells. Permeated concentrations of compounds were able to inhibit the growth of MCF-7 cells, as shown in figure 5.6. PD98059 and LY294002 were able to reduce growth to 71.6 ± 9.98 and 72.1 ± 10.2 % of control growth (P = 0.024, 0.026). The addition of permeated concentrations of 4-hydroxytamoxifen, which was more than the IC_{50} concentration, reduced cell growth to 62.2 ± 5.08 % of control growth (P = 0.004).

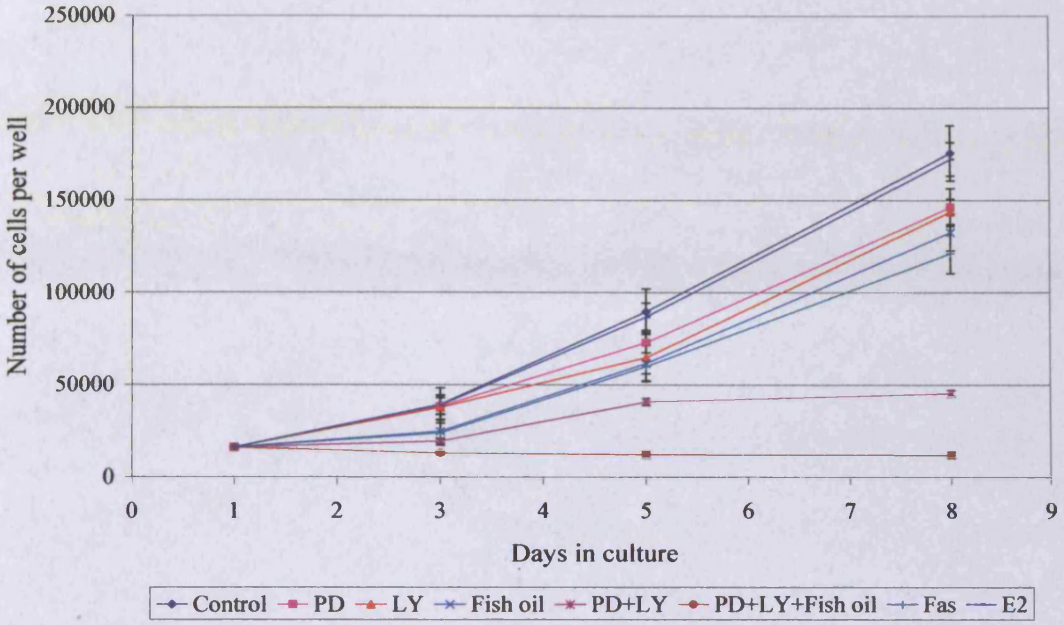

Figure 5.6 Growth assays to detect the effects of permeated concentrations of PD98059, LY294002, 4-hydroxytamoxifen and 1µlml^{-1} fish oil on MCF-7 cell growth. Cells were maintained in wRPMI + 5% SFCS for the duration of the experiment and were incubated at 37°C with 5% CO_2. Cells were dosed on day 1 with permeated concentrations after 48 hours and with permeated concentrations after 24 hours on each day thereafter. Media was replenished on re-treatment. Cell passage numbers were 22, 24 and 29 (n=3 ± SD).

The simultaneous incubation of these three compounds was able to reduce cell growth significantly to 17.27 ± 1.56 % of control growth (P = 0.002). The addition of 1µL mL^{-1} fish oil to these 3 compounds reduced cell growth again, to 9.3 ± 2.1 % of control growth (P = 0.0018).

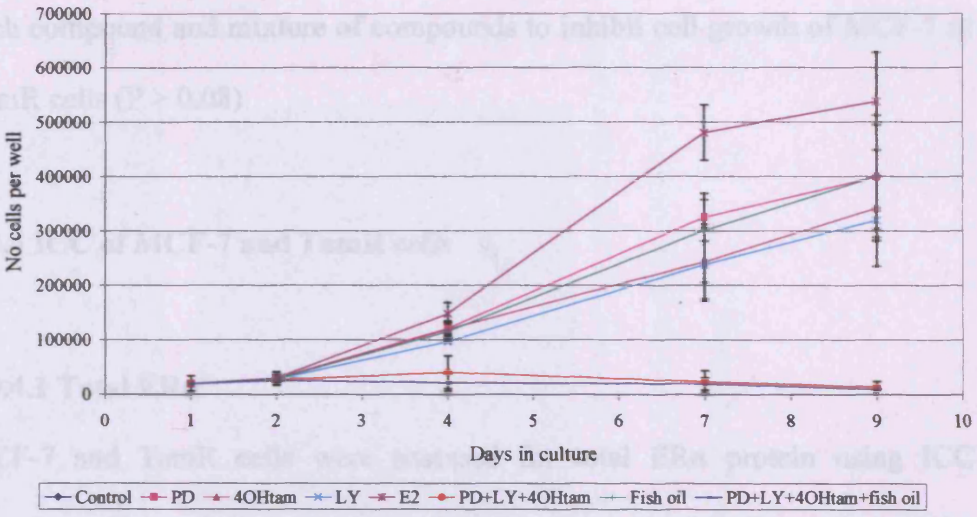

Figure 5.7 Growth assays to detect the effects of permeated concentrations of PD98059, LY294002 and 1µlml^{-1} fish oil on TamR cell growth. Cells were maintained in wRPMI + 5% SFCS for the duration of the experiment and were incubated at 37°C with 5% CO_2. Cells were dosed on day 1 with permeated concentrations after 48 hours and with permeated concentrations after 24 hours on each day thereafter. Media was replenished on re-treatment. Cell passage numbers were 19, 22 and 26 (n=3 ± SD).

Figure 5.7 demonstrates that when incubated simultaneously PD98059 and LY294002 reduced TamR cell growth significantly compared to control growth ($P = 0.001$). The combination reduced cell growth to 25.4 ± 3.9 and 6.4 ± 1.6 % of control growth when incubated without and with 1 µL mL^{-1} fish oil.

Permeated concentrations of PD98059 and LY294002 when incubated singly were also capable of giving a modest reduction in cell growth; 87.5 ± 13.9 and 83.5 ± 11.3 % of control growth respectively, however, this was not a

significant observation. No significant difference was seen in the ability of each compound and mixture of compounds to inhibit cell growth of MCF-7 or TamR cells ($P > 0.08$)

.

5.3.4 ICC of MCF-7 and TamR cells

5.3.4.1 Total ERα

MCF-7 and TamR cells were assessed for total ERα protein using ICC detection. Figure 5.8 demonstrates that ERα is localised to the nucleus of the MCF-7 and TamR cells. The assay also highlights that total ERα is expressed at a higher level in MCF-7 cells than TamR cells. This is reiterated in the H-score analysis, shown in table 5.4, where ERα has a H-score of 213 ± 31 in MCF-7 cells and 122 ± 27 shows that expression of total ERα is significantly reduced in TamR cells compared to MCF-7 cells ($P = 0.034$).

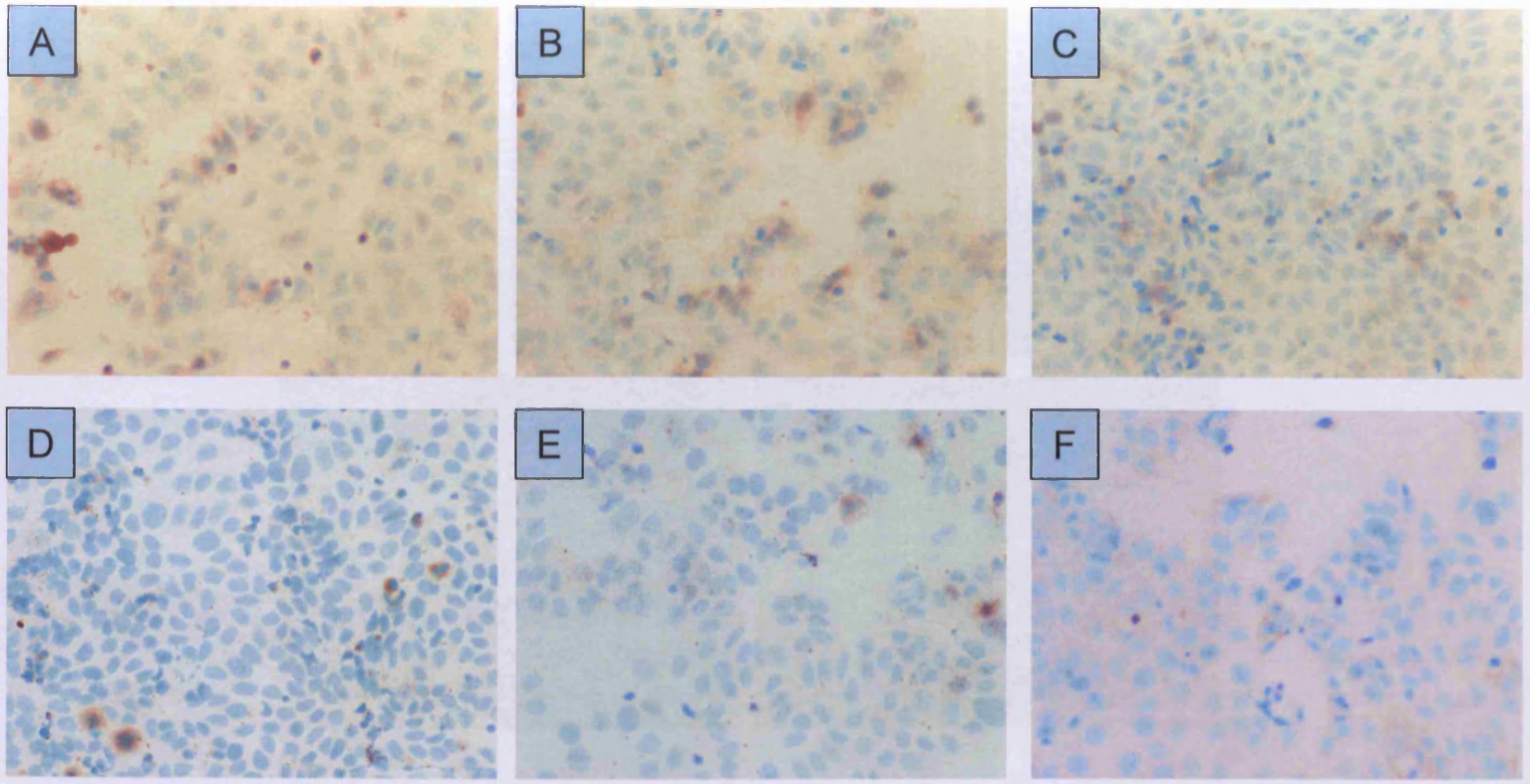

Figure 5.14 A-F MCF-7 cells assayed for pEGFR 1068 (x20). Cells were grown to ~70% confluency on a TESPA coated coverslip. They were then treated with 0.1µlml^{-1} DMSO (A), 25µ PD98059 (B), 5µM LY294002 (C) 1 x 10^{-7}M 4OHTam (D), 1µlml^{-1} fish oil (E) and combination of PD, LY, 4OHTam and fish oil (F) for 3 hours. Fixation was 2.5% Phenol-Formal Saline. Primary antibody was Biosource pEGFR 1068 rabbit primary antibody at 1/75 overnight at 37°C.

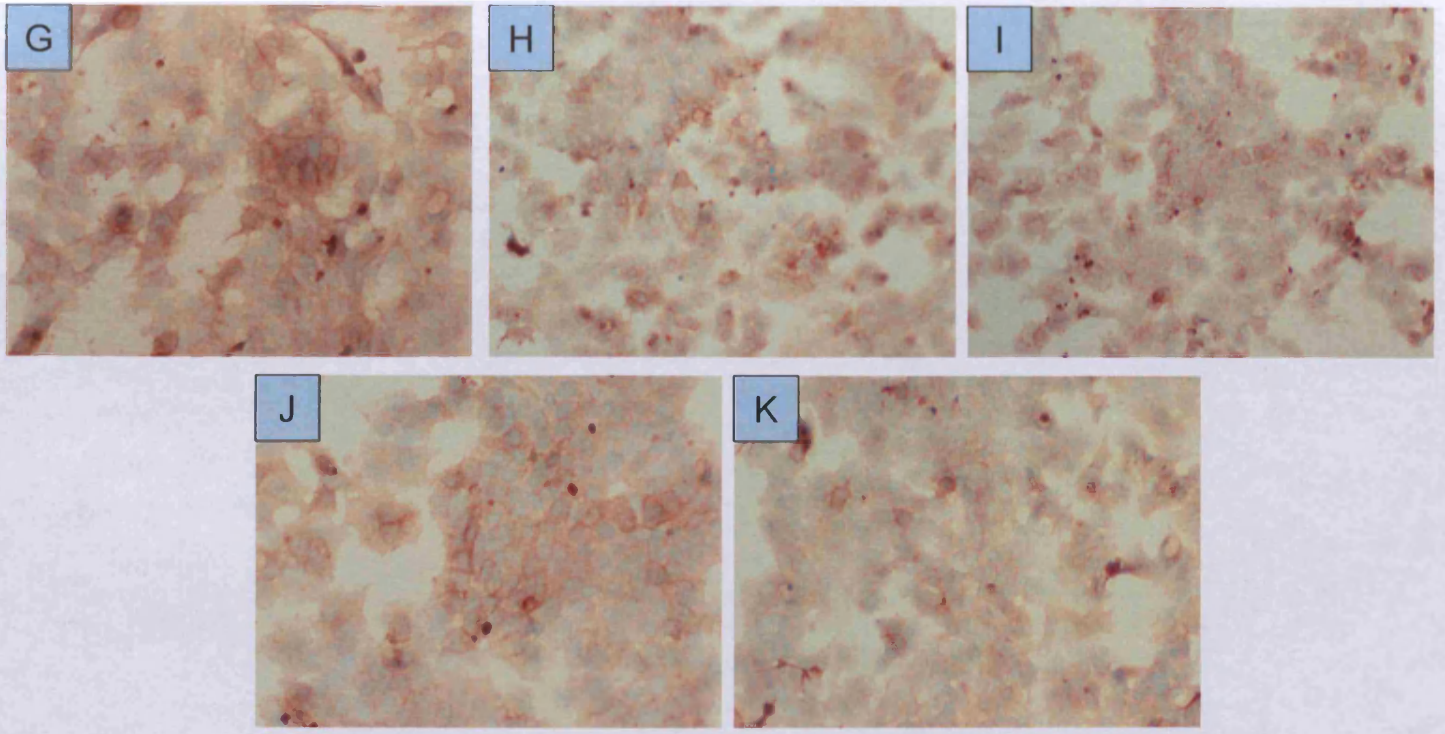

Figure 5.14 G-K TamR cells assayed for pEGFR 1068 (x20). Cells were grown to ~70% confluency on a TESPA coated coverslip. They were then treated with 0.1µlml^{-1} DMSO (G), 25µ PD98059 (H), 5µM LY294002 (I), 1µlml^{-1} fish oil (J) and combination of PD, LY and fish oil (K) for 3 hours. Fixation was 2.5% Phenol-Formal Saline. Primary antibody was Biosource pEGFR 1068 rabbit primary antibody at 1/75 overnight at 37°C

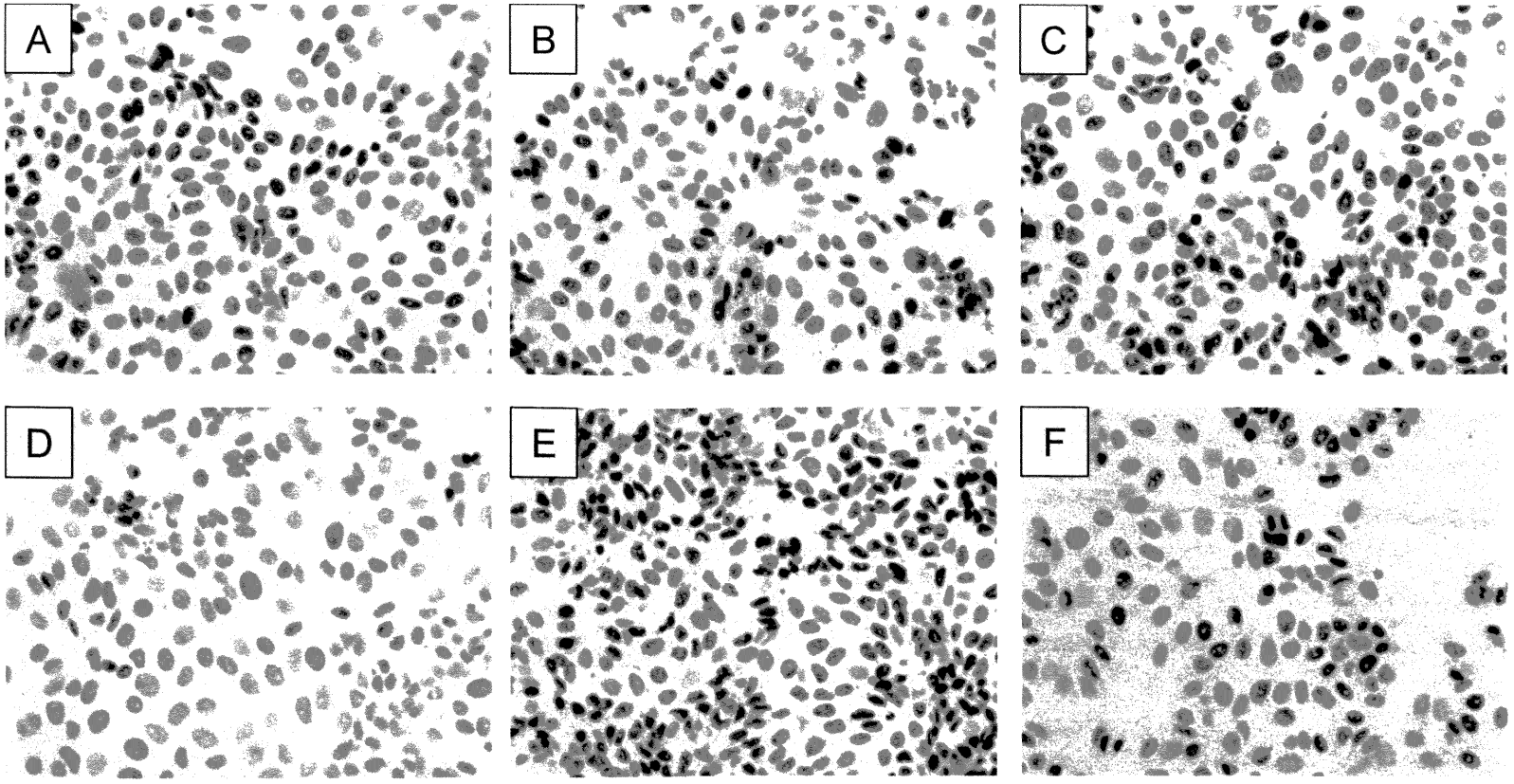

Figure 5.8 A-F MCF-7 cells assayed for total ER (x20). Cells were grown to ~70% confluency on a TESPA coated coverslip. They were then treated with 0.1µlml^{-1} DMSO (A), 25µ PD98059 (B), 5µM LY294002 (C) 1 x 10^{-7}M 4OHTam (D), 1µlml^{-1} fish oil (E) and combination of PD, LY, 4OHTam and fish oil (F) for 3 hours. Fixation was ER-ICA. Primary antibody was DAKO total ER clone ID5 mouse antibody at 1/100 in PBS and was incubated for 60 minutes.

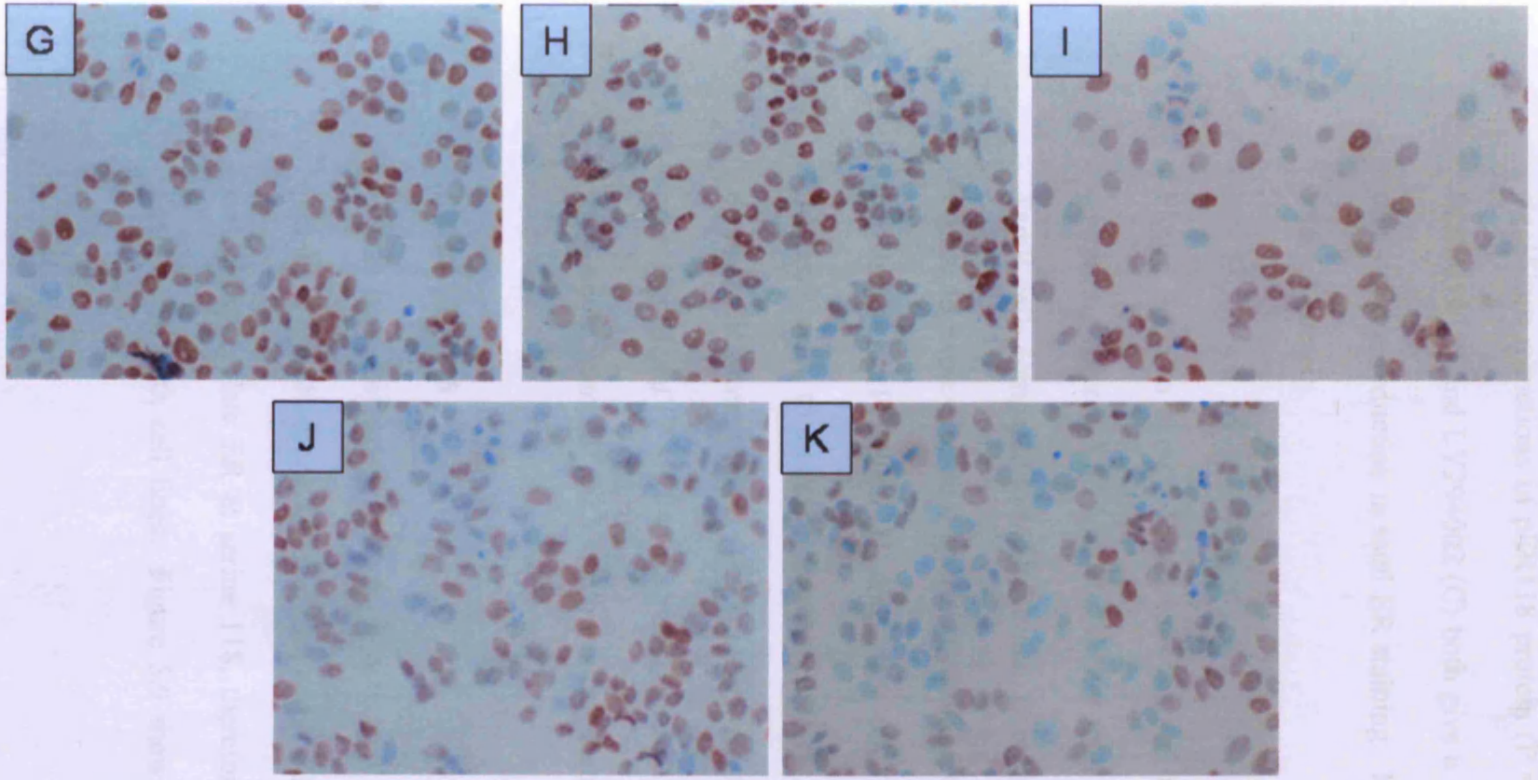

Figure 5.8 G-K TamR cells assayed for total ER (x20). Cells were grown to ~70% confluency on a TESPA coated coverslip. They were then treated with 0.1µlml^{-1} DMSO (G), 25µ PD98059 (H), 5µM LY294002 (I), 1µlml^{-1} fish oil (J) and combination of PD, LY and fish oil (K) for 3 hours. Fixation was ER-ICA. Primary antibody was DAKO total ER clone ID5 mouse antibody at 1/100 in PBS and was incubated for 60 minutes

Figure 5.8 shows total ER staining was nuclear, with no cytoplasmic ER staining seen. 4-hydroxytamoxifen (D) and the cocktail formulation (F) both gave the most obvious reduction in total ER staining in MCF-7 cells, reducing the H-score from 213 ± 31 seen in control, to 81 ± 11 and 75 ± 7, which were significant reductions in pER118 protein ($P = 0.022$ and 0.019 respectively). PD98059 (B) and LY294002 (C) both give a much less prominent and almost unnoticeable reduction in total ER staining. Fish oil (E) gave no reduction in total ER protein.

Figure 5.8 also shows TamR cells stained for total ER. It is obvious by comparing figures 5.8 (A) and (G) that total ER protein is vastly reduced in TamR cells compared to MCF-7 cells. Expression of total ER in TamR cells is similar to expression in 4-hydroxytamoxifen treated MCF-7 cells (D). Figure 5.8 shows that PD98059 (H) and LY294002 (I) both reduced total ER protein in TamR cells, to a similar degree. However, fish oil did not have any effect on total ER protein levels (J). The cocktail of compounds proved to give the most significant ($P = 0.046$) reduction in total ER in TamR cells (K), reducing the H-score from 122 ± 27 seen in control TamR cells, to 51.3 ± 3.67.

5.3.4.2 pER118

It was also important to look at activated ERα as the MAPK and PI3K pathways can phosphorylate and thus activate ERα at specific residues. MAPK can phosphorylate ER at serine 118, therefore pER 118 protein levels were analysed in both cell lines. Figure 5.9 shows, like total ER, pER118 shows

nuclear staining in both cell lines with no cytoplasmic staining. Levels of pER118 protein were much lower than total ERα, with pER118 levels being higher in MCF-7 cells (A) than in TamR cells (G).

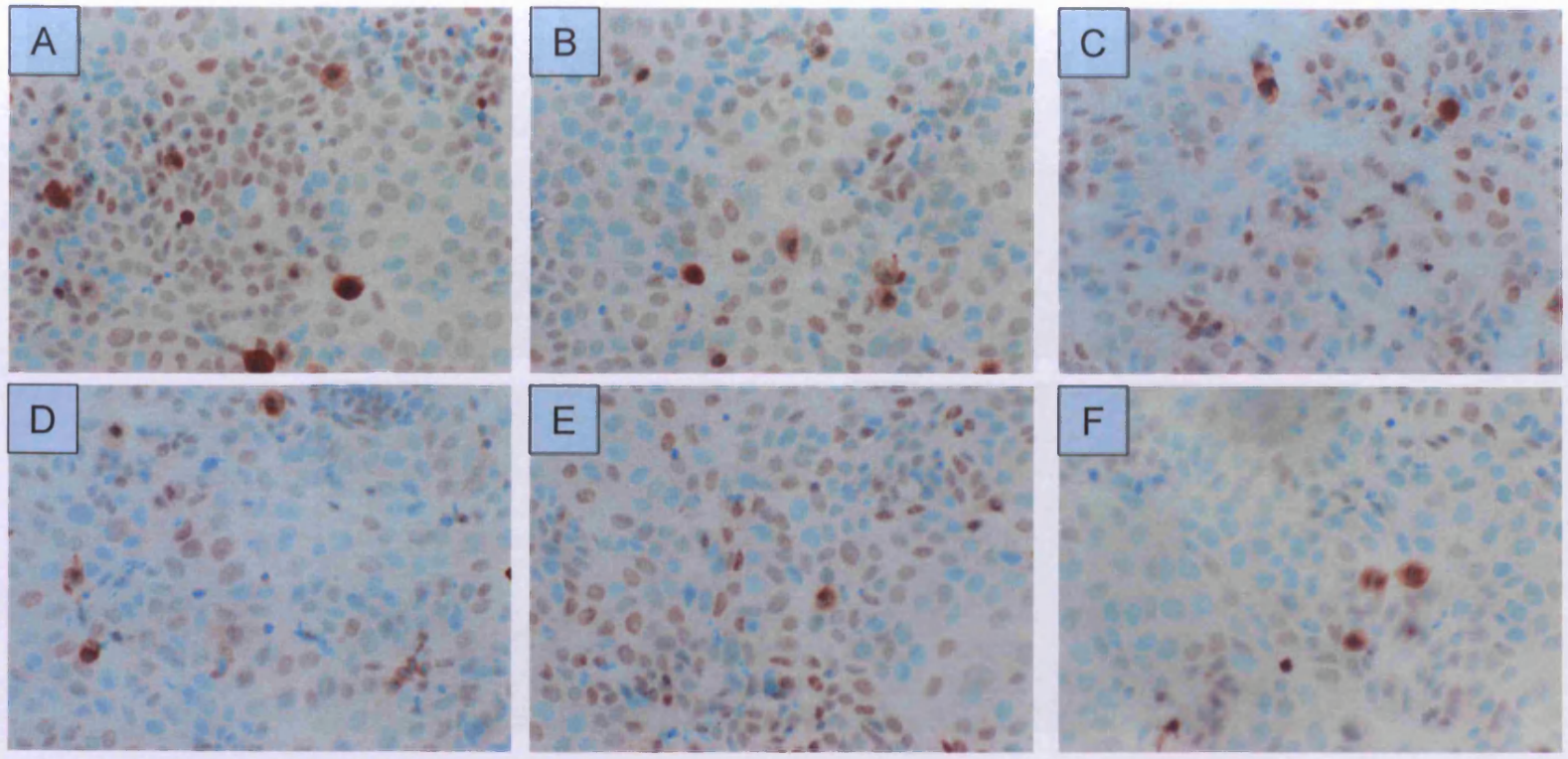

Figure 5.9 A-F MCF-7 cells assayed for pER 118 (x20). Cells were grown to ~70% confluency on a TESPA coated coverslip. They were then treated with 0.1µlml^{-1} DMSO (A), 25µ PD98059 (B), 5µM LY294002 (C) 1 x 10^{-7}M 4OHTam (D), 1µlml^{-1} fish oil (E) and combination of PD, LY, 4OHTam and fish oil (F) for 3 hours. Fixation was 2% paraformaldehyde. Primary antibody was NEB phospho-ER 118 monoclonal antibody at 1/500 in PBS overnight.

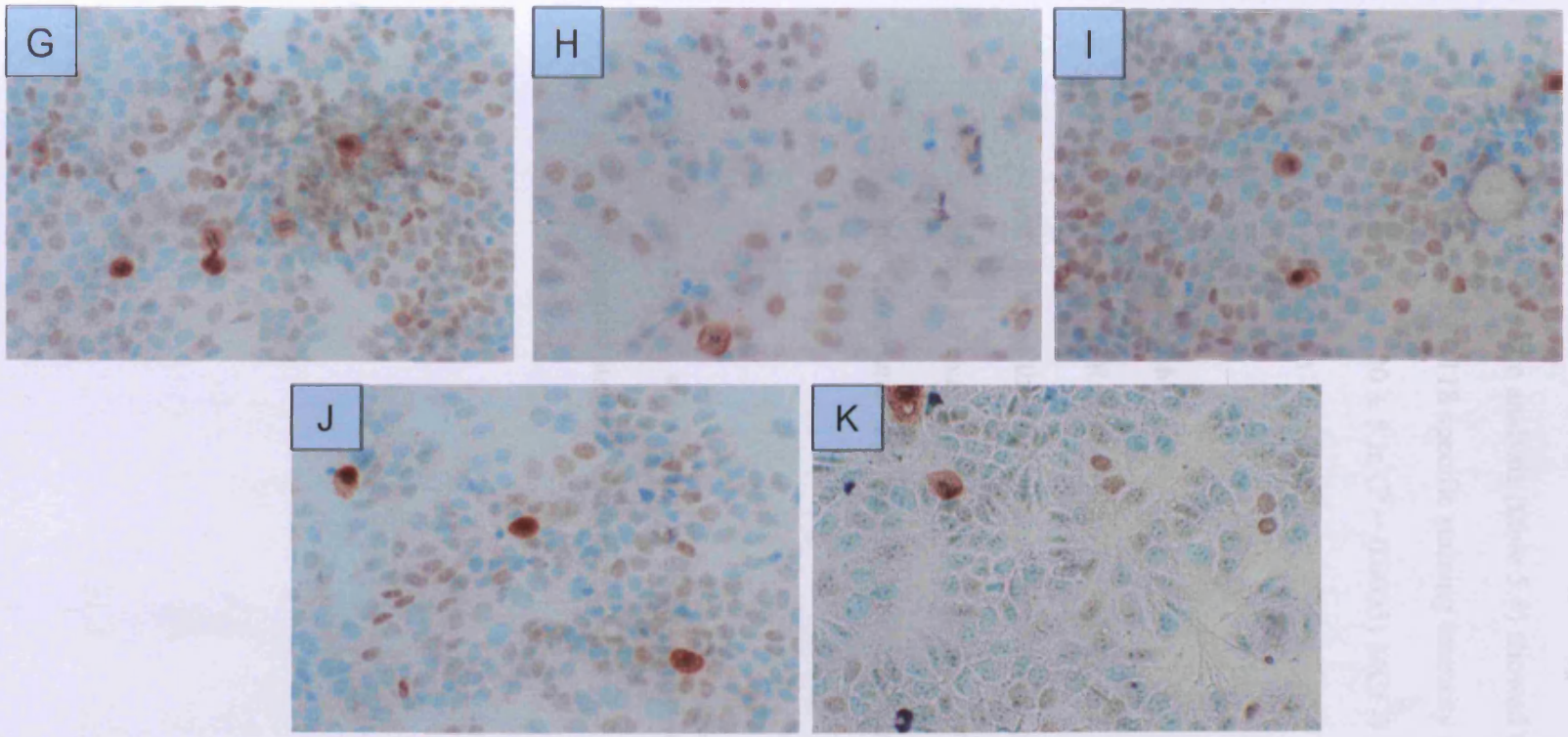

Figure 5.9 G-K TamR cells assayed for pER 118 (x20). Cells were grown to ~70% confluency on a TESPA coated coverslip. They were then treated with 0.1µlml^{-1} DMSO (G), 25µ PD98059 (H), 5µM LY294002 (I), 1µlml^{-1} fish oil (J) and combination of PD, LY and fish oil (K) for 3 hours. Fixation was 2% paraformaldehyde. Primary antibody was NEB phospho-ER 118 monoclonal antibody at 1/500 in PBS overnight.

Figure 5.9 shows that each compound seemed to reduce pER118 protein, with the combination treatment giving the greatest reduction in pER118 in both cell lines. H-score analysis (table 5.4) showed that this combination of compounds reduced pER118 specific staining intensity significantly in both cell lines; from 125 ± 18 to 20 ± 5 in ($P = 0.0005$) MCF-7 cells and from 59 ± 4 to 16.5 ± 2.5 ($P = 0.001$) in TamR cells.

5.3.4.3 pER167

As with pER118, pER167 is a ligand independent activation site, with activation of the PI3K signalling pathway phosphorylating ERα at this residue. Figure 5.10 examines the extent of pER167 in both cell lines and the effect that each compound and the cocktail of compounds had on pER 167 protein expression.

Figure 5.10 shows that pER167 was localised to the nucleus, with no cytoplasmic staining being detected.

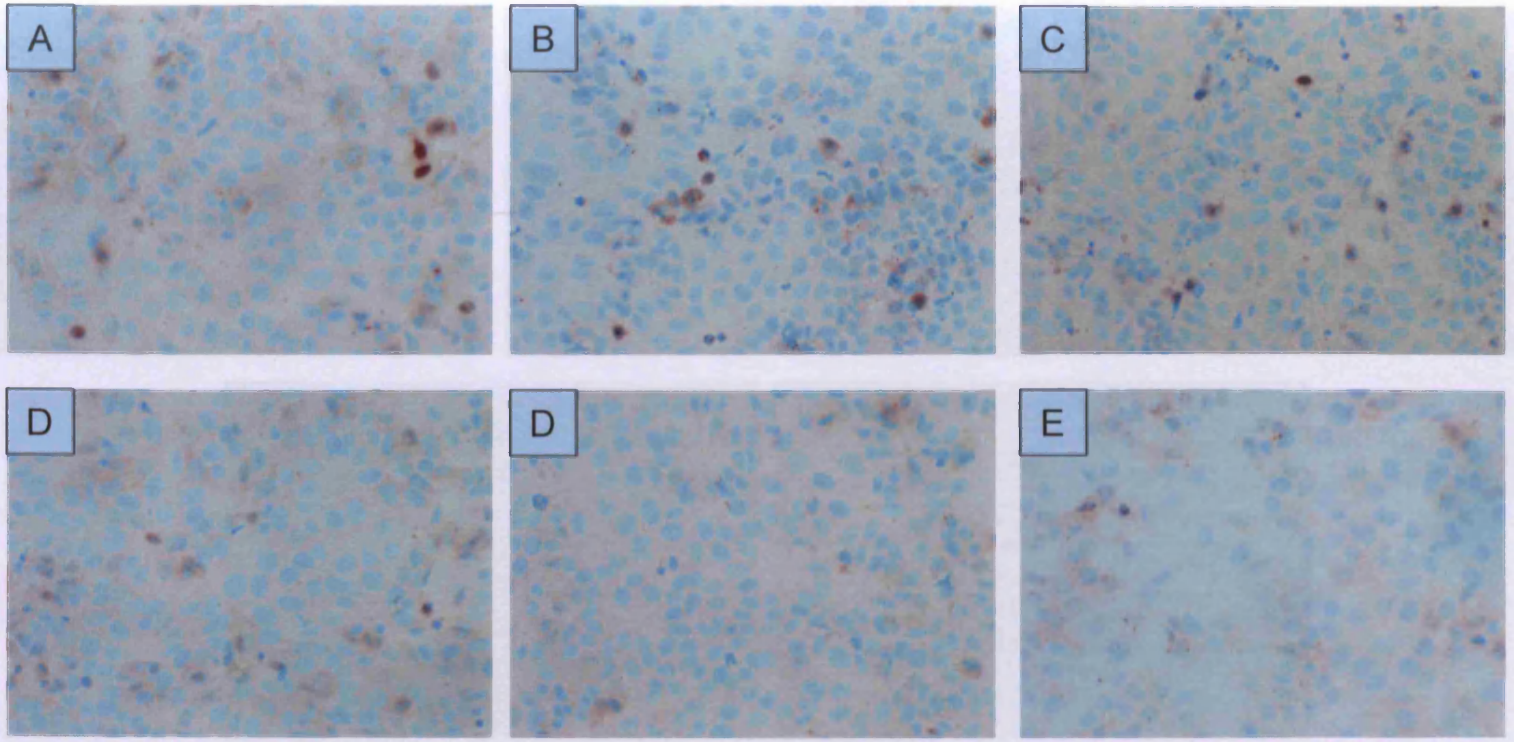

Figure 5.10 A-F MCF-7 cells assayed for pER 167 (x20). Cells were grown to ~70% confluency on a TESPA coated coverslip. They were then treated with 0.1µlml^{-1} DMSO (A), 25µ PD98059 (B), 5µM LY294002 (C) 1 x 10^{-7}M 4OHTam (D), 1µlml^{-1} fish oil (E) and combination of PD, LY, 4OHTam and fish oil (F) for 3 hours. Fixation was ER-ICA. Primary antibody was CST phospho-ER 167 antibody at 1/25 in PBS overnight.

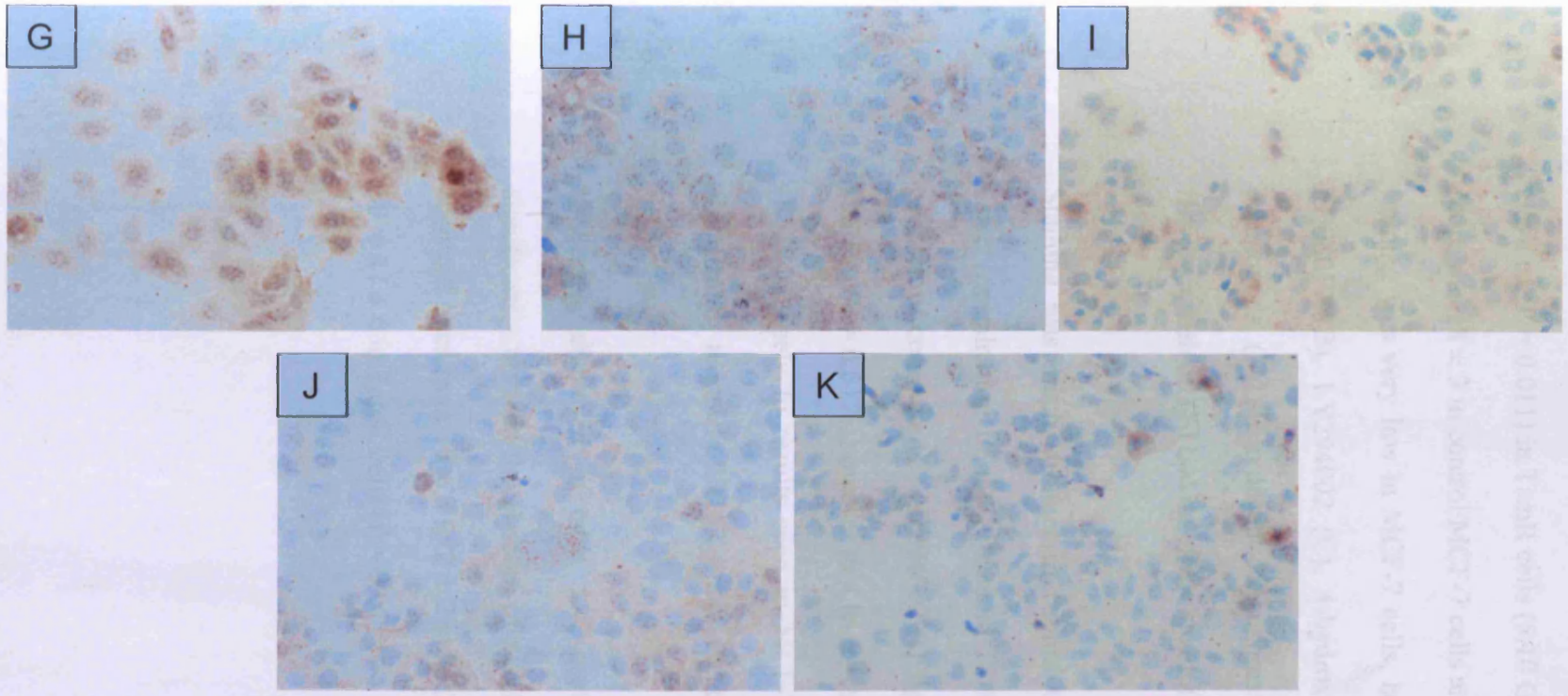

Figure 5.10 G-K TamR cells assayed for pER 167 (G x 40 H-K x20). Cells were grown to ~70% confluency on a TESPA coated coverslip. They were then treated with 0.1µlml^{-1} DMSO (G), 25µ PD98059 (H), 5µM LY294002 (I), 1µlml^{-1} fish oil (J) and combination of PD, LY and fish oil (K) for 3 hours. Fixation was ER-ICA. Primary antibody was CST phospho-ER 167 antibody at 1/25 in PBS overnight.

Unlike total ER and pER118, pER167 protein expression was significantly elevated (P = 0.011) in TamR cells (5.10 G) compared to MCF-7 cells (A). H-score was 18 ± 3 in control MCF-7 cells and 182 ± 30 in TamR cells. pER167 staining was very low in MCF-7 cells, however, it was possible to tell that PD98059 (B), LY294002 (C), 4-hydroxytamifen (D) and the cocktail of compounds (F) all reduced the expression of pER167 in MCF-7 cells, However, fish oil (E) had no effect, quantified in the H-scores in table 5.4.

Staining was much stronger in control treated TamR cells, which allowed easier examination of the effects of PD98059, LY294002, fish oil and the cocktail of compounds. LY294002 (I) significantly reduced pER167 specific staining (P = 0.017), however to a lesser extent than the cocktail of compounds (K). Inversely to results seen in MCF-7 cells, in TamR cells fish oil (J) significantly reduced pER167 protein levels (P= 0.027).

H-scoring, displayed in table 5.4, showed that the cocktail formulation significantly reduced the H-score of pER167 staining compared to control in both cell lines from 18 ± 3 to 2 ± 2 in MCF-7 cells (P = 0.05) and from 182 ± 30 to 11 ± 6 in TamR cells (P = 0.011).

		H-Score						
Cell line	**Treatment**	**Total ER**	**pER118**	**pER167**	**pERK1/2**	**pAkt**	**Total EGFR**	**pEGFR1068**
MCF-7	**Control**	213 ± 31	125 ± 18	18 ± 3	105 ± 26	121 ± 8	52 ± 18	34 ± 6
	PD	183 ± 24	61 ± 4.	10 ± 2	37 ± 5	125 ± 7	44.2 ± 4	21 ± 8
	LY	198 ± 18	81 ± 9	16 ± 4	96 ± 8	45 ± 3	36 ± 4	12 ± 4
	4OHTam	81 ± 11	54 ± 6	13 ± 3	108 ± 19	111 ± 9	66 ± 12	0 ± 0
	FO	213 ± 34	93 ± 13	5 ± 4	64 ± 17	77 ± 7.5	32 ± 6	9 ± 4
	PD, LY, 4OHTam, FO	75 ± 7	20.5 ± 5	2 ± 2	15 ± 3	30 ± 5	19 ± 5	0 ± 0
TamR	**Control**	122 ± 27	59 ± 4	182 ± 30	210 ± 33	175 ± 11	256 ± 17	277 ± 21
	PD	112 ± 14	57 ± 3	141 ± 6	70 ± 21	180 ± 9	235 ± 27	162 ± 22
	LY	102 ± 10	53 ± 7	46 ± 7	159 ± 18.5	40± 6	253 ± 24	168 ± 15
	FO	122 ± 17	41 ± 6.5	71 ± 11	118 ± 22	109 ± 12.5	130 ± 21	222 ± 33
	PD, LY, FO	51.3 ± 3.67	16.5 ± 2.5	11 ± 6	17 ± 3	15 ± 7	126 ± 30	132 ± 10

Table 5.4 H-score analysis of MCF-7 and TamR cells when assayed for the immunocytochemical detection of ER, pER118, pER167, pERK1/2, pAkt, total EGFR and pEGFR1068. Cells were treated with control (0.1μlml^{-1} DMSO), 25μM PD, 5μM LY, 1 x 10^{-7} M 4OHTam, 1μlml^{-1} fish oil for 3 hours (n=3 ± SD).

5.3.4.4 pERK 1/2

The protein expression of pERK1/2 was analysed in both cell lines when insulted with the cocktail formulation as this is the target of PD98059. Figure 5.11 shows that pERK1/2 was detected in both the cytoplasm and nucleus. MCF-7 cells (5.11A) showed significantly less pERK1/2 protein expression than TamR cells (5.11G) did ($p = 0.022$). PD98059 gave a significant knockdown in pERK1/2 protein expression in both cell lines with p values of 0.045 and 0.008 for MCF-7 and TamR cells respectively (5.11B & H). This was quantified by the H-score analysis, where PD98059 reduced the H-score of ERK1/2 from 105 ± 26 to 37 ± 5 in MCF-7 cells and from 210 ± 33 to 70 ± 21 in TamR cells. Fish oil also gave a modest decrease in pERK1/2 staining in both cell lines (5.11E & J). The cocktail formulation of PD98059, LY294002, 4-hydroxytamoxifen and fish oil in MCF-7 cells and PD98059, LY294002 and fish oil in TamR cells gave the most significant knockdown in pERK1/2 protein expression ($p = 0.026$ and 0.01 respectively), which almost silenced pERK1/2 expression completely. This was confirmed in H-score analysis shown in table 5.4.

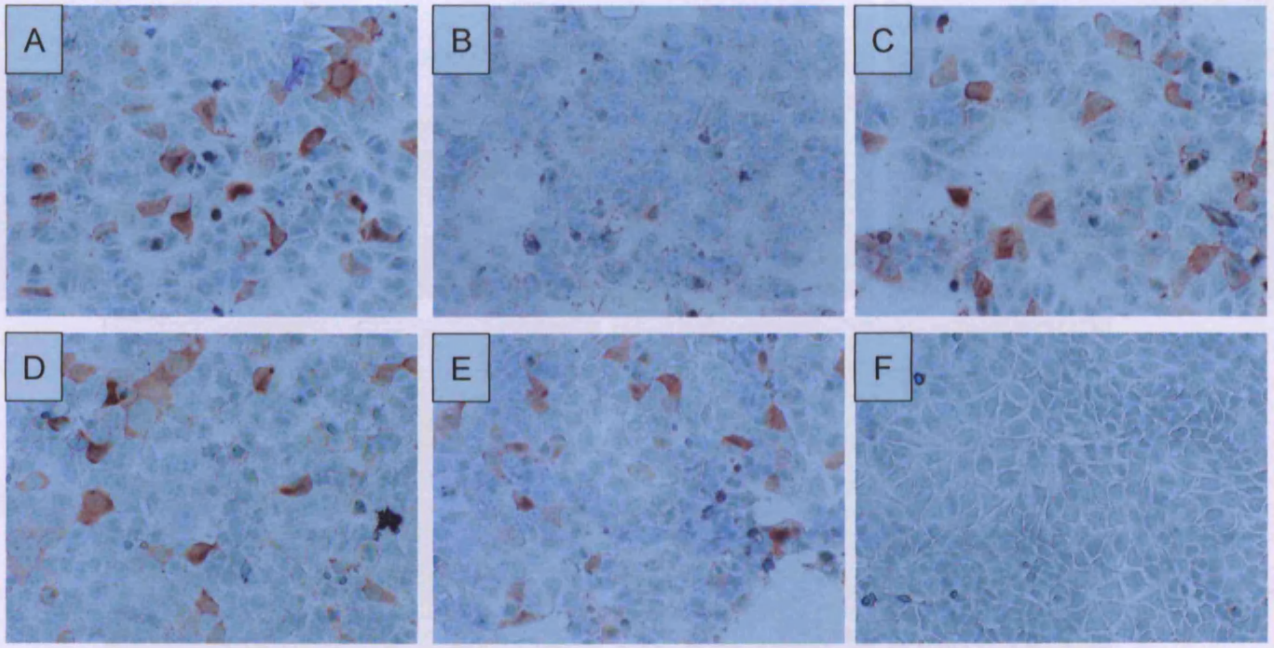

Figure 5.11 A-F MCF-7 cells assayed for pERK1/2 (x20). Cells were grown to ~70% confluency on a TESPA coated coverslip. They were then treated with 0.1µlml^{-1} DMSO (A), 25µ PD98059 (B), 5µM LY294002 (C) 1 x 10^{-7}M 4OHTam (D), 1µlml^{-1} fish oil (E) and combination of PD, LY, 4OHTam and fish oil (F) for 3 hours. Fixation was formal saline. Primary antibody was CST phospho-ERK1/2 antibody at 1/20 in PBS for 1 hour.

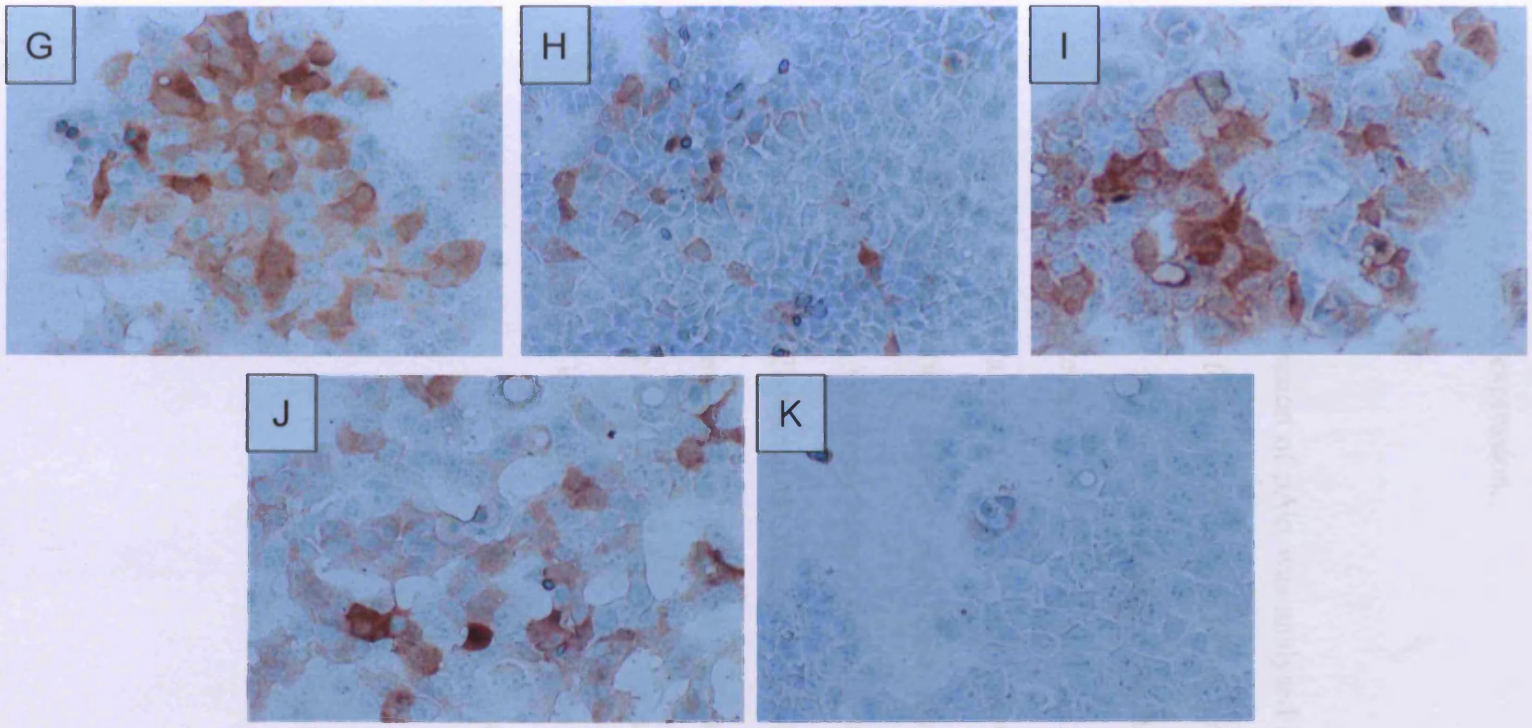

Figure 5.11 G-K TamR cells assayed for pERK1/2 (x20). Cells were grown to ~70% confluency on a TESPA coated coverslip. They were then treated with 0.1µlml^{-1} DMSO (G), 25µ PD98059 (H), 5µM LY294002 (I), 1µlml^{-1} fish oil (J) and combination of PD, LY and fish oil (K) for 3 hours. Fixation was formal saline. Primary antibody was CST phospho-ERK1/2 antibody at 1/20 in PBS for 1 hour.

LY294002 (5.11 C & I) did not affect pERK1/2 expression in either cell line, while incubation of MCF-7 cells with 4-hydroxytamoxifen did not affect pERK1/2 protein expression.

5.3.4.5 pAkt

The protein expression of pAkt was analysed in both cell lines when insulted with the cocktail formulation as this is the target of LY294002. Figure 5.12 shows that pAkt was mainly localised to the cytoplasm but some nuclear staining was detected. MCF-7 cells (5.12A) showed less pAkt protein expression than TamR cells (5.12G) did, however this was not significant ($P = 0.079$). LY294002 gave a significant knockdown ($P = 0.013$, 0.0002 respectively) in pAkt protein expression in both cell lines (5.12B & H). Fish oil also had no effect on pAkt staining in MCF-7 or TamR cells (5.12E & J). The cocktail formulation of PD98059, LY294002, 4-hydroxytamoxifen and fish oil in MCF-7 cells and PD98059, LY294002 and fish oil in TamR cells gave the greatest knockdown in pAkt protein expression ($P = 0.009$, 0.0001 respectively for MCF-7 and TamR cells).

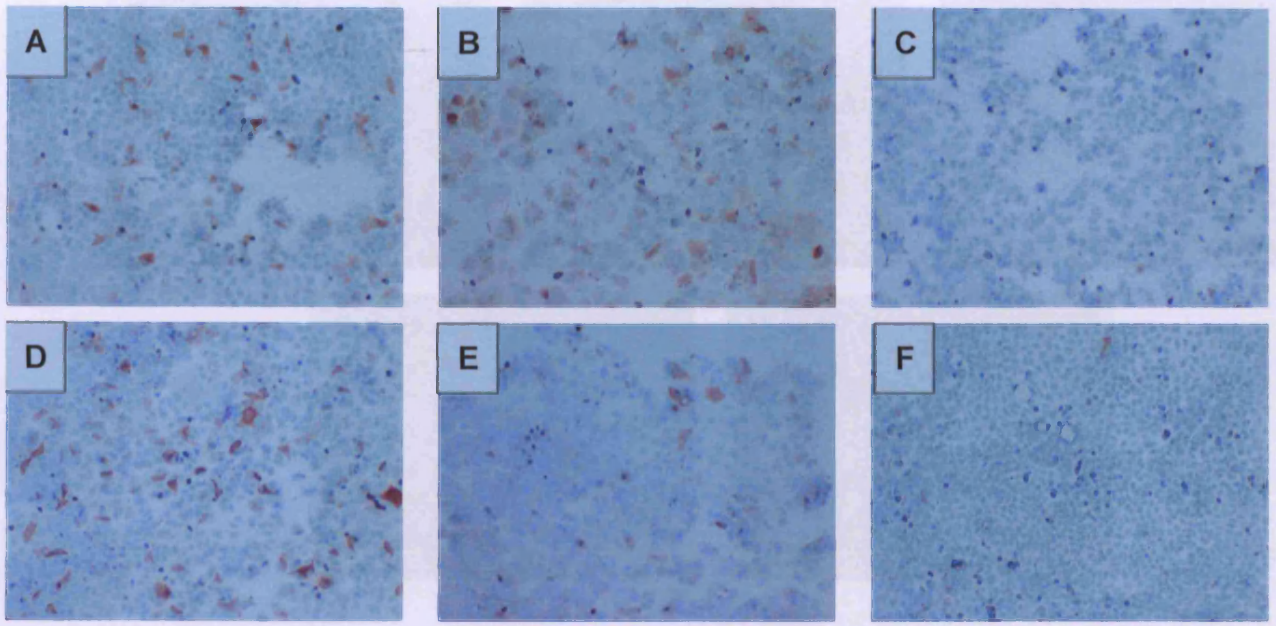

Figure 5.12 A-F MCF-7 cells assayed for pAkt (x20). Cells were grown to ~70% confluency on a TESPA coated coverslip. They were then treated with 0.1µlml^{-1} DMSO (A), 25µ PD98059 (B), 5µM LY294002 (C) 1 x 10^{-7}M 4OHTam (D), 1µlml^{-1} fish oil (E) and combination of PD, LY, 4OHTam and fish oil (F) for 3 hours. Fixation was ER-ICA. Primary antibody was CST phospho-Akt antibody at 1/100 in PBS for 2 hours.

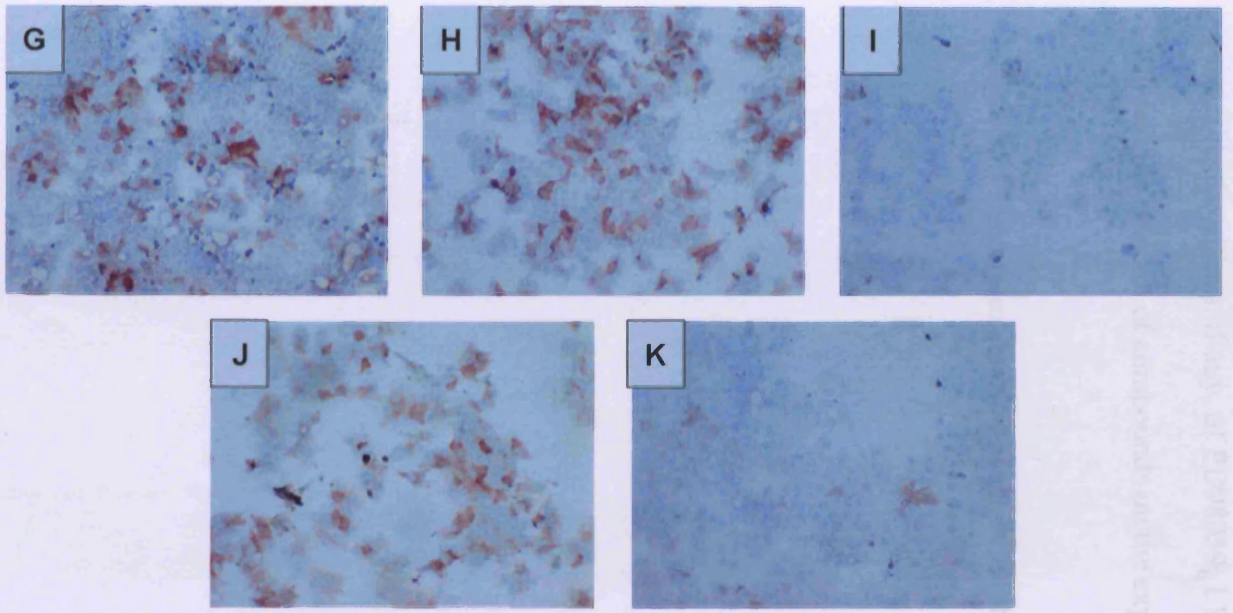

Figure 5.12 G-K TamR cells assayed for pER 167 (G x 40 H-K x20). Cells were grown to ~70% confluency on a TESPA coated coverslip. They were then treated with 0.1µlml^{-1} DMSO (G), 25µ PD98059 (H), 5µM LY294002 (I), 1µlml^{-1} fish oil (J) and combination of PD, LY and fish oil (K) for 3 hours. Fixation was ER-ICA. Primary antibody was CST phospho-Akt antibody at 1/100 in PBS for 2 hours.

5.3.4.6 Total EGFR

PI3K and MAPK are downstream mediators of EGFR. Therefore total EGFR was measured to assess the expression of EGFR in both cell lines and to examine the effects, if any, of PD98059, LY294002, 4-hydroxytamoxifen, fish oil and the cocktail of compounds on the expression of total EGFR.

Figure 5.13 shows expression of total EGFR in MCF-7 and TamR cells.

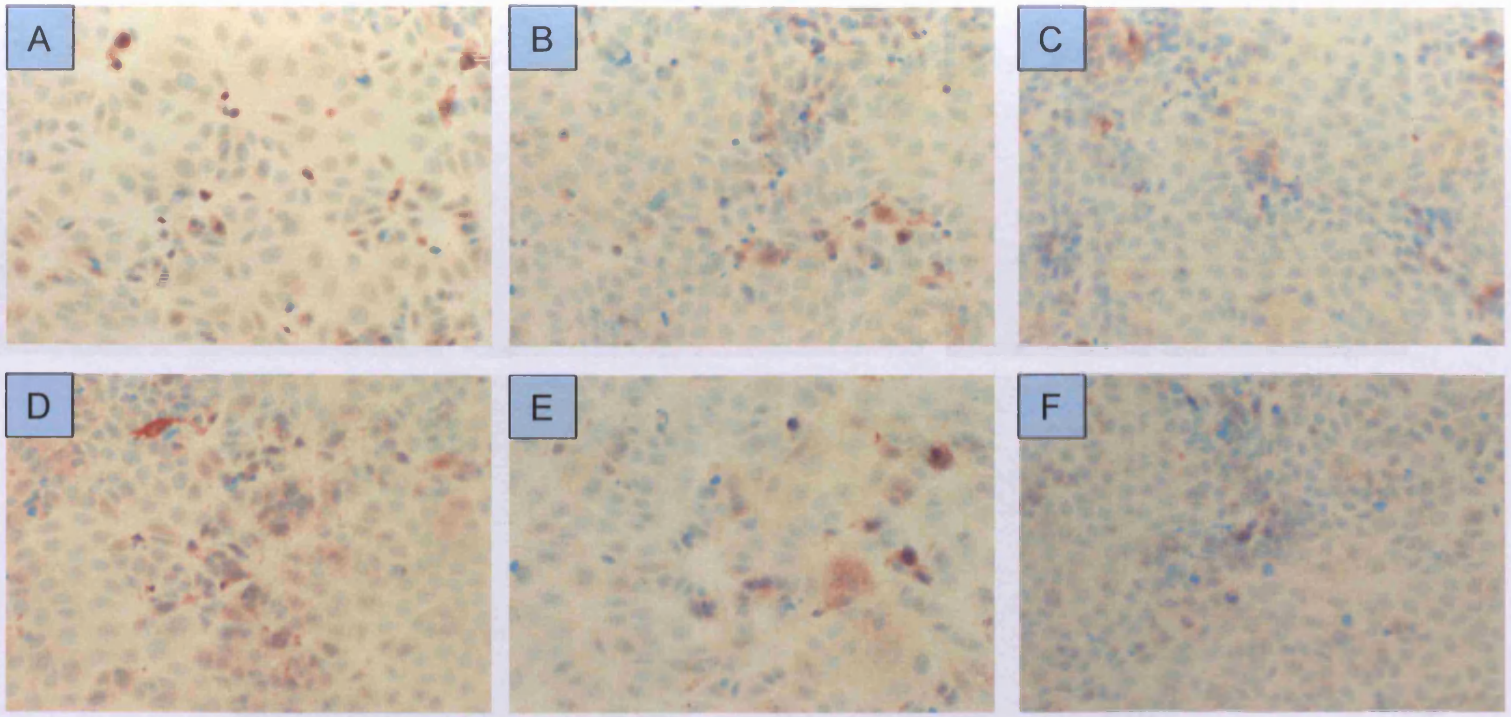

Figure 5.13 A-F MCF-7 cells assayed for total EGFR (x20). Cells were grown to ~70% confluency on a TESPA coated coverslip. They were then treated with 0.1µlml^{-1} DMSO (A), 25µ PD98059 (B), 5µM LY294002 (C) 1 x 10^{-7}M 4OHTam (D), 1µlml^{-1} fish oil (E) and combination of PD, LY, 4OHTam and fish oil (F) for 3 hours. Fixation was 2.5% Phenol-Formal Saline. Primary antibody was NeoMarkers EGFR mouse monoclonal antibody at 1/20 in PBS overnight.

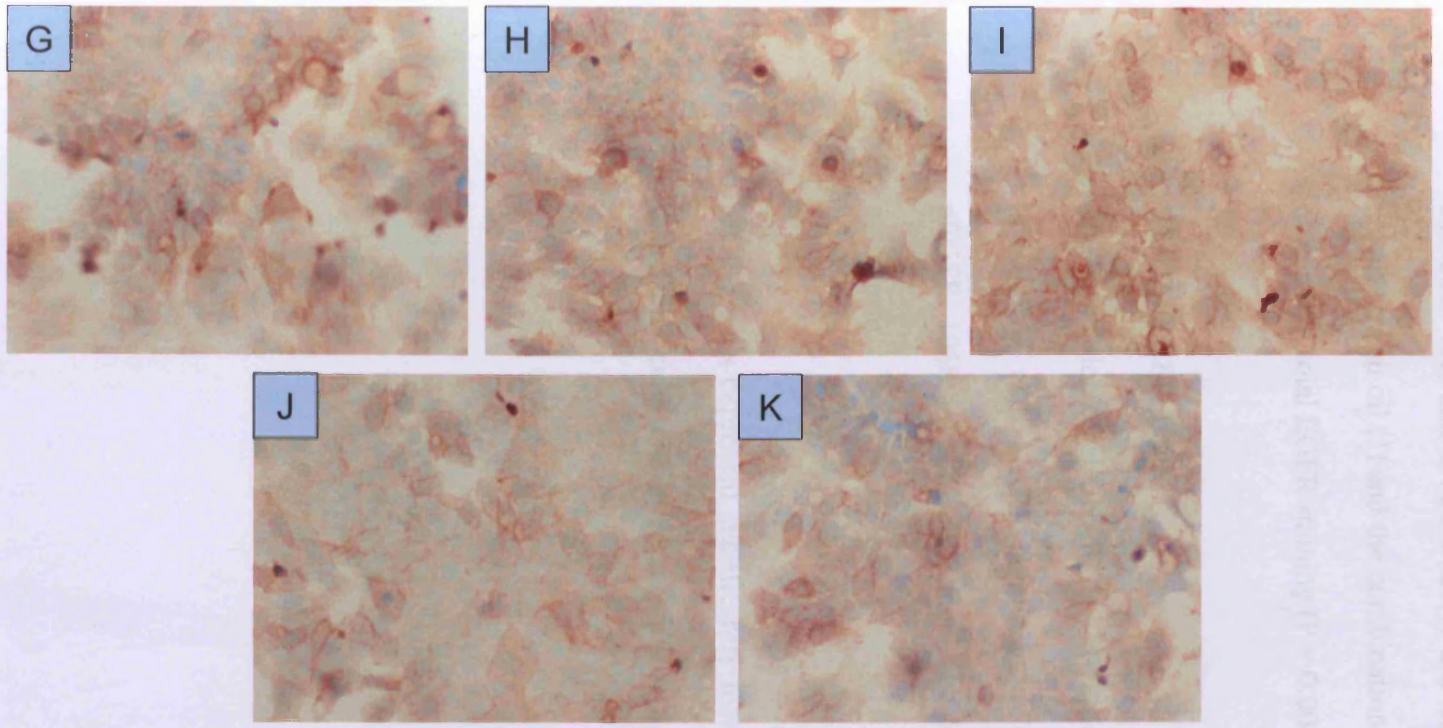

Figure 5.13 G-K TamR cells assayed for total EGFR (x20). Cells were grown to ~70% confluency on a TESPA coated coverslip. They were then treated with 0.1µlml^{-1} DMSO (G), 25µ PD98059 (H), 5µM LY294002 (I), 1µlml^{-1} fish oil (J) and combination of PD, LY and fish oil (K) for 3 hours. Fixation was 2.5% Phenol-Formal Saline. Primary antibody was NeoMarkers EGFR mouse monoclonal antibody at 1/20 in PBS overnight.

Figure 5.13 shows that total EGFR was expressed at significantly higher levels in TamR cells compared to MCF-7 cells, compared in figure 5.13 A and G (P = 0.01). Total EGFR displayed membrane and cytoplasmic localization. PD98059 (H) and LY294002 (I) did not affect total EGFR in TamR cells, however, fish oil (J) and the combination of compounds (K) gave a significant decrease in total EGFR staining (P = 0.004 and 0.007 respectively).

5.3.4.7 pEGFR 1068

The expression of pEGFR1068 was also examined as this phosphorylation site is involved with MAPK signalling. Figure 5.14 shows the expression of pEGFR 1068 in both cell lines was localised to the cell membrane and cytoplasm.

MCF-7 cells expressed significantly lower (P = 0.003) levels of pEGFR1068 than TamR cells, displayed in figure 5.14 A and G.

PD98059 (H), LY294002 (I) and the cocktail formulation (K) all showed significant inhibition of pEGFR1068 protein expression in TamR cells (P = 0.007, 0.005, 0.008 respectively). Fish oil (J) gave a modest inhibition in pEGFR expression in TamR cells, however this was not significant (P = 0.093).

5.3.5 Western blot

To confirm the results seen in the ICC analysis of MCF-7 and TamR cells, western blot was carried out to assess the protein expression of total ER, pER118, pER167, pAkt, pERK1/2, total EGFR and pEGFR when treated with either 0.1µlml^{-1} DMSO (control)or 25µ PD98059, 5µM LY294002, 1 x 10^{-7}M 4OHTam, 1µlml^{-1} fish oil (test).

5.3.5.1 ERα

The cocktail formulation gave a reduction total, p118 and p167 ERα in both cell lines. Figure 5.15 shows western blot analysis for total ER, pER118 and pER167 in MCF-7 and TamR cells.

Western blot of β actin revealed equal protein loading was achieved, as shown in figure 5.15A. All densitometry was normalised for actin.

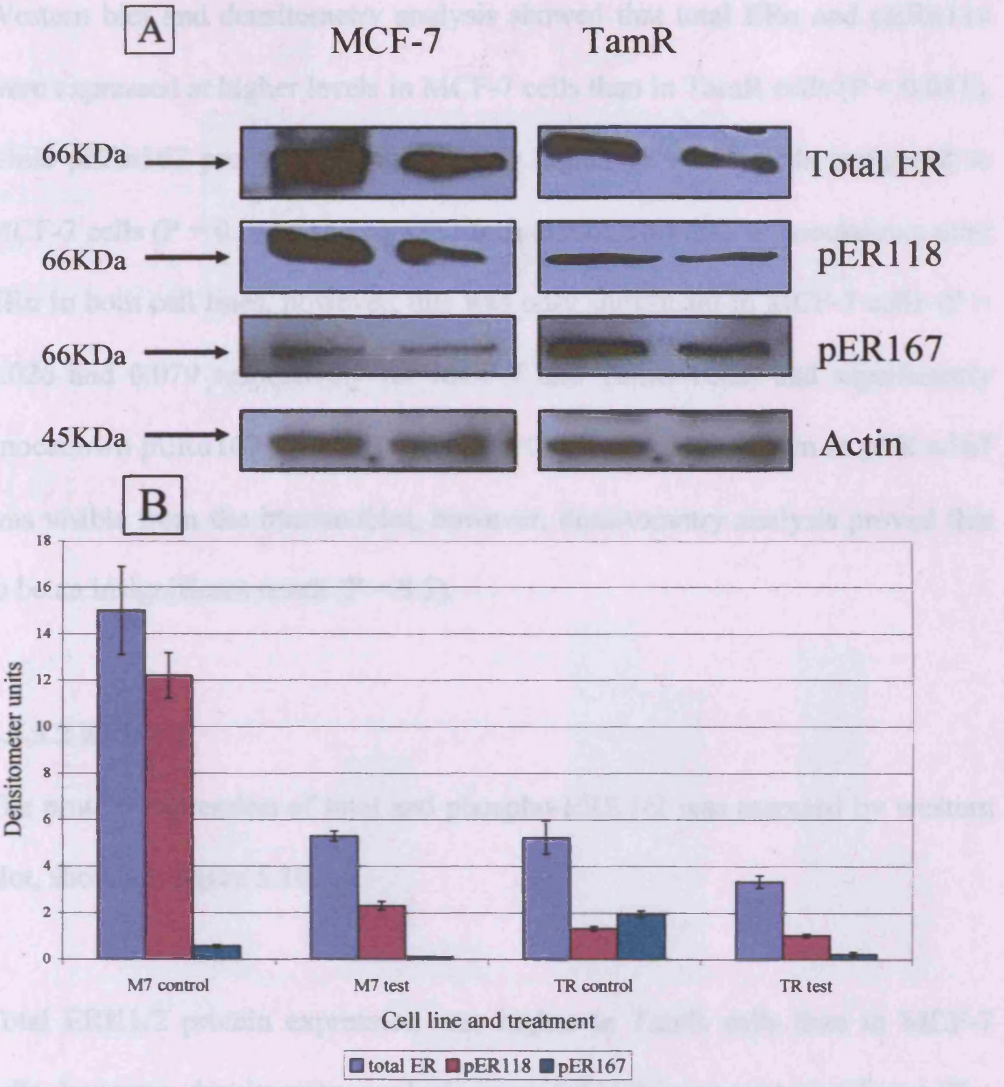

Figure 5.15 Western Blot for the levels of total ERα, pERα118, pERα167 and β-actin protein. MCF-7 and TamR cells were incubated with 1µlml^{-1} fish oil, 25µM PD98059, 5µM LY294002 and 1 x 10^{-7}M 4OHTam (MCF-7 cells only) for three hours. Cells were lysed and protein extracted and quantified for equal loading. Protein was separated by SDS-PAGE, immobilised on a nitrocellulose membrane and immunoprobed using a total ERα, pERα118 or pERα167 primary antibody. Passage numbers 37, 29, 31 for MCF-7 cells and 23, 26 and 28 for TamR cells. **B** Densitometry analysis of total ERα, pERα118 and pERα167 protein (n=3 ± SEM). M7- MCF-7 cells, TR- TamR cells. Densitoetry was normalised to actin. Densitometry was performed using Alpha Digi Doc ™ RT camera and image analysis system, Genetic Research Instrumentation, Essex, UK.

Western blot and densitometry analysis showed that total ERα and pERα118 were expressed at higher levels in MCF-7 cells than in TamR cells (P = 0.011), while pERα167 protein was significantly higher in TamR cells compared to MCF-7 cells (P = 0.01). The cocktail formulation was able to knockdown total ERα in both cell lines, however, this was only significant in MCF-7 cells (P = 0.026 and 0.079 respectively for MCF-7 and TamR cells) and significantly knockdown pERα167 in TamR cells (P = 0.038). A knockdown in pER α167 was visible from the immunoblot, however, densitometry analysis proved this to be an insignificant result (P = 0.5).

5.3.5.2 ERK1/2

The protein expression of total and phospho-ERK1/2 was assessed by western blot, shown in figure 5.16.

Total ERK1/2 protein expression was higher in TamR cells than in MCF-7 cells; however, densitometry analysis proved that this was not significant (P = 0.077). Incubation with PD98059, LY294002, 4-hydroxytamoxifen (MCF-7 cells only) and fish oil did not affect the expression of total ERK1/2 in either cell line.

The expression of pERK1/2 was significantly higher in TamR cells than in MCF-7 cells (P = 0.025). The cocktail of compounds reduced the expression of pERK1/2 significantly in TamR cells only (P = 0.036).

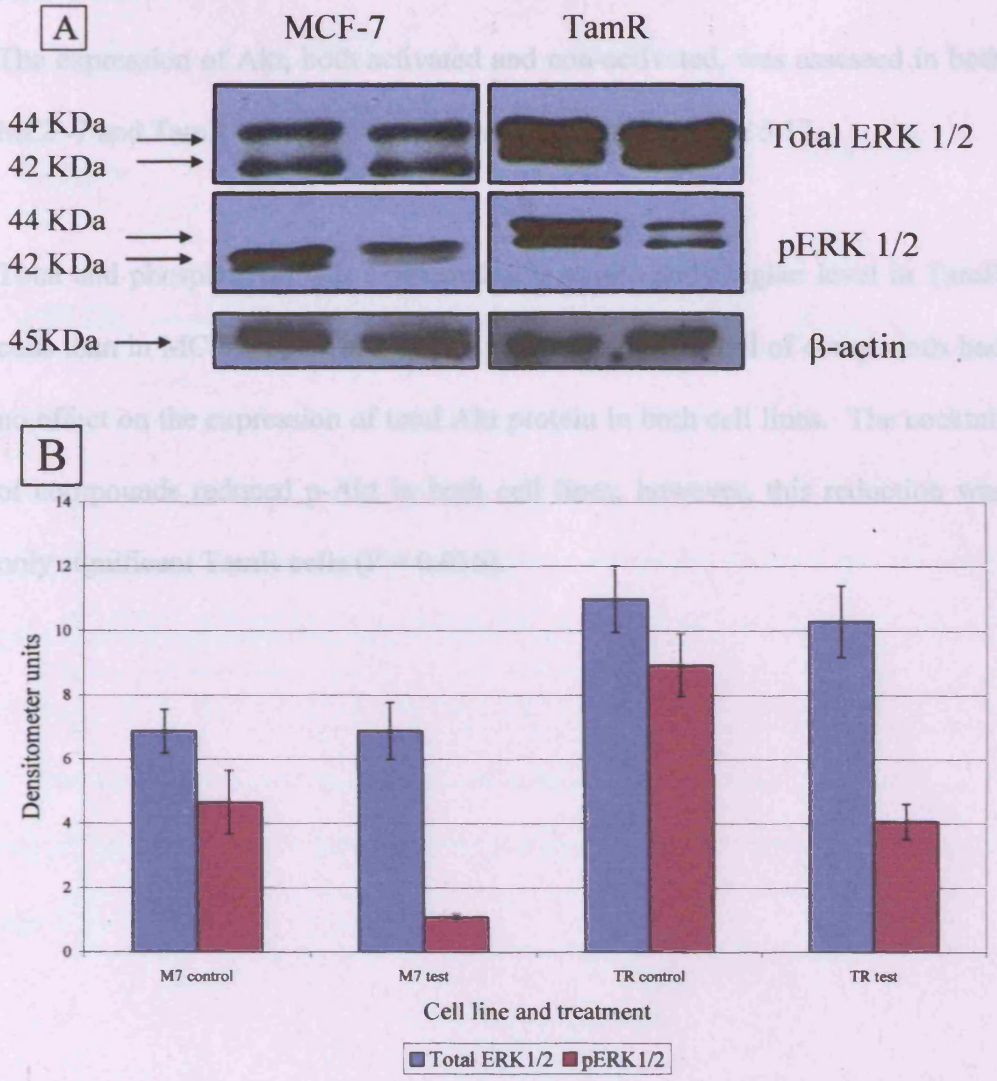

Figure 5.16 Western Blot for the levels of total ERK1/2, pERK1/2 and β-actin protein protein. MCF-7 and TamR cells were incubated with 1μlml^{-1} fish oil, 25μM PD98059, 5μM LY294002 and 1 x 10^{-7}M 4OHTam (MCF-7 cells only) for three hours. Cells were lysed and protein extracted and quantified for equal loading. Protein was separated by SDS-PAGE, immobilised on a nitrocellulose membrane and immunoprobed with either a CST total ERK1/2 or pERK1/2 (Thr202/Tyr204) primary antibody. Passage numbers 37, 29, 31 for MCF-7 cells and 23, 26 and 28 for TamR cells.**B** Densitometry (normalise to actin) analysis of total ERK1/2 and p-ERK1/2 protein (n=3 ± SEM). M7- MCF-7 cells, TR- TamR cells. Densitometry was performed using Alpha Digi Doc ^{TM} RT camera and image analysis system, Genetic Research Instrumentation, Essex, UK.

5.3.5.3 Akt

The expression of Akt, both activated and non-activated, was assessed in both MCF-7 and TamR cells by western blot, displayed in figure 5.17.

Total and phospho-Akt was expressed at a significantly higher level in TamR cells than in MCF-7 cells (P = 0014), however, the cocktail of compounds had no effect on the expression of total Akt protein in both cell lines. The cocktail of compounds reduced p-Akt in both cell lines; however, this reduction was only significant TamR cells (P = 0.016).

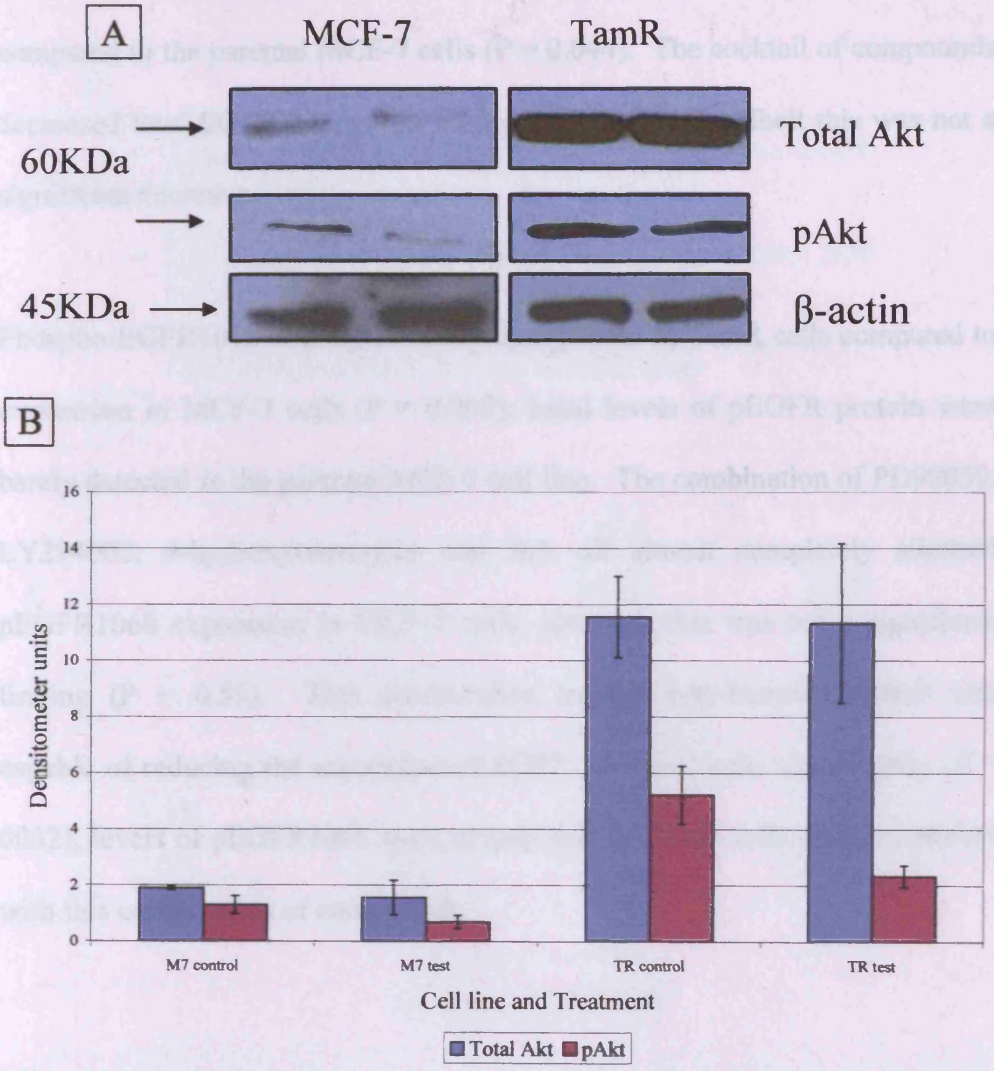

Figure 5.17 Western Blot for the levels of total Akt, phospho-Akt and β-actin protein. MCF-7 and TamR cells were incubated with 1µlml^{-1} fish oil, 25µM PD98059, 5µM LY294002 and 1 x 10^{-7}M 4OHTam (MCF-7 cells only) for three hours. Cells were lysed and protein extracted and quantified for equal loading. Protein was separated by SDS-PAGE, immobilised on a nitrocellulose membrane and immunoprobed using a total Akt or pAkt (ser473) primary antibody. Passage numbers 37, 29, 31 for MCF-7 cells and 23, 26 and 28 for TamR cells.**B** Densitometry (normalised to actin) analysis of total Akt or pAkt protein (n=3 ± SEM). M7- MCF-7 cells, TR- TamR cells. Densitometry was performed using Alpha Digi Doc ™ RT camera and image analysis system, Genetic Research Instrumentation, Essex, UK.

5.3.5.4 EGFR

Total EGFR protein was expressed at a significantly higher level in TamR cells compared to the parental MCF-7 cells (P = 0.044). The cocktail of compounds decreased total EGFR expression modestly in both cells, albeit this was not a significant decrease.

Phospho-EGFR1068 was significantly upregulated in TamR cells compared to expression in MCF-7 cells (P = 0.005); basal levels of pEGFR protein were barely detected in the parental MCF-7 cell line. The combination of PD98059, LY294002, 4-hydroxytamoxifen and fish oil almost completely silenced pEGFR1068 expression in MCF-7 cells, although this was not a significant finding (P = 0.55). This combination (minus 4-hydroxytamoxifen) was capable of reducing the expression of EGFR in TamR cells significantly (P = 0032), levels of pEGFR1068 were around half in TamR cells when incubated with this combination of compounds.

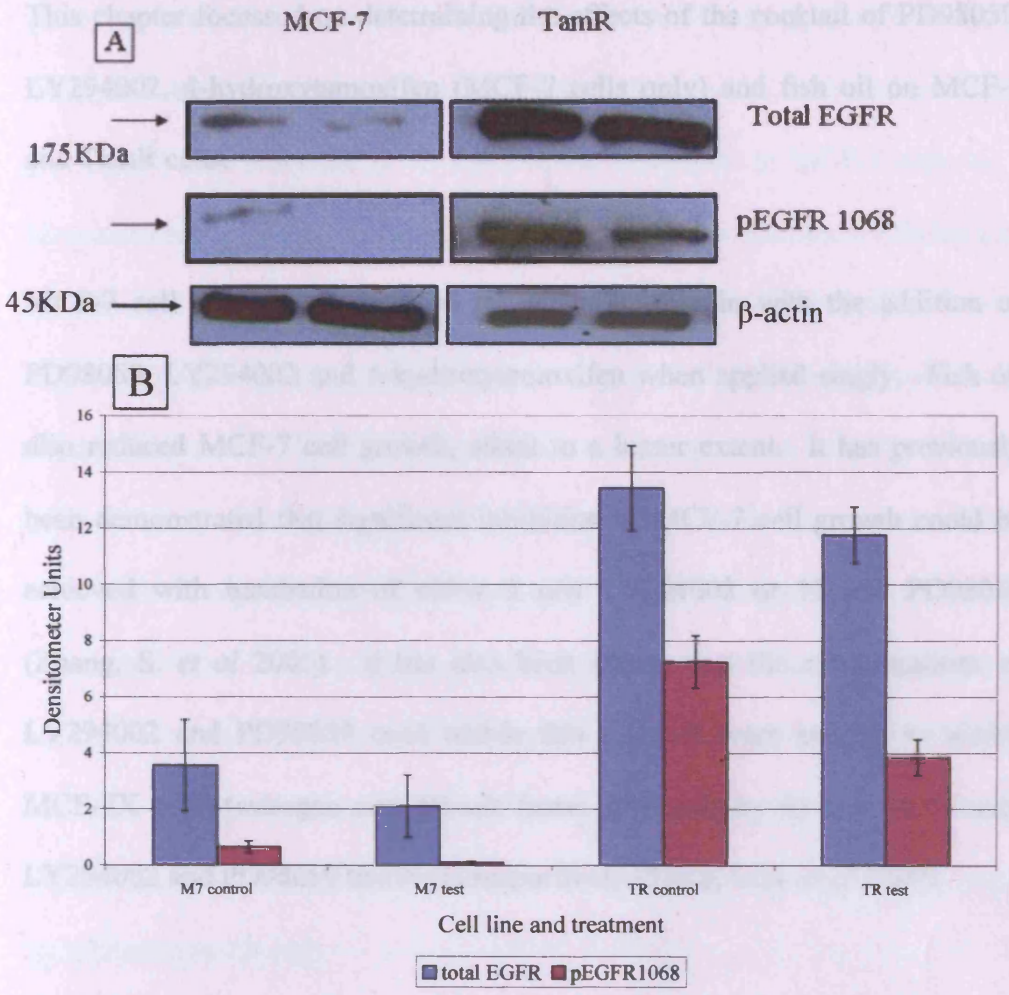

Figure 5.18 Western Blot for the levels of total EGFR, phospho-EGFR1068 and β-actin protein. MCF-7 and TamR cells were incubated with 1μlml^{-1} fish oil, 25μM PD98059, 5μM LY294002 and 1 x 10^{-7}M 4OHTam (MCF-7 cells only) for three hours. Cells were lysed and protein extracted and quantified for equal loading. Protein was separated by SDS-PAGE, immobilised on a nitrocellulose membrane and immunoprobed using a total EGFR or p-EGFR1068 primary antibody. Passage numbers 37, 29, 31 for MCF-7 cells and 23, 26 and 28 for TamR cells.**B** Densitometry (normalised to actin) analysis of total EGFR and phospho-EGFR1068 protein (n=3 ± SEM). M7- MCF-7 cells, TR- TamR cells. Densitometry was performed using Alpha Digi Doc ™ RT camera and image analysis system, Genetic Research Instrumentation, Essex, UK.

5.4 Discussion

This chapter focussed on determining the effects of the cocktail of PD98059, LY294002, 4-hydroxytamoxifen (MCF-7 cells only) and fish oil on MCF-7 and TamR cells.

MCF-7 cell growth was reduced by a similar margin with the addition of PD98059, LY294002 and 4-hydroxytamoxifen when applied singly. Fish oil also reduced MCF-7 cell growth, albeit to a lesser extent. It has previously been demonstrated that significant inhibition of MCF-7 cell growth could be achieved with incubation of either 5 μM LY294002 or 15 μM PD98059 (Zhang, S. *et al* 2005). It has also been shown that the concentrations of LY294002 and PD98059 used within this research were enough to inhibit MCF-7X cells (estrogen and growth factor depleted) by 65 and 35 % with LY294002 and PD98059 treatment respectively (Staka, C.M. *et al* 2005).

Greatest inhibition in MCF-7 growth was seen when cells were insulted with combinations of 25 μM PD98059, 5 μM LY294002, 1 x 10^{-7} M 4-hydroxytamoxifen and 25 μM PD98059, 5 μM LY294002, 1 x 10^{-7} M 4-hydroxytamoxifen and 1 μL mL^{-1} fish oil simultaneously. Staka, C.M. and colleagues (2005) also observed the synergistic actions of PD98059 and LY294002, reporting that this combination reduced cell growth to 15 % of control growth.

It was interesting to see that PD98059 and LY294002 inhibited MCF-7 cell growth to a lesser extent as seen in TamR cells (shown in figure 5.3 and 5.4). This may be explained by the knowledge that TamR cells express both pERK1/2 and PI3K/pAkt at elevated levels compared to MCF-7 cells as a compensatory growth pathway induced by tamoxifen resistance (Nicholson, R.I. *et al* 2005). This was exemplified in this chapter in both ICC of cells (figure 5.11 and 5.12) and western blot analysis of MCF-7 and TamR cells (figure 5.16 and 5.17), which showed elevated expression of pERK1/2 and pAkt in TamR cells compared to the parental MCF-7 cell line. A recent study demonstrated similar results by comparing MAPK activity in several breast cancer cell lines. Results showed that MAPK activity was increased in cell lines overexpressing growth factor signalling mediators, such as MDA-MD-231 and BT-474 cells. There was a significant correlation with IGF-IR expression and MAPK activity in these cell lines, in which PD98059 showed an enhanced sensitivity.

Incubation of MCF-7 and TamR cells with 5 μM LY4002 reduced cell growth significantly compared to control growth. PI3 kinase/Akt signalling has previously been linked to cell cycle abnormalities in human malignancies, driving increased cell proliferation. Akt is a key mediator involved in preventing cyclin D1 degradation by its regulation of cyclin D1 kinase glycogen synthase kinase 3β. Overactivation, of Akt, as seen in malignancies of the breast, allows accumulation of cyclin D1. LY294002 has been shown to greatly decrease the expression of cyclin D1 and induced G1 cell cycle arrest in

ovarian cancer cells (Gao, N. *et al* 2004). Arrest of cell cycle may have been the way in which LY294002 reduced cell proliferation as described in this chapter.

Several studies have also shown that MAP kinase activation is critical for cancer cell growth. A study assessing the levels of pERK1/2 in MCF-7 and T47D compared to non-malignant cell lines revealed that expression of pERK1/2 expression was higher in both MCF-7 and T47D compared to non-malignant cell lines. The study also showed that PD98059 was capable of reducing this expression and the growth of MCF-7 and T47D cells (Hermanto, U. *et al* 2000). Overexpression of MAPK signalling has been shown to alter cell cycle progression by deregulating $p27^{kip1}$, which is a kinase inhibitory protein that regulates cell cycle transitions. Overactivation of MAPK signalling compromises the inhibitory function of p27 and allows elevated growth rate in breast cancer cells; however, MAPK inhibitors were able to reduce growth rate. Upon tamoxifen resistance mitogen-activated protein kinase phophatase is upregulated (Zhou, B. *et al* 2001). This has been shown to de-activate MAPK activity in normal cells via a negative feedback loop, however, in the continued presence of tamoxifen, it is downregulated, which leads to accentuated MAPK activity. PD98059 was able to inhibit the growth of tamoxifen resistant cells in this study and also increased the phosphorylation of c-Jun NH_2-terminal kinase, suggesting a role for MAPKP3 in this resistant growth (Cui, Y. *et al* 2006).

TamR cells were developed in-house to mimic the considerable clinical challenge represented by anti-hormone resistance exemplified by that seen with tamoxifen treatment. These cells were insensitive to 4-hydroxytamoxifen and E_2, however still showed growth inhibition when incubated with Faslodex, as shown in figure 5.2. Incubation of TamR cells with PD98059 and LY294002 singly gave similar inhibition in growth, while fish oil only modestly inhibited TamR growth. Greatest inhibition was seen when PD98059 and LY294002 were incubated with TamR cells simultaneously with and without fish oil present.

Upon acquisition of tamoxifen resistance, elevated EGFR signalling is detected both *in vitro* and *in vivo*. This was portrayed in ICC detection and western blot analysis of total EGFR and PEGFR1068. Further dissection of the EGFR signalling pathway has elucidated that this is, in part, responsible for tamoxifen resistant growth. It is also hypothesised that downstream pathways of the EGFR, including the MAPK and PI3K pathway are also responsible for many aspects of tamoxifen resistant tumorogenesis (Nicholson, R.I. *et al* 2005). This chapter showed that total EGFR, pEGFR1068, pERK1/2 and pAkt were upregulated in TamR cells, suggesting that resistant growth was driven by these signalling pathways. Interestingly, pER167 was significantly upregulated in TamR cells, as displayed in figure 5.10 and 5.15. This could be explained by the increased MAPK and PI3K signalling within TamR cells compared to MCF-7 cells. Activation of these pathways can result in the ligand independent activation of ERα at key serine residues (Sun, M. *et al*

2001). Activated PI3K/Akt are known to phosphorylate ERα at ser167. As this signalling pathway is activated to a greater extent in TamR cells, this may have lead to an elevation in ligand independent activation of ERα by phosphorylation at ser167. The significant knockdown in pERα167 signal when TamR cells were incubated with LY294002 and the cocktail of compounds may have been mainly due to the inhibition of the PI3K/Akt pathway by the actions of LY294002 (Campbell, R.A. *et al* 2001). In fact, a number of discreet and unrelated observations have led to the understanding that this signalling pathway confers to tamoxifen resistant cell growth. It was noticed that patients suffering from Cowdens disease, which presents as a germ line mutation of PTEN, are more susceptible to breast cancer development. PTEN is a tumor suppressor that inhibits Akt.

Fish oil was capable of inhibiting the growth of both MCF-7 and TamR cells, giving a more exaggerated effect on TamR cells. Many studies have investigated the effect of dietary fat on tumor progression and have suggested that the anti-tumor properties of PUFAs arise from their ability to inhibit the COX enzymes. This chapter, however, revealed that fish oil was capable of reducing the expression of EGFR, pEGFR1068, pAkt and pERK1/2, suggesting that n-3 PUFAs may also exert anti-tumorogenic via actions on these key mediators.

There are 12 different fatty acids that are essential to the body but are not endogenous. These can be divided into two main sub-groups dependant on the

saturation state. N-3 (ω-3) PUFAs are unsaturated at the third carbon from the methyl terminus, whereas n-6 (ω-6) PUFAs are unsaturated at carbon 6. The position of this first double bond seems to have significant effects on the actions of PUFAs, with n-6 PUFAs, such as AA and GLA being cancer cell growth promoting, while n-3 PUFAs, such as EPA and DHA show cell growth inhibition (Xia, S. *et al* 2006).

Investigations into the effects of n-3 PUFAs on tumorogenesis have revealed that these fatty acids are potent protein kinase inhibitors at low concentrations. EPA (IC_{50} concentrations of 2-36 μM) was capable of inhibiting the activity of protein kinase c (PKC), cyclic AMP dependent protein kinase A and ERK1/2. Furthermore, this inhibition was ω-3 specific and was not as a result of competitive inhibition of ATP (Mirnikjoo, B. *et al* 2003). This could explain the effect that fish oil gave on the expression of pAkt and pERK1/2.

Several studies have proposed that n-3 PUFAs show efficacy as anti-angigenic therapeutic by inhibiting microvessel formation in tumor tissues (Mukutmoni-Norris, M. *et al* 2000). Only recently has a mechanism behind this observation been proposed, suggesting that n-3 PUFAs inhibit VEGF expression through negative regulation of COX-2/ERK1/2 pathways (Calviello, G. *et al* 2004). This study shows that n-3 PUFAs, in particular EPA, were able to inhibit COX-2 and the phosphorylation of ERK1/2, which downregulated the expression of VEGF.

The n-6 PUFA, AA, was capable of stimulating the activity of PI3K and transiently phosphorylating Akt on Thr-308 and Ser-473 (Hii, C.S.T. *et al* 2001). Another notable finding of this study was that AA was capable of activating ERK1/2, however, this was independent of PI3K activation.

Conversely, n-3 PUFAs have shown opposite effects on PI3K and Akt activation. EPA (and DHA to a less extent) showed a dose-dependent decrease in insulin-induced Akt activity and reduced activity by 67% compared to control. This effect of EPA and DHA (found at high levels in fish oil) could explain the decrease in pAkt in both MCF-7 and TamR cells. It could also rationalise that fact that fish oil had a more prominent affect on TamR cells compared to MCF-7 cells, since the resistant cell line showed higher basal pAkt than MCF-7 cells.

N-3 PUFAs have also displayed EGFR inhibitory effects. Investigations into membrane biology have revealed that lipid rafts may play an important role in cell signalling by aiding the association of signalling molecules such as the EGFR (Brown, D.A. & London, E. 1998). A recent study showed that EPA and DHA altered the lipid composition of lipid rafts in MDA-MB-321 cells. This study also discovered that EPA and DHA decreased EGFR protein levels in lipid rafts, however, the PUFAs increased pEGFR signalling in MDA-MB-231 cells (Schley, P.D. *et al* 2004). The study by Schley and colleagues corroborated results found in a previous study suggesting that EPA and DHA were the most effective unsaturated fatty acids at inducing EGFR

autophosphorylation, leading to p38 MAPK activation (Vacaresse, N. *et al* 1999). However, PGE_2 is known to transactivate EGFR through a Src dependent mechanism to facilitate ligand independent EGFR signalling in COX-2 over-expressing cells (Buchanan, F.G. *et al* 2003). N-3 PUFAs such as EPA and DHA compete with AA for the COX-2 enzyme and hinder the production of series 2 prostanoids, including PGE_2. Instead, series 3 prostanoids are synthesised offering a much weaker inflammatory mediator (Uauy, R. & Valenzuela, A. 2000). The n-3 PUFAs within the fish oil may have decreased the levels of PGE_2, thus inhibiting the transactivation of EGFR induced by this prostanoid.

It was not straightforward to compare the amounts of drug delivered across the skin to the amounts used in the cell growth experiments. On the face of it, the 25×10^{-6} M of PD98059 used to stop the cell proliferation does not compare favourably with the maximum delivery of 0.06 μmol cm^{-2} after 48 hours - an area of application ~ 400 cm^2 would be necessary. Even then this does not take into consideration the precise location within breast tissue of the cancer to be reached via passive diffusion or the proportion of drug cleared by the dermal microvasculature (although the amount in the systemic circulation would probably be beneficial). Such considerations point to the chemo-prevention of breast cancer a more plausible goal for transcutaneous delivery of these agents, rather than a cure.

However, permeated concentrations were applied to MCF-7 cells in a patch application model system, by which concentrations permeated after 48 hours were first applied and the concentrations permeation after 24 hours were applied every 24 hours after this. Although the concentrations that were added were significantly lower previously used in the IC_{50} experiments, cell growth was still reduced to 13.78 ± 0.63 % of control when both compounds were added together. Although this seems surprising, it could be explained by the uptake rates of the compounds into MCF-7 cells. The IC_{50} value concentrations were only dosed twice during the week-long experimentation, whereas the permeated concentrations were dosed on a daily basis. If the uptake of compounds into cells was less or around equal to the concentrations dosed per day in the permeated concentrations investigations then increasing the concentration would not improve the growth inhibition seen. However it has been reported previously through western blot techniques that 100nM PD98059 was adequate to block ERK1/2 significantly (Lassarre, C. *et al* 2003). This concentration is lower than the 0.65μM used in these experiments, which suggests that the inhibition was specific to ERK1/2 inhibition.

Conclusions

This work has shown that the levels at which PD98059, LY294002 and 4-hydroxytamoxifen permeate the skin, are sufficient to exert substantial growth inhibitory effects on MCF 7 and TamR cancer cells *in vitro.* This work has also provided confirmatory evidence that n-3 PUFAs found in fish oil have

intrinsic anti-tumorogenic properties and that they are capable of inhibiting several key tamoxifen-resistant growth mediators.

Chapter 6

Probing the Anti-Metastatic Properties of LY294002, PD98059 and fish oil

6.1 Introduction

6.1.1 COX-2 and Metastasis

An increasing body of evidence supports a role for COX-2 in many malignancies, including those of the colon, prostate and breast (Masferrer, J.L. *et al* 2000). A study investigating the relationship between COX-2 and various clinical markers involved in breast cancer tumorogenesis revealed that up-regulation of COX-2 was significantly correlated with distant metastasis (Ranger, G.S. *et al* 2004). Many authors have reported a link between up-regulation of COX-2 and elevated angiogenesis. Davies, G. and colleagues (2003) reported the first significant relationship between COX-2 and angiogenesis measured by CD31 (platelet –endothelial cell adhesion molecule), an immunoglobulin involved in invasion, migration and angiogenesis.

6.1.2 Breast Cancer and Metastasis

Unfortunately, breast cancer shows a high incidence of metasizing, usually via the lymphatic system, giving a much poorer patient prognosis (Cunnick, G.H. *et al* 2008). Lymph node metastasis is the most common site of secondary colonization of breast cancer cells, with the likelihood of metastatic spread increasing with increasing tumor grade and in hormone receptor negative cancers. As mentioned previously, metastasis from the point of origin seems to be organ of origin specific. It has been established for over a decade that breast cancer cells preferentially metastasize to bone and lung (Fidler, I.J. 2003).

6.1.3 Aims

It has previously been shown in chapter 5 that PD98059, LY294002 and fish oil could suppress the growth of both MCF-7 and TamR cells. The MAPK and PI3K pathways have already been implicated in metastasis (Alfiya, F. *et al* 2006, Jia, Y. *et al* 2004) and so PD98059 and LY294002 are proposed to have ant-metastatic properties.

Insights into the mechanisms involved in metastasis of breast cancer have discerned a possible role for COX-2 in both tumorogenesis and metastatic spread of breast cancer. This short study was aimed at determining whether COX-2 alone, and in combination with LY294002 and PD98059 had a role in TamR cell migration. Also this investigation aimed to see if the constituents of the developed formulation could curb this migratory potential.

6.2. Materials and Methods

6.2.1 Materials

The materials used within this chapter were detailed in section 2.2.1

6.2.2 Methods

6.2.2.1 Growth assays

Growth assays were performed as described in chapter 2. Firstly, the growth rates of three in-house cell lines were compared. MCF-7, TamR and FasR cells were grown to 70 % confluency as previously described, passaged, and seeded into 24 well plates at a density of 1.5 million cells per plate. Cells were trypsinized and counted on days 1, 4, 7 and 9.

Secondly, using both MCF-7 and TamR cells, the effect of the PD98050, LY294002 and 4-hydroxitamoxifen (MCF-7 cells only) and fish oil were determined on the growth rate of both cell lines. The treatment strategies were as detailed in table 6.1. Cells were seeded (1.5×10^6 per plate) on day 0, counted and treated on day 1 and counted on days 2, 4, 7 and 9. Cells were retreated on day 4.

Cell Line	Treatments	Concentrations
MCF-7	DMSO	0.1μL mL^{-1}
	4OHTam	1 x 10^{-7}M
	PD98059	25μM
	LY294002	5μM
	PD+LY+4OHTam	As in single treatments
	Fish oil	1 μL mL^{-1}
	Fish oil+ PD+LY+4OHTam	As in single treatments
	E2	1 x 10^{-9}M
TamR	DMSO	0.1 μL mL^{-1}
	PD98059	25μM
	LY294002	5μM
	PD+LY	As in single treatments
	Fish oil	1 μL mL^{-1}
	Fish oil+ PD+LY	As in single treatments
	E2	1 x 10^{-9}M
	Fas	1 x 10^{-7}M

Table 6.1 Table to show the treatments used in growth assays to detect the effects of formulation constituents on the growth rate of both MCF-7 cells and TamR cells. Cells were seeded at a density of 1.5 million cells per plate on day 0. On day 1 cells were counted and then treated. Additional counts were at days 4, 7 and 9 and treatments replenished on day 4.

6.2.2.2 Migration assays

Migration assays were performed using the method outlined in section 2.2.2.4. Initially migration assays were carried out to compare the migratory potential

of three breast cancer cell lines; MCF-7, TamR and FasR. Secondly the effects of fish oil and fish oil plus PD98059 and LY294002 on the migration of TamR cells were assessed. The assays were assembled as described previously; however, the wells of the modified plate were filled with wRPMI (SFCS, fungicide and antibacterial) with either 0.1 μL mL^{-1} DMSO (control), 1 μL mL^{-1} fish oil or 1 μL mL^{-1}fish oil, 25μM PD98059 and 5 μM LY294002. Detection of migrated cells was as previously outlined (2.2.2.4).

6.2.2.3 Western blot analysis for c-Src and COX-2

MCF-7 and TamR cells were cultured for western blot analysis as detailed in section 2.2.4. After reaching 70% confluency, the cultured cells were incubated, for three hours, with compounds as detailed in table 6.2.

Cell line	Treatment
MCF-7	0.1 μL mL^{-1}DMSO (Control)
	1μlml^{-1} Fish oil
	1 x 10^{-7}M 4OHTam, 25μM PD98059, 5μM LY294002
	1 μL mL^{-1} Fish oil,1 x 10-7M 4OHTam, 25μM PD98059, 5μM LY294002
TamR	0.1 μL mL^{-1} DMSO (Control)
	1 μL mL^{-1}Fish oil
	25μM PD98059, 5μM LY294002
	1 μL mL^{-1} Fish oil, 25μM PD98059, 5μM LY294002

Table 6.2 Treatments for MCF-7 and TamR cells prior to Western blot and ICC analysis. PD98059 and LY294002 were made up in DMSO, while 4OHTam was made up in ethanol. Treatments were incubated for 3 hours, after which protein was extracted for western blot assays and cells were fixed for ICC assays. Cells were maintained at 37°C with 5% CO_2.

Compound(s) were incubated with the cells for 3 h as ICC analysis of porcine skin sections revealed knock down of several markers, including COX-2 after 3 h (described in chapter 5). Protein was then extracted, quantified and analysed via western blot using the methods described in 2.2.4.

Gels were immunoprobed for β-actin as an internal control to ensure equal protein loading.

6.2.2.4 Immunocytochemical detection of c-Src and COX-2 in MCF-7 and TamR cells

MCF-7 and TamR cells were cultured and set up for immunocytochemical assays as detailed in section 2.2.3.2. On reaching 70 % confluency the cells were treated with treatments for 3 hours, as detailed in table 6.2. The fixation of cells for all assays and the detection of total-Src, phospho-Src and total COX2 were conducted as detailed in section 2.2.3.2.

6.3. Results

6.3.1 Growth Assays

Figures 6.1 and 6.2 show repeats of growth studies performed in chapter 5. This repetition was of paramount importance to ensure that cells were behaving phenotypically. Figure 6.1 shows the growth rate of un-treated MCF-7, TamR and FasR cells over 9 days. It is obvious that upon hormone resistance, growth rate accelerates, as shown with TamR and FasR cells compared to the parental and hormone sensitive MCF-7 cells.

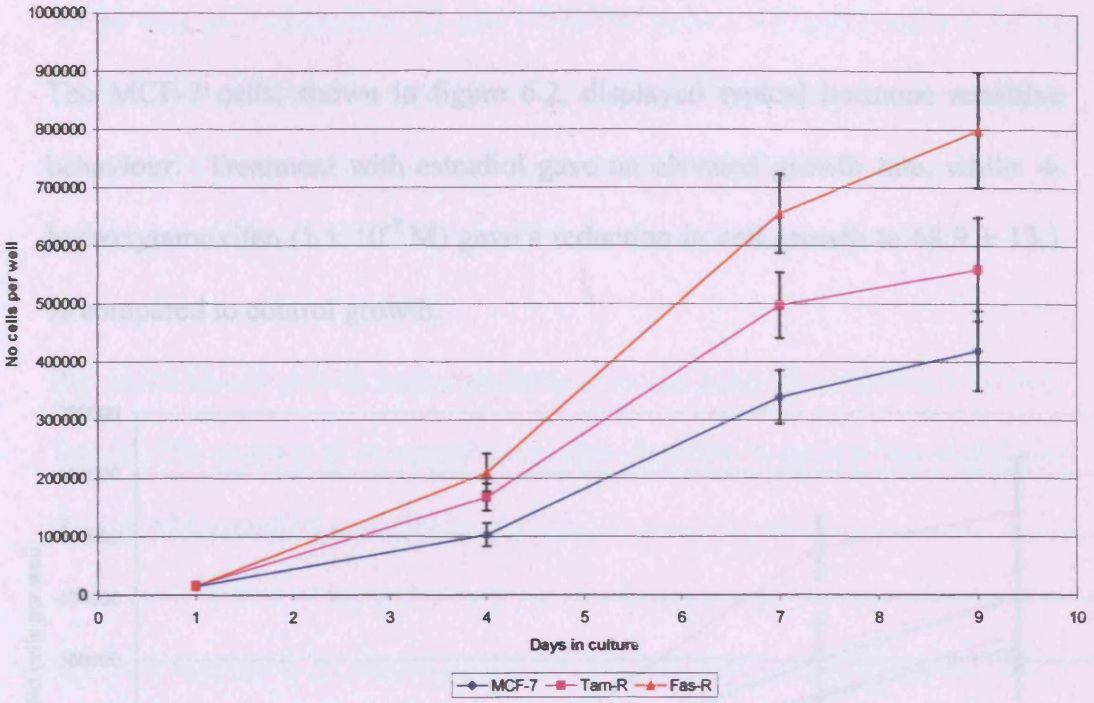

Figure 6.1 Growth assay to show the growth rates of MCF-7, TamR and FasR cells. Cells were seeded at a density of 1.5 million cells per plate on day 0. Cells were counted on days 1, 4, 7 and 9 and media was replenished on day 4. Cells were incubated at 37°C with 5% CO_2. Cell counts represent the mean number per 3 counts (n=3 ± SD). Passage numbers were 12, 14, 20 for MCF-7 cells, 22, 25, 30 for TamR cells and 31, 35 and 40 for FasR cells.

The growth assay shown in figure 6.1 shows that TamR cells have a faster growth rate than the parental MCF-7 cells, however this was not a significant observation (P = 0.120). FasR cells showed a significantly elevated growth rate compared to both TamR and MCF-7 cells (P = 0.012 and 0.05 respectively).

The effect of the active constituents of the final formulation on the growth of both MCF-7 and TamR cells were then examined.

The MCF-7 cells, shown in figure 6.2, displayed typical hormone sensitive behaviour. Treatment with estradiol gave an elevated growth rate, whilst 4-hydroxytamoxifen (1 x 10^{-7} M) gave a reduction in cell growth to 68.9 ± 13.1 % compared to control growth.

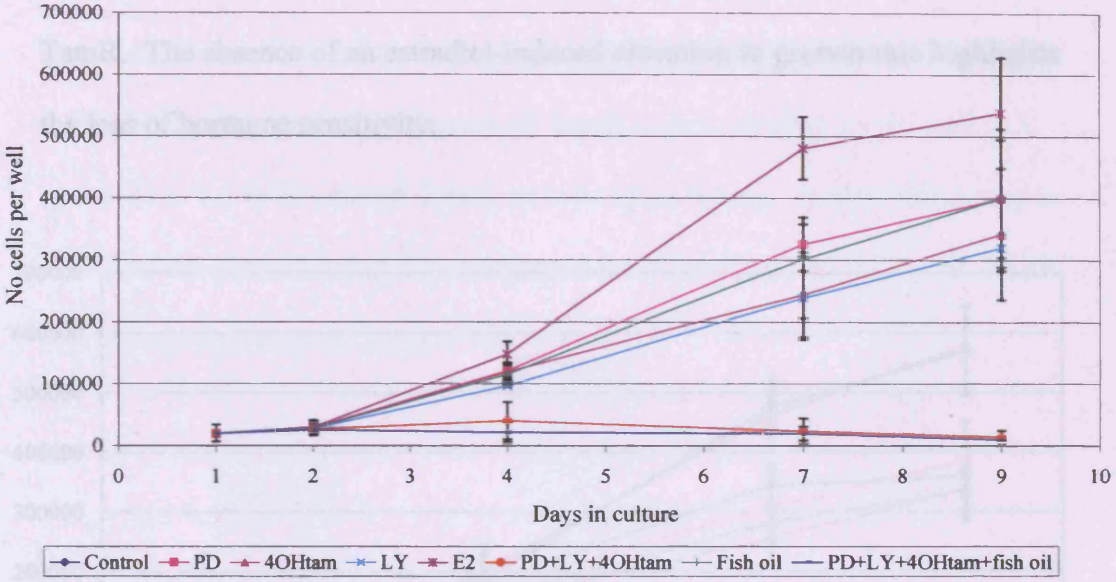

Figure 6.2 Growth assay to show the growth rates of MCF-7 cells when treated with 4-hydroxytamoxifen, PD98059, LY294002 and fish oil (both singly and in combination) and also estradiol. Cells were seeded at a density of 1.5 million cells per plate on day 0. Cells were counted on days 1, 2, 4, 7 and 9 and media and treatments were replenished on day 4. Cells were incubated at 37°C with 5% CO_2. Cell counts represent the mean number per 3 counts (n=3 ± SD). Passage numbers were 19, 21, 24.

The addition of 25 μM PD98059, 5 μM LY292002 and 1 μL mL^{-1} fish oil, separately, reduced MCF-7 growth to 81.5 ± 11.4, 66.2 ± 14.5 and 81.7 ± 13.7 % of control MCF-7 growth respectively. The combination treatments of 1 x

10^{-7}M 4-hydroxytamoxifen, 25 μM PD98059, 5μM LY292002 and 1 x 10^{-7}M 4-hydroxytamoxifen, 25 μM PD98059, 5 μM LY292002 plus 1 μL mL^{-1} fish oil gave, by some margin, the greatest retardation in MCF-7 cell growth by reducing it to 3.2 ± 0.18 and 2.2 ± 0.2 % of control growth respectively.

Figure 6.3 shows growth assays performed on the tamoxifen resistant cell line: TamR. The absence of an estradiol-induced elevation in growth rate highlights the loss of hormone sensitivity.

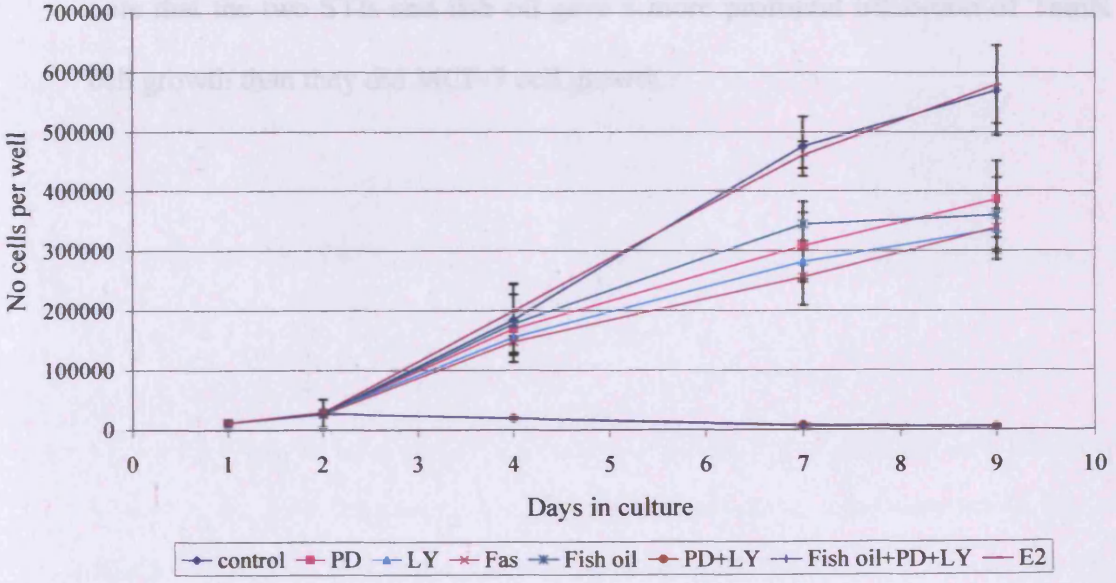

Figure 6.3 Growth assay to show the growth rates of TamR cells when treated with PD98059, LY294002 and fish oil (both singly and in combination) and also faslodex and estradiol. Cells were seeded at a density of 1.5 million cells per plate on day 0. Cells were counted on days 1, 2, 4, 7 and 9 and media and treatments were replenished on day 4. Cells were incubated at 37°C with 5% CO_2. Cell counts represent the mean number per 3 counts (n=3 ± SD). Passage numbers were 25, 27 and 32.

Although the TamR cells displayed insensitivity to E_2, they were still sensitive to the true anti-estrogen Faslodex (Fulvestrant). Incubation with 1 x 10^{-7} M faslodex reduced growth to 58.4 ± 8.3 % of control TamR growth suggesting that the cells were still sensitive to anti-estrogen challenge. The addition of 5μM LY292002 reduced TamR growth to a similar degree, as seen with faslodex: 58.3 ± 9.3 % of control growth. Incubation with 25 μM PD98059 or 1μlml^{-1} fish oil inhibited the growth of TamR cells to similar levels: 68.1 ± 8.1 and 64.9 ± 7.4 % of control TamR growth respectively. It was interesting to note that the two STIs and fish oil gave a more profound inhibition of TamR cell growth than they did MCF-7 cell growth.

6.3.2 Migration Assays

The migratory potential of three in house cell lines was firstly assessed. Figure 6.4 shows the number of MCF-7, TamR and FasR cells migrating after 48 h.

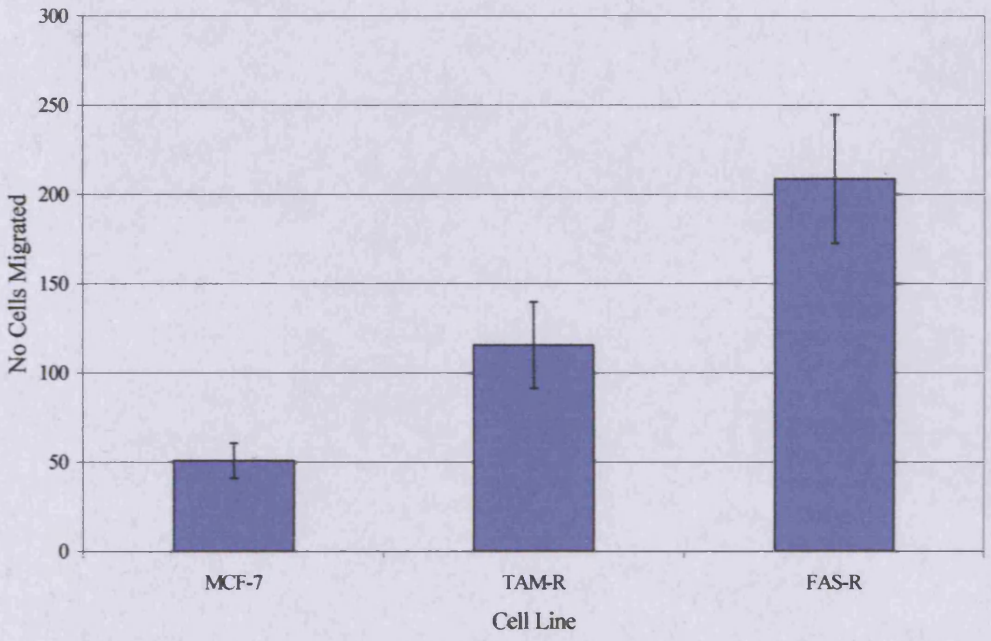

Figure 6.4 Migration assay to show the number of MCF-7, TamR and FasR cells migrating after 48 hours. Cells were seeded onto fibronectin coated porous membranes at a density of 80,000 cells per well, incubated and allowed to migrate for 48 hours at 37°C with 5% CO_2. No of cells migrated represents the mean number of cells per field of view (7 fields per insert were counted) (n=3 ± SD). Passage numbers were 12, 14, 20 for MCF-7 cells, 22, 25, 30 for TamR cells and 31, 35 and 40 for FasR cells.

It was obvious that TamR cells migrated significantly more than MCF-7 cells ($P = 0.004$) and FasR cells migrated significantly more than both MCF-7 and TamR cells ($P = 0.001$ and 0.001). One-way ANOVA determined that there

was a significant difference in the migratory potential of these three cell lines ($P < 0.001$). Although FasR cells displayed the greatest migratory potential, TamR cells have been previously used throughout this thesis as a model for tamoxifen resistance, therefore this cell line was chosen to investigate the anti-migratory potential of fish oil and the two signal transduction inhibitors.

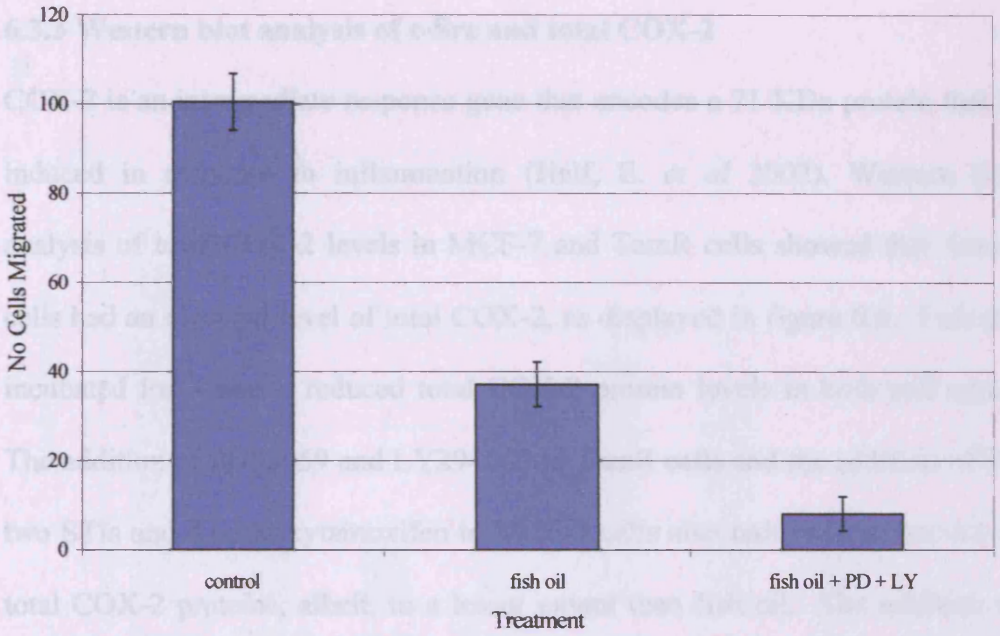

Figure 6.5 Migration assay to show the number of TamR cells migrating after 48 hours, when incubated with control, 1µlml^{-1} fish oil or 1µml^{-1} fish oil plus 25µM PD98059 and 5µM LY294002 treatments. Cells were seeded at a density of 80,000 cells per well and incubated at 37°C with 5% CO_2 No of cells migrated represents the mean number of cells per field of view (7 fields per insert were counted) (n=3 ± SD). Passage numbers were 23, 27 and 30.

Figure 6.5 shows the effect of fish oil alone and in combination with PD98059 and LY294002 on the migration of TamR cells. Fish oil gave a significant reduction in the number of TamR cells migrating after 48 hours ($P = 0.05$),

while the addition of the two signal transduction inhibitors decreased the migratory potential of TamR cells significantly compared to both control cells ($P = >0.001$) and fish oil treated cells ($P = 0.003$). One-way ANOVA analysis revealed that the migratory potential of control, fish oil treated and fish oil plus STIs are significantly different ($P<0.001$)

6.3.3 Western blot analysis of c-Src and total COX-2

COX-2 is an intermediate response gene that encodes a 71 KDa protein that is induced in response to inflammation (Half, E. *et al* 2002). Western blot analysis of total COX-2 levels in MCF-7 and TamR cells showed that TamR cells had an elevated level of total COX-2, as displayed in figure 6.6. Fish oil, incubated for 3 hours, reduced total COX-2 protein levels in both cell types. The addition of PD98059 and LY294002 to TamR cells and the addition of the two STIs and 4-hydroxytamoxifen to MCF-7 cells also reduced the amount of total COX-2 proteins, albeit, to a lesser extent than fish oil. The addition of fish oil to the two treatments mentioned previously, allowed a further additive reduction of the total COX-2 protein in both MCF-7 and TamR cells.

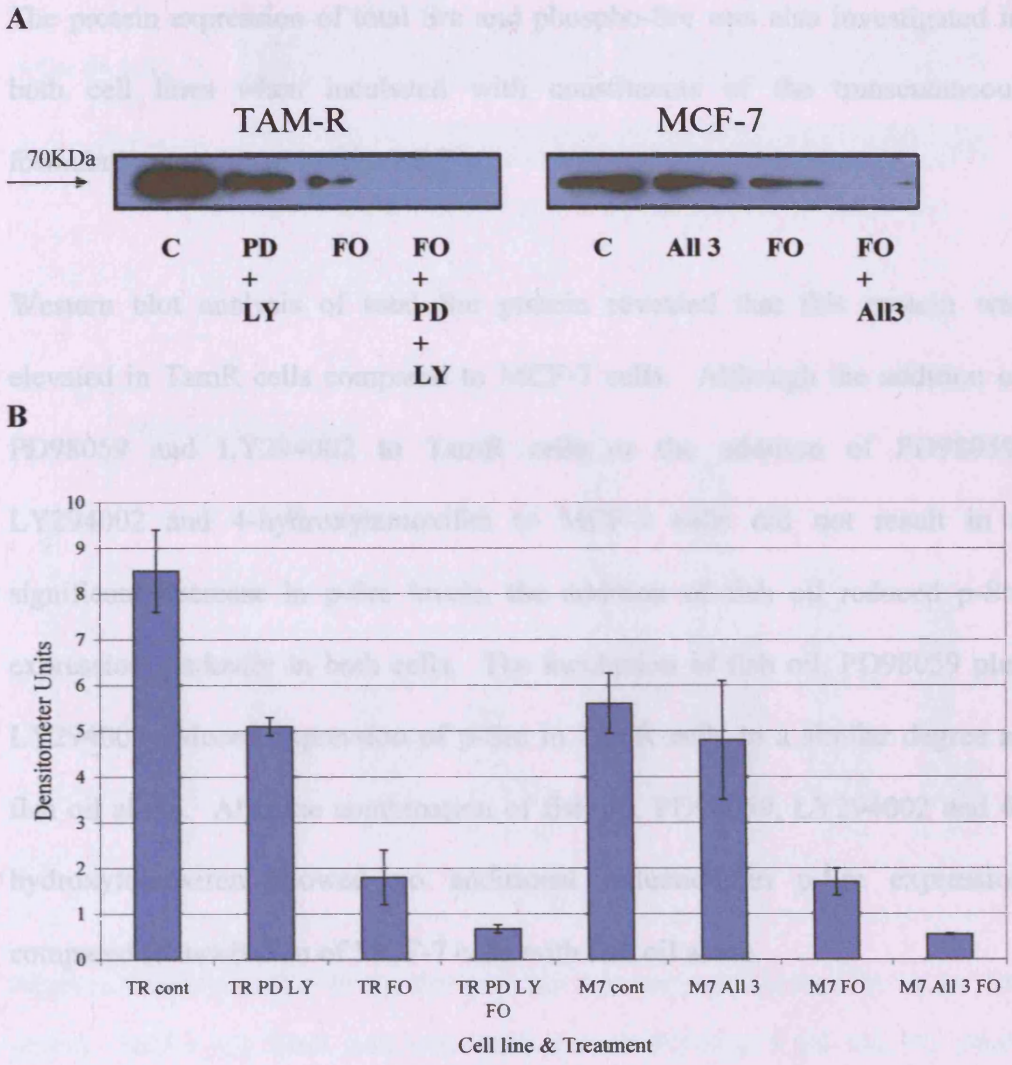

Figure 6.6 A Western Blot for the levels of total COX-2 protein. MCF-7 and TamR cells were incubated with FO (1μml^{-1} fish oil), PD (25μM PD98059), LY (5μM LY294002) and 1 x 10^{-7}M 4-hydroxytamoxifen (MCF-7 cell only) for three hours. Cells were lysed and protein extracted and quantified for equal loading. Protein was separated by SDS-PAGE. Proteins were immobilised on a nitrocellulose membrane and immunoprobed using a total COX-2 primary antibody. **B** Densitometry analysis of total COX-2 protein. Densitometry was performed using Alpha Digi Doc ™ RT camera and image analysis system, Genetic Research Instrumentation, Essex, UK. M7- MCF-7 cells, TR- TamR cells (N=3 ±SD). Results were normalised to actin. Passage numbers were 23, 27 and 30.

The protein expression of total Src and phospho-Src was also investigated in both cell lines when incubated with constituents of the transcutaneous formulation, as shown in figure 6.7

Western blot analysis of total Src protein revealed that this protein was elevated in TamR cells compared to MCF-7 cells. Although the addition of PD98059 and LY294002 to TamR cells or the addition of PD98059, LY294002 and 4-hydroxytamoxifen to MCF-7 cells did not result in a significant decrease in p-Src levels, the addition of fish oil reduced p-Src expression markedly in both cells. The incubation of fish oil, PD98059 plus LY294002 reduced expression of p-Src in TamR cells to a similar degree as fish oil alone. Also the combination of fish oil, PD98059, LY294002 and 4-hydroxytamoxifen showed no additional reduction in p-Src expression compared to incubation of MCF-7 cells with fish oil alone.

A

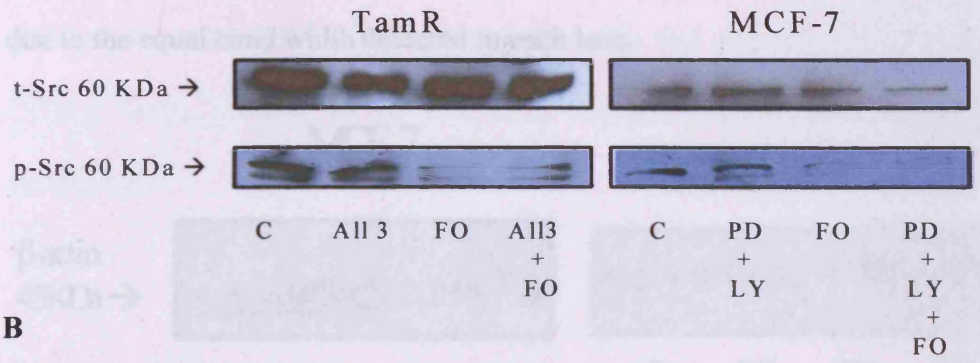

B

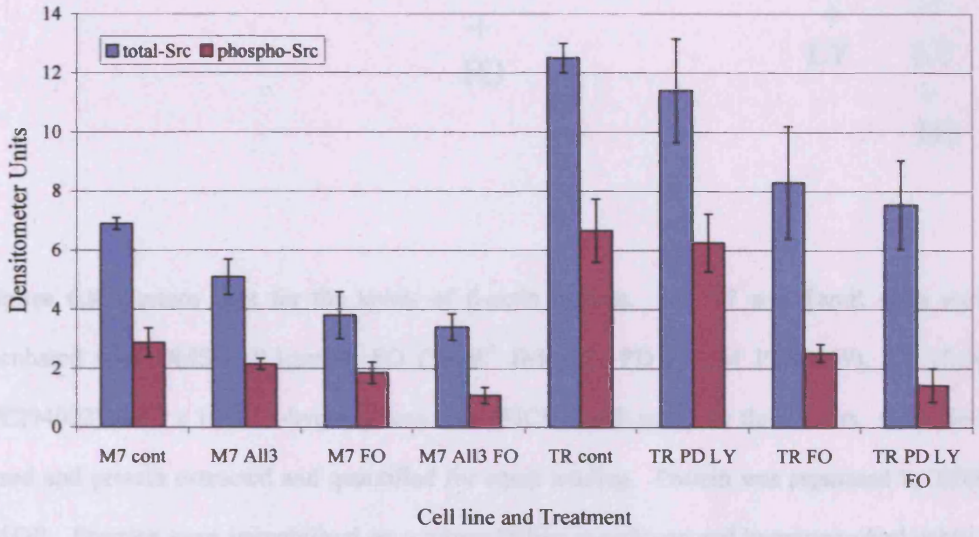

Figure 6.7 A Western Blot for the levels of total Src, and phosphorylated Src (at tyr 416) protein. MCF-7 and TamR cells were incubated with FO (1μml^{-1} fish oil), PD (25μM PD98059), LY (5μM LY294002) and 1 x 10^{-7}M 4-hydroxytamoxifen (MCF-7 cells only) for three hours. Cells were lysed and protein extracted and quantified for equal loading. Protein was separated by SDS-PAGE. Proteins were immobilised on a nitrocellulose membrane and immunoprobed using a cell signalling technology total Src or phospho-Src primary antibody. **B** Densitometry analysis of total Src, and phosphorylated Src (at tyr 416) protein. M7- MCF-7 cells, TR- TamR cells. Densitometry was performed using Alpha Digi Doc ™ RT camera and image analysis system, Genetic Research Instrumentation, Essex, UK. Results were normalised to actin. Passage numbers were 23, 27 and 30

Western blot of β-actin, shown in figure 6.8, confirmed equal protein loading due to the equal band width detected in each lane.

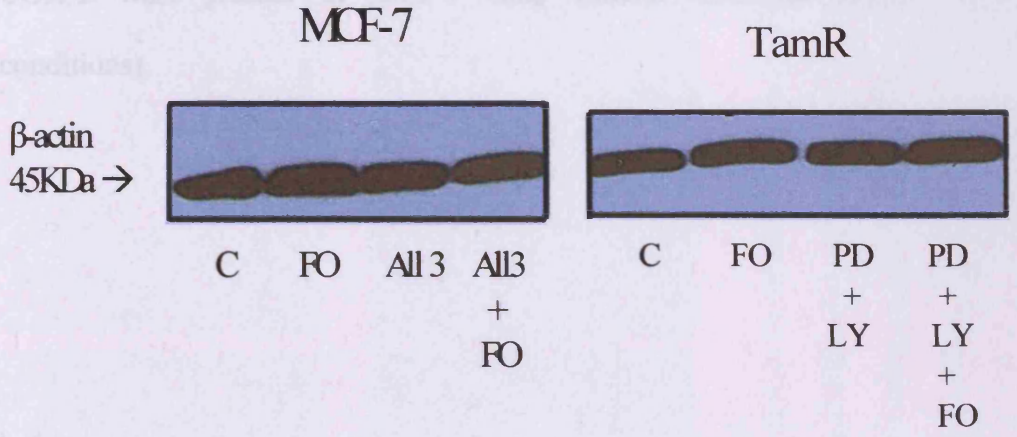

Figure 6.8 Western Blot for the levels of β-actin protein. MCF-7 and TamR cells were incubated with DMSO (0.1μml^{-1}), FO (1μml^{-1} fish oil), PD (25μM PD98059), LY (5μM LY294002) and 1 x 10^{-7}M 4-hydroxytamoxifen (MCF-7 cells only) for three hours. Cells were lysed and protein extracted and quantified for equal loading. Protein was separated by SDS-PAGE. Proteins were immobilised on a nitrocellulose membrane and immunoprobed using a cell signalling technology β-actin primary antibody.

6.3.4 Immunocytochemical detection of p-Src and total COX-2 in MCF-7 and TamR cells

To verify results seen in the western blot analysis of p-Src and total COX-2, immunocytochemical detection of these proteins was carried out on both cell lines.

Figure 6.9 shows the results for the detection of total COX-2 in MCF-7 and TamR cells. Staining in both cell lines was granular and localised to the

cytoplasm, similar to previous immunocytochemical analysis for COX-2 (Davies, G. *et al* 2003). Figure 6.9A-B shows that small amounts of total COX-2 were present in MCF-7 cells without treatment (under basal conditions).

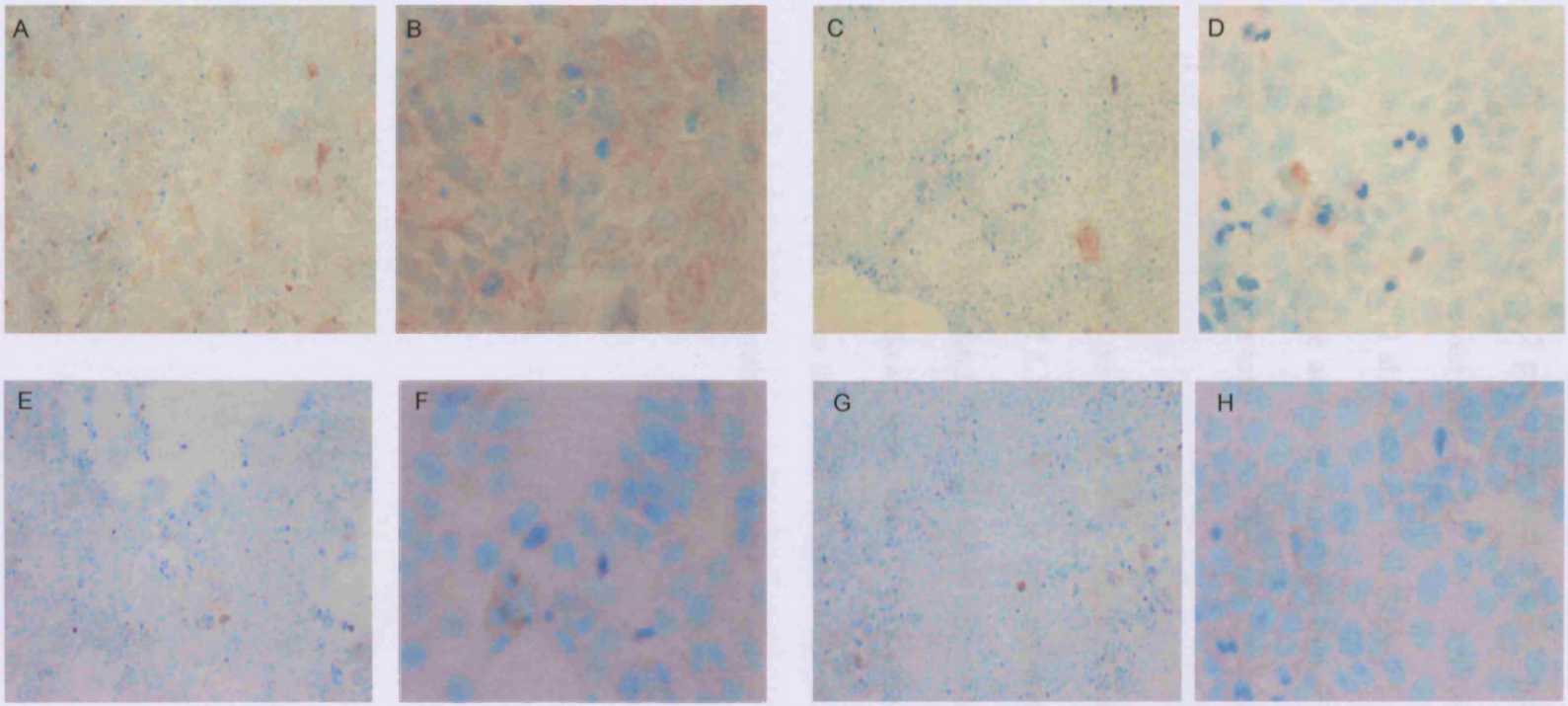

Figure 6.9 A-H ICC detection of total COX-2 in MCF-7 cells incubated with 0.1µlml^{-1} DMSO (A & B), 1µlml^{-1} fish oil (C & D), 1 x 10^{-7}M 4-hydroxytamoxifen, 25µM PD98059 and 5µM LY294002 (E & F) or 1µlml^{-1} fish oil, 1 x 10^{-7}M 4-hydroxytamoxifen, 25µM PD98059 and 5µM LY294002 (G & H) for three hours. Cells were grown to 70% confluency on TESPA coated glass coverslips and fixed using formal saline. 1° antibody was NEB total COX-2 rabbit primary at 1/40 for 1.5 hours. Secondary antibody was DAKO Rabbit EnVision peroxidase labeled polymer antibody for 1.5 hours. A, C, E, G x 10 and B, D, F, H x 40. Passage numbers were 22, 27 and 33.

Total COX-2 protein was lower in MCF-7 cells (6.9 A-B) compared to TamR cells, shown in figure 6.9 I-J. Incubation for three hours with fish oil reduced the levels of COX-2 protein in both MCF-7 cells (6.9 C-D) and TamR cells (6.9 K-L). Incubation with 1x 10^{-7} M 4-hydroxytamoxifen, 25μM PD98059 and 5μM LY294002 also reduced total COX-2 levels in MCF-7 cells, shown in figure 6.9 E-F. The addition of fish oil to this cocktail treatment seemed to completely abolish a total COX-2 protein signal, shown in figure 6.9 G-H.

Figure 6.9 M-N shows TamR cells incubated with the combination of 25 μM PD98059 and 5 μM LY294002. It demonstrates that although this treatment does knock down total COX-2 protein expression after 3 hours, it is not as great as the knock down seen with the incubation of 1 μL mL^{-1} fish oil. The addition of fish oil to the two STIs gave a knock down of total COX-2 protein similar to that seen with fish oil alone.

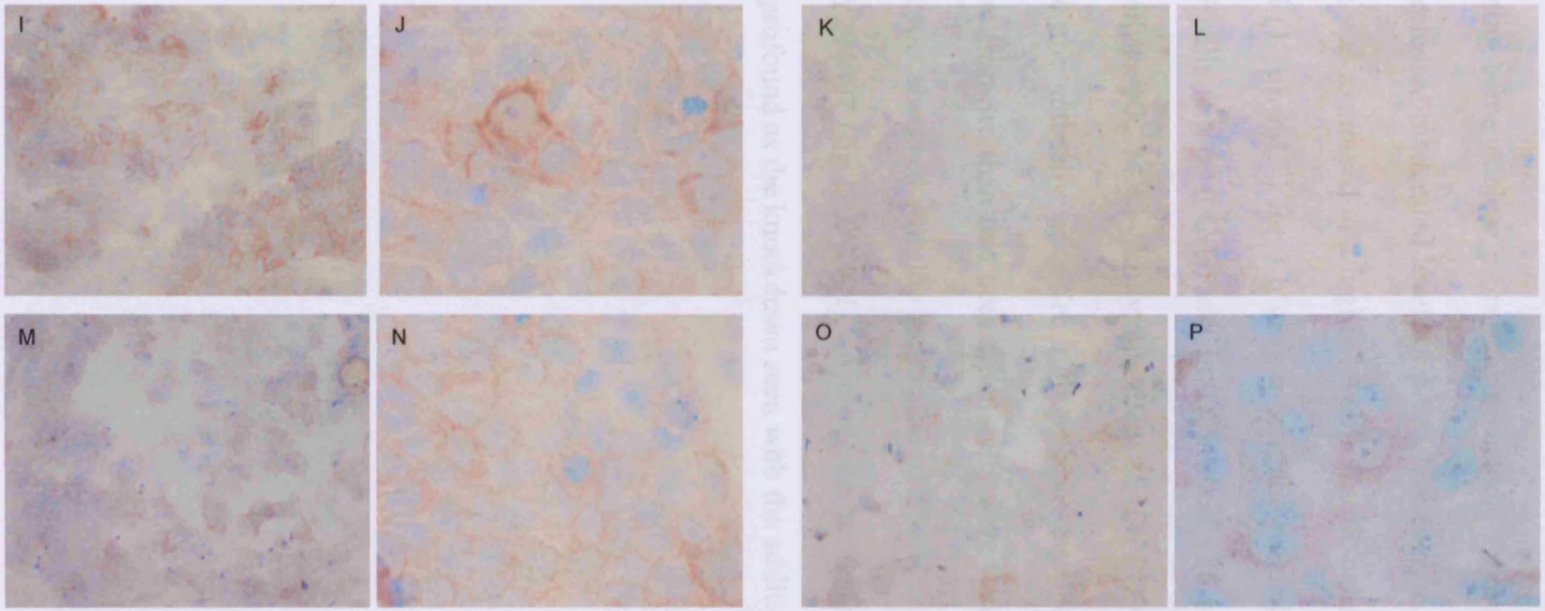

Figure 6.9 I-P Immunocytochemical detection of total COX-2 in TAMR cells. Cells were incubated with 0.1μlml^{-1} DMSO (I & J), 1μlml^{-1} fish oil (K & L), 25μM PD98059 and 5μM LY294002 (M & N) or 1μlml^{-1} fish oil, 25μM PD98059 and 5μM LY294002 (O & P) for three hours. Cells were grown to 70% confluency on TESPA coated glass coverslips and fixed using formal saline. Primary antibody was NEB total COX-2 rabbit primary antibody at 1/40 for 1.5 hours. Secondary antibody was DAKO Rabbit EnVision peroxidase labeled polymer antibody for 1.5 hours. I, K, M, O x 10, L x 20 and J, N, P x 40. Passage numbers were 15, 19 and 30.

Both cell lines were also analysed for p-Src levels, as displayed in figure 6.10. This data shows cytoplasmic localization of p-Src in both cell lines; however, at high levels of staining some nuclear p-Src was detected. Figure 6.10 A-B shows that MCF-7 cells expressed moderated levels of p-Src, however, as with total COX-2 levels; p-Src protein was expressed at a higher level in TamR cells (figure 6.10 I-J). Addition of fish oil (1 $\mu L\ mL^{-1}$) for 3 h gave a dramatic reduction in p-Src protein staining in MCF-7 cells (fig 6.10 C-D) and in TAMR cells (6.10 K-L). Incubation of MCF-7 cells with $1x\ 10^{-7}$ M 4,hydroxytamoxifen, 25 μM PD98059 and 5 μM LY294002 also reduced the intensity of p-Src staining, however, this was a much more subtle decrease in p-Src than that seen when cells were incubated with fish oil. A similar pattern was observed with the incubation of TamR cells with 25 μM PD98059 and 5 μM LY294002 (fig 6.10 M-N). A moderate reduction was observed, however, was not as profound as the knockdown seen with the addition of fish oil.

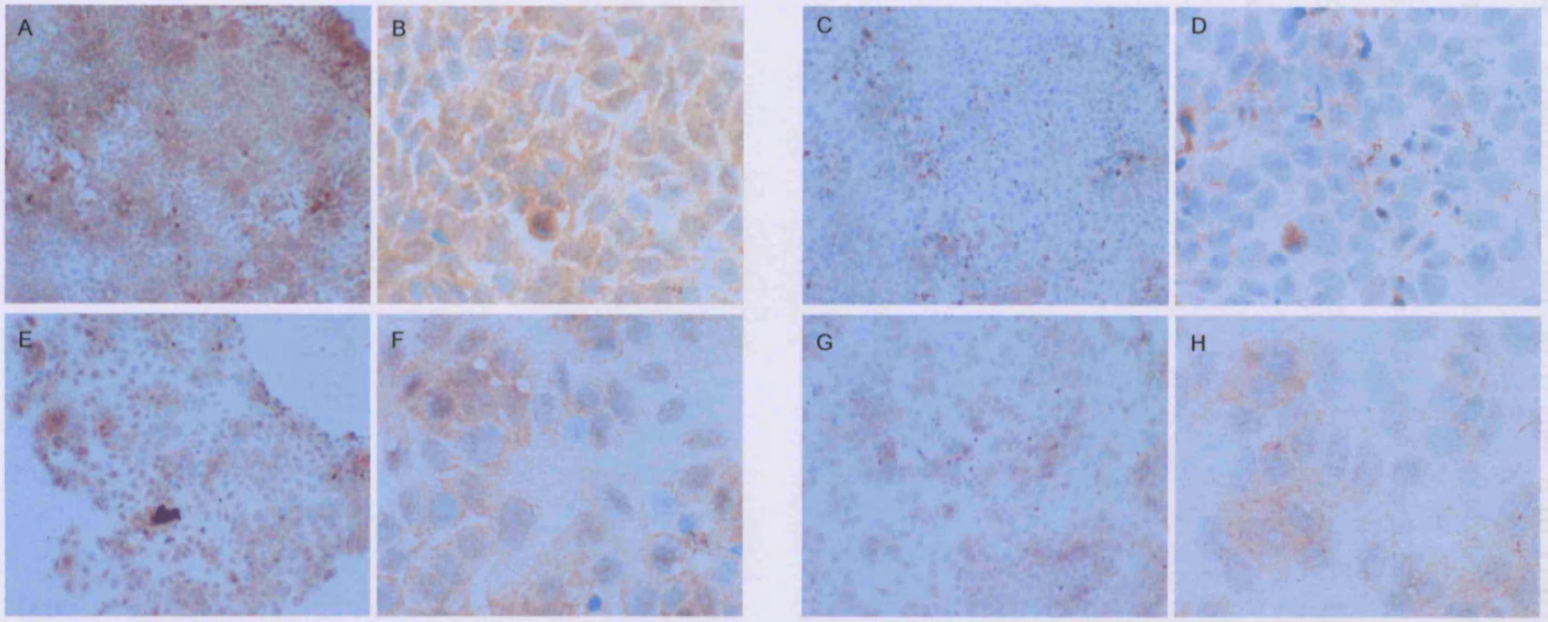

Figure 6.10 A-H Immunocytochemical detection of phospho-Src in MCF-7 cells. Cells were incubated with 0.1µlml^{-1} DMSO (A & B), 1µlml^{-1} fish oil (C & D), 1 x 10^{-7}M 4-hydroxytamoxifen, 25µM PD98059 and 5µM LY294002 (E & F) or 1µlml^{-1} fish oil, 1 x 10^{-7}M 4-hydroxytamoxifen, 25µM PD98059 and 5µM LY294002 (G & H) for three hours. Cell were grown to 70% confluency on TESPA coated glass coverslips and fixed using formal saline. Primary antibody was Cell Signal Technology phoshpo-Src rabbit primary antibody at 1/40 for 2 hours. Secondary antibody was DAKO Rabbit EnVision peroxidase labeled polymer antibody for 2 hours. A, C, E, G x 10 and B, D, F, H x 40. Passage numbers were 22, 27 and 33.

Upon incubation of MCF-7 cells with the combination of 4-hydroxytamoxifen, PD98059, LY294002 and fish oil (figure 6.10 G-H), p-Src protein levels were reduced to levels similar to those seen with incubation with fish oil alone (6.10 C-D). Figure 6.10 O-P shows that incubation of TamR cells with 1μlmL^{-1} fish oil 25μM PD98059 and 5μM LY294002 gave the greatest knockdown in p-Src protein expression in this cell line.

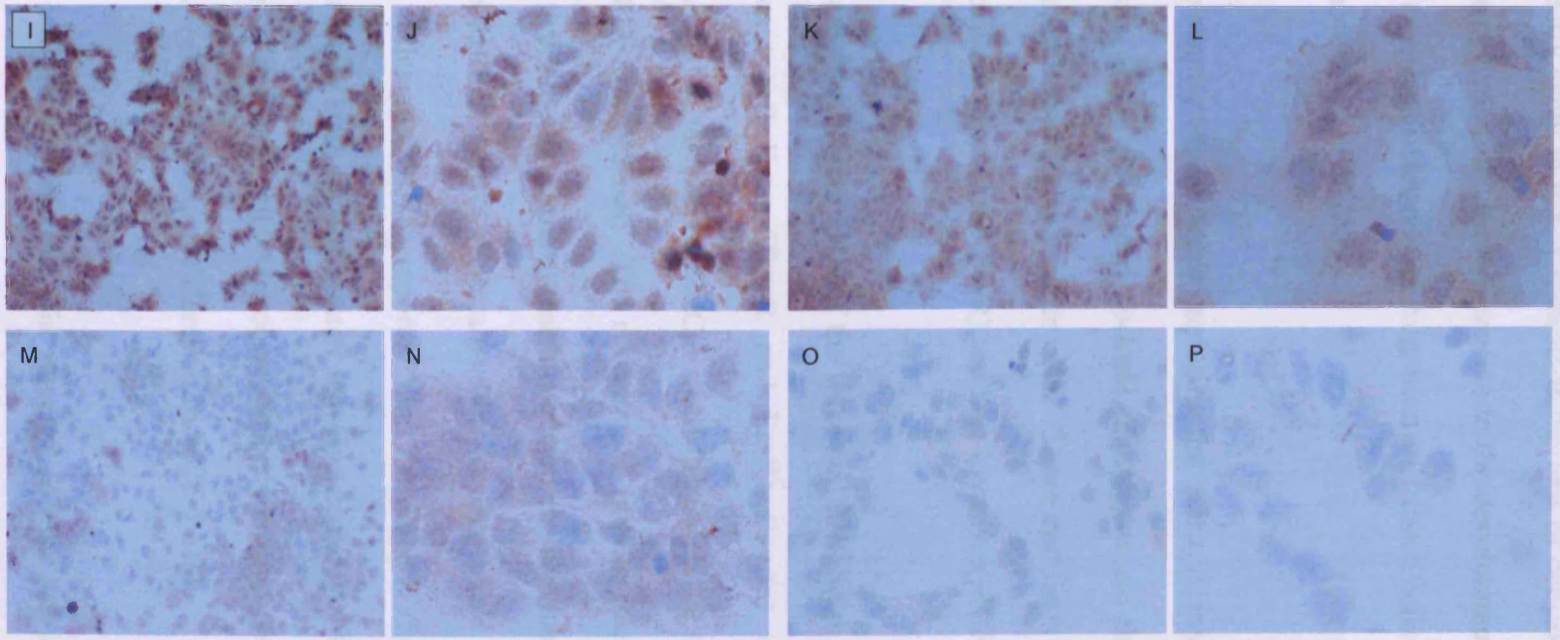

Figure 6.10 I-P Immunocytochemical detection of phospho-Src in TamR cells. Cells were incubated with 0.1µlml^{-1} DMSO (I & J), 1µlml^{-1} fish oil (K & L), 25µM PD98059 and 5µM LY294002 (M & N) or 1µlml^{-1} fish oil, 25µM PD98059 and 5µM LY294002 (O & P) for three hours Cell were grown to 70% confluency on TESPA coated glass coverslips and fixed using formal saline. Primary antibody was Cell Signal Technology phoshpo-Src rabbit primary antibody at 1/40 for 2 hours. Secondary antibody was DAKO Rabbit EnVision peroxidase labeled polymer antibody for 2 hours. I, K, M, x 10, O x 20 and J, L, N, P x 40. Passage numbers were 15, 19 and 30.

This chapter was aimed at exploring the effect, if any, of fish oil and the oth actives of the developed cocktail therapeutic on the migratory potential cultured human breast cancer cells. Three cell lines were chosen to represe an invasive (TamR and FasR) and non-invasive (MCF-7) phenotype.

Initially, the growth rates of the three cell lines were examined. The hormo resistant cell lines (TamR and FasR) showed accelerated growth rat compared to the parental MCF-7 cell line, with the order in growth rate bei MCF-7<TamR<FasR. The elevation in growth rates seen in both tamoxif and faslodex (fulvestrant) resistance has been previously demonstrated and it accepted that growth factor signalling is responsible for this trend. Hiscox, and colleagues (2005) reported that TamR cells displayed enhanced grow rates along with an augmented invasive capacity. The increased growth ra seen with TamR cells was observed previously, correlating to similar grow seen with E_2 induced proliferation in MCF-7 cells.

Growth curves examined in chapter 5 were repeated to ensure the ce displayed the same phenotype and behaved in the same way when insulted wi

fish oil, PD98059, LY294002 and 4-hydroxytamoxifen. Figure 6.2 and 6.3 showed that both MCF-7 and TamR cells behaved very similarly when incubated with these compounds as in chapter 5. Interestingly, no significant difference in growth rates between control and treated MCF-7 and TamR cells were observed after 2 days. This indicated that the results of 2-day migration assays, performed in this chapter, were a consequence of altered migratory potential of the cells rather than an effect on cell number.

Investigations into the migratory potential of the three cell lines followed the same pattern as growth rates, as shown in figure 6.4, where the order of metastatic potential was MCF-7<TamR<FasR. This observation of a correlation existing between loss of hormone sensitivity, elevated growth rate and elevated invasive behaviour has been reported previously (Hiscox, S. *et al* 2005, Sommer, A. *et al* 2003), with the switch to growth factor signalling suggested as being responsible for this phenomenon. EGFR signalling is involved in a wide array of processes in tumor biology and tumorogenesis, including invasion and metastasis (Baselga, J. 2002). Indeed, several studies using cells engineered to overexpress certain growth factors and their ligands have uncovered that growth factor signalling is sufficient to induce migration and invasion (Kruger, J.S. & Reddy, K.B. 2003, Wells, A. *et al* 2002). The elevated migratory potential of the cells is thought to arise form an altered cell-to-cell and cell-to-matrix adhesion (Hiscox, S. *et al* 2004)

The involvement of COX-2 in tumorogenesis was first brought to light with the discovery that regular NSAID use was inversely correlated to colon cancer risk. Since then COX-2 expression has been correlated to higher tumor grade and metastatic potential of many solid cancers such as colon, lung, prostate and breast (Masferrer, J.L. *et al* 2000). In breast cancer, as with other cancers, the exact role of COX-2 in tumorogenisis remains vague, although many reports suggest a role for it in many processes involved in metastasis, including invasion, chemotaxis and angiogenesis as well as proliferation (Costa, C. *et al* 2002).

The data in this chapter indicate that total COX-2 protein is expressed in both hormone sensitive MCF-7 and tamoxifen resistant TamR breast cancer cells, albeit at much lower levels in MCF-7 cells, as shown in both the western blot and ICC experiments. In breast cancer cell lines COX-2 expression has only been demonstrated previously in hormone insensitive cells with an increased invasive capacity, such as MDA-MB-231 cells (Larkins, T.L. *et al* 2006). Expression of COX-2 has previously been shown in MCF-7 cells by Lui, X-H. and Rose, D.P. (1996), however, this expression was only seen post tetradecanoyl phorbol acetate induction. Results in this chapter show constitutive basal COX-2 expression in MCF-7 cells. The expression of COX-2 in TamR cells has been previously demonstrated in house, which correlates with its expression in other highly motile cells such as MDA-MB-231 (Liu, X-H. & Rose, D.P. 1996).

Overexpression of COX-2 has been linked to an increase in invasive and metastatic potential both *in vitro* and *in vivo*. Elevated COX-2 has been shown to enhance the levels of expression and secretion of vascular endothelial growth factor-C (VEGF-C), a potent mediator of lymphangiogenesis. It was further revealed that knockdown of VEGF-C expression reduced the migration of the highly migratory cell line MDA-MB-231 (Timoshenko, A.V. *et al* 2005). Stasinopoulos and colleagues (2007) showed that silencing of COX-2 in MDA-MB-231 showed a reduction in oncogenic markers such as MMP-1, interleukin 11 and chemokine receptor 4. The COX-2 knockdown also induced up-regulation of anti-metastatic markers such as thrombospondin-1 and Epstein-Barr-Induced 3. These cells also showed a decreased migratory and invasive capacity. Overexpression of COX-2, and so over production of PGE_2, can also promote migration via cross-talk with the EGFR. PGE_2 can induce shedding of active EGFR ligands from the PM, thus activating EGFR signalling pathways (Pai, R. *et al* 2002). PGE_2 can also transactivate EGFR through Src stimulation (Buchanan, F.G. *et al* 2003).

Addition of PD98059 and LY294002 caused a slight reduction in COX-2 protein in both MCF-7 and TamR cells. A study by Börsch-Haubold, A.G and co-workers in 1998 described how PD98059, previously thought to be a specific inhibitor of the p42/44 MAPK signalling pathway, inhibited the conversion of AA into thromboxanes (Tx) A_2. The authors showed that PD98059 was capable of preventing platelet aggregation induced by collagen and AA but not by thrombin. Further experiments revealed that this was a

result of inhibition of cyclooxygenase 1 and 2 and not the inhibition of thromboxane synthase. This inhibition of cyclooxygenase by PD98059 may have been the reason for the additive knockdown in COX-2 protein in the western blot analysis of total COX-2 protein seen when TamR cells were simultaneously incubated with both fish oil and PD98059 plus LY294002 for two hours.

The migration assay displayed in figure 6.5 revealed that incubation with 1 μL mL^{-1} fish oil reduced the migratory potential of TamR cells significantly. Dietary fat has been the topic of much debate in its effect on tumorogenesis. Much work has concentrated on the type of fat intake and the different effects they have on both prostanoid/eicosanoid synthesis and on tumor growth, proliferation and apoptosis, however, their involvement in metastasis remains largely unknown and unexplored.

It has been previously shown that the n-3 PUFAs EPA and DHA, which are contained at high concentrations in fish oil, are capable of inhibiting cell growth in the highly invasive MDA-MB-231 breast cancer cell line (Rose, D.P. & Connolly, J.M. 1990), which correlated with results obtained in this chapter (figure 6.2 and 6.3). In the study conducted by Rose and Connolly, the use of selective COX or LOX inhibitors revealed that the inhibition of cell growth was as a result of LOX inhibition and reduction in leukotriene production rather than as a result of reduced prostaglandin production. Subsequent studies by the same group then explored the role of COX and LOX in metastasis of

MDA-MB-231 cells in a nude mice model. This study showed that the growth of the tumors was lessened when the rats were fed with a diet rich in EPA and DHA, however the tumors of mice fed on a diet high in n-6 PUFAs displayed increased growth rates. The occurrence and severity of lung metastasis in mice fed a diet rich in n-3 PUFAs was significantly less than control or mice fed a diet rich in n-6 FAs. The authors also correlated this with the type of prostanoids produced in the tumor cells. The mice fed a diet rich in n-3 FAs showed high levels of series 3 prostaglandins and leukotrienes while mice fed a diet high in n-6 FAs showed no series 3 PGs or LKs but showed high levels of AA metabolites such as PGE_2 (Rose, D.P. *et al* 1995).

The most accepted mechanism for the chemopreventative actions of n-3 PUFAs, such as EPA is the suppression of AA derived prostanoids, in particular, PGE_2 (Horia, E. & Watkins, B.A. 2007). PGE_2 is known to have a role in tumor progression through effects on proliferation and apoptosis. However the role for this prostanoid in metastasis is still vague. It has recently been observed that PGE_2 can reverse the antiangiogenic effects of NSAIDs in CRC cells (Hernandez, G.L. *et al* 2001). N-3 PUFAs compete with AA for the cyclooxygenase enzyme and instead of forming series 2 prostanoids, which are highly inflammatory, series 3 prostanoids are produced. Series 3 prostanoids display a far weaker inflammatory action compared to series 2 prostanoid, which is believed to be the mechanism by which n-3 PUFAs give rise to anti-inflammatory actions. The biological role of PGE_3, derived from n-3 PUFAs has received scant attention. Human cells lack the ability to convert n-6

PUFAs into n-3 PUFAs due to the lack of the *fat-1* gene. Kang, Z.B and colleagues in 2001 transfected A549 cells with the *Caenorhabditis elegans fat-1* gene that encodes for an n-3 desaturase that converts n-6 PUFAs to n-3 PUFAs. They showed in this study that transfection efficiency was 90% and resulted in a rapid and remarkable modification of the n-6:n-3 ratio of fatty acids in the cell without need for dietary intervention. In fact a reversal in the ratio was seen whereby n-3 levels were twice as high as n-6 levels. The same group later used this model to explore the role of high n-3 PUFA concentrations on the metastatic potential of A549 cells. This subsequent study again showed 90% transfection efficiency and highlighted several interesting observations. The authors showed that *fat-1* gene expression led to an inhibition of adhesion and invasive potential of A549 cells, along with an elevation in apoptosis. They also used a low density array and RT-PCR to reveal and verify that MMP-1, ITG-α2 and NM23-H4, which are all involved in the metastatic process, were down regulated in A549 cells (Xia, S-H. *et al* 2005).

The addition of the two STIs also inhibited the migration of TamR cells. Dissection of Src signalling in migration and invasion of hormone resistant cell lines has exposed a role in this process for both the MAPK/ERK1/2 pathway and the PI3K pathway. The acquisition of endocrine resistance is paralleled with an elevation in the activity of Src kinase. Activated Src kinase has the ability to interact with many molecules such as growth factor receptors, steroid receptors, integrins and cell-cell adhesion receptors and thus is involved in

many tumorogenic processes such as proliferation, differentiation, migration and invasion (Hiscox, S. *et al* 2004). Inhibition of Src kinase activity is known to decrease the motility and invasion of TamR cells by reducing the levels of activated FAK and paxillin and by elongating focal adhesions. Interestingly, concomitant incubation with the EGFR inhibitor Gefitinib augmented this decrease in motility and invasion suggesting a role for the EGFR signalling pathway and downstream mediators (Hiscox, S. *et al* 2006). The MAPK (or ERK 1/2) signalling pathway has been correlated to and proved to be necessary for the invasive capability of Dunning rat prostatic adenocarcinoma cell lines, furthermore, the addition of PD98059 significantly reduced the invasive capability of such cell lines. However, PD98059 inhibited cell motility independent of any effects on adherence to the ECM or the secretion of ECM degrading proteases such as MMP2 (Suthiphongchai, T. *et al* 2006). A more recent study, conducted by Mendes, O. and co-workers (2007) found contradictory results regarding MMP2. They confirmed the role of ERK 1/2 in breast cancer metastasis to the brain, however, blockade of this pathway with PD98059 suppressed the secretion of MMP2, which they suggest was the main mechanism by which ERK 1/2 increased metastatic potential due to MMP2 being a pivotal candidate in cell motility.

PGE_2 has been shown to change the morphology of colorectal cancer cells by inducing reorganisation of actin stress fibres and focal adhesion complexes (Sheng, H. *et al* 2001). These changes were later attributed to the binding of PGE_2 to the EP4 receptor. This binding activated Akt through an EGFR/Src

mediated mechanism and was reversed by the addition of LY294002 (Buchanan, F.G. *et al* 2003). This data supports a role for PI3K/Akt in migration. The over expression of COX-2 in TamR cells in this study would give rise to elevated levels of PGE_2 and thus elevated activation of Akt. This could explain the inhibition in migration of TamR cells, seen in this chapter, when incubated with PD98059 and LY294002 (figure 6.3). The overexpression of Akt2 has also been linked to an increased β integrin expression, which in turn led to increased invasion and metastasis of human breast and ovarian cancer cells (Arboleda, M.J. *et al* 2003). This suggests that the blockade of Akt with LY294002 would reverse this event. The Rho family of proteins belongs to the Rho-GTPases, which are responsible for the assembly of the contractile actomyosin machinery that is imperative for most types of cell motility. Overpression of the Akt1 protein has been shown to phosphorylate and target the tumor suppressor TSC2 (tuberous sclerosis 2) for degradation. This led to reduced Rho-GTPase activity, which led to decreased actin stress fibres, focal adhesions and cell motility and invasion (Lui, H. *et al* 2006).

MAPK signalling is also involved in migration and invasion. TGF-β is a potent mediator of immune response, inflammation, tumor growth and metastasis. Three mitogen activated protein kinase signalling pathways (Jun, ERK1/2 and p38 MAPK contribute to TGF-β induced increased tumor migration and invasion. Work by Safina, A.F and colleagues in 2006 showed that constitutive activation of TGF-β type 1 receptor gave rise to elevated

migratory potential of MDA-MB-231 cells and that this could be reversed by blockade of MAPK signalling. It has recently been discovered that MAPK signalling contributes to metastasis of renal cell carcinoma. ERK 1/2 has been shown to be overexpressed in this malignancy and blockade of MAPK signalling reduced cell proliferation by the disruption of tumor vasculature (Huang, D. *et al* 2008).

The addition of fish oil reduced p-Src protein in both cell lines. PGE_2 is known to stimulate Src, which in turn activates EGFR signalling leading to increased cell motility (Shao, J. *et al* 2003). The addition of fish oil may have reduced levels of PGE_2 and thus decreased the stimulation of Src and so reduced the levels of phosphorylated Src in both cell lines.

6.5 Conclusion

The processes of invasion, migration and metastasis are complex and involve many signalling pathways. The literature suggests that cross-talk between several of these pathways is responsible for these events. Figure 6.11 is modified from (Meric, J.B. *et al* 2006) and highlights the cross talk between COX-2, PGE_2, PI3K, ERK 1/2, Src and EGFR. This diagram represents only a fraction of the mediators involved in metastasis. It highlights the complexity that researchers face when trying to dissect the biology of this event.

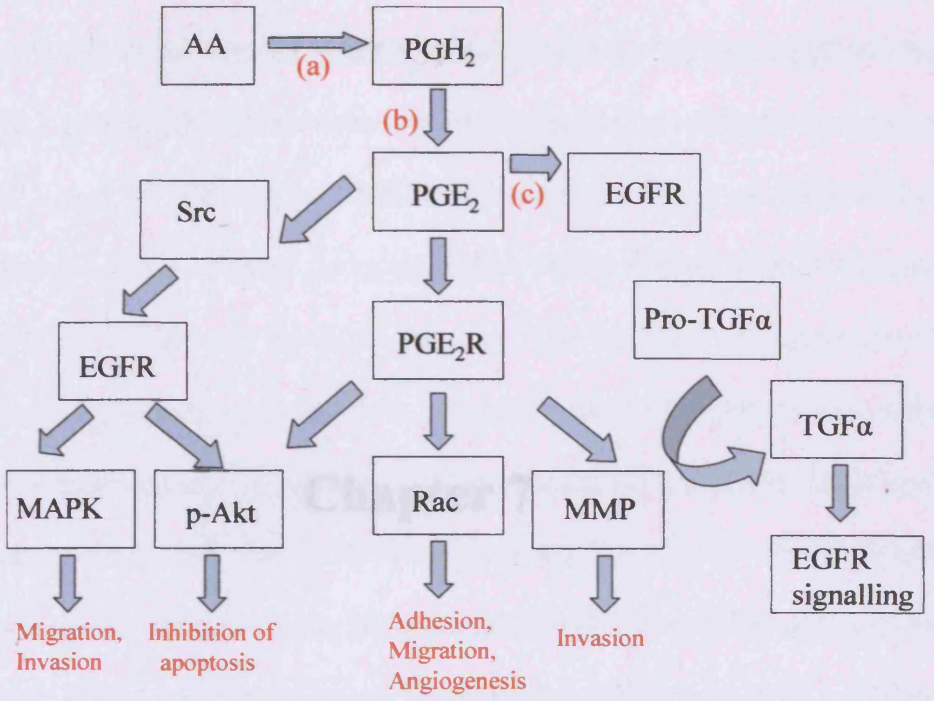

Figure 6.11 Schematic to show pathways involved in metastasis (a) Cyclooxygenase, (b) Cyclooxygenase (c) liberated EGF.

This short study has demonstrated the constituents of the cocktail formulation inhibit both p-Src and COX-2, both of which, although the exact mechanisms remain uncertain, are mediators of motility and invasion. They also decrease migration of TamR cells significantly. The results therefore suggest that the transcutaneous formulation developed in previous chapters may demonstrate anti-metastatic properties in tamoxifen resistant and invasive cells.

Chapter 7

Towards a Franz Diffusion Cell Model for the in vitro Assessment of Topical Breast Cancer Therapeutics I: Control of Microbial Contamination of Receptor Phase

7.1 Introduction

The plausibility of delivering a cocktail of anti-breast cancer agents: PD98059, LY294002 and 4-hydroxytamoxifen across skin was demonstrated *in vitro* in chapters 3 and 4. Furthermore, cell culture and growth assay studies also found that the levels of agent permeating skin were sufficient to significantly inhibit MCF-7 cell growth, shown in chapter 5. The current work is part one of two concerning the development of a composite transcutaneous model, with the aim of more closely reflecting *in vivo* situations. In this model, the target breast cancer cell line (MCF-7) were cultured directly into the receptor compartments of all-glass Franz diffusion cells (FDC), and the cell is then assembled with the inclusion of excised full thickness skin. When contemplating a model such as the one proposed here, where viable cells are to be cultured directly within receptor compartments, the issue of microbial contamination becomes paramount as this can have a profound affect on cultured cell viability and growth.

The use of porcine skin as a model for human skin is now widespread, with numerous studies suggesting parity in terms of histology, morphology and permeability compared to the human counterpart (Sekkat, N. *et al* 2002). It is accepted that in order to serve as a model for human skin, the tissue must not have been subjected to any of the disinfection processes that pigs undergo immediately post slaughter. The clean, pink butcher products familiar to many are far removed from the animal within its farm environment and at the time of slaughter. To the skin scientist, the main problem is that the cleaning process

is highly effective in liberating all traces of epidermis, rendering the material useless as a penetration model. Another, more insidious issue involves the lifestyle of the pig and the close and prolonged exposure to faecal and other materials that make pre-disinfected porcine skin a haven for the proliferation of microorganisms.

7.1.2 Microorganisms

Microorganisms are described as organisms too small to see with the naked eye, thus needing the aid of a microscope. Microorganisms include fungi, bacteria, protists, and archaea however this group of mainly single celled organisms does not include viruses and prions. Microorganisms have the capability of living almost anywhere and the skin has its own resident microorganisms that act beneficially to the health of the skin (Roth, R.R. & James, W.D. 1989).

7.1.2.1 Bacteria

Bacteria belong to a group of organisms termed Prokaryotes. This term is used to descibe organisms that lack a cell nuclues and other organelles. The have a genome made up of one single loop of DNA, however, they have the capability of harbouring small pieces of DNA called plasmids. They range in size between 0.5μm to 8μm in diameter (Spellman, F.R. 1998).

The skin has its own resident bacteria in the form of skin microflora. This microflora normally consists of staphylococci, micrococci, corynebacteria, and

propionibacteria (Ramero-Steiner, S. *et al* 1990). The variety of bacterial inhabitants differs with anatomical site, according to temperature, pH, availability of nutrients and humidity. Personal hygiene also contributes to the level of colonization. The axilla presents as the optimum body location for bacterial population (Leyden, J. *et al* 1981). A balance or relationship between species of bacteria found in the skin microflora has also been described. It is this relationship in species that maintains the symbiotic relationship of the bacteria and the skin (Marples, R.R. & Williamson, P. 1969). Upsetting this balance with antibacterial remedies can result in elimination of non-pathogenic bacteria, which then are replaced by more harmful species. It has been reported that persistent use of antibacterial soap on the foot suppressed gram-positive bacteria, which allowed enterobacteria to colonize this region of the skin. This in turn allowed *Pseudomonas* to inhabit this region which gave rise to lesion formation. These lesions allowed infection with *Candida Albicans* (Ehrenkrans, N.J. *et al* 1967).

7.1.2.2 Fungi

Fungi are also microorganisms; however they are eukaryotes, meaning they contain organelles such as a nucleus, golgi apparatus and mitochondria. Fungi were originally thought to be most similar to plants but are now thought to have more characteristics in common with animals. Fungi may be unicellular but most strains string their cells together, forming a mycelium that may be visible to the naked eye.

There are five distinct characteristics that are used to classify fungi detailed below.

1. Fungi cells contain a nucleus and chromosomes.

2. They cannot photosynthesise.

3. They develop hyphae, which are long, tubular branching filaments used to absorb food.

4. Fungi absorb their food by osmosis.

5. They reproduce via spores, which develop on the fungi and are released by it.

Little is known about the incidence of fungi on normal human skin (McBride, M.E. *et al* 1979). However it is now understood that *Pityrosporum* (*Malassezia* spp.) is commonly detected in normal, healthy skin (Elsner, P. 2006). *Candida Albicans* is a common pathogenic fungi found in skin (Ehrenkrans, N.J. *et al* 1967).

7.1.2.3 The 0.22μm cyclopore track etched membrane

The trademark registered cyclopore track etched membranes are filters that are manufactured by Cyclotron technology giving accurate pore size and uniform distribution compared to general filter pore creation.

The pore size of membrane used throughout these studies was 0.22μm in diameter. This size was used to prohibit the passage of microorganisms, such

as bacteria and fungi. These microorganisms can be as small as 0.25μm in diameter but should be retained cyclopore track etched membrane.

7.1.3 Aims

The aim of the work was to examine the microorganisms colonising freshly excised porcine ears. Secondly, the possibility of excluding such microorganism contamination from receptor phases was explored by the inclusion of a 0.22 μm Cyclopore track etched membrane between the skin and receptor compartment, as it is established and widely agreed by microbiologists that most, if not all, recognised fungal and bacterial organisms are above 0.25 μm in diameter.

7.2 Materials and Methods

7.2.1 Materials

Most materials used in this chapter were discussed in chapter 2 (section 2.1). Tryptone soya agar (TSA) and sabouraud dextrose agar (SDA) were from Oxoid LTD, Basingstoke, Hampshire, England. Cyclopore track etched membrane (47mm diameter, 0.22μm) petri dishes and Dow Corning high vacuum grease were from Fisher Scientific, Loughborough, England. Crystal violet solution, Gram's iodine solution and safranin were from Sigma-Aldrich Ltd, Poole, England.

7.2.2 Methods

7.2.2.1 Preparation of the porcine ears

Porcine ears were collected from a local abattoir and kept on ice during transportation. The ears were then washed with cool water, patted dry and kept in the fridge until the following day.

7.2.2.2 Preparation of the agar

TSA is a broad range culture medium, used in the culture of microorganisms. It is not selective over aerobes or anaerobes. TSA media was made up by dissolving 40g thoroughly in 1L of deionised water and was then autoclaved. This was then left to cool at room temperature. It was then poured into sterile Petri dishes in a laminar flow cabinet and allowed to set overnight. SA was introduced by Sabouraud in 1910 as a selective medium for fungi and yeasts. Using this medium inhibits the growth of most bacteria due to its acidic pH of 5.6. To achieve these properties 65g was dissolved thoroughly in 1L of deionised water, and autoclaved to sterilise the media according to the manufacturer's guidelines.

7.2.2.3 Swabs of whole porcine ears

Swabs of the porcine ear were taken to show the extent of colonisation on the skin surface. Swabs were taken from three different locations on the ear; swab A was taken from skin closest to the point of dissection, swab B was from the

tip of the ear and swab C was taken from the middle of the ear. Individual sterile swabs were rubbed across the skin and the rotated 5 times in the described area. They were then rubbed across the agar in a similar manner to ensure all swabbed material was transferred to the agar plates.

Swabs a, b and c were transferred to TSA containing plates to detect bacterial growth and swab d was transferred to SDA containing plates to detect fungal growth. Plates containing swabs a, b and d were incubated at 37°C while the plates containing swab c were kept at 30°C. Plates were removed from the incubators after 48 hours and placed in the fridge until required.

Single colonies were isolated using a flame sterilised wire loop. The loop was rubbed across one place of the agar and then sterilised further. The wire was then used to spread out the swabbed colony onto the rest of the agar plate. The agar plates were then incubated according to the previous incubation. This was able to produce sufficient single colonies to perform gram staining. Colonies were photographed using an Olympus DP-12 digital camera (Olympus, Oxford, UK).

7.2.2.4 Swabbing of receptor phase with and without cyclopore track etched membrane in place

Franz diffusion cells were cleaned and autoclaved and kept in a sterile environment until required. Prior to experimentation, ears were prepared as stated in chapter 2; however, the stratum corneum was swabbed with 70% ethanol made up with de-ionised water. Cells were set up as stated in table 7.1

Cell number	CTEM	Excised skin	Fungizone and streptomycin
1-5	Present	Present	Present
6-10	Present	Present	Absent
11-15	Present	Absent	Present
16-20	Present	Absent	Absent
21-25	Absent	Present	Present
26-30	Absent	Present	Absent

Table 7.1 Table to show the diffusion cell set up to assess the ability of the CTEM in preventing microbiological contamination of the receptor solution. Cells were maintained in a sterile environment at 37 °C to provide a skin surface temperature of 32 °C. Receptor solution was wRPMI plus 5% SFCS. Fungizone and streptomycin were added as stated in the table.

Cells were set up with both the excised porcine skin membrane and the cyclopore track etched membrane in place; with the membrane filter being in contact with the receptor compartment and being greater in diameter than the skin membrane, so to prevent contamination of the receptor compartment. This methodology was to determine the capability of the CTEM to prevent

bacterial and fungal passage from the skin surface to the receptor compartment. This was repeated in the presence and absence of antibacterial and anti fungal solutions to assess the importance of the presence of these compounds in the receptor phase. Cells were set up in the absence of the CTEM, to gauge the necessity of this filter being in place and to assess its ability to prevent contamination of the receptor phase. This was again done in the presence and absence of antibacterial and antifungal. Cells were also set up with just CTEM present. It was deemed essential to calculate the sterility of such membranes to ensue they themselves could not contaminate the receptor phase. Receptor phase in all diffusion cell set-ups was wRPMI with 5% SFCS.

7.2.2.5 Gram's stain

Christian Gram developed the method followed in this thesis in 1884. The protocol relies on a fundamental difference in the structure of the bacterial cell wall. This cell wall is the outermost structure of bacteria and confers to its rigidity and mechanical strength. Gram-positive bacteria have up to 40 layers of peptidoglycan giving it high mechanical strength; however gram-negative bacteria only possess 1 or 2 layers of peptidoglycan and so are mechanically weak. It is this difference in cell wall thickness that allows the gram reaction to differentiate the two sub types of bacteria. The presence of multiple layers of pepidoglycan allows crystal violet-iodine complex stain to be retained in the bacteria, even after an ethanol/acetone wash. The absence of these pepidoglycan layers allows the crystal violet stain to be washed off by ethanol/acetone and the bacteria are susceptible to safranin counterstain. The

method described by Lesher. J.L & Aly, R. (2000) was closely followed. Single colonies were isolated using a wire loop, emulsified in water and spread upon glass microscope slides. This slide was then heated over a Bunsen burner to attach the bacteria to the glass slide and allowed to cool.

The bacterial specimen was then flooded with crystal violet solution for 10 seconds, which was subsequently washed off with tap water. The slides were then flooded with Gram's iodine solution for 10 seconds, which was subsequently washed off with tap water. The slides were then washed with ethanol-acetone solution until the solvent ran clear. The bacterial specimens were the counterstained with safranin for 10 seconds and washed carefully with tap water. The slides were then air dried and analysed using microscopy and images captured using an integrated Olympus DP-12 digital camera system (Olympus, Oxford, UK)..

7.3 Results

7.3.1 Microbiological examination of porcine ear

7.3.1.1 Swabbing of whole porcine ear skin

The microbiological examination of the porcine ear swabs firstly revealed that 3 main types of colonies grew at both 37 °C and that anatomical site showed no difference. This was shown across all 3 ears swabbed also. Isolation revealed another two strains. Table 7.2 describes bacterial colonies grown

from each swab and results from the Gram's stain, to ascertain the species of bacteria, are shown in figure 7.2.

Swab	Incubation temperature	Description of colony grown
A	37° C	Small yellow and small white colony, large white, colony
B	37° C	Small yellow and small white colony, large white, colony
C	30° C	White diffused colony, diffused yellow colony
D	37° C	No bacterial growth

Table 7.2 Descriptions of bacterial colonies grown from swabs of porcine skin, taken at different locations on the upper surface of the ear skin after 48 hours. Swabs a-c were grown up on TSA, while swab d was grown up on SDA.

Repeated isolation and re-swabbing of colonies determined that 5 distinct bacterial colonies were present on the surface of porcine ear skin. Unsurprisingly, no bacterial colonies were detected on the SDA plates, as this agar in specifically for the growth of fungal colonies.

Figure 7.1 shows digital photos of the result of the Gram's stain. 7.1 A shows that the small white colony, grown on TSA at 37° C, stained a violet colour, revealing that this was a Gram-positive bacterium.

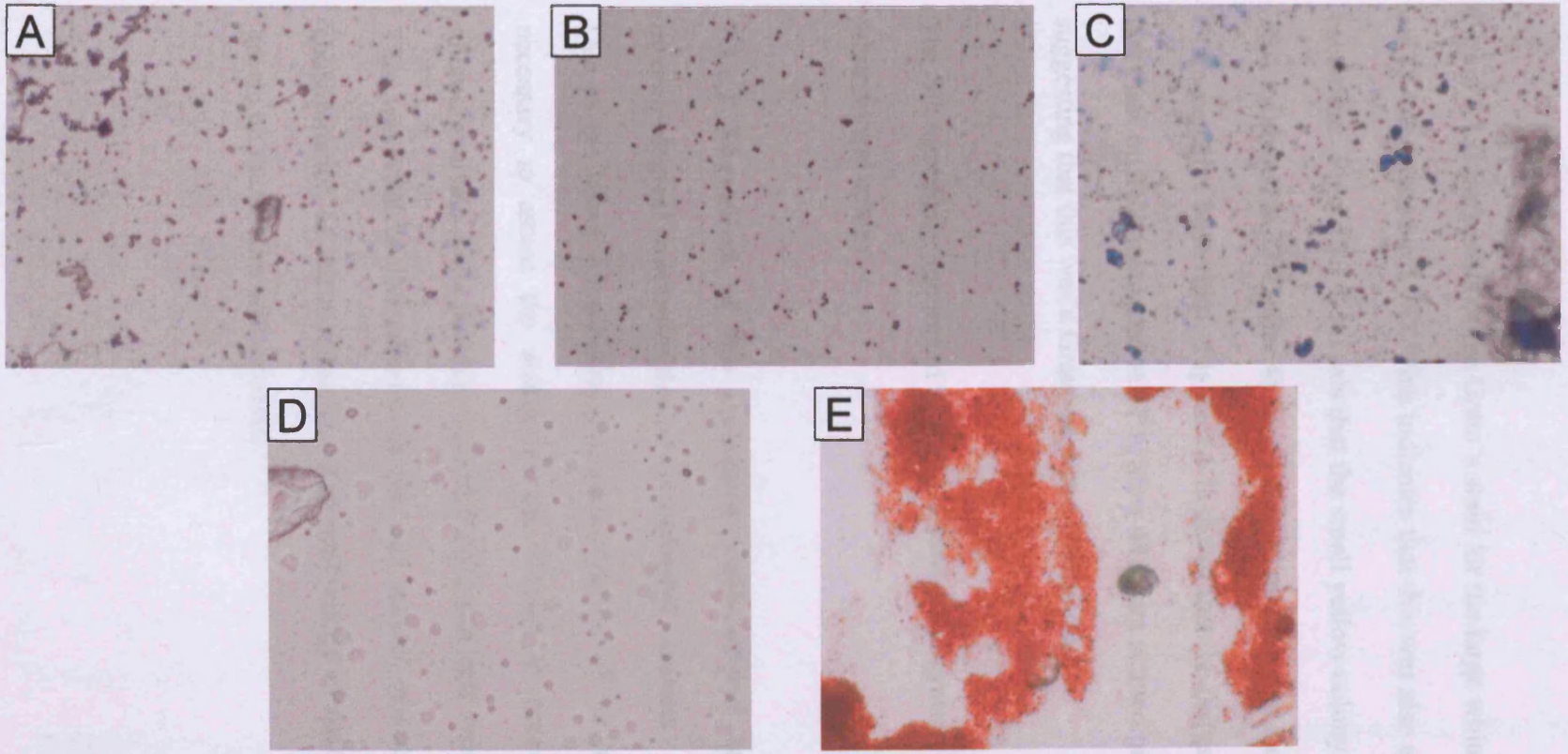

Figure 7.1 A-E Gram's stain of bacterial colonies (x80). A = small white colony, B = diffused white colony, C = large white colony, D = smell yellow colony, E = diffused yellow colony photos of gram stain were taken using an Olympus BH-2 phase microscope and photographed using an integrated Olympus DP-12 digital camera system (Olympus, Oxford, UK).

Figure 7.1 B shows that the diffused white colony, grown on TSA at both 30°C after 48 hours, stained violet indicating this too was a Gram-positive bacterium.

Figure 7.1 C the results of the Gram's stain for the large white colony, grown on TSA incubated at 37°C. This indicates that this was also a gram-positive bacterium. Figure 7.1 D reveals that the small yellow colony, which grew on TSA incubated at 37°C after 48 hours stained pink/orange indicating this was a Gram-negative bacterium. Figure 7.1 E shows that the diffused yellow colony that grew on TSA incubated at 37°C after 48 hours stained pink/orange suggesting that this was a Gram-negative bacterium

The SD agar plate, incubated at 37°C, allowed the growth of a large diffused white fungal colony.

7.3.1.2 The effect of the cyclopore track etched membrane on the microbiological contamination of the receptor solution

Due to the heavy microbiological contamination of the porcine ears, it was necessary to assess the ability of the CTEM to prevent the ingress of microorganisms from the skin into the diffusion cell receptor compartment. This was vital to the success of the full model system, as any bacterial contamination of the receptor compartment would almost certainly kill cells grown on the bottom of this vessel.

CTEM	Skin	AB and AF	Growth after 6 hours	Growth after 24 hours	Growth after 48 hours
Present	Present	Present	No growth	No growth	No growth
Present	Present	Absent	No growth	White diffused (30 °C)	White diffused (30 °C)
Present	Absent	Present	No growth	No growth	No growth
Present	Absent	Absent	No growth	No growth	No growth
Absent	Present	Present	Small white & yellow (37 °C)	Small white & yellow (37 °C)	Small white & yellow (37 °C)
Absent	Present	Absent	Large white, small white, small yellow (37 °C) white diffused (30 °C)	Large white, small white, small yellow (37 °C) white diffused (30 °C)	Large white, small white, small yellow (37 °C) white diffused and yellow diffused (30 °C)

Table 7.3 Table to show the diffusion cell set up to assess the ability of the CTEM in preventing bacterial contamination of the receptor solution. Cells were maintained in a sterile environment at 37 °C to provide a skin surface temperature of 32 °C. Receptor solution was wRPMI plus 5% SFCS. Fungizone (AF) and streptomycin (AB) were added as stated in the table. Samples of the receptor solution were taken at 6, 24 and 48 hours (n=5).

The data displayed in table 7.3 shows that bacterial growth was not seen when diffusion cells were set up with CTEM membrane alone both with and without antibacterial and antifungal present and at all time points, suggesting that this membrane was reliably sterile. Bacterial growth was detected in diffusion cells set up with skin, without the CTEM present, both with and without antibacterial and antifungal present and at all time points. The diffusion cells with both porcine skin and CTEM showed no bacterial growth at each time point when the antibacterial and anti-fungal were present. However, in the absence of the antibacterial and antifungal bacterial contamination was seen in the 24 and 48 hour sample.

CTEM	Skin	AB and AF	Growth after 6 hours	Growth after 24 hours	Growth after 48 hours
Present	Present	Present	No growth	No growth	No growth
Present	Present	Absent	No growth	No growth	Large white diffused
Present	Absent	Present	No growth	No growth	No growth
Present	Absent	Absent	No growth	No growth	No growth
Absent	Present	Present	Large white diffused	Large white diffused	Large white diffused
Absent	Present	Absent	Large white diffused	Large white diffused	Large white diffused

Table 7.4 Table to show the diffusion cell set up to assess the ability of the CTEM in preventing fungal contamination of the receptor solution. Cells were maintained in a sterile environment at 37 °C to provide a skin surface temperature of 32 °C. Receptor solution was wRPMI plus 5% SFCS. Fungizone (AF) and streptomycin (AB) were added as stated in the table. Samples of the receptor solution were taken at 6, 24 and 48 hours (n=5). Incubation of Petri dishes was at 37°C.

The data displayed in table 7.4 shows that fungal contamination of the receptor phase was prevented when both the CTEM and antibiotic and antifungal were present. The presence of just the skin and CTEM, without antibiotic and antifungal present, delayed fungal contamination for 24 hours. Inclusion of the skin and the antibiotic and antifungal were present without the addition of the CTEM gave rise to contamination at the first sample point of 6 hours.

7.4 Discussion

This chapter has highlighted the extent of microbial contamination to which transdermal/transcutaneous permeation studies are subjected to, however, the normal cleansing routine post-slaughter would be a compromise but not an acceptable one for permeation studies due to the stripping of SC and epidermis. Microbial contamination of receptor phase is not normally considered a major pitfall in permeation studies, however, when developing such a composite transcutaneous model aimed at reflecting *in vivo* situations, this consideration becomes paramount.

This chapter has determined that 5 distinct bacterial colonies and 1 fungal colony exist on excised porcine ear skin. These were detected in three different ears on three separate occasions, suggesting that these microorganisms are commonly found on porcine ear skin.

One species of fungi was also present on excised porcine ear skin, which if human and porcine skin share the same resident fungi, this could be *Pityrosporum* (*Malassezia spp*).

It is widely acknowledged by microbiologists that the sizes of bacteria and fungi are in excess of 0.22 μm, suggesting that this would provide a suitable filter to stop the ingress of these microorganisms from the skin to the receptor phase cyclopore track etched membrane.

Diffusion experiments with CTEM present beneath the skin membrane delayed bacterial contamination of the receptor phase, however complete inhibition of contamination was only seen when AB and AF were included into the receptor phase. This suggests that either species of bacteria exist that are smaller than 0.22 μm in diameter and that are not widely documented in microbiology texts or that the pore sizes were not uniformly accurate at 0.22 μm in diameter. Another plausible explanation could be that the bacteria could pass around the edges of the CTEM and enter between the CTEM and receptor compartment flanges.

The amounts of bacteria entering the receptor phase in the presence of the CTEM was much reduced compared to that entering without the CTEM present as the AB present within the receptor phase was capable of killing these. Streptomycin and penicillin were added to the receptor phase and act on Gram-negative and Gram-positive bacteria respectively. Streptomycin is a

bactericidal agent, capable of killing many species of bacteria (Donald, P.R. 2002). Streptomycin delivers the bactericidal by binding to the 30S subunit of bacterial ribosomes, changing their shape. This leads to misreading of bacterial messenger RNA, thus inhibits bacterial protein synthesis (Rang, H.P. *et al* 2000). Penicillins are also bactericidal; however, they inhibit bacterial wall synthesis. Data in this chapter suggests that the inclusion of these Abs is crucial in maintaining a sterile receptor phase in which MCF-7 cells may later be cultured.

7.5 Conclusions

The 0.22 μm cyclopore track etched membrane proved sufficient in retarding the ingress of microorganisms. It is established that most, if not all, recognised fungal and bacterial organisms are above 0.5 μm in diameter (Spellman, F.R. 1998) and therefore it is not surprising that the 0.22 μm pore size of the membrane was sufficient to prevent the passage of the microorganisms.

Chapter 8

Towards a Franz Diffusion Cell Model for the in vitro Assessment of Topical Breast Cancer Therapeutics II: Effect of Permeants on MCF-7 Cells Seeded Within the Receptor Phase

8.1 Introduction

In chapters 3 and 4 the plausibility of delivering PD98059, LY294002 and 4-hydroxytamoxifen across excised porcine skin was demonstrated and discussed. Furthermore, chapter 5 revealed that concentrations permeated were enough to inhibit MCF-7 cell growth significantly.

Throughout the literature, there is scant evidence of any intermediate between *in vitro* transcutaneous delivery studies and *in vivo* animal studies. Little effort has been made to further develop the diffusion cell methodology to incorporate post skin targets.

This chapter examined the plausibility of a composite model, incorporating elements of both skin permeation and cell culture. The first part of the model consists of MCF-7 cells grown at the bottom of a glass Franz diffusion cell (FDC) receptor compartment. This, in itself, provides a major challenge as uncoated glass is not considered to be an effective substrate for the growth of this type of cell line. The second part of the model involves a full-thickness skin membrane, mounted between the greased flanges of the diffusion cell, shown in Figure 8.1. Drug solutions applied to the skin in the donor phase permeating the skin enter the receptor phase and diffuse to the cells, where their pharmacological activities would be exerted.

Figure 8.1 An illustration to show the experimental set up of the "composite model".

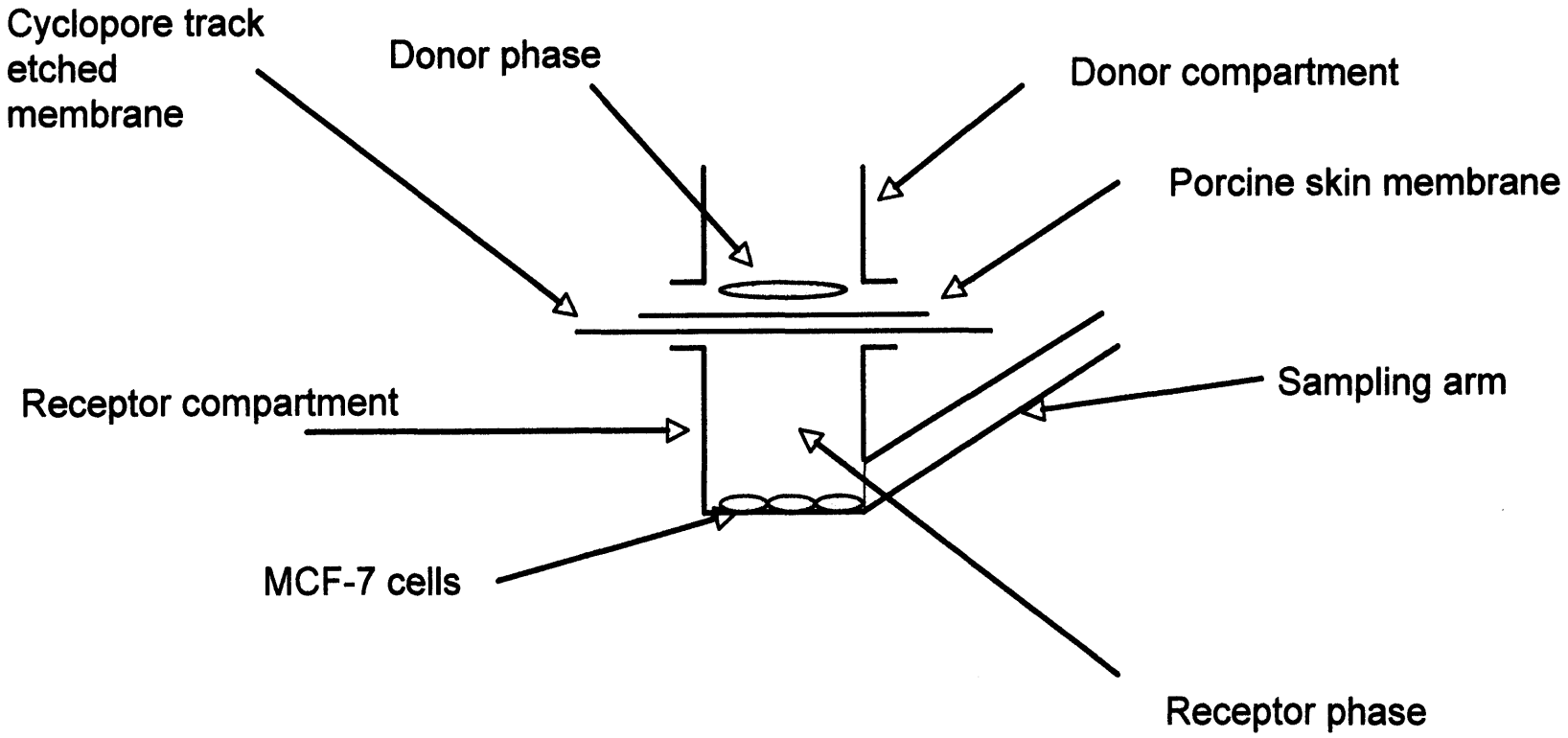

The final part of the model surrounds the necessity to prevent microbial contamination of the receptor phase/cell growth medium. To this end a 0.22 μm cyclopore track etched membrane was used- these are filters that contain highly accurate and uniform pore distribution compared to general filter pore creation. This was placed between the lower surface of the skin and receptor phase, chapter 7 validated the prevention of bacteria and fungal entry into the receptor phase when both AB and AF were present.

A successful composite system based on the above would mimic a topical drug delivery system scenario more closely than two disparate experiments. In this work, the individual elements of the proposed model were validated and ultimately used to determine the effects of the aforementioned drug combination on the cells cultured within the FDC receptor compartment. This composition of the separate methodologies has not been presented in the literature, and thus it can be presumed has not been attempted or been successful, therefore optimisation of all aspects had to be performed (described in chapter 7 and section 8.2.2).

8.1.3 Aims

The aim of the work in this chapter was to probe a novel composite model for studying in vitro the activity of topically applied compounds against breast cancer cells (figure 8.1).

8.2 Material & Methods

8.2.1 Materials

Most materials used in this chapter were introduced in chapter 2 (section 2.1) Cyclopore track etched membranes (CTEM), 47mm diameter, 0.22 μm and Dow Corning high vacuum grease were from Fisher Scientific, Loughborough, UK.

8.2.2 Methods

8.2.2.1 Cell culture in glass Franz diffusion cells

Franz diffusion cells were cleaned and autoclaved and stored in a sterile environment until required. MCF-7 cells were grown in plastic flasks, in RPMI plus 5% FCS until 70% confluent. At this point cells were passaged, using the protocol outlined in chapter 2 and 1 million cells per Franz diffusion cell were seeded into each diffusion cell in 1ml of wRPMI. The media was supplemented with 5% SFCS, 10UmL^{-1} and 10 μg mL^{-1} penicillin/streptomycin and 2.5 μg mL^{-1} fungizone. The diffusional area of the receptor compartment was sealed with a sterile cover slip, while the sampling arm was sealed with sterile tin foil. This time point was taken as day 0. On day 2 the media was removed and replenished with fresh media, on this instance the whole receptor compartment was filled. On day 4, media was replenished and on day 7 cells were counted, as outlined previously. Counts were corrected for the area of the receptor compartment.

8.2.2.2 Permeation studies through 0.22 μm pore membrane filters

All studies were conducted in a laminar flow cabinet and under sterile conditions. A sterile cyclopore track etched membrane (CTEM) was necessary in the whole model as it has been previously demonstrated that this is sufficient to prevent the ingress of bacteria and fungus, described in chapter 7. It was hoped that the 0.22μm pores would be sufficiently small to prevent microorganisms from entering the receptor phase from the skin but large enough so as not to impede the permeation of the three compounds. This section was aimed at ensuring that the cyclopore track etched membrane was not a limiting factor in the permeation of the compounds.

Glass diffusion cells were washed, autoclaved and set up as described in chapter 3. However, a cyclopore track etched membrane was added in place of the skin membrane. The CTEM was soaked in receptor phase prior to incorporation into the diffusion cell apparatus to ensure that any drug penetration was not out-balanced by the upward movement of receptor phase into the CTEM. A donor compartment was clamped to the upper surface of the membrane with a stainless steel clamp. Both donor and receptor flanges were greased with high vacuum silicon grease to ensure no leakage of donor phase. Receptor phase was cetrimide (30 mg mL^{-1}) and donor phase was 2.54 x 10^{-4} M 4-hydroxytamoxifen, PD98059 and LY294002 in a fish oil vehicle. The donor compartment was occluded to mimic a patch application. Samples were

taken at 1,2,3,4,5,6 and 24 h (n=5 for both experiments). Samples were analysed for the three compounds and for EPA as described in chapter 2.

8.2.2.3 Permeation studies through both excised porcine skin and 0.22 μm cyclopore track etched membrane

Franz diffusion cells were set up as stated in 8.2.2.2, however, excised porcine skin was placed onto the uppermost surface of the membrane, stratum corneum upward. Again, a donor compartment was clamped into place. Donor phase was 2.54 x 10^{-4} M PD98059, LY294002 and 4-hydroxytamoxifen in a fish oil vehicle. Samples were taken at 3, 6, 12, 24, 36 and 48 h and analysed as above.

8.2.2.4 Cell growth studies with trans-CTEM dosing of 4-hydroxytamoxifen, PD98059 and LY294002

Franz diffusion cells were cleaned and autoclaved prior to use and all experimentation was conducted in a laminar flow cabinet to maintain a sterile environment. Diffusion cells were set up as described in section 8.2.2.1. MCF-7 cells were seeded at a density of 1 x 10^6 cells per diffusion cells on day 0. Flanges of the receptor compartment were greased to ensure no leakage and the receptor compartment was sealed with a sterile cover slip. On day 1 media was removed from the receptor compartment and replenished with fresh, on this occasion the whole receptor compartment was filled. The receptor the compartment was sealed in this circumstance with a 0.22 μm CTEM and a pre-greased donor compartment was clamped into place. A donor phase of 2.54 x

10^{-4} M 4-hydroxytamoxifen, PD98059 and LY294002 in a fish oil vehicle or fish oil alone (control) was applied to the surface of the track-etched membrane. On day 6 cells were trypsinized and counted using the method outlined previously.

8.2.2.5 Composite model

Experimental protocol described in the section 8.2.2.4 was repeated, however, a porcine skin membrane was placed above the CTEM, stratum corneum upward facing. It was ensured that the CTEM was greater in diameter than the porcine skin membrane to restrict passage of microorganisms under the CTEM.

8.2.3 Statistics

One-way ANOVA was used to assess the similarity in cell growth between FDCs. Cell counts were deemed statistically insignificantly different at $P < 0.05$. Un-paired t-tests were used to compare the permeation of PD98059, LY294002, 4-hydroxytamoxifen and EPA through full thickness skin, the CTEM and both skin and CTEM. T-tests were also used to assess the effect of the cocktail formulation on MCF-7 cell growth when cultured in FDCs. P values less than 0.05 were deemed to represent statistically significant results

8.3 Results

8.3.1 MCF-7 cell culture in glass Franz diffusion cells

Figure 8.2 shows cell counts after 7 days of culture in all glass Franz cells. Six diffusion cells were investigated, which gave consistent cell counts between the 6 different diffusion cells and between the 5 repeats (P = 0.870). A P value above 0.05 suggests that no significant difference was seen between cell counts.

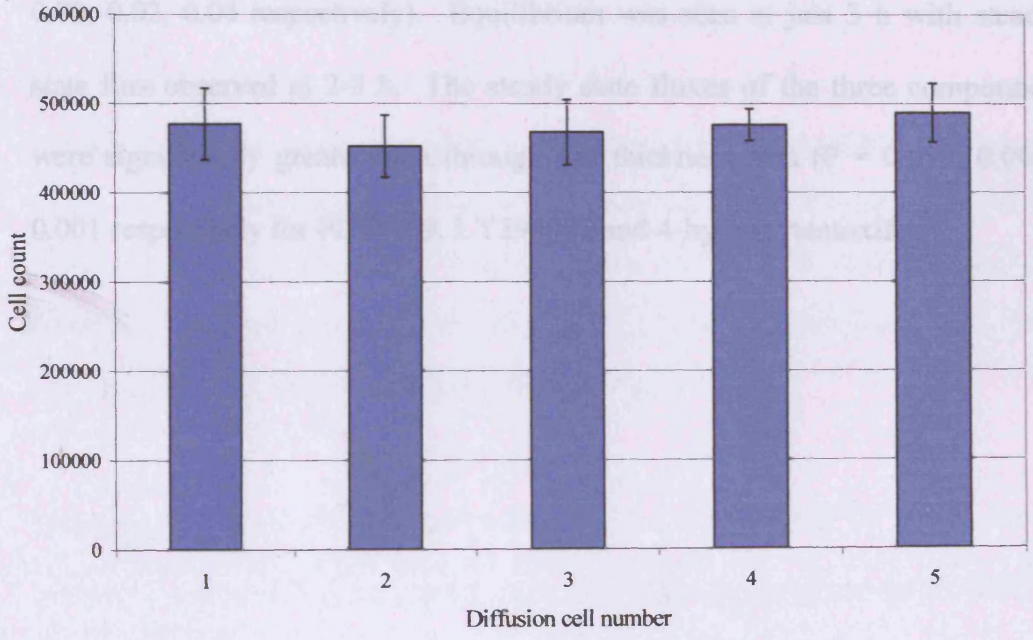

Figure 8.2 Histogram to show diffusion cell MCF-7 counts after 1 week incubation (n=5 ± SD). Passage numbers were 12, 13, 14, 19, 22.

Each diffusion cell allowed a cell count of between 40,000 and 50,000 cells, with no significant difference in cell count between each diffusion cell. Reproducible cell counts meant that any effects on cell growth occurring in

treated diffusion cells could confidently be attributed to the effects of the compounds.

8.3.2 Permeation of 4-hydroxytamoxifen, PD98059 and LY294002 through a 0.22μm cyclopore track etched membrane

Figure 8.3 shows the permeation of all compounds through the CTEM. The CTEMs allowed 0.0167 ± 0.0026, 0.011 ± 0.001 and 0.016 ± 0.0025 mg cm^{-2} of PD98059, LY294002 and 4-hydroxytamoxifen respectively, which was significantly greater than the mass permeating through full thickness skin (P = 0.03, 0.02, 0.04 respectively). Equilibrium was seen at just 3 h with steady state flux observed at 2-3 h. The steady state fluxes of the three compounds were significantly greater than through full thickness skin (P = 0.013, 0.008, 0.001 respectively for PD98059, LY294002 and 4-hydroxytamoxifen).

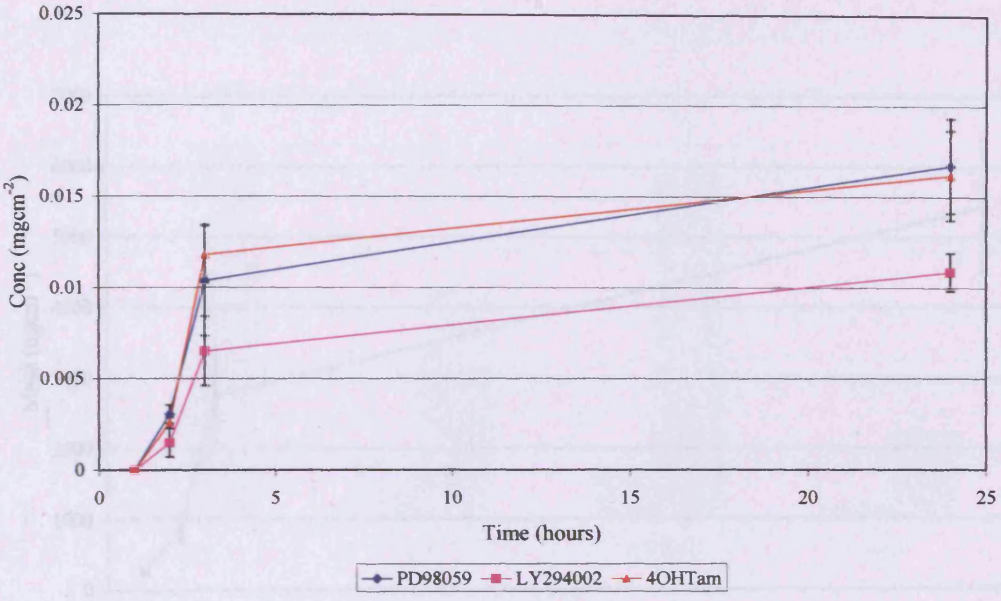

Figure 8.3 Permeation profiles for 4-hydroxytamoxifen, PD98059 and LY294002 through a 0.22µm cyclopore track etched membrane. Diffusion cells were kept in a water bath at 37°C to mimic normal diffusion experiments. Donor phase was 2.54 x 10^{-4} M 4-hydroxytamoxifen, PD98059 and LY294002 in fish oil (plus 0.05 v/v BHA, 2.5% DMSO/ethanol and 4% w/v cab-o-sil). Receptor phase was 30mgml^{-1} cetrimide solution (n=5 ± SD).

These were 7.55 ± 1.72, 5.03 ± 1.4 and 9.225 ± 1.28 µg cm^{-2} h^{-1}. Lag times were 1.53 ± 0.18, 1.7 ± 0.13 and 1.72 ± 0.01 hours respectively for PD98059, LY294002 and 4-hydroxytamoxifen, these were also significantly less than those seen across full thickness skin (P = 0.01, 0.05, 0.05 respectively).

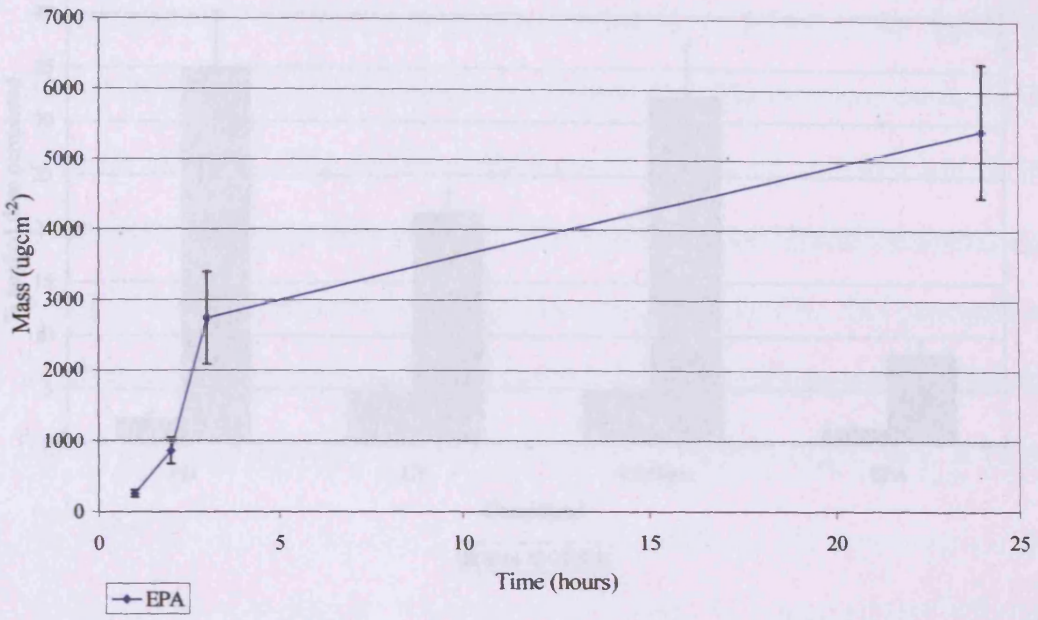

Figure 8.4 Permeation profile for EPA through a 0.22µm cyclopore track etched membrane. Diffusion cells were kept in a water bath at 37°C to mimic normal diffusion experiments. Donor phase was 2.54 $x10^{-4}$ 4-hydroxytamoxifen, PD98059 and LY294002 in fish oil (plus 0.05 v/v BHA, 2.5% DMSO/ethanol and 4% w/v cab-o-sil). Receptor phase was 30mgml^{-1} cetrimide solution (n=5 ± SD).

Figure 8.4 shows the permeation of EPA through the CTEM. The CTEM allowed 5543.494 ± 955.9 µ gcm^{-2} of EPA to permeate after 24 h, which was significantly greater than the mass permeating through excised porcine skin after 24 h (P = 0.016). The steady state flux of EPA through the CTEM was significantly higher also (P = 0.02). This was seen between 2-3 hours and was 1878.75 ± 139.1 µg cm^{-2} h^{-1}. The lag time was 1.54 ± 0.02 hours under these conditions, which was much reduced compared with permeation through skin membranes, however, this was not statistically significant (P = 0.08).

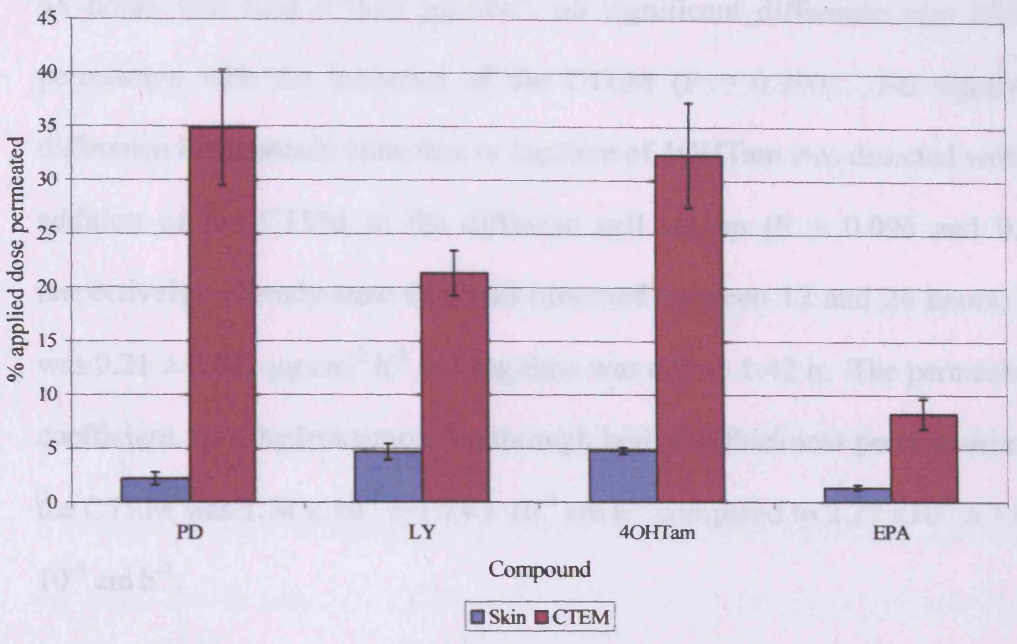

Figure 8.5 Histogram to show the percentage of applied dose permeating after 24 hours, comparing the percentage permeating through skin and the cyclopore track etched membrane.

Figure 8.5 compares the percentage of applied dose permeated of each active of the formulation. It also compares this against the percentage of applied dose permeating full thickness porcine skin. It demonstrates very comprehensibly that permeation through the CTEM was greater than through the porcine skin membranes for each active constituent of the formulation.

8.3.3 Permeation studies through both excised porcine skin and 0.22µm cyclopore track etched membrane

Figure 8.6 shows permeation data for 4-hydroxytamoxifen, PD98059 and LY294002 across both excised porcine skin membrane and the CTEM. The

mass of 4-hydroxytamoxifen that permeated through both skin and CTEM after 48 hours was 6.22 ± 0.29 μg cm^{-2}, no significant difference was seen in permeation with the inclusion of the CTEM (P = 0.990). No significant difference in the steady state flux or lag time of 4OHTam was detected with the addition of the CTEM to the diffusion cell set up (P = 0.096 and 0.169 respectively). Steady-state flux was observed between 12 and 24 hours, flux was 0.21 ± 0.021 μg cm^{-2} h^{-1} and lag time was 6.03 ± 1.42 h. The permeability coefficient for 4-hydroxtamoxifen through both full thickness porcine skin and the CTEM was 1.74 x 10^{-3} ± 1.74 x 10^{-4} cm h^{-1} compared to 2.27 x10^{-3} ± 1.65 x 10^{-4} cm h^{-1}.

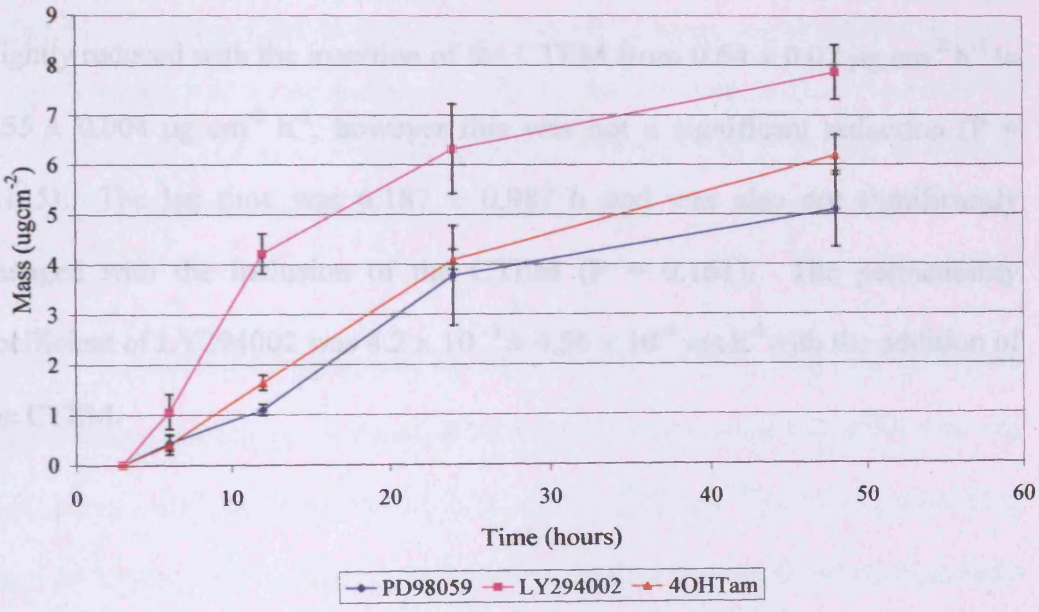

Figure 8.6 Permeation profile for 4-Hydroxytamoxifen, PD98059 and LY294002 through both full thickness excised porcine skin and a 0.22μm cyclopore track etched membrane. Diffusion cells were kept in a water bath at 37°C. Donor phase was 2.54 x10^{-4} 4-hydroxytamoxifen, PD98059 and LY294002 in fish oil (plus 0.05 v/v BHA, 2.5% DMSO/ethanol and 4% w/v cab-o-sil). Receptor phase was 30mgml^{-1} cetrimide solution (n=5 ± SD).

The inclusion of the CTEM to the diffusion cell set up gave no significant effect (P = 0.996) on the mass of PD98059 permeating after 48 hours, this was 5.06 ± 0.74 μg cm^{-2}. The steady state flux of PD98059 was 0.23 ± 0.04 μg$cm^{-2}h^{-1}$ and was observed between 12 and 24 h. It was not significantly altered with the inclusion of the CTEM (P = 0.1115). The lag time of PD98059 was 6.43 ± 1.1 h in the presence of the CTEM, which was not significantly different from the lag time seen when PD98059 was applied to skin only (P = 0.432). The permeability coefficient for PD98059 was 2.16 x 10^{-3} ± 4.1 x 10^{-4} cm h^{-1}.

The mass of LY294002 that permeated both skin and CTEM was 7.89 ± 0.68 μg cm^{-2}, which was not significantly different to the mass permeating full thickness skin without CTEM present (P = 0.316). The flux of LY294002 was slightly reduced with the insertion of the CTEM from 0.64 ± 0.07 μg cm^{-2} h^{-1} to 0.55 ± 0.004 μg cm^{-2} h^{-1}, however this was not a significant reduction (P = 0.115). The lag time was 6.187 ± 0.987 h and was also not significantly changed with the inclusion of the CTEM (P = 0.161). The permeability coefficient of LY294002 was 4.2 x 10^{-3} ± 4.56 x 10^{-4} cm $h^{-1}$with the addition of the CTEM.

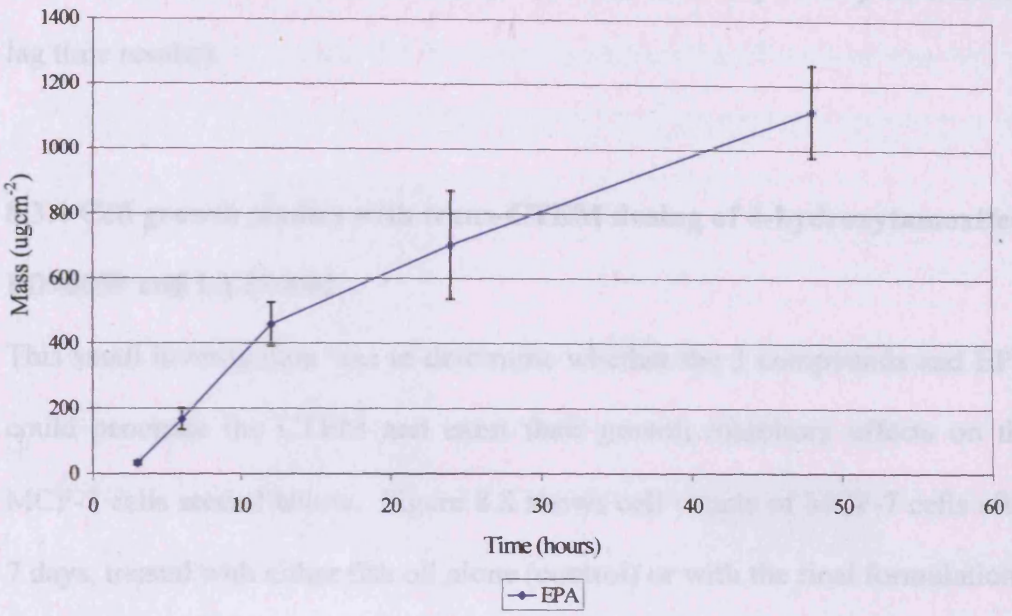

Figure 8.7 Permeation profile for EPA through both full thickness excised porcine skin and a 0.22 µm cyclopore track etched membrane. Diffusion cells were kept in a water bath at 37 °C. Donor phase was 2.54 $x10^{-4}$ 4-hydroxytamoxifen, PD98059 and LY294002 in fish oil. Receptor phase was 30mgml^{-1} cetrimide solution (n=5 ± SD).

Figure 8.7 shows the permeation of EPA through both a skin and cyclopore track etched membrane. It demonstrates that the permeation of EPA was not significantly different with the addition of the CTEM. The mass permeating after 48 h was 1159 ± 168.9µgcm^{-2}, which was not a significant change from the mass permeating through full thickness skin without CTEM present (P = 0789). Steady-state flux of EPA was seen between 3-12 h. The flux was 57.67 ± 10.26 µg cm^{-2} h^{-1} and lag time was 5.83 ± 1.042 hors, with neither of these results showing a significant difference from results obtained for permeation of

EPA through just full thickness skin (P = 05 and 0162 respectively for flux and lag time results).

8.3.4 Cell growth studies with trans-CTEM dosing of 4-hydroxytamoxifen, PD98059 and LY294002

This small investigation was to determine whether the 3 compounds and EPA could penetrate the CTEM and exert their growth inhibitory effects on the MCF-7 cells seeded below. Figure 8.8 shows cell counts of MCF-7 cells after 7 days, treated with either fish oil alone (control) or with the final formulation.

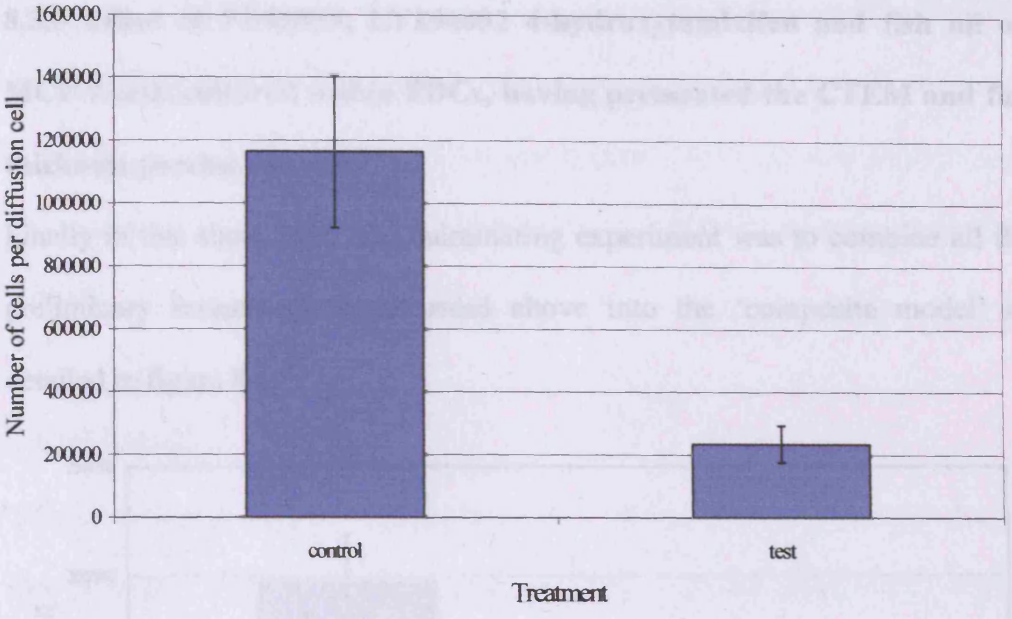

Figure 8.8 Histogram to show the effect of CTEM dosed 4-hydroxytamoxifen, PD98059 and LY294002 on MCF-7 cells seeded in glass diffusion cells. Control formulation consisted of fish oil (plus 2.5% v/v DMSO/ethanol, 0.05% v/v BHA, 4% w/v Cab-o-sil. Test formulation was the same however included 2.54 x 10^{-4} 4-hydroxytamoxifen, PD98059 and LY294002. Receptor phase was wRPMI + 5% v/v SFCS + 1% antibacterial and antifungal. Diffusion cells were maintained in a Diffusion cells were maintained in a Sanyo MCO-17AIC incubator (Sanyo, E&E Europe BV, Loughborough, UK) at 37°C in a humidified atmosphere of 5% CO_2 in air throughout the experiment (n=6 for control and 12 for test ± SD). Passage numbers were 12, 17 and 27.

Figure 8.8 shows that the formulation permeated the CTEM and reduced cell growth significantly to 20.8 ± 5.1 % of control cell growth (P = 0.01. This inhibition in cell growth is less than seen when MCF-7 cells were treated directly with IC_{50} concentrations of the three compounds, which reduced cell growth to 2.6 ± 0.5 % of control.

8.3.5 Effect of PD98059, LY294002 4-hydroxytamixifen and fish oil on MCF-7 cells cultured within FDCs, having permeated the CTEM and full thickness porcine ear skin

Finally in this short study, the culminating experiment was to combine all the preliminary investigations discussed above into the 'composite model' as detailed in figure 8.1.

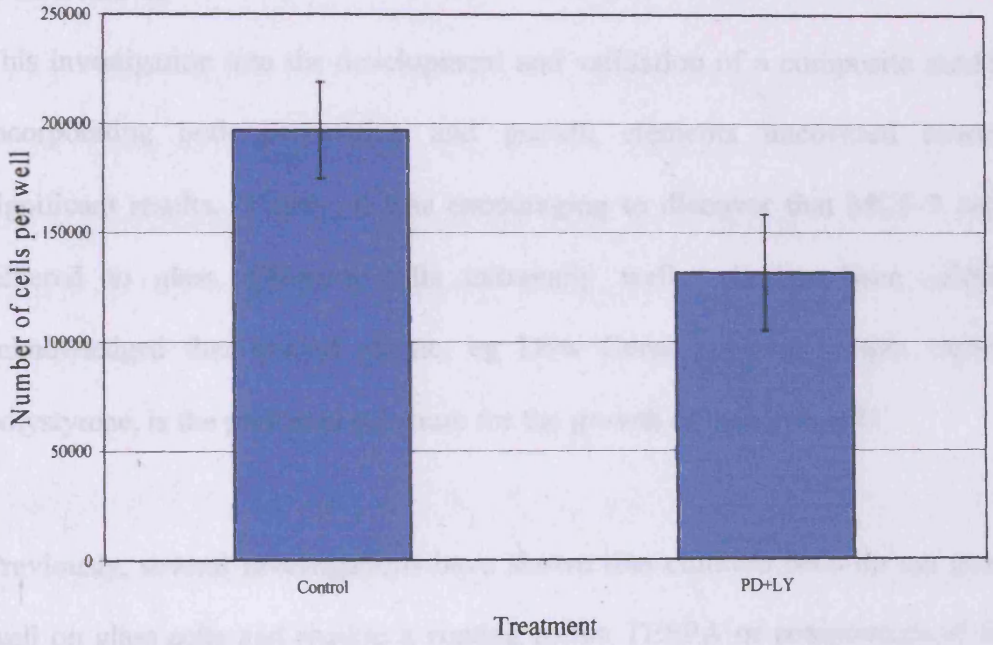

Figure 8.9 Histogram to show the effect of porcine skin and CTEM dosed 4-hydroxytamoxifen, PD98059 and LY294002 on MCF-7 cells seeded in glass diffusion cells. Control formulation consisted of fish oil (plus 2.5% v/v DMSO/ethanol, 0.05% v/v BHA, 4% w/v Cab-o-sil). Test formulation was the same however included 2.54 $x10^{-4}$ 4-hydroxytamoxifen, PD98059 and LY294002. Receptor phase was wRPMI + 5% v/v SFCS + 1% antibacterial and antifungal. Diffusion cells were maintained in a Sanyo MCO-17AIC incubator (Sanyo, E&E Europe BV, Loughborough, UK) at 37°C in a humidified atmosphere of 5% CO_2 in air throughout the experiment (n=6 x 3 for control and 12 x 3 for test ±SD). Passage numbers were Passage numbers were 22, 30 and 35.

Figure 8.9 showed that the test formulation was capable of permeating the skin and significantly inhibiting MCF-7 cell growth to 66.68 ± 13.41 % compared to control growth (P = 0.044). This was a significantly smaller inhibition in cell growth than that seen with IC_{50} concentrations of the three compounds (P = 0.023).

8.4 Discussion

This investigation into the development and validation of a composite model, incorporating both permeation and growth elements uncovered several significant results. Firstly, it was encouraging to discover that MCF-7 cells adhered to glass diffusion cells extremely well. It has been widely acknowledged that treated plastic, eg Dow Corning tissue culture treated polystyrene, is the preferred substrate for the growth of cultured cells.

Previously, several investigations have shown that cultured cells do not grow well on glass cells and require a coating (often TESPA or components of the ECM such as lamanin or fibronectin) for adequate seeding and growth. Ability of cell to adhere to glass is also cell specific. Bovine aortic endothelial cells show good attachment to glass, enabling normal growth of this cell line; however, human umbilical vein epithelial cells attached and grew poorly when the same methodology was followed. These two cell lines both attached and proliferated on plastic surfaces equally well (Grabowski, E. F. & McDonnell, S.L. 1982). It has been suggested that the mechanism of cell attachment to

glass is not a result of interactions between substrate and charged regions of the cell surface, but as a result of interactions with non-polar regions of the cell surface, however, in the presence of serum, electrostatic forces may be responsible for cellular attachment George, J.N *et al* 1970)..Another study suggested that red blood cell attachment to glass was a result of long-range electrostatic repulsive and electrodynamic attractive forces (Tommler, A. *et al* 1985).

A possible explanation for the unexpected cell attachment could be due to the cleaning process with Decon 90, which may have made the inner surfaces of the FDC rough and uneven. It has previously been shown that grit blasted glass equates to better cell attachment than smooth glass surfaces (Banks, B. *et al* 2001).

The flux of all 4 of the active constituents was not hindered by the presence of the CTEM. This was evident from comparing diffusion studies through CTEM alone, skin alone and composite CTEM and skin. The flux of the permeants through the CTEM was significantly greater than across the skin and there was virtually no lag time seen. This is most probably a result of the relative sizes of the drugs being in the nanometre range, while the pore sizes of the CTEM are 0.22μm, suggesting that the pores would offer no resistance to the passage of the compounds and the CTEM was not rate limiting to the permeation of PD98059, LY294002, 4,hydroxytamoxifen or EPA.

Due to the presence of the MCF-7 cells at the bottom of the receptor compartment, the micro magnetic stirrer normally inserted into the receptor compartment to agitate the receptor solution could not be used in this work. Thus an additional barrier, in the form of a stagnant diffusion layer, would have existed at the membrane/receptor solution interface. The average area of the receptor compartment used was 3.2 mL, thus it would be necessary for the permeants to diffuse through this medium prior to interacting with the MCF-7 cells. These stagnant diffusion layers, in some way mimics permeation through sub-skin tissues. Post skin targets would not be subjected to large concentration gradients as seen in standard diffusion experiments caused by the constant agitation of the receptor phase. Instead passive diffusion through the tissue would dominate the route of entry and passage through tissues. The lack of agitation of the receptor phase in these diffusion experiments would reduce the impact of the concentration gradient, especially at lower stagnant diffusion layers of the receptor phase, and so passage of compounds through this media would be by passive diffusion.

Finally, it is acknowledged that dermal clearance will remove some permeating drug, and some skin scientists argue that transcutaneous delivery of compounds is made impossible due to the extent of this phenomenon (Krestos, K. *et al* 2007). This was mimicked, in this chapter, by replenishment of media on day 4 and by daily agitation of the receptor compartment. In spite of this media removal and agitation, sufficient concentrations of compounds were capable of

reaching the under-laying cells and inhibiting their growth significantly (P = 0.044).

8.5 Conclusions

There are two major conclusions from this work. Firstly, MCF-7 breast cancer cells can be successfully cultured directly within glass Franz diffusion cells. Secondly, a composite diffusion cell/ cell culture model can be used to indicate the potential efficacy of topically delivered anti breast cancer therapeutic agents. The model may be considered as an intermediate between *in vitro* and *in vivo* experiments. By combining two separate and time consuming experiments, such a model could be used as a high throughput experiments screen in other transcutaneous drug delivery systems.

Chapter 9

Delivery of PD98059, LY294002 and 4-hydroxytamoxifen via the mammary papilla

9.1 Introduction

Previous chapters have considered the potential of delivering PD98059, LY294002, 4, hydroxytamoxifen and EPA across full thickness porcine skin, and their effects on breast cancer cells having diffused through the multiple layers of the skin. Thereafter, it has been hypothesised that the agents will diffuse further through and pervade the breast tissue providing therapeutic levels *in situ*. The fact that little control can be exerted over the ultimate localisation of the drugs could limit the efficacy of the system. However, an encouraging clinical study was recently published describing the effect of a 4-hydroxy tamoxifen gel on cyclical mastalgia in premenopausal women, where symptoms were found to diminish after 4 months of topical application to the breast (Mansel, R. *et al* 2007).

This chapter is concerned with a somewhat different approach for delivering the aforementioned compounds, involving permeation across the mammary papilla (nipple). To the best of our knowledge, the approach is novel.

The rationale for this study was centralised around the location in which breast cancers originate from. Most breast carcinomas and pre-cancers are believed to originate in the lining of the milk duct or in the lobule (figure 9.1), making such areas the major target for any topical delivery system.

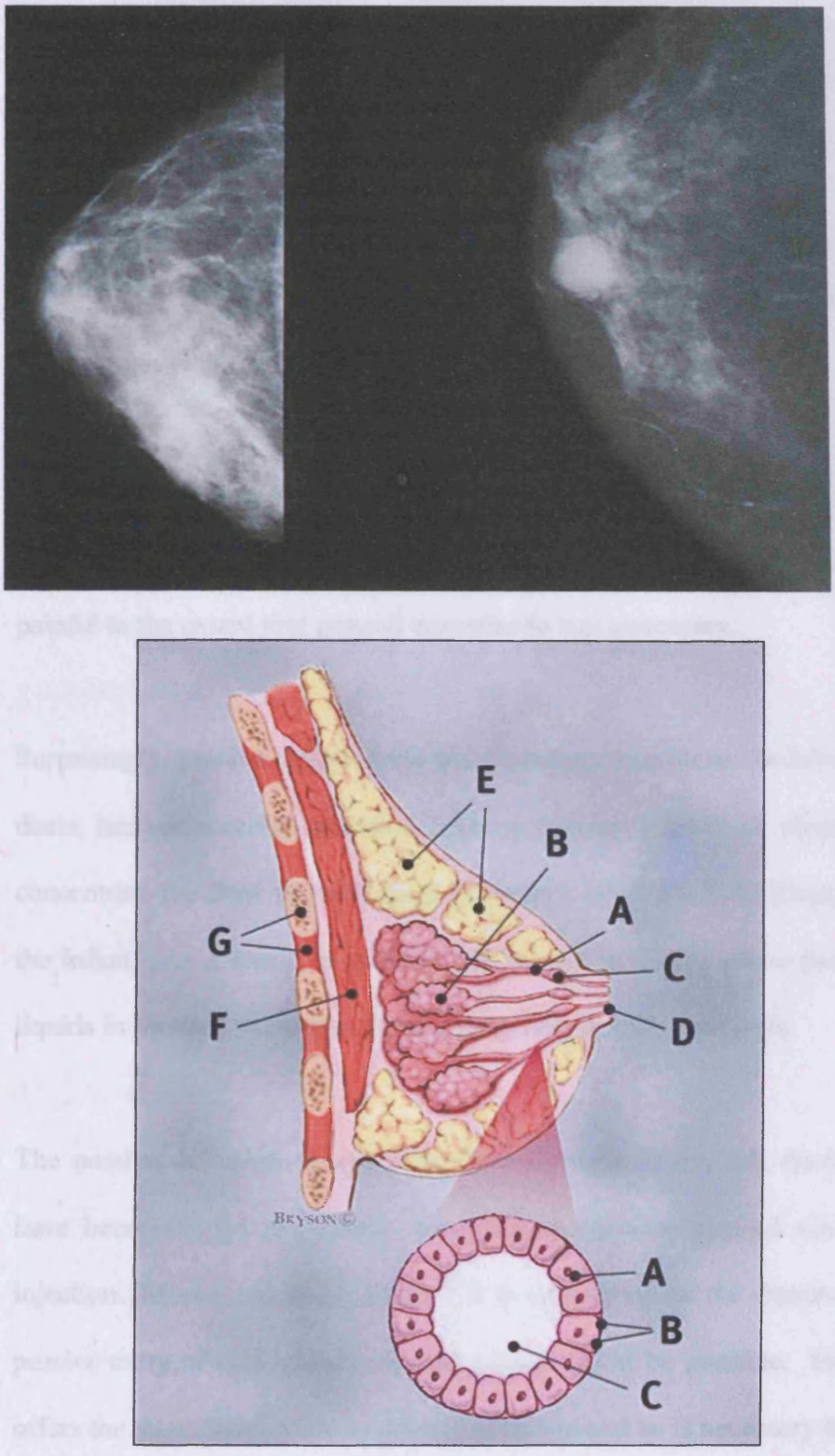

Figure 9.1 Upper: Normal (left) versus cancerous (right) mammography images (National Cancer Institute, http:// history.nih.gov/exhibits/genetics/sect2.htm) Lower: Anatomy of the mammary papilla and breast. A-milk duct, B-lobule, C-dilated section of duct to hold milk, D-nipple, E-fatty tissue, F-pectoralis major muscle, G-chest wall/ribs (www.breastcancer.org).

Until recently direct access to this area has been by core biopsy or fine needle aspiration only (Shen, K.W. *et al* 2000), although the newer techniques of 'ductography' and 'fiberoptic ductoscopy' have been explored and proposed for visualisation in the diagnosis of breast cancer and other diseases of the breast (Yamamoto, D. *et al* 2001).

Ductoscopy has also been investigated for delivering breast cancer treatment to the tumor directly. Although deemed 'minimally invasive' this procedure was painful to the extent that general anaesthesia was necessary.

Surprisingly, passive delivery via the mammary papilla to the lobules, via the ducts, has not received attention. The mammary papilla, or nipple, exists to concentrate the flow of milk from the breast lobules and facilitate transfer to the infant. As a tissue, it is leaky and would in theory allow the transfer of liquids in forward or reverse directions in non-lactating subjects.

The passive diffusion of chemical dyes throughout the full ductal networks have been mapped previously, however, these were applied via intraductal injection (Murata, S. *et al* 2006). It is not stated in the literature whether passive entry of compounds into the nipple would be possible. However this offers the most direct route to the site of action and so is necessary to explore.

9.1.1 Aims

The aim of the work in this chapter was to explore in vivo the potential of delivering the previously developed formulation via the mammary papilla. It was hypothesised that the applied drugs would be capable of passively migrating through the ducts of the breast and be detected by the use of regular Franz diffusion cells.

9.2 Materials and Methods

9.2.1 Materials

Most of the materials used within this chapter were detailed in section 2.1. Strips of porcine sow breasts were obtained from a local abattoir prior to cleansing procedure. These were transported to the lab on ice and maintained in HHBBSS.

9.2.2 Methods

9.2.2.1 Preparation of porcine mammary papilla

Freshly excised strips of porcine mammary papilla were washed in tepid water to remove surface dirt.

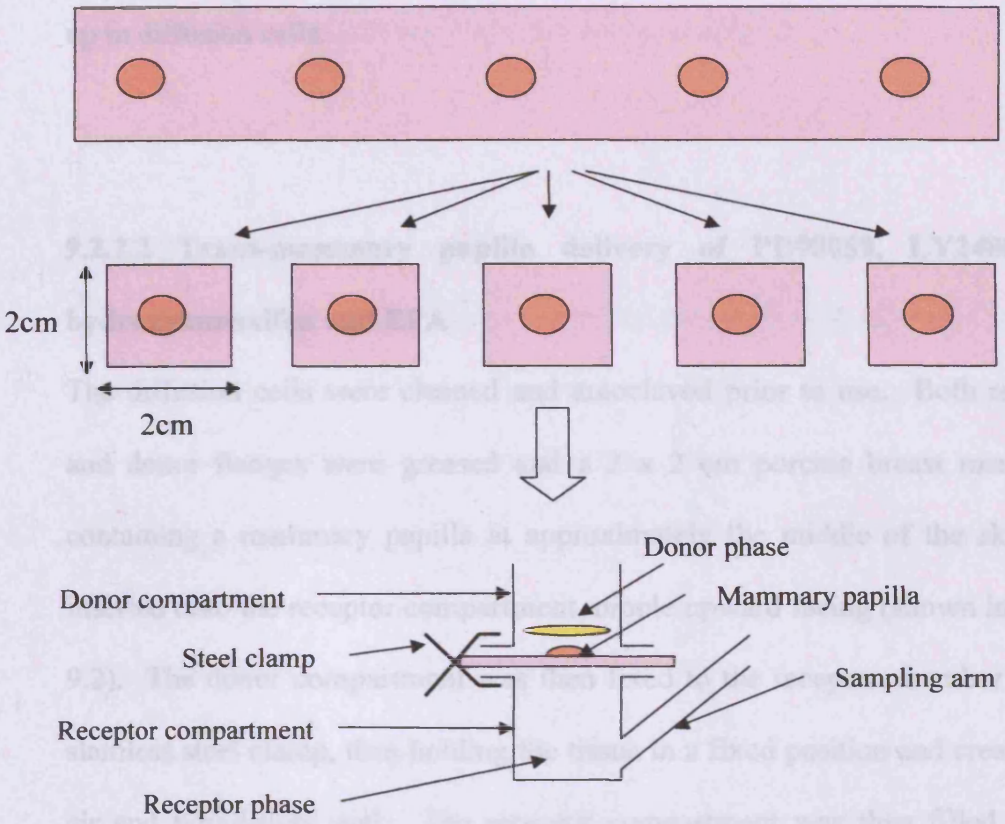

Figure 9.2 Diagram to illustrate the dissection of mammary papilla and their set up in Franz diffusion cells.

Mammary papilli, surrounded by 2 x 2 cm of belly skin, were excised by blunt dissection as illustrated in figure 9.2. Subcutaneous fatty tissue was also removed by blunt dissection and pieces were maintained in HHBBSS until set up in diffusion cells.

9.2.2.2 Trans-mammary papilla delivery of PD98059, LY24002, 4, hydroxytamoxifen and EPA

The diffusion cells were cleaned and autoclaved prior to use. Both receptor and donor flanges were greased and a 2 x 2 cm porcine breast membrane containing a mammary papilla at approximately the middle of the skin was inserted onto the receptor compartment, nipple upward facing (shown in figure 9.2). The donor compartment was then fixed to the receptor chamber with a stainless steel clamp, thus holding the tissue in a fixed position and creating an air and liquid-tight seal. The receptor compartment was then filled with a $30mgml^{-1}$ cetrimide solution (which had previously been degassed), to which, a micro-stirrer bar was then added. The diffusion cells were then placed onto a submersible stirrer plate in a water bath set at 37° C and allowed to equilibrate. After 30 minutes, equimolar concentrations of PD98059, LY294002 and 4, hydroxytamoxifen (2.54×10^{-4} mol) were simultaneously applied to the surface of the skin in 200μL fish oil (containing 0.05% v/v BHA 2.5% DMSO, 2.5% ethanol v/v and 4% Cabosil w/v) as developed in chapter 4. Samples of receptor phase were collected, over a 24 h period.

9.2.2.3 Quantification of amounts of PD98059, LY24002, 4, hydroxytamoxifen and EPA passing through the mammary papilla

HPLC analysis was performed as described in chapter 2.

9.2.3 Statistical analysis

Permeation through the nipple was compared to that through skin via the use of unpaired t-tests. These were conducted on Minitab for Windows. P values of less than 0.05 were deemed as statistically significant.

9.3 Results

9.3.1 Delivery of PD98059, LY24002 and 4-hydroxytamoxifen via the mammary papilla

Figure 9.3 shows the mass of PD98059, LY294002 and 4-hydroxytamoxifen reaching the receptor phase after application to the nipple. This figure shows that saturation was reaches very quickly compared to delivery across skin: after just 5 hours.

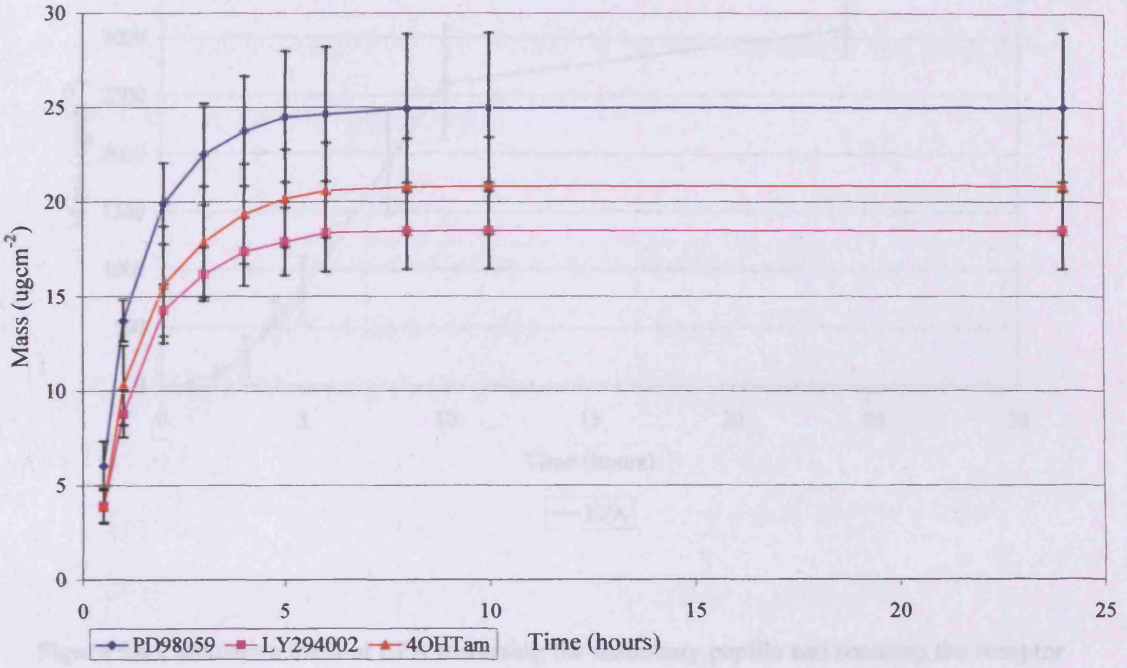

Figure 9.3 Cumulative mass of PD98059, LY294002 and 4, hydroxytamoxifen traversing the mammary papilla and reaching the receptor phase over 24 hour period. Receptor phase was 30mgml-1 cetrimide solution, which was stirred with a micro-stirrer and maintained in a water bath set at 37°C to give a skin surface temperature of 32°C. Donor phase was dosed with 2.54 x 10^{-4}mol PD98059, LY294002 and 4, hydroxytamoxifen in 200µl fish oil with 0.05% BHA 2.5% DMSO and ethanol and 4% Cabosil (n=5 ± SD).

At 5 h, 24.69 ± 3.31, 17.87 ± 2.44, 20.13 ± 2.89 µg cm^{-2} PD98059, LY294002 and 4-hydroxytamoxifen passed into the receptor phase respectively.

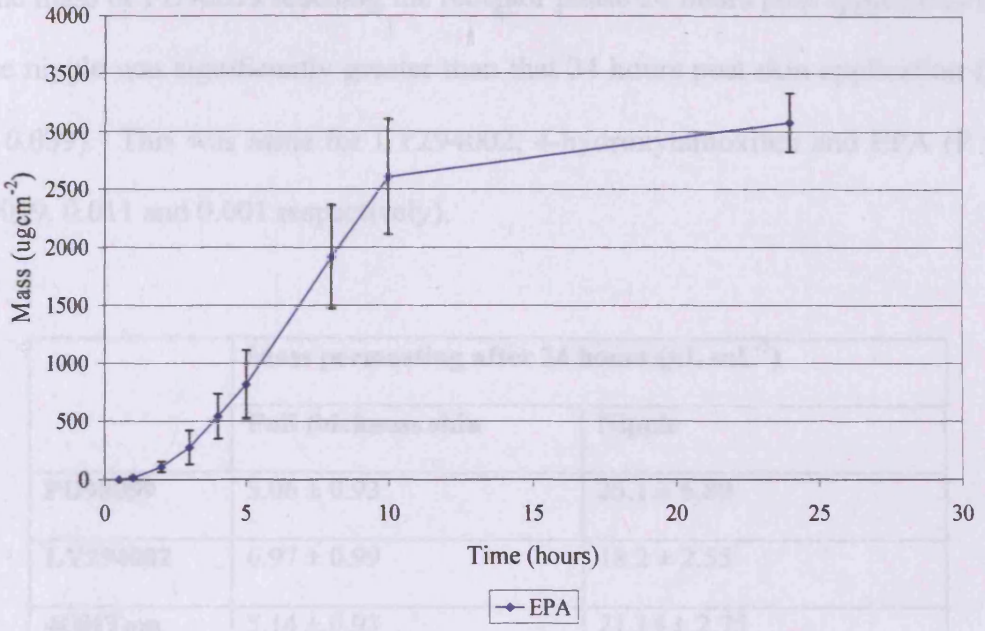

Figure 9.4 Cumulative mass of EPA traversing the mammary papilla and reaching the receptor phase after 24 hours. Receptor phase was 30mgml-1 cetrimide solution, which was stirred with a micro-stirrer and maintained in a water bath set at 37°C to give a skin surface temperature of 32°C. Donor phase was dosed with 2.54 x 10^{-4}mol PD98059, LY294002 and 4, hydroxytamoxifen in 200µl fish oil with 0.05% BHA 2.5% DMSO and ethanol and 4% Cabosil (n=5 ± SD).

Figure 9.4 shows the mass of EPA able to reach the receptor phase also increased compared to delivery across full thickness skin. Saturation was reached at 10 h, when, which was almost exactly half the applied dose of each compound. After 10 h, 2611.4 ± 497.5 µg cm^{-2} EPA passed into the receptor phase. After the 24-hour investigation 3081 ± 252.7 µg cm^{-2} EPA passed into the receptor phase.

The mass of PD98059 reaching the receptor phase 24 hours post application to the nipple was significantly greater than that 24 hours post skin application (P = 0.039). This was same for LY294002, 4-hydroxytamoxifen and EPA (P = 0.019, 0.011 and 0.001 respectively).

	Mass permeating after 24 hours ($\mu L\ mL^{-1}$)	
	Full thickness skin	**Nipple**
PD98059	5.06 ± 0.93	25.1 ± 6.89
LY294002	6.97 ± 0.99	18.2 ± 2.55
4OHTam	5.14 ± 0.93	21.14 ± 2.75
EPA	1121.6 ± 143	3081.2 ± 252.7

Table 9.1 Comparison of the mass of PD98059, LY294002, 4-hydroxytamoxifen and EPA reaching the receptor phase after 24 hours when applied to full thickness skin or to the mammary papilla (nipple). Donor phase was 2.54 x 10^{-4}mol PD98059, LY294002, 4-hydroxytamoxifen in 200µl fish oil plus 0.05% BHA 2.5% v/v DMSO and ethanol with 4% w/v Cabosil. Receptor phase was 30mgml^{-1} cetrimide solution, previously degassed, agitated with a magnetic micro-stirrer and maintained to give a skin surface temperature of 32°C (n=5 ± SD).

Table 9.1 compares the mass of each active constituent of the cocktail reaching the receptor phase after 24 h when dosed onto full thickness skin and onto the nipple. It is obvious that trans-mammary papilla dosing was superior to transcutaneous dosing.

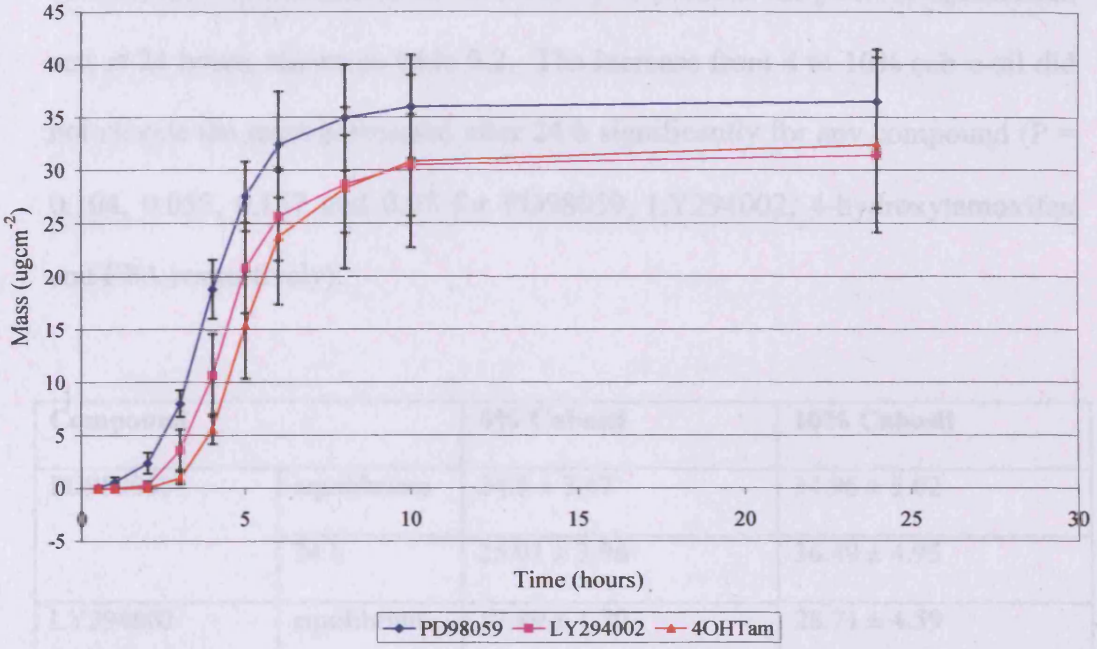

Figure 9.5 Cumulative mass of PD98059, LY294002 and 4, hydroxytamoxifen traversing the mammary papilla and reaching the receptor phase after 24 hours. Receptor phase was 30mgml-1 cetrimide solution, which was stirred with a micro-stirrer and maintained in a water bath set at 37°C to give a skin surface temperature of 32°C. Donor phase was dosed with 2.54 x 10^{-4}mol PD98059, LY294002 and 4, hydroxytamoxifen in 200µl fish oil with 0.05% BHA 2.5% DMSO and ethanol and 10% Cab-o-sil (n=5 ± SD).

Figure 9.5 shows the effect of increasing the weight in volume of cabosil added to the formulation. At 4% cab-o-sil the formulation remained liquid, while increasing the percentage of cab-o-sil to 10% gave a more viscous gel formulation, which remained at the point of application (on the top of the nipple) rather than collecting at the base of the nipple. This increase of cab-o-sil lengthened the time taken to reach equilibrium for PD98059, LY294002 or

4-hydroxytamoxifen from 5 to 8 h and also increased the mass of all 3 compounds that was able to reach the receptor phase at the point of equilibrium and at 24 hours, shown in table 9.2. The increase from 4 to 10% cab-o-sil did not elevate the mass permeated after 24 h significantly for any compound (P = 0.104, 0.055, 0.157 and 0.07 for PD98059, LY294002, 4-hydroxytamoxifen and EPA respectively).

Compound		**4% Cabosil**	**10% Cabosil**
PD989059	equilibrium	24.5 ± 3.47	34.96 ± 5.02
	24 h	25.01 ± 3.96	36.49 ± 4.95
LY294002	equilibrium	17.89 ± 1.79	28.71 ± 4.59
	24 h	18.5 ± 2.1	31.42 ± 5.01
4-hydroxytamoxifen	equilibrium	20.2 ± 2.58	28.35 ± 7.6
	24 h	20.86 ± 2.58	32.4 ± 8.28
EPA	equilibrium	2611.4 ± 497.6	3508 ± 747.2
	24 h	3081.03 ± 252.7	4794 ± 780.4

Table 9.2. The mass of PD98059, LY294002, 4-hydroxytamoxifen and EPA reaching the receptor phase at the point of equilibrium and after 24 hours when applied to the nipple with either 4 or 10 % Cab-o-sil. Donor phase was 2.54 x 10^{-4}mol PD98059, LY294002, 4-hydroxytamoxifen in 200µl fish oil plus 0.05% BHA 2.5% v/v DMSO and ethanol with either 4 or 10% w/v Cab-o-sil. Receptor phase was 30mgml^{-1} cetrimide solution, previously degassed, agitated with a magnetic micro-stirrer and maintained to give a skin surface temperature of 32°C. (n=5 ± SD).

Figure 9.6 shows the mass of EPA able to reach the receptor phase when applied to the mammary papilla when formulated with 10 % cab-o-sil. Figures 9.4 and 9.6 show that the mass of EPA able to reach the receptor phase after 24 hours was increased when fish oil was thickened with 10 % w/v cab-o-sil compared to with 4 % w/v Cab-o-sil, as highlighted in table 9.2.

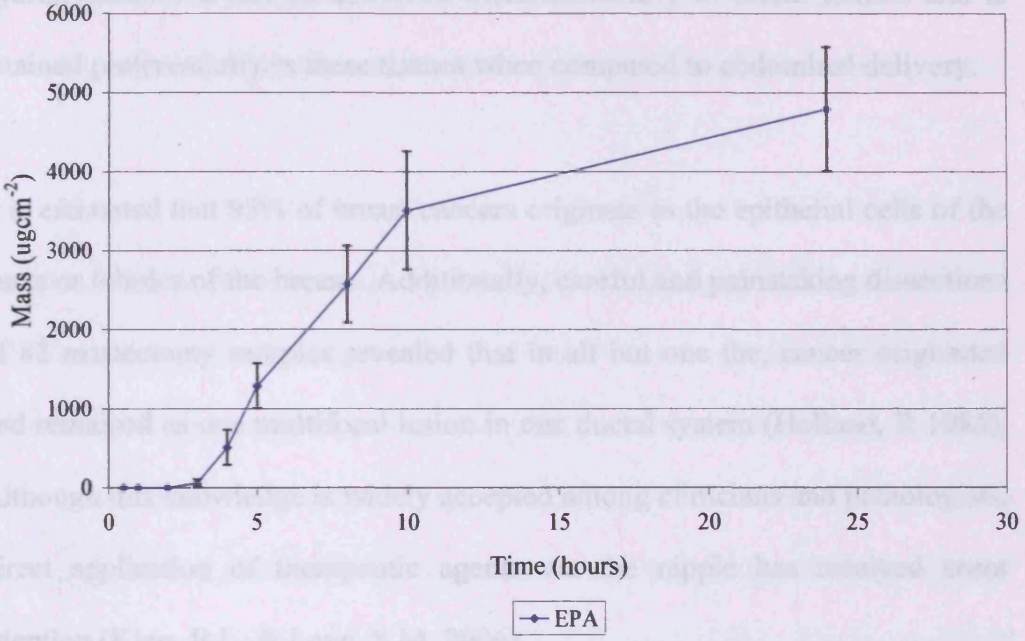

Figure 9.6 Cumulative mass of EPA traversing the mammary papilla and reaching the receptor phase after 24 hours. Receptor phase was 30mgml-1 cetrimide solution, which was stirred with a micro-stirrer and maintained in a water bath set at 37°C to give a skin surface temperature of 32°C. Donor phase was dosed with 2.54mol PD98059, LY294002 and 4, hydroxytamoxifen in 200µl fish oil with 2.5% DMSO and ethanol and 10% Cabosil (n=5 ±stdev).

Equilibrium of EPA between donor and receptor phase may not have been reached in the 24-hour investigation; however, the diffusion of EPA slows after 10 h.

9.4 Discussion

This short study has demonstrated the possibility of passively delivering anti-breast cancer agents via the nipple. As discussed in previous chapters, breast cancer therapies are predominantly delivered orally or by i.v. injections. This method has been relied upon for many years and only recently has the idea of localised delivery received attention. Several studies have shown that 4-hydroxytamoxifen can be delivered transcutaneously to breast tumors and is retained preferentially in these tissues when compared to abdominal delivery.

It is estimated that 95% of breast cancers originate in the epithelial cells of the ducts or lobules of the breast. Additionally, careful and painstaking dissections of 82 mastectomy samples revealed that in all but one the, cancer originated and remained as one multifocal lesion in one ductal system (Holland, R 1985). Although this knowledge is widely accepted among clinicians and pathologists, direct application of therapeutic agents via the nipple has received scant attention (King, B.L. & Love, S.M. 2006).

However the development of ductoscopy and intraductal injection by nipple block and cannulation have lead to a surge of interest in this area and more recent studies have sought to explore the validity of delivering anti-breast cancer agents directly to the site of action via the mammary papilla (nipple). These studies involved intraductal injections, which required hospital day visits, however proved to have favourable effects to i.v or oral treatments. Murata, S. and colleagues (2006) demonstrated that an intraductal injection of

crystal violet was capable of reaching all parts of the mammary gland including the terminal end buds, in which the majority of cancers originate. They also showed that intraductal injection of either 4-hydroxytamoxifen or pegylated liposomal doxorubicin (PLD) was as effective at preventing N-methyl-N'-nitrosourea induced mammary tumorogenesis in the rat as systemically administered tamoxifen. They also showed that intraductal administration resulted in lower circulating levels of PLD when compared to i.v. administration and furthermore, resulted in no systemic or mammary gland toxicity.

Another study explored the plausibility of delivering adenovirus vectors for the delivery of genes via the nipple. The study showed that intraductal injection of the adenovirus vector gave transduction efficiency in epithelial cells of the duct that varied from 7-25% and failed to evoke an inflammatory response. Although the study did not explore gene delivery, it highlighted the possibility of delivering genes in this manner (Russell, T.D. *et al* 2003). The treatment of DCIS or LCIS by intraductal injection has one major flaw. The nipple presents with, on average, 5-9 ductal orifices (Love, S. & Barsky, S.H. 2004). Before treatment can begin the correct ductal orifice must be found, which drains the affected ductal canal. This may be obvious in a minority of cases due to spontaneous discharge that localises the affected duct but in most cases it is impossible to guess and so ductoscopy must be performed beforehand (Murata, S. 2006).

The passive delivery of compounds through the ductal components of the breast has not been explored within the literature. It has been accepted that because nipple discharge and milk secretion occurs in the opposite direction, the passive ingress of compounds from the outside down the ducts to the lobules would not be viable and therefore this route of administration has been dismissed. This short study has illustrated that this dismissal may have been too hasty, but may be restricted to non-lactating individuals.

The study by Rząsa, A. in 2005 stated that the anatomy of the porcine sow mammary gland compares adequately to that of the human mammary gland (Rząsa, A. *et al* 2005). The mammary gland of a lactating sow has a short *ductus papilares* canal that extends between 3-4mm. There are 9-14 big and 6-10 small lactiferous ducts that branch from this canal, which in turn branch into numerous smaller ducts and terminate as intra-lobular ducts (Rząsa, A. *et al* 2005, Frandson, R.D. *et al* 2003).

The cocktail treatment of PD98059, LY294002 and 4-hydroxytamoxifen in fish oil plus 2.5 % v/v DMSO/etOH and 4 % w/v cab-o-sil was capable of delivering 6.92 ± 0.55, 9.17 ± 0.77, 8.25 ± 0.36 and 1420.12 ±119 μg cm^{-2} PD98059, LY294002, 4-hydroxytamoxifen and EPA respectively across full thickness porcine skin after 48 hours, which was vastly less than was delivered across the nipple in a formulation containing 10% cab-o-sil after 24 h, as shown in table 9.1.

The formulation containing 10% cab-o-sil did not hinder the delivery of EPA through the nipple. However at percentages over 4% had a retarding effect on the permeation of EPA across full thickness skin (Philpot, I. *et al* manuscript in preparation). This could be explained by the lack of barrier properties in the nipple compared to the many barriers presented in the skin. This in turn suggests whole formulation; including cab-o-sil migrated into the nipple. The safety of cab-o-sil has been determined in chapter 4, and the fact that it is used to thicken food such as tomato ketchup suggests that the ingress of cab-o-sil into the nipple would raise no adverse toxicological action, however much more extensive safety screening would be required.

The ease of permeation from the nipple surface into the receptor phase suggests that this route of administration may be superior to classical routes; however, several issues must be assessed beforehand.

Firstly, the formulation was capable of passing down the major and larger ducts relatively well; however it was impossible, in this study, to map the exact route of the compounds throughout the breast. For adequate treatment a sufficient dose must reach the desired duct or lobule, for example, the tumor may reside in a major duct or may be in a narrow duct or lobule toward the base of the breast and so it would be important to measure the levels of drugs able to reach these narrow ducts that branch from the main duct.

Secondly, this study has shown adequate passage of compound from the nipple surface, through to the receptor phase. However, this study used excised breasts that were dosed facing upwards. In the human, the nipple is verticle, which may reduce to passage of compounds through the breast structure. This may mean that the patient would need to lie flat upon application and remain there for up to 5 hours.

Further work could involve dosing the nipple with a biological dye to map its passage through the breast. Also the nipple could be dosed with compounds and after set times, the breast dissected and ICC employed to detect p-MAPK, p-Akt, ER and COX-2 throughout the breast structure.

Passive passage throughout the ductal network within the breast is only part of the picture, as the mass of drug able to partition into the inner epithelial lining of the ducts would need to be calculated.

9.5 Conclusions

This study confirmed that all 4 actives of the formulation developed in chapters 3 and 4 could be delivered successfully and high concentrations by this route and overcome the normal direction of milk secretion and discharge. Additionally, the delivery via this route surpassed the concentrations of the 4 compounds that could be delivered transcutaneously.

Work in chapter 4 showed that EPA was not released from Cab-o-sil formulations above 4% w/v. This study shows that EPA was detected in the receptor phase when formulated at 10% Cab-o-sil, suggesting that the formulation penetrated the mammary papilla as a whole.

Chapter 10

General Discussion

10. General Discussion

10.1 Overview

Breast cancer is the most common female malignancy in the western world. Each year in the UK in excess of 44, 000 women and 300 men are diagnosed with breast cancer (www.cancerresearchuk) and incidence rates are increasing each year. Tamoxifen remains the therapy of choice in patients with ER+ breast cancer. However, new insights into the biology of ER+ breast cancer and the long-term genetic implications of tamoxifen treatment have highlighted key concerns among cancer and endocrine biologists.

The biology of endocrine resistance is poorly understood and complex to even the competent endocrinologist. Many mechanisms of anti-hormone resistance have been proposed including loss of or mutation of ERα, lack of progesterone receptor expression, increased ERβ and elevated growth factor signalling. The clinical extrapolation of some of these mechanisms lacks evidence, however, high homology between *in vitro* models of endocrine resistance and clinical observations exist in regards to the involvement of growth factor signalling. The increase in growth factor signalling is thought to arise from the effect of tamoxifen on AF-1 mediated gene transcription.

Inappropriate involvement of growth factor signal transduction pathways have now been accepted as mechanisms of acquired anti-hormone resistance. Their increased involvement can occur via a number of methods; activation of target receptors, an increased supply of growth factor ligands or an increased

activation of downstream mediators. Epidermal growth factor receptor expression is often increased in endocrine resistance, which is paralleled in the clinical setting. However, the targeted and specific inhibition of EGFR has shown disappointing results both in vitro and in vivo, with resistance to anti-EGFR agents developing in a matter of months. Furthermore, expression of EGFR does not confer to therapeutic response to anti-EGFR challenge. These data revealed that the complexity of EGFR signalling was greatly underestimated. Only recently has it been discovered that cross talk between a diverse array of growth signalling pathways exists which renders cancer cell extremely adaptable in regards to cell growth and survival. Upon blockade of one growth pathway, cancer cells possess the intrinsic ability to switch to and utilise alternative pathways in order to evade growth inhibition (Jones, H.E. *et al* 2006).

10.2 Aims of the thesis

The aims of this thesis were to develop a transcutaneous breast cancer therapeutic and evaluate its effects on breast cancer cells. This formulation was hoped to overcome hypothesized adverse effects of oral administration and prevent or delay resistance, seen both clinically and *in vitro*, with tamoxifen treatment.

10.3 Transcutaneous formulation Development

The first issue to be addressed was the compounds to include in this cocktail therapeutic. Two downstream pathways of EGFR and IGFR signalling were

targeted due to their role in resistant growth. These were the PI3K and MAPK pathways. Inhibitors of these pathways were investigated for their skin penetrating capabilities. LY294002, a widely explored PI3K inhibitor and PD98059, a MAPK inhibitor often used as a scientific tool to block ERK1/2 signalling gave superior skin permeation profiles compared to other inhibitors of these pathways and so were taken forward to develop, along with tamoxifen, in to a transcutaneous gel or patch.

Formulation choice is fundamental to both maximising penetration and clinical safety and toxicology. Preliminary permeation studies used DMSO as vehicle, which has received a great deal of press regarding its permeation enhancement of a wide array of compounds. As a skin scientist, this is one, but not all criteria of a high-quality transcutaneous vehicle. Delving deeper into the effects of DMSO lead to concerns on the subject of toxicity, which were visualised in immunohisto- and immunocytochemical analysis of DMSO treated porcine skin. At concentrations exceeding 60% DMSO is proposed to give irreversible SC and keratinocyte toxicity (Williams, A.C. 2003). It advocates these events by removing SC lipids and keratinocyte cell membrane lipid. Concentrations below 60% are deemed 'safe' and proposed as reversible effects; however, modulation of SC function and keratinocyte viability by such a severe mechanism suggests that clinically acceptable formulations would not permit the inclusion of this solvent even at percentages < 60%.

Chapter 4 investigated fish oil as a replacement vehicle and initial IHC and ICC analysis revealed a far superior toxicological profile with no SC or keratinocyte damage and maintenance of viability up to 12 hours. This chapter also highlighted, again, that formulation choice radically effects extent of permeation, luckily the permeation of all 4 components of the therapeutic were enhanced to the greatest extent by the addition of DMSO/ethanol.

10.3 The effects of the cocktail formulation on post skin targets

Once an optimal formulation was found, it was necessary to evaluate the post skin effects of the formulation. Results throughout chapters 5 and 6 looked at the effects of PD98059, LY294002, 4-hydroxytamoxifen and fish oil the growth of hormone sensitive (MCF-7) and tamoxifen resistant (TamR) cells. The expression of ER, pAkt, pERK1/2, EGFR, COX-2, and Src was also described. The effect of fish oil and fish oil plus PD98059 and LY294002 on the migratory potential of TamR cells was also determined.

10.4.1 PI3K and MAPK signalling

PI3K and MAPK signalling have been shown to be important in cell proliferation, avoidance of apoptosis and in metastasis. The cocktail formulation was capable of decreasing the expression of pAkt and pERK1/2 in both MCF-7 and TamR cells, which have previously been shown to give rise to anti-tumor effects. It was also capable of inhibiting MCF-7 and TamR cell growth significantly. The cocktail therapeutic also showed anti-metastatic potential.

10.4.2 Cyclooxgenase signalling

COX-2 overexpression is often seen in breast cancer, and has been linked to increased metastatic potential. COX-2 expression has also been shown to be sufficient to induce tumorogenesis in mice. It is suggested that it is the accumulation of PGE_2 that gives rise to the tumorogenic actions of COX-2, with crosstalk between COX-2/ PGE_2/EGFR/Src giving rise to pro-metastatic effects.

10.5 Suggested future work

This thesis has generated several exciting results, several of which could be expanded on and developed.

Many tyrosine kinase inhibitors, which target growth factor signalling pathways, are small molecules and so may also be candidates for transcutaneous delivery. These include Gefitinib (EGFR inhibitor) and Axitinib (VEGFR inhibitor). These two inhibitors are around 400KDa, making them suitable candidates for topical drug delivery.

Other dominant pathways involved in resistant growth centralise around such mediators as NFκB and IGF-IR. It would be extremely interesting to explore the potential of delivering inhibitors of these, both individually and simultaneously with various constituents of the cocktail already developed.

Although porcine skin shows good homology to human skin, it is not ideal to use *in vitro* models for permeation studies. It would be advantageous to use *in vivo* models, either animal or human, to explore the post skin transport of the delivered compounds. A study mapping the transport of radiolabelled 4-hydroxytamoxifen has already been conducted, where it was showed that the compound had a significantly greater half-life in breast tissue, compared to when dosed to the abdomen (Mauvis-Jarvis, P. *et al* 1986).

The results obtained from chapters 7 and 8, detailing the development of a composite model, highlight an interesting possibility to develop a high-throughput assay for candidate transcutaneous breast cancer therapeutics, and serves as a proof of principle for this. It could possibly save the researcher weeks of investigation, which is extremely valuable in cancer therapeutics research and development.

Finally, maybe the most exciting results came from the shortest study conducted. Chapter 9 investigated the credibility of delivering the aforementioned cocktail therapeutic via the mammary papilla (nipple). Although the gross anatomy of the sow mammary gland may differfrom human, this chapter saw up to a 7-fold increase in the penetration of the actives of the formulation when delivered trans-mammary papilla rather than across skin. Furthermore, the compounds would be delivered to the site of action, without need of diffusing through several millimetres of tissue. These results warrant further examination of this delivery route, with particular emphasis on

delivery through human, *ex-vivo*, tissue. It would also be critical to pin point the route of drug passage through the complex ductal network, to ensure homogenous spread of the compound is attainable.

If possible, it would ideal to analyse a cohort of mastectomy tissue, where the cancerous lesion could be subjected to core biopsy. This could then be assayed for the expression of mediators such as pAkt, pERK, EGFR, IGFR. This tissue would the be subjected to the cocktail therapeutic via the mammary papilla and subsequently re-analysed to detect and visualise any effects on the expression of such mediators within the ductal network.

10.6 Conclusions

This transcutaneous cocktail anti-breast cancer therapeutic shows promising skin permeating properties, with permeating concentrations capable of diffusing through stagnant diffusion layers and inhibiting under-laying MCF-7 cells. It serves as a prototype topical therapy that may be modified or developed further and suggests that a patch or gel formulation may be useful as an adjuvant to surgery or as a chemopreventative device.

Bibliography

A Karim, S.S., Zulfahar, H. & Heard, C.M. (2008) Probing the penetration enhancement of caffine by oleic acid and influence of receptor phase in the *in vitro* percutaneous absorbtion of oleic acid. Welsh School of Pharmacy, MPharm Abstract; 1.

Adeyinka, A., Nui, Y., Cherlet, T., Snell, L., Watson, P.H. & Murphy, L.C. (2002). Human breast tumorigenesis and breast cancer progression (1). Clinical Cancer Research; 8:1747-1753.

Alessi, D.R., Cuenda, A., Cohen, P., Dudley, D.T., Saltiel, A.R. (1995) PD 98059 is a specific inhibitor of the activation of mitogen-activated protein kinase kinase in vitro and in vivo. Journal of Biological Chemistry, 270: 27489-27494.

Ali, S. & Coombes, R.C. (2002) Endocrine-responsive breast cancer and strategies for combating resistance. National Review of Cancer, 2;101-112.

Anigbogu, A.N.C., Williams, A.C., Barry, B.W. & Edwards, H.G.M. (1995) Fourier transform Raman spectroscopy of interactions between the penetration enhancer dimethyl sulfoxide and human stratum corneum. International Journal of Pharmaceutics, 125: 625-682.

Arboleda, M.J., Lyons, J.F., Kabbinavar, F.F., Bray, M.R., Snow, B.E., Ayala, R., Danino, M., Karlan, B.Y. & Slamon, D. (2003) Overexpression of AKT/protein kiase Bβ leads to upregulation of β1 integrins, increased invasion and metastasis of human breast and ovarian cancer cells. Cancer Research, 63: 196-206.

Atalay, G., Cardoso, F., Awada, A. & Piccart, M.J. (2003) Novel therapeutic strategies targeting the epidermal growth factor receptor (EGFR) family and its downstream effectors in breast cancer. Annals of Oncology, 14; 1346–1363.

Atkins, C.M., Selcher, J.C., Petraitis, J.J., Trzaskos, J.M., Sweatt, J.D. (1998). The MAPK cascade is required for mammalian associative learning.
Nature Neuroscience, 1: 602-609.

Banks, B., Miller, S. & deGroh, K. (2001) The development of surface roughness and implications for cellular attachment in biomedical applications. National Aeronautics and Space Administration Fall Meeting, 1-7.

Barker, J.N.W.N., Mitra, R.S., Griffiths, C.E.M., Dixit, V.M. & Nickoloff, B.J. (1991) Keratinocytes as initiators of inflammation. The Lancet, 337: 211-214.

Barkhem, T., Carlsson, B., Nilsson, Y., Enmark, E., Gustafsson, J. & Nilsson, S. (1998). Differential response of estrogen receptor alpha and estrogen receptor beta to partial estrogen agonists/antagonists. Molecular Pharmacology, 54; 105–12.

Baselga, J. (2002) Why the Epidermal Growth Factor Receptor? The Rationale for Cancer Therapy. Oncologist, 7; 2 - 8.

Beatson, G.T. (1898) On the treatment of inoperable cases of carcinoma of the mammary. Suggestions for a new method of treatment with illustrative cases. Lancet,2;104-107.

Bedogni, B, O'Neill, M.S., Welford, S.M., Bouley, D.M., Giaccia, A.J., Denko, N.C. & Broome Powell, M. (2004) Topical treatment with inhibitors of the phosphatidylinositol 3-kinase/Akt and Raf/mitogen-activated protein kinase kinase/extracellular signal-regulated kinase pathways reduces melanoma development in severe combined immunodeficient mice. Cancer Research, 64: 2552-2560.

Berditchevski, F., Chang, S., Bodotova, J. & Helmer, M.E. (1997) Generation of monoclonal antibodies to integrin –associated proteins. Journal of Biological Chemistry, 272: 29174-29180.

Björnström, L. & Sjöberg, M. (2006) Mechanisms of estrogen receptor signaling: convergence of genomic and nongenomic actions on target genes. Molecular Endocrinology, 19 :833–842.

Boggon, T.J. & & Eck, M.J. (2004) Structure and regulation of Src family kinases. Oncogene,23; 7918-7927.

Bonina, F., Lanza, M., Montenegro, L., Puglisi, C., Tomaino, A., Trombetta, D., Castelli, F. & Saija, A. (1996). Flavonoids as potential protective agents against photo-oxidative skin damage. International Journal of Pharmaceutics, 145: 87–94.

Borgna, J-L. & Rochefort, H. (1981) Hydroxylated metabolites of tamoxifen are formed *in Vivo* and bound to estrogen receptor in target tissues. The Journal of Biological Chemistry, 256; 859-868.

Börsch-Haubold, A.G., Pasquet, S. & Watson, S.P. (1998) Direct inhibition of cyclooxygenase-1 and –2 by the kinase inhibitors SB 203580 and PD 98059. The journal of Biological Chemistry, 273: 28766-28772.

Bronaugh, R.L., Stewart, R.F., Congdon, E. & Giles Jr., A.L. (1982) Methods for in vitro percutaneous studies I. Comparison with in vivo results. Toxicology and Applied Pharmacology, 62; 474-480.

Brown, D.A. & London, E. (1998) Structure and origin of ordered lipid domains in biological membranes. Journal of Membrane Biology, 164; 103-14.

Brunton, V. G., Avizienyte, E., Fincham, V. J., Serrels, B., Metcalf, C. A., Sawyer, T. K., & Frame, M. C. (2005) Cancer Research, 65: 1335–1342

Buchanan, F.G., Wang, D., Bargiacchi, F. & DuBois, R. (2003) Prostaglandin E2 regulates cell migration via the intracellular activation of the epidermal growth factor receptor. The Journal of Biological Chemistry, 278: 35451-35457.

Bugaj, A., Iani,V., Juzeniene, A., Juzenas, P., Ma, L-W. & Moan, J. (2006) The effect of dimethylsulfoxide, 1-[2-(decylthio)ethyl]azacyclopentan-2-one and Labrafac®CC on porphyrin formation in normal mouse skin during topical application of methyl 5-aminolevulinate: A fluorescence and extraction study. Photodiagnosis and Photodynamic Therapy, 3; 27-33.

Calviello, G., Di Nicuolo, F., Gragnoli, S., Piccioni, E., Serini, S., Maggiano, N., Tringali, G., Navarra, P., Ranelletti, F.O. & Palozza, P. (2004) n-3 PUFAs reduce VEGF expression in human colon cancer cells modulating the COX-2/PGE_2 induced ERK-1 and -2 and HIF-1α induction pathway. Carcinogenesis, 25; 2303 - 2310.

Campbell, R.A., Bhat-Nakshatri, P., Patel, N.M., Constantinidou, D., Ali, S. & Nakshatri, H. (2001) Phosphatidylinositol 3-Kinase/AKT-mediated activation of estrogen receptor α. A NEW MODEL FOR ANTI-ESTROGEN RESISTANCE. The Journal of Biological Chemistry, 276; 9817-9824.

Casagrande, R., Georgetti, S.R., Verri, W.A., Borin, M.F., Lopez, R.F.V. & Fonseca, M.J.V. (2007) *In vitro* evaluation of quercetin cutaneous absorption from topical formulations and its functional stability by antioxidant activity. International Journal of Pharmaceutics, 328 183–190.

Chandrasekharan, N.V., Dai, H. & Roos K.L. (2002) COX-3, a cyclooxygenase-1 variant inhibited by acetaminophen and other analgesic/antipyretic drugs: cloning, structure and expression. Proceedings of the National Academy of Science in the United States of America, 99: 13926-13931.

Chang,L. & Karin, M. (2001) Mammalian MAP kinase signalling cascades. Nature, 410; 37-40.

Chapkin, R.S., Ziboh, V.A. & McCullough, J.L. (1987) Dietary influences of evening primrose and fish oil on essential fatty acid-deficient guinea pigs. The American Journal of Nutrition, 117: 1360-1370.

Charalambopoulou, G.C., Steriotis, T.A., Hauss, T., Stubos, A.K. & Kanellopoulos, N.K. (2004). Structural alterations of fully hydrated human stratum corneum. Physica B; 350: 603-606.

Chin, G. & Yeston, J. (2007) More than skin deep. Applied Phyiology Letters, 91; 171906.

Choi, K-C., Auersperg, N. & Leung, P. (2003). Mitogen-activated protein kinase I normal and (pre)neoplastic ovarian surface epithelium. Reproductive biology and endocrinology; 1:71-79.

Costa, C., Soares, R., Reis-Filho, J.S., Leitão, D., Amendoeira, I. & Scmitt, F.C. (2002) Cyclo-oxygenase 2 expression is associated with angiogenesis and lymph node metastasis in human breast cancer. The Journal of Clinical Pathology, 55; 429-434.

Cross, S.E., Anissimov, Y.G., Magnusson, B.M. & Roberts, M.S. (2003) Bovine-serum-albumin-containing receptor phase better predicts transdermal absorption parameters for lipophilic compounds. The Journal of Investigative Dermatology, 120; 589-591.

Cui, Y., Parra, I., Zhang, M., Hilsenbeck, S.G., Tsimelzon, A., Furukawa, T., Horii, A., Zhang, Z-Y., Nicholson, R.I. & Fuqua, S.A.W. (2006) Elevated expression of mitogen-activated protein kinase phosphatase 3 in breast tumors: a mechanism of tamoxifen resistance. Cancer Research, 66; 5950-5959.

Cunnick, G.H., Jiang, W.J., Douglas-Jones, T., Watkins, G., Gomez, K.F., Morgan, M.J., Subramanian, A., Mokbel, K. & Mansel, R.E. (2008). Lymphangiogenesis and lymph node metastasis in breast cancer. Molecular Cancer. Article in Press.

Dandekar, D.S. & Lokeshwar, B.L. (2004) Inhibition of Cyclooxygenase (COX)-2 Expression by Tet-Inducible COX-2 Antisense cDNA in Hormone-Refractory Prostate Cancer Significantly Slows Tumor Growth and Improves Efficacy of Chemotherapeutic DrugsClin. Cancer Research, 10; 8037 - 8047.

Dash, P.K., Mach, S.A. & Moore, A.N. (2002) The role of extracellular signal-regulated kinase in cognitive and motor deficits following experimental traumaticbrain injury. Neuroscience, 114: 775.

Datta, S.R., Brunet, A. & Greenberg, M.E. (1999). Cellular survival: A play I three Akts. Genes and development; 13: 2905-2927.

Davidson, B., Konstantinovsky, S., Nielson, S., Dong, H.P., Berner, A., Vyberg, M. & Reich, R. (2004) Altered expression of metastasis-associated and regulatory molecules in effusions from breast cancer patients: A novel model for tumor progression. Clinical Cancer Research, 10: 7335-7346.

Davies, G., Salter, J., Hills, M., Martin, L-A., Sacks, N. & Dowsett, M. (2003) Correlation between cyclooxygenase-2 expression and angiogenesis in human breast cancer. Clinical Cancer Research, 9: 2651-2656.

Davis, S., Vanhoutte, P., Page, C., Caboche, J. & Laroche, S. (2000) The MAPK/ERK cascade targets both Elk-1 and cAMP response element-binding protein to control long-term potentiation-dependent gene expression in the Dentate Gyrus *In Vivo.* The Journal of Neuroscience, *20*: 4563–4572.

Degim, I.T. (2005) Understanding skin penetration: computer aided modeling and data interpretation. Current Computer-Aided Drug Design, 1; 11-19 11.

deGraffenried, L.A., Fulcher, L., Friedrichs, W.E., Grünwald, V., Ray, R.B. & Hidalgo, M. (2004) Reduced PTEN expression in breast cancer cells confers susceptibility to inhibitors of the PI3 kinase/Akt pathway. Annals of Oncology,15; 1510–1516.

Dehal, S. & Kupfer, D. (1997) CYP2D6 catalyzes tamoxifen 4-hydroxylation in human liver. Cancer Research, 57; 3402-3406.

Dommels, Y.E.M., Haring, M.M.G., Keestra, N.G.M., Alink, G.M., van Bladeren, P.J. & van Ommen, B. (2003) The role of cyclooxygenase in n-6 and n-3 polyunsaturated fatty acid mediated effects on cell proliferation, PGE2 synthesis and cytotoxicity in human colorectal carcinoma cell lines. Carcinogenesis, 24; 385–392.

Donald, P.R., Sirgel, F.A., Venter, A., Smit, E., Parkin, D.P., Van de Wal, B.W., Doré, C.J. & Mitchison, D.A. (2002) The early bactericidal activity of streptomycin. The International Journal of Tuberculosis and Lung Disease, 6; 693-698.

Dubois, R.N., Abramson, S.B., Crofford, L., Gupta, R.A., Simon, L.S., Van De Putte, L.B.A. & Lipsky, P.E. (1998) Cyclooxygenase in biology and disease. Federation of American Societies for Experimental Biology, 12: 1063-1073.

Dudley, D.T., Pang, L., Decker, S.J., Bridges, A.J., Saltiel, A.R. (1995). A synthetic inhibitor of the mitogen-activated protein kinase cascade. Proc.Natl. Acad. Sci. USA 92: 7686-7689.

Elias, P.M. (1983) Epidermal lipids, barrier function and desquamation. Journal of Investigative Dermatology, 88; 44s-49s.

Elias, P.M. (1988) The structure and function of the stratum corneum permeability barrier. Drug Development Research, 13; 97-105.

Essa, E.A., Bonner, M.C. & Barry, B.W (2002) Human skin sandwich for assessing shunt route penetration during passive and iontophoretic drug and liposome delivery. Journal of Pharmaceutics and Pharmacology, 54; 1481-90.

Frandson, R.D., Wilke, W.L. & Fails, A.D. (2003) Anatomy and physiology of farm animals, Blackwell Publishing, London, Uk. 416-421.

Fidler, I. J. (2003) The pathogenesis of cancer metastasis: the 'seed and soil' hypothesis revisited. Nature Review Cancer,3: 53-58.

Fisher, B., Costantino, J.P., Redmond, C.K., Fisher, E.R., Wickerham, L. & Cronin, W.M. (1994). Endometrial cancer in tamoxifen-treated breast cancer patients: findings from the National Surgical Adjuvant Breast and Bowel Project (NSABP) B-14. Journal of the National Cancer Institute; 86: 527-537.

Fisher, B., Dignam, J., Bryant, J., Decillis, A., Wickerham, D.L., Wolmark, N., Constantino, J., Redmond, C., Fisher, E.R., Bowman, D.M., Deschênes, L., Dimitrov, N.V., Margolese, R.G., Robidoux, A., Shibata, H., Terz, J., Paterson, A.H.G., Feldman, M.I., Farrar, W., Evans, J. & Lickley, H.L. (1996). Five versus more than five years of tamoxifen therapy for breast cancer patients with negative

lymph nodes and estrogen receptor-positive tumors. Journal of the National Cancer Institute; 88 (12): 1529-1542.

Formica, J.V. & Regelson, W. (1995) Review of the biology of quercetin and related bioflavonoids. Food Chemical Toxicology, 33: 1061-1080.

Forslind, F (1994) A domain mosaic model of the skin barrier. Acta Derm Venereol, 74; 1-6.

Fox, M.E., Bernaciak, T.M., Wen, J., Weaver, A.E., Shupnik, M.A. & Silva, C.M. (2008) STAT5b, c-Src, and EGFR signaling play integral roles in estrogen-stimulated proliferation of ER-positive breast cancer cells. Molecular Endocrinology, article in press.

Freeman, D.J., Sheth, N.V. & Spruance, S.P. (1986) Failure of topical acyclovir in ointment to penetrate human skin. Antimicrobial Agents and Chemotherapy, 29: 730-732.

Fry, M.J. (2001). Phosphoinositide 3-kinase signaling in breast cancer: how big a role might it play? Breast Cancer Research; 3: 304-312.

Gallagher, S.J., Trottet, L. & Heard, C.M. (2003) Ketoprofen: release from, permeation across and rheology of simple gel formulations that simulate increasing dryness. International Journal of Pharmaceutics, 268: 37–45.

Gao, S. & Singh, J. (1998) In vitro percutaneous absorption enhancement of a lipophilic drug tamoxifen by terpenes. Journal of Controlled Release, 51: 193-199.

Gee, J.M.W., Harper, M.E., Hutcheson, I.R., Madden, T.A., Barrow, D., Knowlden, J.M., McClelland, R.A., Jordan, N., Wakeling, A.E. & and Nicholson, R.I. (2003) The antiepidermal growth factor receptor agent Gefitinib (ZD1839/Iressa) improves antihormone response and prevents development of resistance in breast cancer *in vitro*. Endocrinology, 144; 5105-5117.

Gee, J.M., Robertson, J.F., Gutteridge, E., Ellis, I.O., Pinder, S.E., Rubini, M. & Nicholson, R.I. (2005) Epidermal growth factor receptor/HER2/insulin-like growth factor receptor signalling and oestrogen receptor activity in clinical breast cancer. Endocrine-Related Cancer, 12; S99–S111.

Gee, J.M.W., Shaw, V.E., Hiscox, S.E., McClelland, R.A., Rushmere, N.K. & Nicholson, R.I. (2006) Deciphering antihormone-induced compensatory mechanisms in breast cancer and their therapeutic implications. Endocrine-Related Cancer, 13; S77–S88.

Going, J.J. & Moffat, D.F. (2004) Escaping from Flatland: clinical and biological aspects of human mammary duct anatomy in three dimensions. Journal of Pathology, 203; 538-544.

Golden, G.M., Guzek, D.B, Kennedy, A.H., McKie, J.E. & Potts, R.O. (1987) Stratum corneum lipid phase transitions and water barrier properties. Biochemistry, 26: 2382-2388.

Gonza´lez, L., Agullo´ -Ortun˜o, M.T., Garcı´a-Martı´nez, J.M., Calcabrini, A., Gamallo, C., Palacios, J., Aranda, A., & Martı´n-Pe´rez, J. (2006). Role of c-Src in human MCF7 breast cancer cell tumorigenesis. The Journal of Biological Chemistry, 281; 20851–20864.

Gottlicher, M., Heck, S. & Herrlich, P. (1998) Transcriptional cross-talk, the second mode of steroid hormone receptoraction. Journal of Molecular Medicine, 76: 480–489.

Grabowski, E.F. & McDonnell, S.L. (1993) Adhesion of human erythrocytes to glass: The nature of the interaction and the effect of serum and plasma. Methods in Cell Science, 15; 190-198.

Grände, M., Franzen, A., Karlsson, J-O., Ericson, L.E., Heldin, N-E. & Nilsson, M. (2002) Transforming growth factor-b and epidermal growth factor synergistically stimulate epithelial to mesenchymal transition (EMT) through a MEKdependent mechanism in primary cultured pig thyrocytes. Journal of Cell Science, 115; 4227-4236.

Granger, G.S., Thomas, V., Jewell, A. & Mokbel, K. (2004) Elevated cyclooxygenase-2 expression correlates with distant metastases in breast cancer. Anticancer Research, 24: 2349-2351.

Green, P.G., Guy, R.H. & Hadgraft, J. (1988) In vitro and in vivo enhancement of skin permeation with oleic and lauric acids. International Journal of Pharmaceutics, 48: 103-111.

Grubauer, G., Feingold, K.R., Harris, R.M. & Elias, P.M. (1989) Lipid content and lipid type as determinants of the epidermal permeability barrier. The Journal of Lipid Research, 30; 89-96.

Guo, H., Li, R., Zucker, S. & Toole, B.P. (2000) EMMPRIN (CD147), an inducer of matrix metalloproteinase synthesis, also binds interstitial collagenase to the tumor surface. Cancer Research, 60: 888-891.

Haberland, A., Schreiber, S., Maia, C.S., Rubbelke, M.K., Schaller, M., Korting, H.C., Kleuser, B., Schimke, I. & Schafer-Korting, M. (2006) The impact of skin viability on drug metabolism and permeation -- BSA toxicity on primary keratinocytes. Toxicology In Vitro, 20; 347-354.

Hagemann, T., Robinson, S.C., Schulz, M., Trümper, L., Balkwill, F.R. & Binder, C. (2004) Enhanced invasiveness of breast cancer cell lines upon co-cultivation with macrophages is due to TNF-α dependent up-regulation of matrix metalloproteases. Carcinogenesis, 25; 1543 - 1549.

Half, E., Tang, X.M., Gwyn, K., Sahin, A., Wathen, K., Sinicrope, F.A. (2002) Cyclooxygenase-2 expression in human breast cancers and adjacent ductal carcinoma *in situ.* Cancer Research, 62: 1676-1681.

Hanstein, B., Djahansouzi, S., Dall, P., Beckmann, S.J. Bender, H.G. (2004) Insights into the molecular biology of the estrogen receptor define novel therapeutic targets for breast cancer. European Journal of Endocrinology, 150; 243 - 255.

Harris, A.L., Nicholson, S., Sainsbury, J.R., Farndon, J. & Wright, C. (1989) Epidermal growth factor receptors in breast cancer: association with early relapse and death, poor response to hormones and interactions with neu. Jornal of steroid Biochemistry, 34; 123-131.

Harris Wooge, C., Nilsson, G.M. Heierson, A., McDonnell, D.P. & Katzenellenbogen B.S. (1992) Structural requirements for high affinity ligand binding by estrogen receptors: A comparative analysis of truncated and full length estrogen receptors expressed in bacteria, yeast, and mammalian cells. Molecular Endocrinology 6; 861-869.

Hermanto, H., Zong, S.C. & Wang, L-H. (2000). Inhibition of mitogen-activated protein kinase kinase selectively inhibits cell proliferation in human breast cancer cells displaying enhanced insulin-like growth factor I-mediated mitogen-activated protein kinase activation 1. Cell Growth & Differentiation: 11: 655–664.

Hernandez, G.L., Volpert, O.V., Iniguez, M.A., Lorenzo, E., Martinez-Martinez, S., Grau, R., Fresno, M. & Redondo, J.M. (2001) Selective inhibition of vascular growth factor-mediated angiogenesis by cyclosporin A: roles of the nuclear factor of activated T cells and cyclooxygenase 2. Journal of Experimental Medicine, 193: 607-620.

Heard, C.M., Gallagher, S.J., Congiato, C., Harwood, J., Thomas, C.P., McGuigan, C., Němcová, M., Nouskova, T. (2005) Preferential π–π complexation between tamoxifen and borage oil/γ linolenic acid: Transcutaneous delivery and NMR spectral modulation. International Journal of Pharmaceutics, 302: 47-55.

Heard, C.M., Gallagher, S.J., Harwood, J. & Maguire, P.B. (2003) The in vitro delivery of NSAIDs across skin was in proportion to the delivery of essential fatty acids in the vehicle-evidence that solutes permeate skin within their solvation cages? International Journal of Pharmaceutics, 261: 165-169.

Heard, CM, Harwood, J Maguire, P, McNaughton, G, Pugh, WJ. (2002) Simultaneous penetration of NSAID and essential fatty acid esters as a dual-action

anti-arthritis therapy. In, Brain KR and Walters K (Eds.) Perspectives in Percutaneous Penetration, Vol 8a STS Publishing, Cardiff pp 93.

Heard, C.M., Kung, D. & Thomas, C.P. (2005) Skin penetration enhancement of mefenamic acid by ethanol and 1,8-cineole can be explained by the 'pull' effect. International Journal of Pharmaceutics, 321: 167-170.

Heard, C.M. & Screen, C. (2007) Probing the permeation enhancement of mefenamic acid by ethanol across full thickness skin, heat-separated epidermal membrane and heat separated dermal membrane. International Journal of Pharmaceutics, 349: 323-325.

Henzl, M. R., Loomba, P. K. (2003) Transdermal delivery of sex steroids for hormone replacement therapy and contraception: A review of principles and practice. The Journal of Reproductive Medicine, 48: 525-540.

Hii, C.S.T., Moghadammi, N., Dunbar, A. & Ferrante, A. (2001) Activation of the phosphatidylinositol 3-kinase-Akt/protein kinase B signaling pathway in arachidonic acid-stimulated human myeloid and endothelial cells. The Journal of Biological Chemistry, 276; 27246-27255.

Hikima, T., Tojo. K. & Maibach, H.I. (2005). Skin metabolism in transdermal therapeutic systems. Skin Pharmacology and Physiology; 18: 153-159.

Hiscox, S., Jiang, W.G., Obermeirer, K., Taylor, K., Morgan, L., Burmi, R., Barrow, D. & Nicholson, R.I. (2006) Tamoxifen resistance in MCF7 cells promotes EMT-like behaviour and involves modulation of b-catenin phosphorylation. International Journal of Cancer, 118: 290-301.

Hiscox, S., Jordan, N.J., Jiang, W., Harper, M., McClelland, R., Smith, C. & Nicholson, R.I. (2006) Chronic exposure to fulvestrant promotes overexpression of the c-Met receptor in breast cancer cells: implications for tumour–stroma interactions. Endocrine-Related Cancer, 13; 1085–1099.

Hiscox, S., Morgan, L., Green, T.P., Barrow, D., Gee, J. & Nicholson, R.I. (2006) Elevated Src activity promotes cellular invasion and motility in tamoxifen resistant breast cancer cells. Breast Cancer Research and Treatment, 97: 263-274.

Ho, S., Calder, R.J., Heard, C.M. & Thomas, C.P. (2004) In vitro transcutaneous delivery of tamoxifen and □ linolenic acid from a borage oil formulation containing ethanol and 1,8-cineole. Journal of Pharmacy and Pharmacology, 56; 1-8.

Holland R, Veling SH, Mravunac M, Hendriks JH (1985) Histologic multifocality of Tis, T1-2 breast carcinomas. Implications for clinical trials of breast-conserving surgery. Cancer 1985, 56: 979-990.

Horia, E. & Watkins, B.A. (2007) Complementary actions of docosahexaenoic acid and genistein on COX-2, PGE2 and invasiveness in MDA-MB-231 breast cancer cells. Carcinogenesis, 28: 809-815.

Hotchkiss, S.A.M. (1998). Dermal metabolism. In: Roberts, M.S., Walters, K.A. (Eds.), Dermal Absorption and Toxicity Assessment. Marcel Dekker, New York, pp. 43–101.

Howard F.A. & Henderson, C. (1999) Hydrogenation of polyunsaturated fatty acids by human colonic bacteria. Letters in Applied Microbiology, 29; 193-196.

Huang, D., Ding, Y., Luo, W-M., Bender, S., Qian, C.N., Kort, E., Zhang, Z.F., VandenBeldt, K., Duesbery, N.S. Resau, J.H. & Teh, B.T. (2008) Inhibition of MAPK Kinase Signaling Pathways Suppressed Renal Cell Carcinoma Growth and Angiogenesis *In vivo.* Cancer Research, 68: 81-88.

Hwang, D-M., Kundu, J.K., Shin, J-W., Lee1, J-C., Lee, H.J. & Surh, Y-J. (2007) cis-9,trans-11-conjugated linoleic acid down-regulates phorbol ester-induced NF-kB activation and subsequent COX-2 expression in hairless mouse skin by targeting IkB kinase and PI3K-Akt. Carcinogenesis, 28: 363–371.

Jantharaprapap, R. & Stagni, G. (2007) Effects of penetration enhancers on *in vitro* permeability of meloxicam gels. International Journal of Pharmaceutics, 343: 26–33.

Jia, Y., Zeng, Z-Z., Markwart, S.M., Rockwood, K.F., Woods Ignatoski, K.M., Ethier, S.P. & Donna L. Livant. (2004) Integrin Fibronectin Receptors in Matrix Metalloproteinase-1–Dependent Invasion by Breast Cancer and Mammary Epithelial Cells. Cancer Research, 64; 8674 - 8681.

Jones, H.E., Gee, J.M.W., Hutheson, I.R., Knowlden, J.M. Barrow, D. & Nicholson, R.I. (2006) Growth factor interplay and resistance in cancer. Endocrine-Related Cancer, 13; S45-51.

Jordan, N.J., Gee, J.M.W., Barrow, D., Wakeling, A.E. & Nicholson, R.I. (2004) Increased constitutive activity of PKB/Akt in tamoxifen resistant breast cancer MCF-7 cells. Breast Cancer Research and Treatment, 87; 167-180.

Jordan, V.C., Gapstur, S. & Morrow, M. (2001). Selective estrogen receptor modulation and reduction in risk of breast cancer, osteoporosis, and coronary heart disease. Journal of the National Cancer Institute; 93: 1449-1457.

Jordan, V.C. & Marrow, M. (1999) Tamoxifen, raloxifen and the treatment of breast cancer. Endocrine Reviews, 20; 253-278.

Kang, Z.B., Ge,Y., Chen, Z., Clnette-Brown, J., Laposata, M., Leaf, A. & Kang, J.X. (2001) Adenoviral gene transfer of Caenorhabditis elegans n-3 fatty acid desaturase optimizes fatty acid composition in mammalian cells. Proc. National Academy of Science USA, 98: 4050-4054.

Karia, C., Harwood, J., Morris, A.P. & Heard, C.M. (2004) Simultaneous permeation of tamoxifen and γ linolenic acid across excised human skin. Further evidence of the permeation of solvated complexes. International Journal of Pharmaceutics, 271: 305-309.

Karande, P., Jain, A., Mitragotri, S. (2006) Insights into synergistic interactions in binary mixtures of chemical permeation enhancers for transdermal drug delivery. Journal of Controlled Release, 115: 85-93.

Kataoka, H., DeCastro, R., Zucker, S. & Biswas, C. (1993) Tumor cell-derived collagenase stimulatory factor increases expression of interstitial collagenase, stromelysin, and 72Kda gelatinase. Cancer Research, 53: 3154-3158.

Kim, H.W., Gwak, H.S. & Chun, I.K. (2004) The effect of vehicles and pressure sensitive adhesives on the percutaneous absorption of quercetin through the hairless mouse skin. Archives of Pharmaceutical Research, 27: 763-768.

King, B.L. & Love, S.M. (2006) The intraductal approach to the breast: raison d'être. Breast Cancer Research, 8: 206-216.

Knowlden, J.M., Hutcheson, I.R., Jones, H.E., Madden, T., Gee, J.M.W., Harper, M., Barrow, D., Wakeling, A.E. & Nicholson, R.I. (2003) Elevated levels of epidermal growth factor receptor/c-erbB2 heterodimers mediate an autocrine growth regulatory pathway in tamoxifen-resistant MCF-7 cells. Endocrinology, 144; 1032-1044.

Knowlden, J.M., Hutcheson, I.R., Barrow, D., Gee, J. M. W. & Nicholson, R.I. (2005) Insulin-like growth factor-I receptor signaling in tamoxifen-resistant breast cancer: A supporting role to the epidermal growth factor receptor. Endocrinology, 146; 4609-4618.

Krasilnikov, M.A. (2000) Phosphotidylinositol 3-kinase dependant pathways: the role in control of cell growth, survival and malignant transformation, 65; 59-67.

Kretsos, K. & Kasting, G.B. (2005). Dermal capillary clearance: Physiology and modeling. Skin Pharmacology and Physiolgy; 18: 55-74.

Kruger, J.S. and Reddy, K.B. (2003) Distinct mechanisms mediate the initial and sustained phase of cell migration in epidermal growth factor -overexpressing cells. Molecular Cancer Research, 1: 801-809.

Kundu, M. & Fulton, A.M. (2002) Selective cyclooxygenase (COX)-1 or COX-2 inhibitors control metastatic disease in a murine model of breast cancer. Cancer Research, 62: 2343-2346.

Larkins, T.L., Nowell, M., Singh, S. & Sanford, G.L. (2006) Inhibition of cyclooxygenase-2 decreases breast cancer cell motility, invasion and matrix metalloproteinase expression. BioMed Central Cancer, 6; 181-192.

Lavinsky, R.M., Jepsen, K., Heinzel, T., Torchia, J., Mullen, T-A., Schiff, R., Del-Rio, A.L., Ricote, M., Ngo, S., Gemsch, J., Hilsenbeck, S., Osborne, C.K., Glass, C.K., Rosenfeld, M.G. & Rose, D.W. (1998) Diverse signaling pathways modulate nuclear receptor recruitment of N-CoR and SMRT complexes. PNAS, 95; 2920 - 2925.

Lee, A.J., King, J.R. & Rogers, T.G. (1996) A multiple-pathway model for the diffusion of drugs in skin. Journal of Mathematics Applied in Medicine & Biology, 54; 1481-1490.

Lee, J.L., Mukhtar, H., Bickers, D.R., Kopelovich, L. & Athar, M. (2003) Cyclooxygenase in the skin: pharmacological and toxicological implications. Toxicology and Applied Pharmacology, 192: 294-306.

Levine, M., Moutquin, J-M.,Walton, R., Feightner, J. (2001). Chemoprevention of breast cancer. A joint guideline from the Canadian Task Force on Preventive Health Care and the Canadian Breast Cancer Initiative's Steering Committee on Clinical Practice Guidelines for the Care and Treatment of Breast Cancer. Canadian Medical Association Journal; 164: 1681-1690.

Leyden, J.J., McGinley, K.J. Holzle, E., Labows, J.N. & Kligman, A.M. (1981) The microbiology of the human axilla and its relationship to axillary odor. Journal of Investigative Dermatology, 77; 413-416.

Liu, H., Li, S., Wang, Y., Yao, H. & Zhang, Y. (2006) Effect of vehicles and enhancers on the topical delivery of cyclosporin A. International Journal of Pharmaceutics, 311: 182-186.

Liu, X.H., Connolly, J.M. & Rose, D.P. (1996) The 12-lipoxygenase gene-transfected MCF-7 human breast cancer cell line exhibits estrogen-independent, but

estrogen and omega-6 fatty acid-stimulated proliferation in vitro, and enhanced growth in athymic nude mice. Cancer Letters, 109; 223-230.

Lui, X-H. & Rose, D. (1996) Differential expression and regulation of cyclooxygenase-1 and –2 in two human breast cancer cell lines. Cancer Research, 56; 5125-5127.

Love, R.R., Wiebe, D.A., Feyzi, J.M., Newcomb, P.A. & Chappell, R.J. (1994). Effects of tamoxifen on cardiovascular risk factors in postmenopausal women after 5 years of treatment. Journal of the National Cancer Institute; 86:1534-1539.

Love, S.M. & Barsky, S.H. (2004) Anatomy of the nipple and breast ducts revisited. Cancer, 101: 1947-57.

Macgregor, J.I. & Jordan, V.C. (1998) Basic guide to the mechanisms of antiestrogen action. Pharmacological Reviews, 50; 151-196.

Maibach, H.A., Feldman, R.J., Milby, T.H. & Serat, W.F. (1971) Regional variation in percutaneous penetration in man. Pesticides. Archives of Environmental Health, 23; 208-211.

Malet, C., Spritzer, P., Cumins, C., Guillaumin, D., Mauvais-Jarvis, P. & Kuttenn. (2002) Effect of 4-hydroxytamoxifen isomers on growth and ultrastructural aspects of normal human breast epithelial (HBE) cells in culture. Journal of Steroid Biochemistry & Molecular Biology, 82: 289–296.

Malkowski, M.G., Thuresson, E.D., Lakkides, K.M., Rieke, C.J., Micielli, R., Smith, W.L. & Garavito, R.M. (2001) Structure of eicosapentaenoic and linoleic acids in the cyclooxygenase site of prostaglandin endoperoxide H synthase 1. The Journal of Biological Chemistry, 276: 37547-37555.

Mansel R, Goyal A, Le Nestour E, Masini-Eteve V, O'Connell K. (2007) A Phase II trial of Amoxifene (4-hydroxytamoxifen gel) for cyclical mastalgia in premenopausal women. Breast Cancer Research and Treatment, 106; 389-397.

Marples, R.R. (1969) Violagabriellae Variant of *Staphylococcus epidermidis* on Normal Human Skin. Journal of Bacteriology, 100-47-50.

Masferrer, J.L., Leahy, K.M., Koki, A.T., Zweifel, B.S., Settle, S.L., Woerner, B.M., Edwards, D.A., Flickinger, A.G., Moore, R.J., & Seibert, K. (2000) Antiangiogenic and antitumor activities of cyclooxygenase-2 inhibitors. Cancer Research, 60: 1306-1311.

Mauvais-Jarvis, P., Baudot, N., Castaigne, D., Banzet, P. & Kuttenn, F. (1986) *Trans*-4-hydroxytamoxifen concentration and metabolism after local percutaneous administration to human breast, Cancer Research, 46: 1521–1525.

McBride, M.E., Duncan, W.C. & Knox, J.M. (1977) The environment and the microbial ecology of human skin. Applied and Environmental Microbiology, 33; 603-608.

McClelland, R., Barrow, D., Madden, T-R., Dutkowski, C.M., Pamment, J., Knowlden, J., Gee, J.M.W. & Nicholson, R.I. (2001) Enhanced epidermal growth factor receptor signalling in MCF7 breast cancer cells after long-term culture in the presence of the pure antiestrogen ICI 182,780 (Faslodex). Endocrinology, 142; 2776-2788.

Mendes, O., Kim, H.T., Lungu, G. & Stoica, G. (2007) MMP2 role in breast cancer brain metastasis development and its regulation by TIMP2 and ERK ½. Clinical Experimental Metastasis, 24: 341-351.

Méric, J-B., Rottey, S., Olaussen, K., Soria, J-C., Khayat, D., Rixe, O. & Spano, J-P. (2006) Cyclooxygenase-2 as a target for anticancer drug development. Clinical Reviews in Oncology/Hematology, 59: 51-64.

Mernard, S., Castronovo, V., Tagliabue, E. & Sobel, M.E. (1997) New insights into the metastasis-associated 67KDa laminin receptor. The Journal of Cell Biochemistry, 67: 155-165.

Mernard, S., Tagliabue, E. & Colnaghi, M.I. (1998) The 67KDa laminin receptor as a prognostic factor in human cancer. Breast Cancer Research and Treatment, 52: 137-145.

Mirnikjoo, B., Brown, S.E., Seung Kim, H.F., Marangell, L.B., Sweatt, J.B. & Weeber, E.J. (2001) Protein Kinase Inhibition by v-3 Fatty Acids. The Journal of Biological Chemistry, 276; 10888-10896.

Moghimi, H.R., Williams, A.C. & Barry, B.C. (1996) A lamellar matrix model for stratum corneum intercellular lipids III. Effects of terpene penetration enhancers on the release of 5-fluorouracil and oestradiol from the matrix. International Journal of Pharmaceutics, 145: 37-47.

Moghimi, H.R., Williams, A.C. & Barry, B.C. (1996) A lamellar matrix model for stratum corneum intercellular lipids IV. Effects of terpene penetration enhancers on the permeation of 5-fluorouracil and oestradiol through the matrix. International Journal of Pharmaceutics,145: 49-59.

Moghimi, H.R., Williams, A.C. & Barry, B.C. (1997) A lamellar matrix model for stratum corneum intercellular lipids. V. Effects of terpene penetration enhancers on the structure and thermal behaviour of the matrix. International Journal of Pharmaceutics, 146: 41-54.

Monti, D., Chetoni, P., Burgalassi, S., Najarro, M., Fabrizio Saettone, M. & Boldrini, E.M. (2002) Effect of different terpene-containing essential oils on permeation of estradiol through hairless mouse skin. International Journal of Pharmaceutics, 237: 209-214.

Moon, J-H., Nakata, R.O., Oshima, S., Inakuma, T. & Terao, J. (2000) Accumulation of quercetin conjugates in blood plasma after the short-term ingestion of onion by women. The American Journal of Physiology - Regulatory, Integrative and Comparative Physiology, 279: R461–R467.

Mukutmoni-Norris, M., Hubbard, N.E. & Erickson, K.L. (2000) Modulation of murine mammary tumor vasculature by dietary n-3 fatty acids in fish oil. Cancer Letters, 150; 101-109.

Murata, S., Kominsky, S.L., Vali, M., Zhang, Z., Garrett-Mayer, E., Korz, D., Huso, D., Baker, S.D., Barber,J., Jaffee, E., Reilly, R.T. & Sukumar, S. (2006) Ductal access for prevention and therapy of mammary tumors. Cancer Research, 66: 638-645.

Nanua, S., Zick, S.M., Andrade, J.E., Sajjan, U.S., Burgess, J.R., Lukacs, N.W. & Hershenson, M.B. (2006) Quercetin blocks airway epithelial cell chemokine expression. American Journal of Respiratory Cell and Molecular Biology, 35: 602–610.

Narishetty, S.T.K. & Panchagnula, R. (2004) Transdermal delivery of zidovudine: effect of terpenes and their mechanism of action. Journal of Controlled Release, 95: 367-379.

Nicholson, R.I., Hutheson, I.R., Hiscox, S.E., Knowlden, J.M., Giles, M., Barrow, D. & Gee, J.M. (2005) Growth factor signalling and resistance to selective oestrogen receptor modulators and pure anti-oestrogens: the use of anti-growth factor therapies to treat or delay endocrine resistance in breast cancer. Endocrine-Related Cancer, 12: s29-s36.

Nicholson, R.I., Hutcheson, I.R., Knowlden, J.M., Jones, H.E., Harper, M.E., Jordan, N., Hiscox, S.E. Barrow, D. & Gee, J.M.W. (2004) Nonendocrine Pathways and Endocrine Resistance: Observations with Antiestrogens and Signal Transduction Inhibitors in Combination. Clinical Cancer Research, 10; S346-S354.

Nicholson, R.I., Staka, C., Boynes, F., Hutheson, I.R. & Gee, J.M.W. (2004) Growth factor-driven mechanisms associated with resistance to estrogen deprivation in breast cancer: new opportunities for therapy. Endocrine-Related Cancer, 11; 1-9.

Normanno, N., Di Maio, E., De Luca, A., de Matteis, A., Giordano, A. & Perrone, F. (2005) Mechanisms of endocrine resistance and novel therapeutic stratergies in breast cancer. Endocrine-Related Cancer, 12; 721-747.

Oh, S.Y., Fujii, M., Takeda, Y., Yoda, K., Utoguchi, N., Matsumoto, M. & Watanabe, Y. (2002) The effect of ethanol on the simultaneous transport and metabolism of methyl *p*-hydroxybenzoate in excised skin of Yucatan micropig. International Journal of Pharmaceutics, 236: 35–42.

O'Lone, R., Frith, M.C., Karlsson, E.K. & Hansen, U. (2004) Genomic targets of nuclear estrogen receptors. Molecular Endocrinology, 18: 1859–1875.

Omran M.O., Al-Hammami., Richards, J.R. (1996) Effects of excipients on the bioavailability of sodium salicylate from orally administered, oily suspensions. Pharmaceutics Acta Helvetiae, 71: 297-303

Ongpipattanakul, B., Bumette, R.R., Potts, O.R. & Francoeur, M.I. (1991) Evidence that oleic acid exists in a separate phase within stratum corneum lipids. Journal of Pharmaceutical Science, 8: 350-354.

Pai, R., Nakamura, T., Moon, W.S. & Tarnawski, A.S. (2003) Prostaglandins promote colon cancer cell invasion; signalling by crosstalk between two distinct growth factor receptors. The FASEB Journal, 17: 1640-1647.

Pastore, S., Mascia, F., Mariotti, F., Dattilo, C., Mariani, V. & Girolomoni, G. (2005) ERK1/2 regulates epidermal chemokine expression and skin inflammation. The Journal of Immunology, 174: 5047-5056.

Patil, S., Singh, P., Szolar-Platzer, C. & Maibach, H. (1996) Epidermal Enzymes as Penetration Enhancers in Transdermal Drug Delivery? Pharmaceutical Sciences, 85: 249-252.

Pecorino, L. (2005). Molecular biology of cancer. Oxford University Press. New York.

Philpot, I., Davison, Z., Nicholson, R.I. & Heard, C.M. (Manuscript in preparation) An oleo gel formulation for the transcutaneous delivery of EGFR signal transduction inhibitors and eicosapentaenoic acid.

Razandi, M., Pedram, A. & Levin, E.R. (2008) Plasma membrane estrogen receptors signal to antiapoptosis in breast cancer. Molecular Endocrinology, 14: 1434–1447.

Razandi, M., Pedram, A., Park, S.T. & Levin, E.R. (2003) Proximal events in signaling by plasma membrane estrogen receptors. The Journal of Biological Chemistry, 278; 2701–2712.

Ribeiro, G. & Swindell, R. (1992). The Christie Hospital adjuvant tamoxifen trial. Monograph National Cancer Istitute; 11: 121-125.

Rhee, Y-S., Choi, J-G., Park, E-S. & Chi, S-C. (2001) Transdermal delivery of ketoprofen using microemulsions. International Journal of Pharmaceutics, 228: 161-170.

Roberts, M.S., Cross, S.E. & Pellett, M.A. (2002) Skin transport. In: Walters, K.A. (Ed.), Dermatological and Transdermal Formulations. Marcel Dekker, New York, pp. 89–196.

Robertson, D.W., Katzenellenbogen, J.A., Long, D.J., Rorke, E.A. & Katzenellenbogen, B.S. (1982) Tamoxifen antiestrogens. A comparison of the activity, pharmacokinetics, and metabolic activation of the cis and trans isomers of tamoxifen. Journal of Steroid Biochemistry, 16; 1-13.

Robertson, J.F.R., Nicholson, R.I. & Hayes, D.F. (2002). Endocrine therapy of breast cancer. Martin Dunitz Ltd. London.

Romero-Steiner, S., Witek, T. & Balish, E. (1990) Adherence of skin bacteria to human epithelial cells. The Journal of Clinical Microbiology, 28; 27-31.

Roskoski Jr, R. (2004) Src protein-tyrosine kinase structure and regulation. Biochemistry and Biophysiology Research and Communication, 324; 1155-1164.

Rose, D.P., & Connolly, J.M. (1999) Omega-3 fatty acids as cancer chemopreventive agents. Pharmacology and Therapeutics, 83; 217-244.

Rose, D.P., Connolly, J.M., Rayburn, J. & Coleman, M. (1995) Influence of diets containing eicosapentaenoic or docosahexaenoic acid on growth and metastasis of breast cancer cells in nude mice. Journal of the National Cancer Institute, 87; 587-592.

Roth, R.R. & James, W.D. (1989) Microbiology of the skin: resident flora, ecology, infection. J of the American Academy of Dermatology, 20; 367-390.

Rouanet, P., Linares-Cruz, G., Dravet, F., Poujol, S., Gourgou, S., Simony-Lafontaine, J., Grenier, J., Kramar, A., Girault, J., Le Nestour, E. & Maudelonde, T. (2005) Neoadjuvant percutaneous 4-Hydroxytamoxifen decreases breast tumoral cell proliferation: A prospective controlled randomized study comparing three doses of 4-hydroxytamoxifen gel to oral tamoxifen. Journal of Clinical Oncology, 23; 2980-2987.

Roymans, D. & Slegers, H. (2001). Phosphatidylinositol 3-kinase in tumor progression. European journal of biochemistry; 268: 487-498.

Russell, T.D., Fischer, A., Beeman, N.E., Freed, E.F., Neville, M.C. & Schaack, J. (2003) Transduction of the mammary epithelium with adenovirus vectors In Vivo. Journal of Virology, 77: 5801-5809.

Russo, J., Hu, Y-F., Yang, X. & Russo, I.H. (2000). Chapter 1: Developmental, Cellular, and Molecular Basis of Human Breast Cancer. Journal of the National Cancer Institute Monographs; 27: 1-37.

Rząsa, A., Poznański, W., Pospieszny, N. & Zawada, Z. (2005) New aspects of the anatomical structure of the sows udder. Electronic Journal of Polish Agricultural Universities, 8.

Safina, A.F., Vandette, E., Varga, A.E. & Bakin, A.V. (2006) TGF-ß-MAPK signaling enhances metastases by stimulating tumor cell invasion and changes in tumor microenvironment. Proc American Association of Cancer Research, 47: Abstract #3524.

Saija, A., Tomaino, A., Trombetta, D., Giacchi, M., De Pasquale, A. & Bonina, F. (1998). Influence of different penetration enhancers on in vitro skin permeation and in vivo photoprotective effect of flavonoids. International Journal of Pharmaceutics, 175: 85–94.

Scheid, M.P., Marignani, P.A. & Woodgett, J.R. (2002) Multiple phosphoinositides 3-kinase-dependent steps in activation of protein kinase B. Molecular and Cellular Biology, 22; 6247-6260.

Schley, P.D., Brindley, D.N. & Field, C.J. (2007) (n-3) PUFA alter raft lipid composition and decrease epidermal growth factor receptor levels in lipid rafts of human breast cancer cells. Journal of Nutrition, 137; 548-553.

Sekkat, N., Kalia, Y.N. & Guy, R.H. (2002) Biophysical study of porcine ear skin in vitro and its comparison to human skin in vivo. Journal of Pharmaceutical Sciences, 91; 2376-2381.

Shaffer, T.E. & Pruitt, A.W. (1983) Dimethyl sulfoxide (DMSO). Pediatrics, 71: 76-77).

Shen, K.W., Wu, J., Lu, J.S., Han, Q.X., Shen, Z.Z., Nguyen, M., Shao, Z.M. & Barsky, S.H. (2000) Fiberoptic ductoscopy for patients with nipple discharge. Cancer, 89: 1512-1519.

Silva, P.J., Fernandes, P.A. & Ramos, M.J. (2003) A theoretical study radical-only and combined radical/carbocationic mechanisms of arachadonic acid cyclooxygenation by prostaglandin H synthase. Theoretical Chemistry Accounts, 110: 345-351.

Simmons, D.L., Botting, R.M., Hla, T. (2004) Cyclooxygenase isozymes: The biology of prostaglandin synthesis and Inhibition. Pharmacological Reviews, 56:387-437.

Simoncini, T., Hafezi-Moghadam, A., Brazil, D.P., Ley. K., Chin. W.W. & Liao, J.K. (2000). Interaction of oestrogen receptor with the regulatory subunit of phosphatidyl-3-OH kinase. Nature; 407: 538-541.

Singh, B., Berry, J.A., Shoher, A. & Lucci, A. (2006) COX-2 induces IL-11 production in human breast cancer cells. Journal of Surgical Research, 131: 267-275.

Sliva, D., Rizzo, M.T. & English, D. (2002). Phosphatidylinositol 3-kinase and NF-$_{\kappa}$B regulate motility of invasive MDA-MB-231 human breast cancer cells by the secretion of urokinase-type plasminogen activator. The Journal of Biological Chemistry; 227: 3150-3157.

Smith, R.F. & Evans, B.L. (1972) Bacteria of porcine skin, xenografts, and treatment with neomycin sulfate. Applied Microbiology, 23; 293-297.

Smith, E.R., Hadidian, Z. & Mason, M.M. (1968) The Toxicity of Single and Repeated Dermal Applications of Dimethyl Sulfoxide. The Journal of Clinical Pharmacology and the Journal of New Drugs, 8; 315-321.

Solanki, K., Matnani, M., Kale, M., Joshi, K., Bavdekar, A., Bhave, S., & Pandit, A. (2005) Transcutaneous absorption of topically massaged oil in neonates. Indian Pediatrics, 42: 998-1005.

Sommer, A., Hoffmann, J, Lichtner, R.B., Schneider, M.R. & Parczyk, K. (2003) Studies on the development of resistance to the pure antiestrogen FaslodexTM in three human breast cancer cell lines. Journal of Steroid Biochemistry & Molecular Biology, 85: 33–47.

Song, R.X-D. & Santen, R.J. (2006) Membrane initiated estrogen signaling in breast cancer. Biology & Reproduction, 75; 9 - 16.

Soslow, R.A., Dannenberg, A.J. Rush, D., Woerner, B.M., Khan, K.N., Masferrer, K. & Koki, A.T (2000) COX-2 is expressed in human pulmonary, colonic, and mammary tumors. Cancer, 89; 2637-2645

Spellman, F.R. (1998) Water biology in: The Science of Water, Concepts and Applications. CRC Press, London, UK.

Spruance, S.L., Mckeough, M.B & Cardinal, J.R. (1984) Penetration of guinea pig skin by acyclovir in different vehicles and correlation with the efficacy of topical therapy of experimental cutaneous herpes simplex virus infection. Antimicrobial Agents and Chemotherapy, 25: 10-15.

Staka, C.M., Nicholson, R.I. & Gee, J.M.W. (2005) Acquired resistance to oestrogen deprivation: role for growth factor signalling kinases/oestrogen receptor cross-talk revealed in new MCF-7X model. Endocrine Related Cancer, 12; S85-S97.

Stasinopoulos, I., O'Brien, D.R., Wildes, F., Glunde, K. & Bhujwalla, Z.M. (2007) Silencing of Cyclooxygenase-2 Inhibits Metastasis and Delays Tumor Onset of Poorly Differentiated Metastatic Breast Cancer Cells. Molecular Cancer Research, 5: 435-442.

Stewart, H.J. (1992). The Scottish trial of adjuvant tamoxifen in node-negative breast cancer. Scottish Cancer Trials Breast Group. Monograph National Cancer Institute; 11: 117-120.

Streuli, C.H. & Haslam, S.Z. (2005) Control of mammary gland development and neoplasia by stromal-epithelial interactions and extracellular matrix. Journal of Mammary Gland Biology and Neoplasia, 3: 107–108.

Suliburk, J., Helmer, K., Kennison, S., Mercer, D. & Robinson, E. (2005) Time-dependent aggrevation or attenuation of lipopolysaccharide-induced gastric injury by nitric oxide synthase inhibition. Journal of Surgical Research, 129; 265-271.

Sun, M., Paciga, J.E., Feldman, R.I., Yuan, Z-Q., Coppola, D., Lu, Y.Y., Shelley, S.A., Nicosia, S.V. & Cheng, J.Q. (2001) Phosphatidylinositol-3-OH kinase

(PI3K)/AKT2, activated in breast cancer, regulates and is induced by estrogen receptor α (ER α) via interaction between ER α and PI3K. Cancer Research, 61; 5985-5991.

Suthiphongchai, T., Phimsen, S., Sakulkhu, U. & Tohtong, R. (2006) PD98059-inhibited invasion of Dunning rat prostate cancer cells involves suppression of motility but not MMP2 or uPA secretion. Oncology Reports, 15: 1605-1610.

Timoshenko, A.V., Chakraborty, C. & Lala, P.K. (2005) COX-2-mediated upregulation of VEGF-C in human breast cancer cells in autocrine stimulation of cancer cell migration. Proc American Association of Cancer Research, 46: abstract #3691.

Thomas, C.P. & Heard, C.M. (2006) Probing the skin permeation of eicosapentaenoic acid and ketoprofen: 2. Comparative depth profiling and metabolism of eicosapentaenoic acid. European Journal of Pharmaceutics and Biopharmaceutics, 67: 156-165.

Thomas, C.P., Davison, Z. & Heard, C.M. (2007) Probing the skin penetration of fish oil/EPA on epidermal COX-2 and LOX. Prostaglandins, Leukotrienes and Essential Fatty Acids, 76; 357-362.

Thomas, C.P., Platts, J., Tatchell, T. & Heard, C.M. (2007) Probing the skin permeation of fish oil/EPA and ketoprofen: 1. NMR spectroscopy and molecular modelling. International Journal of Pharmaceutics, 338: 207-212.

Thomas, S.M., & Brugge, J.S. (1997) Cellular fuctions regulated by Src family kinases. Annual Review in Cell and Developmental Biology, 13: 513–609.

Tominaga, K., Higuchi, K., Sasaki, E., Suto, R., Watanabe, T., Fujiwara, Y., Oshitani, N., Matsumoto, T., Kim, S., Iwao, H. & Arakawa, T. (2004) Correlation of MAP kinases with COX-2 induction differs between MKN45 and HT29 cells. Alimentary Pharmacology & Therapeutics, 20:143–150.

Tommler, A., Gingell, D. & Wolf, H. (1985) Red blood cells experience electrostatic repulsion but make molecular adhesions with glass. Biophysics Journal, 48; 835-841.

Tucker, A.N., Tkaczuk, K.A., LewisL.M., Tomica, D., Limc, C.K. & Flawsa, J.A. (2005) Polymorphisms in cytochrome P4503A5 (CYP3A5) may be associated with race and tumor characteristics, but not metabolism and side effects of tamoxifen in breast cancer patients. Cancer Letters, 217: 61–72.

Uauy, R. & Valenzuela, A. (2000) Marine oils: The health benefits of n-3 fatty acids. Nutrition, 16; 280-284.

Vacaresse, N., Lajoie-Mazenc, I., Augé, N., Suc, I., Frisach, M.F., Salvayre, R. & Nègre-Salvayre, A. (1999) Activation of epithelial growth factor receptor pathway by unsaturated fatty acids. Circulation Research, 85; 892-899.

Vaddi, H. K., Ho, P.C., Chan, W.Y.& Chan, S.Y. (2002) Terpenes in ethanol: haloperidol permeation and partition through human skin and stratum corneum changes. Journal of Controlled Release, 81: 121-133.

Vanhaesebroeck, B., Waterfield, M.D. (1999) Signaling by distinct classes of phosphoinositides 3-kinases. Experimental Cell Research, 253; 239-254.

Vivanco, I. & Sawyer, C.L. () The phosphotidylinositol 3-kinase-Akt pathway in human cancer. Nature Reviews, 2; 489-501.

Vlahos, C.J., Matter, W.F., Hui, K.Y. & Brown, R.F (1994) A specific inhibitor of phosphatidylinositol 3-kinase, 2-(4-morpholinyl)-8-phenyl-4H-1-benzopyran-4-one (LY294002). The Journal of Biological Chemistry, 269: 5241-5248.

Walker, R.B. & Smith, E.W. (1995) The role of percutaneous penetration enhancers. Advanced Drug Delivery Reviews, 18: 295-301.

Wells, A., Kassis, J., Solava, J., Turner, T. & Lauffenburger, D.A. (2002) Growth-factor-induced cell motility in tumor invasion. Acta Oncologica, 41: 124-130.

Wester, R.C., Noonan, P.K., Smeach, S & Kosobud, L. (1983) Pharmacokinetics and bioavailability of intravenous and topical nitroglycerin in the rhesus monkey: estimate of percutaneous first-pass metabolism. Journal of Pharmaceutical Sciences, 72; 745-748.

Williams, A.C. (2003)

Wiseman, H. (1995) Tamoxifen. Molecular basis of use in cancer treatment and prevention. John Wiley and Sons, Chichester, UK.

Xia, S-H., Wang, J. & Kang, J.X. (2005) Decreased n-6/n-3 fatty acid ratio reduces the invasive potential of human lung cancer cells by downregulation of cell adhesion/invasion-related genes. Carcinogenesis, 26:779-784.

Xie, W., Chipman, J.G., Robertson, D.L., Erikson, R.L. & Simmons, D.L.(1991) Expression of a Mitogen-Responsive Gene Encoding Prostaglandin Synthase is Regulated by mRNA Splicing. PNAS, 88; 2692 - 2696.

Yamamoto, D., Shoji, T., Kawanishi, H., Nakagawa, H., Haijima, H., Gondo, H. & Tanaka, K. (2001) A utility of ductoscopy and fiberoptic ductoscopy for patients with nipple discharge. Breast Cancer Research and Treatment, 70: 103-108.

Yang, P., Chan, D., Felix, E., Cartwright, C., Menter, D.G., Madden, T., Klein, R.D., Fischer, S.M. & Newman, R.A. (2004) Formation and antiproliferative effect of prostaglandin E3 from eicosapentaenoic acid in human lung cancer cells. Journal of Lipid Research, 45: 1030-1039.

Zhang, S., Lil, X., Burghardt, R., Smith, R. & Safe, S.H. (2005) Role of estrogen receptor (ER) _ in insulin-like growth factor (IGF)-I-induced responses in MCF-7 breast cancer cells. Journal of Molecular Endocrinology, 35; 433–447.

Zhou, J., Wulfkuhle, J., Zhang, H., Gu, P., Yang, Y., Deng, J., Margolick, J., Liotta, L.A., Petricoin, E. & Zhang, Y. (2007) Activation of the PTEN/mTOR/STAT3 pathway in breast cancer stem-like cells is required for viability and maintenance. PNAS, 104; 16158-16163.

http://146.107.217.178/lab/

www.cancernews.com/data/Article/236.asp

www.ribbonofpink.com

www.natural-skin-health.com

Appendix 1 Western blot recipes

Loading buffer

A stock solution of 4ml 10% SDS 2ml glycerol, 2.4ml 0.5M Tris (pH 6.8), 1.6ml de-ionised H_2O, 1mg bromophenol blue was prepared. Immediately before experimentation 15.5mgml^{-1} DTT was added.

Lysis Buffer

A stock solution of 50mM Trizma HCl, 5nM EGTA, 150mM NaCl, 1% v/v triton X-100. This solution was stored at 4 °C until required. Immediately prior to experimentation, the following were added to the stock solution: 2mM sodium vanadate, 50mM sodium fluoride, 1mM phenylmethyl sulphonyl Fluoride, 20mM phenylarsine oxide, 10mM sodium molybate, 10 μgml^{-1} leupeptin, 2mgml^{-1} aprotinin.

Running buffer

A x 10 stock solution of running buffer was made, which was diluted 1:10 in de-ionised H_2O prior to SDS-PAGE.

The x 10 stock solution included; 0.23M Trizma Base, 1.92M glycine, 0.1% SDS

Separating Gel

1. 7.5 % gel (protein range 70-200 kDa)

2.5ml 30% Acylamide, 4.8ml de-ionised H_2O, 1.5M (2.5ml) tris HCl (pH 8.8), 0.1ml 10% SDS, 0.1ml 10% APS, 10µl temed.

2. 10% gel (protein range 20-100 kDa)

3.3ml 30% acrylamide, 4ml de-ionised H_2O, 1.5M (2.5ml) tris HCl (pH 8.8), 0.1ml 10% SDS, 0.1ml 10% APS, 10µl temed.

Stacking gel

1.7ml 30% Acrylamide, 5.8ml de-ionised H_2O, 2.5ml 1.5M tris HCl (pH 6.8), 0.1ml 10% SDS, 0.1ml 10% APS, 10µl temed.

Transfer buffer

A x 10 stock solution was made, which was diluted 1:10 with de-ionised H_2O prior to transfer.

The x 10 solution comprised of; 0.25M Trizma Base, 1.92M glycine, 20% methanol.

TBS-TWEEN

A x 10 stock solution was made, which was diluted 1:10 with de-ionised H_2O prior to use. The x 10 stock solution was made using; 12.1g Trizma Base 58g NaCl, 5ml Tween 20, 15ml 5M HCl.

Appendix 2. ICC recipes

ER-ICA fixation

Coverslips were placed into a metal rack and fixed in 3.7% formaldehyde for 15 minutes at room temperature. They were then bathed in PBS for 5 minutes at room temperature. Coverslips were then subjected to methanol between -10 and -30°C, acetone at the same temperature for 3 minutes and finally PBS at room temperature for 5 minutes. Coverslips were then stored in sucrose storage media (SSM) at -20°C until required.

Formal Saline

Formal saline was made of 4.5g NaCl, 450ml of tap water and 50ml of 37% formaldehyde solution. The solution was allowed to dissolve thoroughly and stored at room temperature until required.

Formal Saline fixation

Tissue culture media was removed by aspiration and coverslips were incubated with 1ml formal saline solution for 10 minutes. They were then incubated with 1 ml ethanol for 5 minutes, followed by a quick rinse in ethanol. Ethanol was removed and coverslips subsequently incubated with 1ml PBS for 5 minutes, followed by a quick rinse in PBS. They were then stored in SSM at -20°C until required.

Phenol Formal Saline

The preparation of phenol formal saline was conducted under a fume hood, whilst wearing full protective clothing. A 2.5% w/v solution of phenol formal saline was prepared formal saline previously prepared.

Phenol Formal Saline fixation

Tissue culture media was removed by aspiration. Coverslips were incubated with 2ml phenol formal saline solution for 5 minutes. This was the removed and replaced with 1 ml of ethanol for 5minutes followed by a quick rinse in ethanol. Ethanol was then removed by aspiration and coverslips incubated with 1 ml PBS for 5 minutes, followed by a quick rinse in PBS. Coverslips were then stored in SSM at -20°C until required.

Appendix 3.Tissue Culture recipes

Charcoal Stripping

The pH of 100ml FCS was adjusted to 4.2 and left to equilibrate for 30 minutes at 4°C. Meanwhile, an 11% activated charcoal/0.06% dextran C solution was made in 10 ml distilled water. This was agitated vigorously for 1 hour and 5ml was then added to 100ml FCS. This was the incubated at 4°C, with gentle agitation, for 16 hours. Charcoal was then removed by centrifugation at 12000g for 40 minutes. The remaining solution was filtered several times using a Whatman No 4 filter paper and subsequently adjusted to pH 7.2. Finally, the solution was sterilised using a 0.22μm membrane filter.

Isoton Solution

Isoton II azide-free balanced electrolyte solution, coulter counter solution, $7.9gl^{-1}$ NaCl, $1.9gl^{-1}$ disodium hydrogen orthophosphate, $0.4gl^{-1}$ EDTA disodium salt, $0.2gl^{-1}$ orthophosphate and $0.3gls^{-1}$ odium fluoride.

Sucrose Storage Media (SSM)

SSM was made using 0.33g NaCl, 42.8g sucrose in 250ml PBS. After sufficient stirring 250ml glycerol was added. SSM was stored at -20°C until required.